ORIGIN OF CHLORINE-36 IN THE EASTERN SNAKE RIVER PLAIN AQUIFER, IDAHO: IMPLICATIONS FOR DESCRIBING GROUND WATER CONTAMINATION NEAR A NUCLEAR FACILITY

by

L. DeWayne Cecil

A thesis
presented to the University of Waterloo
in fulfillment of the
thesis requirement for the degree of
Doctor of Philosophy
In
Earth Sciences

Waterloo, Ontario, Canada, 2000

Canada

The University of Waterloo requires the signature of all persons using or photocopying this thesis. Please sign below, and give address and date.

ABSTRACT

Isotopic tracers have been used in hydrogeologic investigations for over forty years with a relatively recent increase in the use of radioactive, cosmogenically-produced nuclides. It has been the practice by hydrogeologists to assume that the major source of these radionuclides in ground water is meteoric, with analytical detection as the only limiting factor in utilizing these tracers to describe hydrogeologic processes. However, in many environments, subsurface production as well as anthropogenic sources of these isotopes dominate. This is particularly true of radioactive chlorine-36 (^{36}Cl).

To understand and quantify the sources of ^{36}Cl in the environment, this research was undertaken in the eastern Snake River Plain aquifer system near the Idaho National Engineering and Environmental Laboratory (INEEL). The environment at and near the INEEL has significant inputs of ^{36}Cl from nuclear-fuel and nuclear-waste processing that can be orders of magnitude larger than meteoric, weapons-tests, or *in situ* production. The INEEL is located in southeastern Idaho and is among the U.S. Department of Energy's (DOE) largest nuclear testing facilities. Between 1953 and February 1984, low-level radioactive wastewater containing tritium, iodine-129, and ^{36}Cl, among other radionuclides, was discharged to the eastern Snake River Plain aquifer through a 183-meter-deep disposal well at the Idaho Nuclear Technology and Engineering Center (INTEC). Additionally, wastewater has been discharged to the environment through infiltration ponds at the Test Reactor Area since 1952 and at the INTEC since February 1984 (Cecil and others, 1992).

Since 1966, the U.S. Geological Survey (USGS) routinely has archived at least one suite of ground and surface water samples collected quarterly at the INEEL each year. The samples are available for research purposes. The new data generated from the archived samples, associated historical database, and the capability to detect ^{36}Cl at small environmental

concentrations by accelerator mass spectrometry (AMS), should allow determination of large-scale aquifer hydrogeologic properties and quantification of the sources of this isotope.

The main area of research documented in this dissertation was the quantification of ^{36}Cl inputs to the environment at and near the INEEL. This information was then used to begin to describe the hydrogeology in the far field from the ^{36}Cl source at the INTEC, up to 28 km downgradient. The first research objective was an evaluation of the archived water samples in terms of ^{36}Cl concentrations and possible chloride isotope fractionation through time. Secondly, concentrations of ^{36}Cl in the environment from meteoric, weapons-tests, and *in situ* production were established and compared to releases from nuclear-fuel and nuclear-waste processing at the INEEL. Finally, these ^{36}Cl inputs to the environment were used to determine first arrival times at downgradient observation wells and one-dimensional hydraulic dispersivities in the far field.

To evaluate the suitability of the archived samples as an indicator of historical radionuclide concentrations, water samples from six USGS monitoring wells collected during 1969-93 and one surface water site from 1970 were analyzed for stable chlorine isotopic ratios, chlorine-37/chlorine-35 (^{37}Cl/^{35}Cl). These ratios were measured in water samples and were compared to ^{37}Cl/^{35}Cl in standard mean ocean chloride (δ^{37}Cl) to determine if fractionation of chlorine isotopes had occurred during storage or along apparent flowpaths in the aquifer. This information was used to evaluate if ^{36}Cl concentrations measured in water from the archived samples in the 1990s were representative of the historical concentration at the time of sample collection. The results of this evaluation indicated that no detectable fractionation of chlorine isotopes had taken place during storage. Therefore, ^{36}Cl concentrations measured today in the archived water samples, are representative of the concentrations at the time of sample collection. Additionally, the results suggest an inverse correlation between δ^{37}Cl and radioactive ^{36}Cl concentrations in some of the water samples from this aquifer that warrants further research.

Quantification of ^{36}Cl in the environment at and near the INEEL included calculation of meteoric input, fallout from atmospheric nuclear-weapons tests conducted in the 1950s-60s, and

natural *in situ* production in the aquifer system. After accounting for ^{36}Cl from these three sources, any remaining quantifiable concentration was concluded to originate from nuclear facilities at the INEEL. From the data presented in this dissertation, it was determined that concentrations of ^{36}Cl larger than 1×10^9 atoms per liter (atoms/L) in the environment at the INEEL were a result of nuclear-waste disposal practices. Releases of ^{36}Cl to the environment at the INEEL as a result of site operations are on the order of 10^{11} to 10^{12} atoms/L in ground water near the INTEC source.

To determine first-arrival times of ^{36}Cl from site-disposal practices, analyses were performed on archived ground water samples from selected downgradient observation wells. Estimated first arrival times from ^{36}Cl data in the archived water samples from observation wells indicate minimum ground water flow velocities of 1 to 3 m/day with velocities as large as 6 m/day. Using the results of this research, hydrodynamic dispersion was analytically modeled using a one-dimensional convolution integral in a computer spreadsheet. The results of the system-response modeling suggest one-dimensional dispersion (equivalent to longitudinal dispersion) of less than 5 m. This further suggests that ground water flow in this system may be along preferential flow corridors.

ACKNOWLEDGMENTS

TABLE OF CONTENTS

LIST OF ILLUSTRATIONS

Page

LIST OF TABLES

LIST OF APPENDIX TABLES

Page

CONVERSION FACTORS, VERTICAL DATUM, AND ABBREVIATED UNITS

Multiply	By	To obtain
centimeter per year (cm/yr)	0.394	inch per year
cubic centimeter (cm^3)	0.061	cubic inch
gram (g)	0.035	ounce
gram per cubic centimeter (g/cm^3)	0.578	ounce per cubic inch
gram per liter (g/L)	0.133	ounce per gallon
meter (m)	3.281	foot
meter per kilometer (m/km)	5.28	foot per mile
kilogram (kg)	2.204	pound
liter (L)	0.264	gallon
square centimeter per gram (cm^2/g)	4.394	square inch per ounce
square centimeter per second (cm^2/s)	0.155	square inch per second
square kilometer (km^2)	0.386	square mile
square meter per day (m^2/d)	10.76	square foot per day
degree Celsius (°C)	[°C (9/5) + 32]degree Fahrenheit (°F)	

Sea Level: In this dissertation, "sea level" refers to the National Geodetic Vertical Datum of 1929—a geodetic datum derived from a general adjustment of the first-order level nets of both the United States and Canada.

Other abbreviated units and symbols used in this dissertation (all others explained in the text):

m/day (meters per day)
MeV (million electron volts), keV (thousand electron volts)
mg/kg (milligrams per kilogram)
mg/L (milligrams per liter)
mL (milliliters)
(n/cm^2)/s (neutrons per square centimeter per second)
(n/g)/yr (neutrons per gram of rock per year)
ppm (parts per million)
p (proton)
n (neutron)
γ (gamma radiation)
α (alpha particle)
σ (sigma)
μ⁻ (negative muon)
yr^{-1} (per year)
δ (delta notation)

PREFACE

The research discussed in this dissertation is based on information and data published in journal articles, professional papers, conferences and symposia, and USGS publications over the last 11 years (Cecil, 1989; Cecil and others, 1989, 1991, 1992, 1997, 1998, 1999, 2000a, and 2000b). Additionally, five other publications in the References that list me as the second author were an integral part of the research conducted for this dissertation. Those five references are: (1) Beasley, Cecil, and others, 1993; (2) Davis, Cecil, and others, 1998; (3) Knobel, Cecil, and Woods, 1995; (4) Mann and Cecil, 1990; and (5) Orr and Cecil, 1991. For the research documented in all of these references, I wrote (or co-authored) the proposals and obtained (or assisted in obtaining) the funding, was involved in the major portion of the planning and carrying out of the experimental work, and the interpretation of the data and reporting of the results. For the sample results discussed in this dissertation, I collected and/or processed the samples for analysis, was an integral part of the development of techniques for extracting the chloride from the samples, and prepared most of the targets for the accelerator mass spectrometry measurements.

CHAPTER 1

INTRODUCTION

The Idaho National Engineering and Environmental Laboratory (INEEL) is located in southeastern Idaho and is one of the largest of the United States Department of Energy's (DOE) nuclear testing facilities, covering about 2,300 square kilometers (km) (figure 1.1). The INEEL was established in 1949 and is used by the DOE to construct and test nuclear reactors and to participate in various defense programs. There have been 52 different reactors constructed and tested at this site since 1952 and thirteen of the reactors are still operable.

The DOE requires information about the mobility and/or retardation of radiochemical and chemical wastes released to the environment at the INEEL. In 1949, the DOE (then called the Atomic Energy Commission) requested the United States Geological Survey (USGS) to describe the geology and water resources of the eastern Snake River Plain. Since the completion of that initial site characterization, the USGS has maintained a network of monitoring wells to determine hydrologic trends and to describe the fate of contaminants contained in wastewater released to the environment.

Radiochemical and chemical wastes generated at the INEEL and other DOE facilities have been buried in the subsurface at the site since 1952. Additionally, from 1952-84, wastewater containing tritium (^{3}H), iodine-129 (^{129}I), and chlorine-36 (^{36}Cl), among other radiochemical and chemical constituents, was discharged to the eastern Snake River Plain aquifer through a 183-meter-deep disposal well at the Idaho Nuclear Technology and Engineering Center (INTEC). Since 1984 at the INTEC, and from 1952-93 at the Test Reactor Area, these wastes also were discharged to disposal ponds (fig. 1.2). The wastewater discharged to ponds at these two facilities must travel through about 150 m of alluvium, sedimentary interbeds, and basalt before reaching the aquifer. Historically, the distribution of ^{3}H has been used to define the extent that the Snake River Plain aquifer has been influenced by wastewater-disposal practices (Duffy

1

Figure 1.1. Map showing location of the eastern Snake River Plain, the Idaho National Engineering and Environmental Laboratory, and selected sampling sites.

2

113°
43°37'30"

112° 52' 30"

0   1   2 MILES

0   1   2 KILOMETERS

EXPLANATION

44 ● WELL LOCATION—44 is local well identifier

DISPOSAL PONDS

TEST REACTOR AREA

Big Lost River

Disposal well

IDAHO NUCLEAR TECHNOLOGY AND ENGINEERING PLANT

● 44

● 57

DISPOSAL PONDS

● 77

● 20

● 85

Lincoln Boulevard

CENTRAL FACILITIES AREA

U.S. 20, 26

43° 30'
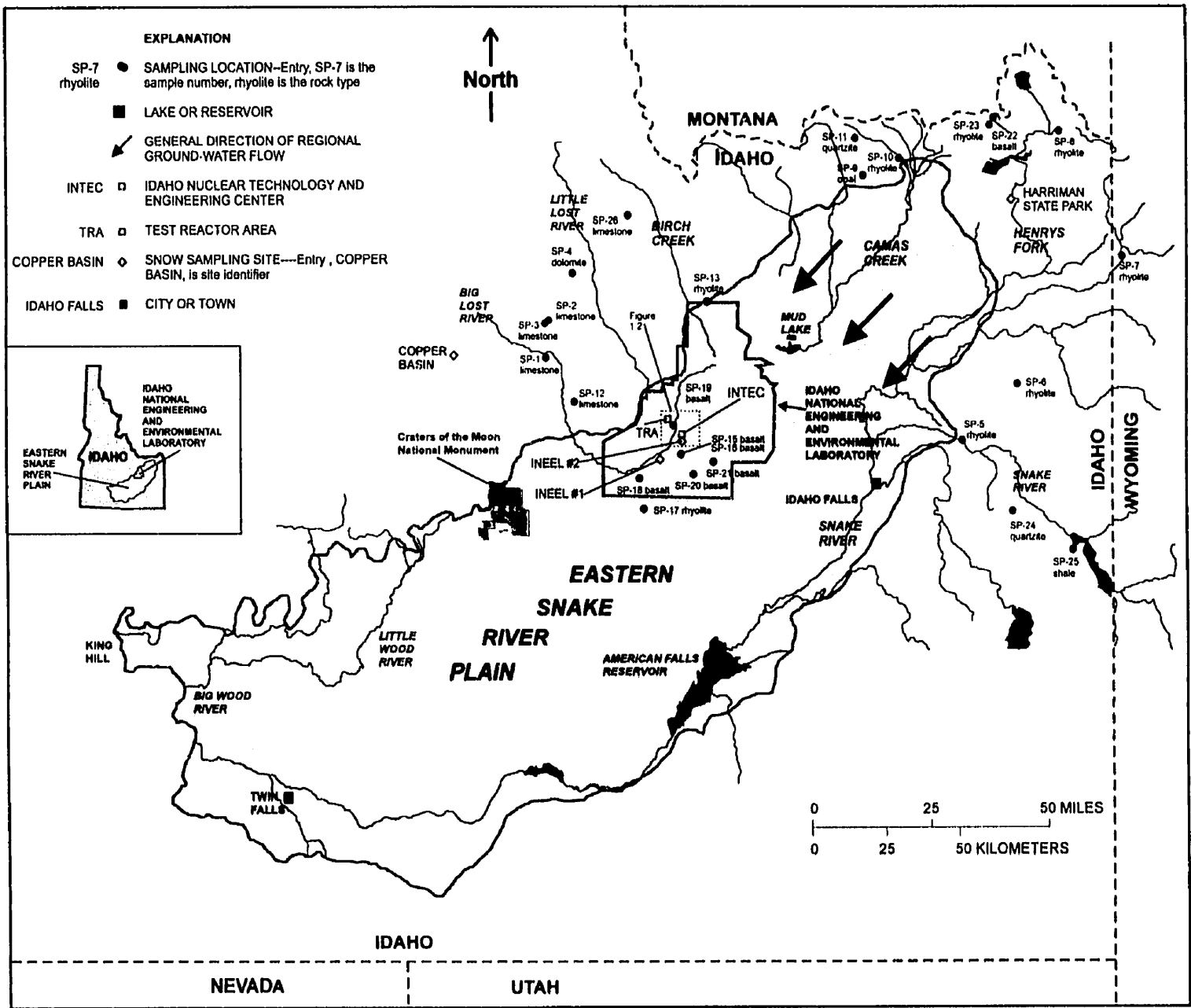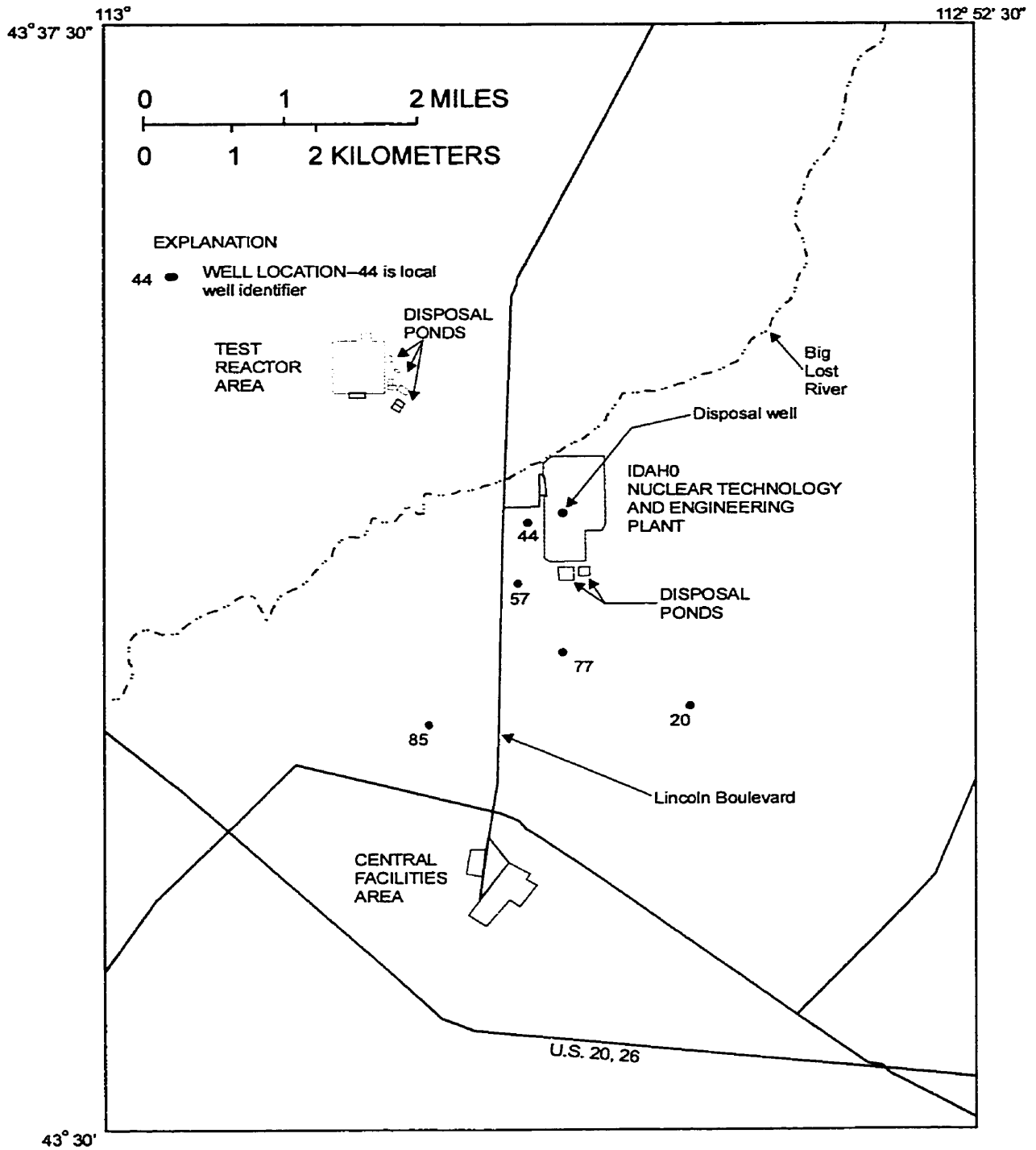
Figure 1.2. Location of observation wells completed in the Snake River Plain aquifer, the wastewater-disposal well, and disposal ponds near the Idaho Nuclear Technology and Engineering Center and the Test Reactor Area.

and Harrison, 1987). However, the relatively short (12.26-year) half-life of ^{3}H and the detection capability that is used at the INEEL in routine monitoring, 500 picocuries per liter (pCi/L), limit the utility of this radionuclide for hydrologic studies. Due to the short half-life and the analytical method utilized, ^{3}H detection in the far field (20+ kilometers downgradient from the INTEC source) is not possible. However, even if a more sensitive analytical method were employed, the short travel time from INTEC and the 12.26 year half-life seriously complicate any attempt to distinguish ^{3}H in ground water as a result of disposal practices from ^{3}H as a result of natural or weapons-tests production in the far field.

Prior to 1990, concentrations of ^{36}Cl (half-life is 301,000 years) at the INEEL were determined by beta-counting methods and ^{129}I (half-life is 15.7 million years) concentrations were determined by neutron activation analysis. Ground water samples analyzed by accelerator mass spectrometry (AMS) in 1990 and 1991 contained concentrations of ^{36}Cl and ^{129}I that previously were not detectable. Therefore, a more accurate description of the area influenced by wastewater disposal can be made because the analytical method detection limit for AMS is several orders of magnitude lower than that for either the beta-counting method or neutron-activation analysis.

Since 1966, the USGS has routinely archived at least one suite of quarterly ground- and surface water samples each year. The samples and a large associated geochemical database are available for research purposes. These archived samples, the historical chemical database, and the capability to detect radionuclides such as ^{36}Cl at small environmental concentrations by AMS should allow determination of large-scale aquifer hydraulic flow properties.

Releases of anthropogenic ^{36}Cl to the environment at the INEEL, as a result of nuclear-fuel and nuclear-waste processing operations, have been well documented (Cecil and others, 1992; Beasley and others, 1993). This ^{36}Cl was produced by neutron activation of stable chlorine-35 (^{35}Cl) present as impurities in nuclear fuel bundles, reactor-cooling water, and other process wastes. Radioactive chlorine (^{36}Cl) is then released to the environment in liquid and

4

gaseous effluents as chlorine gas, nitrosyl chloride, and/or hydrochloric acid. One possible reaction during the waste processing is:

$$HNO_3 + 3H\,^{36}Cl \longrightarrow\,^{36}Cl\,^{35}Cl + NO\,^{36}Cl + 2\ H_2O$$
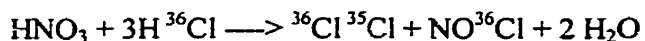
There are three possible sources of ^{36}Cl in the environment at the INEEL in addition to the releases made during nuclear waste-disposal operations. These three sources are meteoric input of cosmogenically produced ^{36}Cl in wet and dry deposition, ^{36}Cl produced during nuclear-weapons tests in the 1950s-60s and transported globally in the upper atmosphere or released during nuclear accidents, and *in situ* production of ^{36}Cl in rocks and soils by nuclear particle interactions with stable elements (fig. 1.3). Until the research reported here was completed, meteoric input, flux from nuclear-weapons tests, and *in situ* production for this nuclide had only been estimated at the INEEL (Cecil and others, 1992; Beasley and others, 1993). In this dissertation, the first measurements and quantitative estimates of meteoric input, weapons-tests production, and *in situ* production for ^{36}Cl at and near the INEEL are presented and are compared to ^{36}Cl concentrations in the environment as a result of nuclear-waste processing.

To aid in determining meteoric input to the environment, 32 surface water and two spring samples collected during 1969-95 were selected from sites on and near the eastern Snake River Plain for ^{36}Cl analyses (table 1.1). Eighteen of these samples were selected from the archive-sample library maintained by the USGS at the INEEL. In addition to the surface water samples, four snow and seven ground water samples(a subset of all ground water samples, table 1.1) were collected at and near the INEEL and analyzed for ^{36}Cl. These samples were selected on the basis of areal distribution, availability of additional historical analytical records, and whether or not they were representative of areal recharge to the eastern Snake River Plain aquifer system.

Chlorine-36 produced during nuclear weapons tests in the 1950s-60s has been identified in polar ice and in the ice sheet in Greenland (Finkel and others, 1980; Elmore and others, 1982). However, ice-core traces of climate, as suggested by the isotopic record in glaciers, have been considered unsuitable for temperate locations such as the continental United States due to the

5
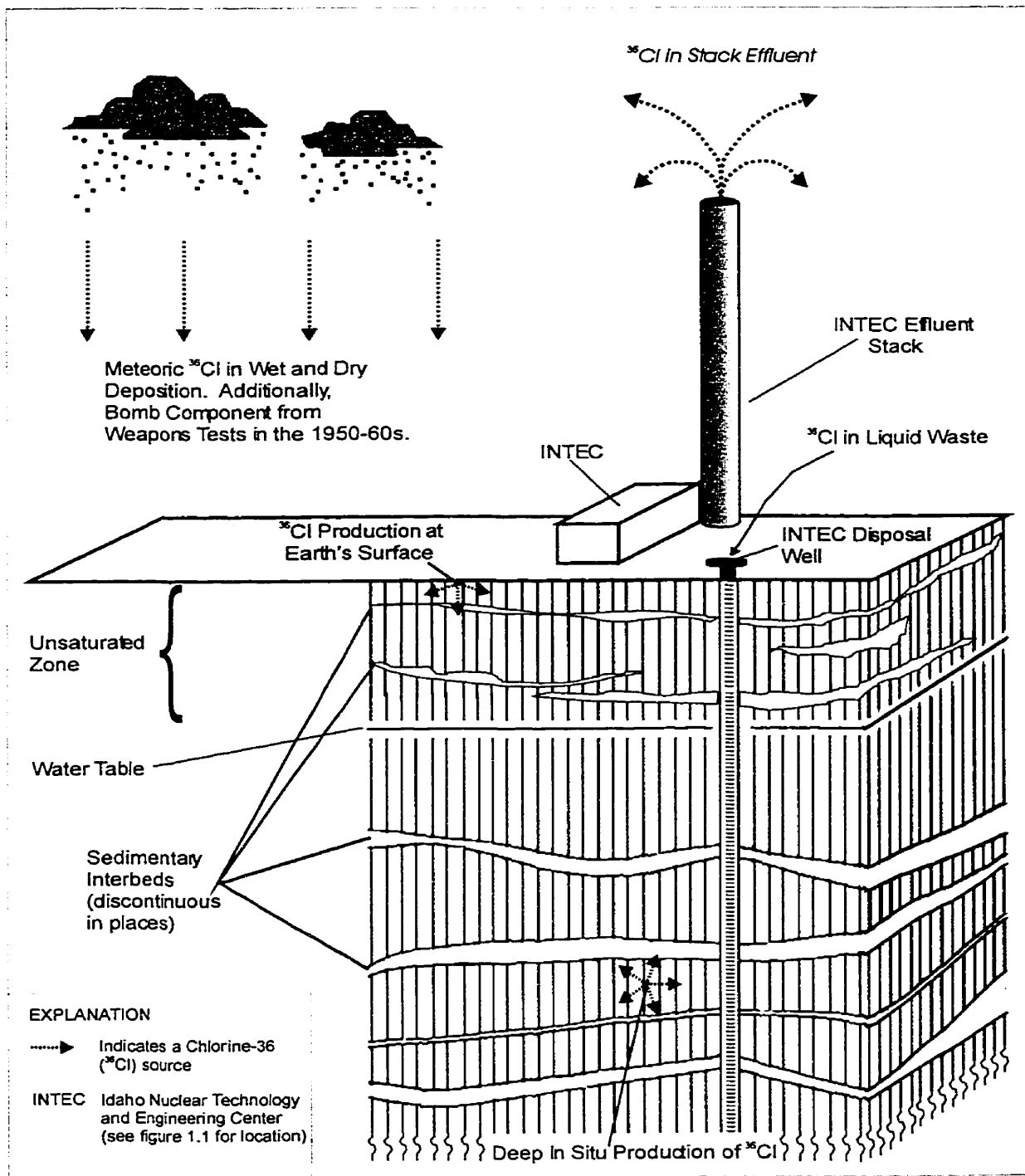
Figure 1.3. Conceptual model showing potential sources of chlorine-36 in the eastern Snake River Plain aquifer.

Note: This figure is not to scale. There are other possible facility sources of ^{36}Cl at the INEEL but the INTEC is the major source.

effects of thawing and refreezing and subsequent meltwater percolation. However, in 1991, a research team from the USGS collected a continuous 160-meter ice core from the Upper Fremont Glacier in the Wind River Range of Wyoming in the western United States (fig. 1.4). From this core, the first successful reconstruction of an isotopic record of paleoclimate from a mid-latitude North American glacier was reported (Naftz and others, 1996). Naftz and others (1996) established a global linkage of the delta oxygen-18 ($\delta^{18}O$) Standard Mean Ocean Water series between the Upper Fremont Glacier and two ice-core records from the Quelccaya Ice Cap in South America. In the research presented here, the first measurements of mid-latitude ^{36}Cl fallout archived in glacial ice in North America are presented.

From the Upper Fremont Glacier ice-core, Naftz and others (1996) identified the 1963 ^{3}H bomb peak at a depth of 29 meters (m) below the surface of the glacier. The ^{3}H concentration at this depth in 1991 was 365 tritium units (TU). Based on this ^{3}H record, eighteen sections of ice core were selected for ^{36}Cl analyses. The core, measuring in length from 0.4 to 0.7 m, was from various depths below the surface of the Upper Fremont Glacier. These sections of ice core were selected to include the peak bomb production of ^{36}Cl that occurred during 1957-58. This ^{36}Cl peak should be slightly deeper in the ice core than the 1963 ^{3}H peak. Additional sections of ice were selected to be representative of pre- and post-bomb ^{36}Cl concentrations. A sample of relatively recent glacial runoff from Galena Creek Rock Glacier, 180 km north of the Upper Fremont Glacier, was analyzed for comparison purposes.

The information gathered from the archive sample evaluation, the quantification of ^{36}Cl inputs to the environment, and the ground water sample results were used to mathematically model one-dimensional (1-D) aquifer dispersivity. Additionally, ^{36}Cl input from disposal practices was reconstructed from ^{3}H input records and used to determine first arrival times at downgradient observation wells and for curve-matching in the modeling process.

1.1   Purpose and Scope

The purpose of the research reported here is to understand and quantify the sources of
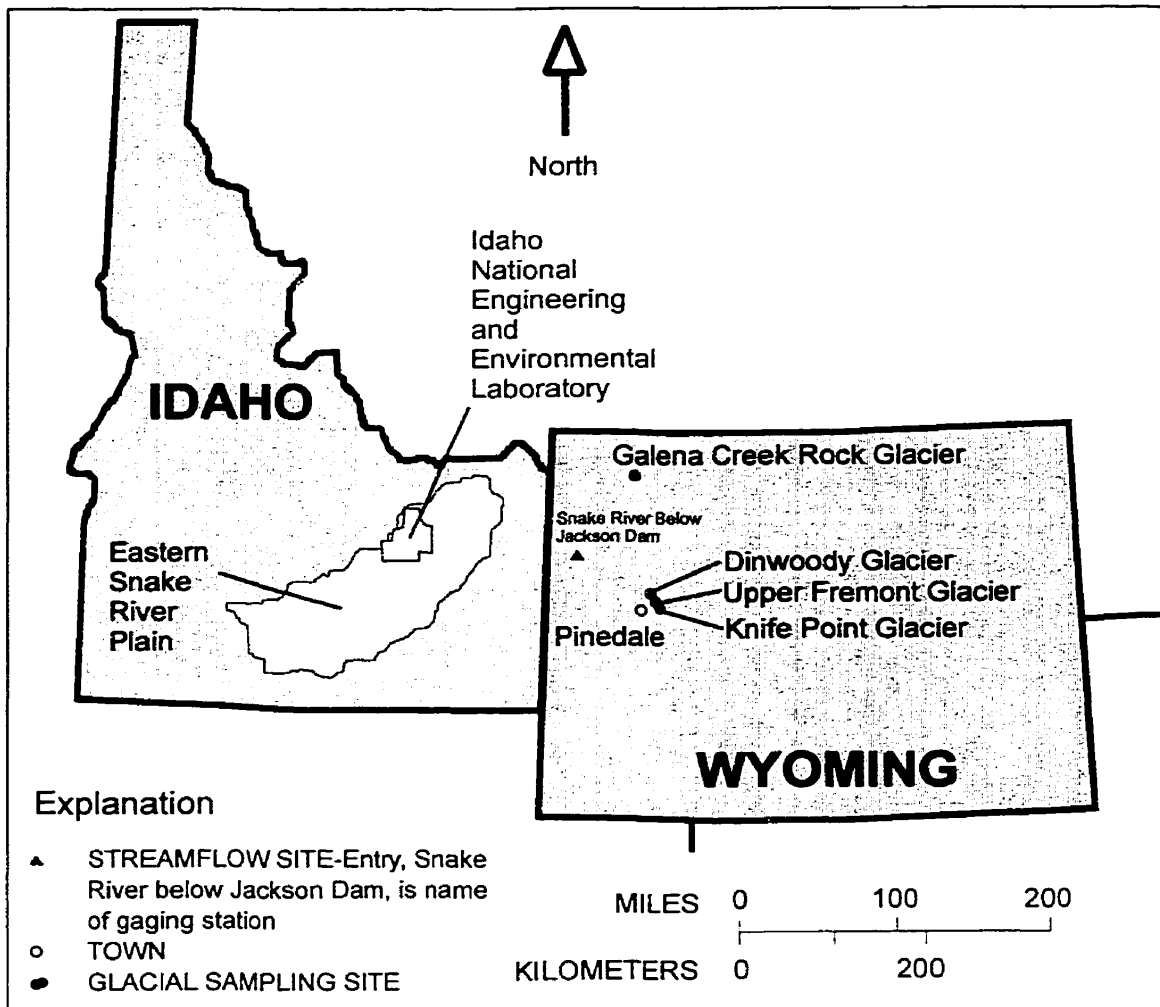
Figure 1.4. Location of the Idaho National Engineering and Environmental Laboratory and selected surface water and glacial sampling sites.

radioactive ^{36}Cl in the environment at and near the INEEL. This information was then applied to an evaluation of 1-D hydrodynamic dispersion in the eastern Snake River Plain aquifer system. The type and number of samples collected to accomplish the purpose and scope of this research are given in table 1.1. These data were used to reconstruct the historical development of wastewater migration in the Snake River Plain aquifer with particular emphasis on ^{36}Cl. Reconstruction permitted the definition of first arrival times of wastewater containing ^{36}Cl at monitoring wells up to 26 km downgradient from the INTEC. An attempt was also made to

Table 1.1.   Type, number, and purpose of environmental samples collected for this study.

[A subset of the ground-and surface water samples was selected for evaluating the suitability of the archived samples for this research. See Chapter 4 for a discussion of this analysis.]

Type of Sample	Number of Samples	Purpose of Samples
Ground Water	70	Determination of ambient and/or background concentrations, 1-D aquifer dispersivity, archive-sample evaluation, Cl^-/Br^- ratios
Surface Water	32	Determination of meteoric and anthropogenic input, effects of evaporation on ^{36}Cl concentrations, archive-sample evaluation, Cl^-/Br^- ratios
Ice Core	18	Determination of meteoric and/or anthropogenic ^{36}Cl input, Cl^-/Br^- ratios
Snow	4	Determination of meteoric and/or anthropogenic ^{36}Cl input
Rock Core	25	Determination of whole-rock geochemistry (22 elements) for *in situ* ^{36}Cl production calculations
Glacial Meltwater	1	Determination of meteoric and/or anthropogenic ^{36}Cl input, Cl^-/Br^- ratios
Spring	2	Determination of meteoric and/or anthropogenic ^{36}Cl input, Cl^-/Br^- ratios

establish 1-D aquifer dispersivities to help constrain future 2-D and 3-D modeling efforts. To accomplish the purpose of the overall study, an evaluation of selected water samples from the USGS archive library for the period 1966-1994 was performed to determine if there was Cl isotope fractionation and thereby establish confidence in utilizing chloride (Cl^-) isotopic data generated from these historical water samples. The evaluation covered the historical record available from selected sites at the INEEL and included, (1) an assessment of paper and computer records for each sample; (2) a determination of $^{37}Cl/^{35}Cl$ ratios; and (3) a determination of ^{36}Cl

concentrations. These assessments and analyses were performed to ascertain if Cl isotope fractionation might have occurred during storage. This information is essential in determining the suitability of using ^{36}Cl concentrations in the archived water samples to aid in determining aquifer hydraulic properties.

Most ^{36}Cl produced in the atmospheric environment originates from cosmic radiation interacting with atmospheric gases. Additionally, large amounts of ^{36}Cl, orders of magnitude greater than naturally produced atmospheric inventories, have been released to the environment during nuclear-weapons tests, nuclear-reactor operations, and nuclear-waste processing. To better determine the inventories of ^{36}Cl at the INEEL, ground and surface water, snow, and glacial- ice and -runoff samples were analyzed to establish inputs from meteoric sources and nuclear-weapons tests. These measurements were performed on samples collected at and near the INEEL in southeastern Idaho and western Wyoming (fig. 1.4).

Additionally, calculations were performed to determine the contribution of ^{36}Cl from *in situ* production in subsurface rocks and ground water in the eastern Snake River Plain aquifer. These concentrations were then compared to ground water concentrations as a result of site disposal practices at the INEEL. The scope included isotopic and chemical analyses and associated ^{36}Cl *in situ* production calculations on 25 whole-rock samples from six major water-bearing rock types found in the eastern Snake River Plain. The rock types investigated were basalt, rhyolite, limestone, dolomite, shale, and quartzite. The calculated contribution included the estimation of neutron production rates based on the elemental composition of the rock samples and the proportion of the resultant neutrons that may be captured by ^{35}Cl atoms within the rock to produce ^{36}Cl.

Finally, a 1-D system response model was constructed in the far field (up to 26 km from the source) to determine aquifer dispersivity. Assuming that tracer arrival times at downgradient observation wells are controlled by preferential flow, the model was used to determine aquifer

dispersivity by comparing the shape of predicted ^{36}Cl-concentration curves to the shape of ^{36}Cl-concentrations measured in archived water from these observations wells.

1.2   Hydrogeologic Setting

The eastern Snake River Plain (fig. 1.1) is a structural basin defined by faulting and downwarping on the southeast and faulting on the northwest. It is predominantly filled with Quaternary basalt of the Snake River Group that is generally covered by up to3 m of alluvium at land surface (Garabedian, 1992; Whitehead, 1992). This structural basin was created by Cenozoic tectonic stresses and is a zone of transition between the northern Rocky Mountain geologic province to the north and east and the Basin and Range province to the northwest, west, north, east, and southeast. Unconsolidated sediments overlie the margins of the basin and are interbedded with the basalts and pyroclastics at depth. The basalts are several hundred to as much as 1,500 m thick, underlie most of the basin, and constitute the major water-bearing rock units of the eastern Snake River Plain aquifer.

Fractures and vesicular zones occur near the surfaces of the basalt flows and may be highly transmissive of ground water. Reported transmissivities for the eastern Snake River Plain aquifer range from 0.1 to more than 70,000 m^2/day, a range of nearly six orders of magnitude (Ackerman, 1991). Depth to ground water at the INEEL varies in the basalt aquifer from about 60 m below land surface in the northern part to more than 275 m in the southern part. The hydraulic gradient at the INEEL is about 1 m/km and horizontal ground water flow velocity ranges from 1 to 6 m/day. This range is based on the distribution of ^{36}Cl through time as determined from analyses of archived samples presented later in this dissertation.

Aquifers at the INEEL consist of layered sequences of basaltic-lava flows and cinder beds intercalated mainly with fluvial and lacustrine sedimentary deposits. Individual lava flows typically are 6 to 7.5 m thick and 130 to 260 square kilometers in areal extent, providing potential for relatively large regional flow systems within individual volcanic-extrusive episodes. Rubble,

clinker zones, fractures, and vesicular zones are prevalent near the surfaces of flows and may serve as preferential pathways for ground water movement. Subsequent lava flows or sedimentary deposits may partly fill fractures and vesicles and thereby restrict ground water flow. The centers of individual flows, especially thick flows, are typically less vesicular and more massive and may be characterized by vertical fractures further complicating the interpretation of the ground water flow system. Well yields can be large because of the highly transmissive nature of the fractured, vesicular interflow zones. The aquifer framework results in a complex, heterogeneous and anisotropic medium.

The geology and hydrology of the Snake River Plain at the INEEL describe a water-table aquifer of large areal extent with overlying perched aquifers near waste-disposal ponds (Cecil and others, 1991). Ground water levels have been relatively stable at the INEEL since measurements began in 1949. However, water levels do respond to climatic trends, and locally, to recharge from intermittent streams. Regional ground water flow is from the northeast to the southwest (fig. 1.1). Perched aquifers form when downward flow from waste ponds is impeded by silt and clay in sedimentary deposits or by dense sections at the interiors of basalt flows.

Long-term (1950-1988) average precipitation in the vicinity of the INEEL is 22 cm/year (Clawson and others, 1989, table D-1). About 40 percent of the long-term average precipitation on the eastern Snake River Plain is rainfall between April and September. However, as a result of evapotranspiration (ET), less than 5 percent of the long-term annual average precipitation infiltrates the surface locally on the eastern Snake River Plain (Cecil and others, 1992). As illustrated later, ET can significantly affect meteoric ^{36}Cl concentrations measured in environmental water samples from the eastern Snake River Plain aquifer system. Recharge to the eastern Snake River Plain aquifer is from snowmelt in the mountains to the east, west, and north, and from irrigation return flow and surface water. The five watersheds that recharge the northern portion of the eastern Snake River Plain aquifer are the Big Lost River, Little Lost River, Birch Creek, Camas Creek/Mud Lake, and the main Snake River drainage (fig. 1.1).

1.3 Reporting of Radionuclide Data

Three measures for the presence of ^{36}Cl are used in this dissertation. They are, ratios of atoms of ^{36}Cl to atoms of total Cl⁻ in the samples (^{36}Cl/Cl), concentrations expressed in atoms/L (Appendix Table C-1), and atmospheric flux of ^{36}Cl in atoms per area per time calculated from concentrations in ice and snow samples (atom/L) and precipitation flux (g/cm^2yr) (Appendix Table C-2). The ratios are reported by the accelerator facilities. The concentrations and fluxes were calculated from the data generated in this research and were used to compare with data sets from other studies reported in the literature. Additionally, concentrations of the radionuclide ^{36}Cl are reported with an estimated sample standard deviation, s, which is obtained by propagating sources of analytical uncertainty in measurements. The following guidelines for interpreting analytical results are based on a method proposed by Currie (1984) and were subsequently prepared as guidelines for the USGS, Water Resources Division (Cecil, 1989).

In the analysis for a particular radionuclide, laboratory measurements are made on a target sample and a prepared blank. Instrument signals for the sample and the blank vary randomly. Therefore, it is essential to distinguish between two key aspects of the problem of detection. First, the instrument signal for the sample must be larger than the signal observed for the blank before the decision can be made that the radionuclide was detected. Second, an estimation must be made of the minimum radionuclide concentration that will yield a sufficiently large observed signal before the correct decision can be made for detection or non-detection of the radionuclide. The first aspect of the problem is a qualitative decision based on an observed signal and a definite criterion for detection. The second aspect of the problem is an estimation of the detection capabilities of a given measurement process.

In the laboratory, instrument signals must exceed a critical level of $1.6s$ before the qualitative decision can be made as to whether the radionuclide was detected. At $1.6s$, there is about a ninety-five percent probability that the correct conclusion, not detected, will be made. Given a large number of samples, as many as 5 percent of the samples with measured

13

concentrations larger than or equal to 1.6s, which were concluded as being detected, might not contain the radionuclide. These measurements are referred to as false positives and are errors of the first kind in hypothesis testing.

Once the critical level of 1.6s has been defined, the minimum detectable concentration may be determined. Concentrations that equal 3s represent a measurement at the minimum detectable concentration. For true concentrations of 3s or larger, there is a 95 percent or larger probability that the radionuclide was detected in a sample. In a large number of samples, the conclusion, not detected, will be made in 5 percent of the samples that contain true concentrations at the minimum detectable concentrations of 3s. These measurements are referred to as false negatives and are errors of the second kind in hypothesis testing.

True radionuclide concentrations between 1.6s and 3s have larger errors of the second kind. That is, there is a larger-than-five-percent probability of false negative results for samples with true concentrations between 1.6s and 3s. Although the radionuclide might have been detected, such detection may not be considered reliable; at 1.6s, the probability of a false negative is about 50 percent. If sample results between 1.6s and 3.0s are reported as non-detects, approximately 50 percent of these results will have true radionuclide concentrations. These reported non-detects, results between 1.6s and 3.0s, are false negatives.

The critical level and minimum detectable concentration are based on counting statistics alone and do not include systematic or random errors inherent in laboratory procedures. The values 1.6s and 3s vary slightly with background or blank counts, with the number of gross counts for individual analyses, and for different radionuclides. In this dissertation, radionuclide concentrations less than 3s are considered to be below a "reporting level." The critical level, minimum detectable concentration, and reporting level aid the reader in the interpretation of analytical results and do not represent absolute concentrations of radioactivity that may or may not have been detected in an environmental sample. With the exception of one snow sample

(Copper Basin, fig. 1.1), all analytical results reported here for radionuclides exceeded three sample standard deviations.

1.4   Previous Investigations

This dissertation is a compilation of work conducted as an employee of the USGS, Water Resources Division, at the INEEL from 1988 until the present. In particular, this work is a summary of a series of USGS publications on which I was senior author (Cecil, 1989, Cecil and others, 1992, 1998, 1999, and 2000). Additionally, the portion of this research dealing with weapons-test fluxes of ^{36}Cl archived in glacial ice has been published in, Cecil, L.D., and Vogt, S., 1997, "Identification of bomb-produced ^{36}Cl in mid-latitude glacial ice of North America" (Nuclear Instruments and Methods in Physics Research, B 123, p. 287-289).

Many investigators have described the geology and hydrology of the eastern Snake River Plain at the INEEL in a continuing series of reports published by the USGS. Robertson and others (1974) described the regional hydrogeology and the influence of wastewater disposal on ground water geochemistry for 1952-70, Barraclough and others (1976) described hydrologic conditions during 1971-73, Barraclough and others (1982) for 1974-78, Lewis and Jensen (1985) for 1979-81, Pittman and others (1988) for 1982-85, Orr and others (1991) for 1986-88, and Bartholomay and others (1995) for 1989-91. Cecil and others (1991) also described the hydrogeology and influence of wastewater disposal in perched ground water zones for 1986-88.

Several studies have also been made to mathematically model waste plumes in the fractured basalt. Robertson (1974) was the first to describe the construction of a computer model to represent the transport of radioactive and chemical wastes in the eastern Snake River Plain aquifer at the INEEL. Robertson calibrated a two-dimensional (2-D) flow and transport model using data from the USGS for 1952-72 and predicted solute spreading in the Snake River Plain aquifer at the INEEL to the year 2000. The calibrated longitudinal (α_L) and transverse (α_T) dispersivities were about 90 and 140 m respectively. This characteristic, $\alpha_T > \alpha_L$, is not expected

theoretically and is still unique among field-scale investigations. Gelhar and others (1992) critically reviewed investigations of 59 different field sites on field-scale dispersion in aquifers and found that for 24 values of horizontal transverse dispersivities reported, all but those by Robertson were one to two orders of magnitude less than longitudinal values. Subsequent reevaluation of Robertson's work and new attempts at modeling flow and transport at the INEEL has not resolved this apparent discrepancy (Duffy and Harrison, 1987, Fryar and Domenico, 1989, and Goode and Konikow, 1990).

Pre-weapons tests ^{36}Cl/Cl ratios have been predicted for the continental United States (Bentley and others, 1986). These researchers used calculations done by Lal and Peters (1967) for meteoric ^{36}Cl fallout with latitude divided by Cl$^-$ deposition from Eriksson (1960). Similar ratios as those predicted by Bentley and others for the latitude of the INEEL (300 to 600 × 10^{-15}, fig. 1.5) have been reported by Cecil and others (1992) for pre-weapons tests soil water extracted from the shallow alluvium at the Radioactive Waste Management Complex (RWMC). It was determined that soil water representative of pre-weapons tests ^{36}Cl/Cl ratios from depths ranging from 2.4 to 5.6 m below land surface had values near 300 × 10^{-15}; 290±14 × 10^{-15}, 260±12 × 10^{-15} and 280±15 × 10^{-15}. Chlorine-36 concentrations and estimated fluxes have also been reported for the eastern United States (Hainsworth and others, 1994) and for the central United States (Knies and others, 1994). The values reported in these studies for pre- and post-weapons tests fluxes were nearly the same as the values reported here. Cecil and Vogt (1997) reported the first identification of bomb-produced ^{36}Cl in glacial ice of North America.

Recently, Moysey (1999) and Sterling (2000) reevaluated the meteoric fallout of ^{36}Cl across the continental United States using total chloride data in precipitation from the National Atmospheric Deposition Program. The results of their work for southeastern Idaho and western Wyoming are similar to the results of the research presented here and will be discussed in section 5.1 "Meteoric Production". Appendix D-1 is a comprehensive list of global research from the

literature concerning ^{36}Cl studies in various geologic and hydrologic environments.

Bentley and others (1982) initially demonstrated the feasibility of using the bomb-^{36}Cl pulse in ground water near Borden, Ontario, to identify recharge. Since then, numerous studies have been conducted to identify ground water that has been recharged since 1954 (Bentley and others, 1986a; Phillips and others, 1986; Andrews and others, 1994; Purdy and others, 1996; Herczeg and others, 1997). In contrast to such application of ^{36}Cl to identify recharge, little use has been made of the bomb-^{36}Cl peak, or other anthropogenic ^{36}Cl sources, as tracers to determine ground water hydraulic properties.

Although an evaluation of sampling and preservation methods for strontium-90 has been performed at the INEEL (Cecil and others, 1989), no previous investigations on variations in stable Cl isotopic ratios have been reported for the eastern Snake River Plain aquifer.
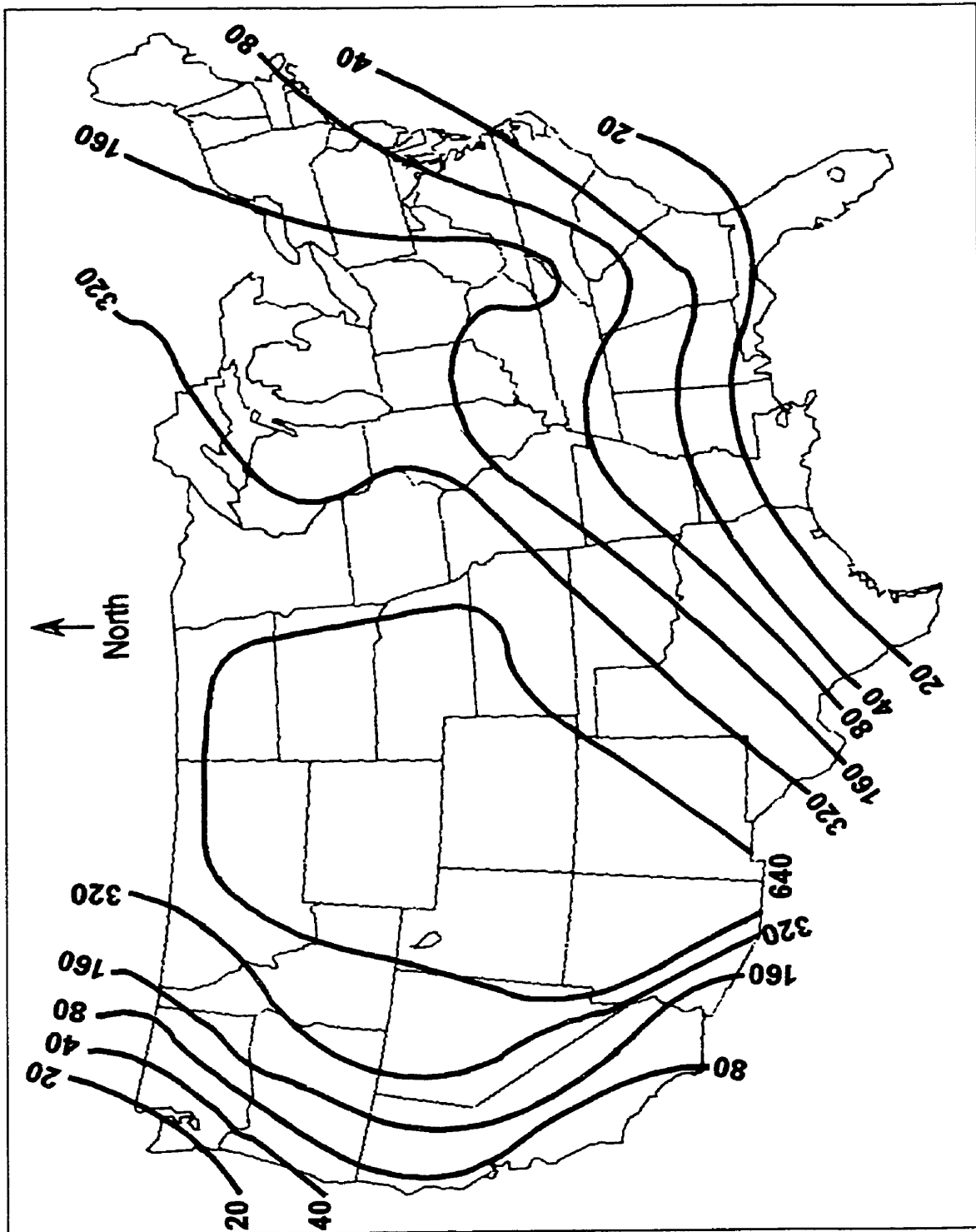
Figure 1.5. Calculated chlorine-36/chlorine ($\times$ 10^{-15}) ratios in precipitation and dry dallout over the United States.

Note: This figure was modified from Bentley and others, 1986.

18

CHAPTER 2

CHLORINE ISOTOPES

Fifteen isotopes of Cl are known to exist; two are stable and thirteen are radioactive. Of the stable isotopes, ^{35}Cl is the most common in nature with 75.77 percent abundance and an atomic weight of 34.9689 g (CRC Handbook, 1991). The remaining stable isotope, ^{37}Cl, has an abundance in nature of 24.23 percent and an atomic weight of 36.9659 g. Of the thirteen radioactive isotopes, only ^{36}Cl has a half-life greater than one hour; the half-life for ^{36}Cl is 301,000 years (Walker and others, 1989). Several oxidation states for Cl isotopes are found in nature but with the exception of a few rare instances, the -I oxidation state as the Cl⁻ ion is dominant. Oxidation states of +VII for perchlorates (ClO_4^-) and +I for hypochlorites (HOCl) have been reported (Erickson, 1981; Sienko and Plane, 1966). Once the Cl⁻ ion is dissolved in the ground water, sinks for removing this ion from solution do not exist due to the highly hydrophilic nature of this element (Eggenkamp, 1994).

Absolute isotopic ratio measurements of elements are difficult to perform because variations in isotopic composition are small. Therefore, the isotopic ratio of ^{37}Cl/^{35}Cl is measured relative to the same ratio in a standard sample and expressed in the delta chlorine-37 (δ^{37}Cl) permil notation defined as:

$$\delta^{37}Cl = \left(\frac{R_{sample} - R_{standard}}{R_{standard}} \right) \times 1000 \qquad \text{2.1-1}$$

where: R_{sample} = ratio of ^{37}Cl/^{35}Cl in the sample, and

$R_{standard}$ = ratio of ^{37}Cl/^{35}Cl in the standard.

Variations in δ^{37}Cl in ground waters may be a result of diffusion, ion-filtration, mixing, dissolution of evaporites along a flow path, and/or temperature and pressure effects in geothermal

systems. Diffusion has been suggested to be a process that may cause significant variations in Cl⁻ isotopic ratios (Desaulniers and others, 1986). Additionally, Eggenkamp (1994) showed significant $\delta^{37}Cl$ variations in geothermal water and possible significant variations through diffusion modeling. None of these processes are expected to be an effective means of fractionation of Cl⁻ isotopes in water from the eastern Snake River Plain aquifer system because: (1) diffusion is unlikely with ground water flow velocities ranging from 1 to 6 m/day (Desaulniers and others, 1986); (2) there are no significant ion-filtration processes operable along the flowpath such as large-scale ground water flow through clay beds; (3) regional ground water mixing is minimal; (4) there are no significant deposits of evaporites along the flowpath from recharge to discharge; and (5) geothermal effects are minimal. Additionally, the archived samples have been in temperature- and light- controlled storage since the date of sample collection. Measurements of $\delta^{37}Cl$ were made on selected samples to document possible variations through time and to ensure that ^{36}Cl concentrations measured in the 1990s, for water samples collected in the 1960s-90s, were representative of the concentration at the time of sample collection.

The internationally accepted standard for $\delta^{37}Cl$ is Standard Mean Ocean Chloride (SMOC) as defined by Kaufmann and others (1984); the ratio of $^{37}Cl/^{35}Cl$ was shown to be constant in fifteen ocean water samples worldwide. The standard for the research reported here was collected near Fairfax, Nova Scotia, and was compared with measurements performed on the same standard at the University of Arizona. The measured $\delta^{37}Cl$ SMOC for the sample collected near Fairfax, Nova Scotia, was 0.00 ± 0.18 indicating that this standard is the same as SMOC measured at the University of Arizona.

Chlorine-36, a beta-particle emitter, is cosmogenically produced in the atmosphere by two major processes; (1) spallation (cosmic-ray interaction with ^{40}Ar), and (2) neutron activation of ^{36}Ar according to the following reactions (Andrews and Fontes, 1992):

^{40}Ar (p, n α) ^{36}Cl   (67 percent of total natural atmospheric production), and

^{36}Ar (n, p) ^{36}Cl   (33 percent of total natural atmospheric production)
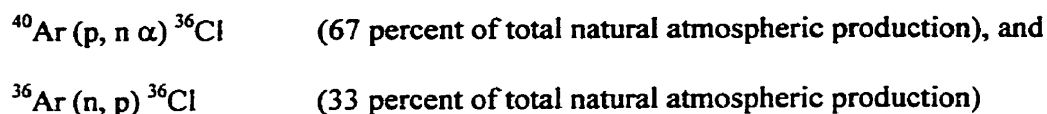
Another significant source of ^{36}Cl in the environment is the neutron activation of stable ^{35}Cl:

$$^{35}\text{Cl (n, } \gamma) \, ^{36}\text{Cl.}$$
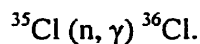
This reaction is the source of ^{36}Cl produced during atmospheric weapons tests conducted by the United States and Great Britain over the Pacific Ocean during 1952-58 (Schaeffer and others, 1960). This reaction may also produce significant ^{36}Cl *in situ* in certain subsurface environments that have a neutron source in reasonably close proximity to stable ^{35}Cl. In basalt, rhyolite, sandstone, and carbonate rocks, the following reactions on potassium-39 (^{39}K) and to a lesser extent, on calcium-40 (^{40}Ca), can contribute to *in situ* production:
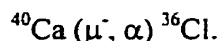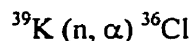
$$^{39}\text{K (n, } \alpha) \, ^{36}\text{Cl}$$

$$^{40}\text{Ca } (\mu^-, \alpha) \, ^{36}\text{Cl.}$$

Chlorine-36 can be produced at detectable concentrations in both the deep and shallow subsurface. However, the ^{35}Cl (n, γ) ^{36}Cl reaction is the only one that produces significant ^{36}Cl in the subsurface at a depth greater than 10 m (Andrews and others, 1989; Davis and others, 1998; and Fabryka-Martin, 1988). Later in this dissertation, the factors that determine *in situ* production of ^{36}Cl in the deep subsurface at the INEEL will be discussed in detail.

Bentley and others (1986) predicted pre-weapons test ^{36}Cl/Cl ratios for the continental United States (fig. 1.5). These predictions are based on long-term deposition of both wet precipitation and dry fallout and represent integrated ratios expected for ground water that has not been exposed to anthropogenic or significant *in situ* produced ^{36}Cl. This model assumes that ET processes increase the absolute concentration of Cl⁻ isotopes in ground water but do not affect meteorically derived ratios. In many ground water environments, the Cl⁻ concentration increases along a flow path (Davis and others, 1998) and the meteoric input of ^{36}Cl may be diluted by the

21
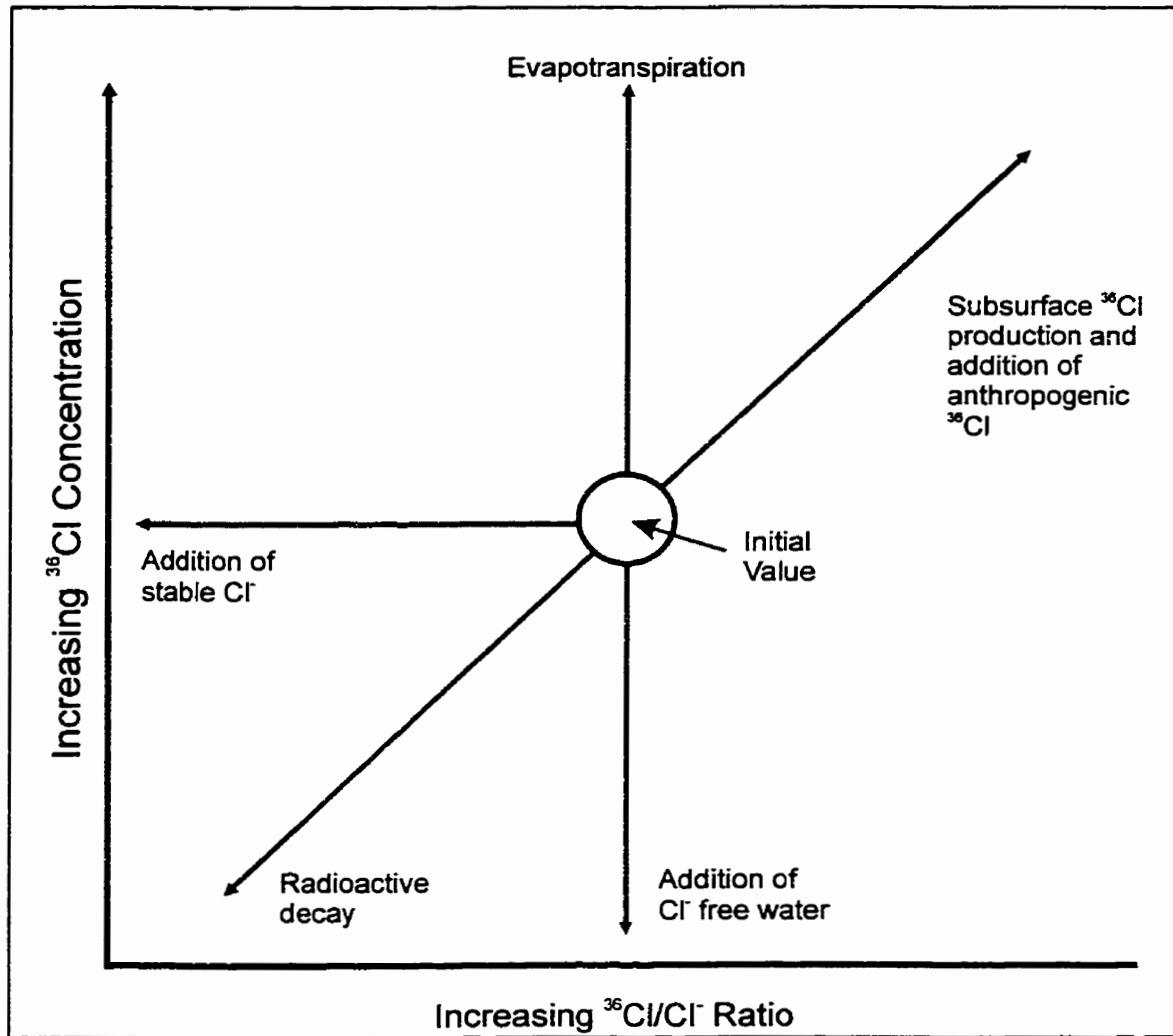
Figure 2.1. **Mechanisms that can change ^{36}Cl concentrations and (or) ^{36}Cl/Cl ratios.**
Note: **This figure was modified from Davis and others, 1998.**

addition of Cl$^-$ containing no measurable radioactive Cl$^-$ from the aquifer matrix or from the un-saturated zone that recharge must travel through (fig. 2.1). This type of total Cl$^-$ would have a ^{36}Cl/Cl ratio that is in equilibrium with the *in situ* activated stable ^{35}Cl and would not fit the integrated box model postulated by Bentley and others.

Bentley and others (1986) predicted that spallation of ^{40}Ar produces a global ^{36}Cl fallout of 11 atoms/m^2/sec and neutron activation of ^{36}Ar produces 5 atoms/m^2/sec. However, Hossain (1988) published new data on the capture cross section of the ^{36}Ar (n, p) ^{36}Cl reaction that

22

indicate that the probability of this reaction is reduced to less than 1.5 millibarns as opposed to 1.83 barns as was used for the calculations of Bentley and others. This complicating factor was pointed out by Andrews and Fontes, 1992, p. 247. They suggested that the global fallout values used in this box model should be reduced by 11/16 because neutron activation of ^{36}Ar appears to be an insignificant meteoric source. This apparent reduction of the significance of neutron activation of ^{36}Ar is important to establishing pre-bomb ^{36}Cl/Cl ratios because the values in the model are modified by prevailing winds and orographic effects (as one moves away from coastal to continental areas) and latitudinal variations. It is the latitudinal variations that are most affected by the differences in the probability of the neutron activation of ^{36}Ar. Another even more complicating factor in attempting to determine the meteoric input function is the fact that calculations of the ^{36}Cl content of an ice core from Greenland, collected at the Dye 3 site, show that the fallout rate from ^{40}Ar spallation is larger than the value originally calculated by Lal and Peters (1967). The significance of these difficulties in determining the atmospheric flux of ^{36}Cl from natural production will be discussed with the results of the ice-core analyses later in this dissertation.

Chlorine-36 can be produced at detectable concentrations in both the deep and shallow subsurface. In the deep subsurface, neutron activation of ^{35}Cl and ^{39}K are the dominant sources for the production of ^{36}Cl. The neutrons required for these reactions are produced by the interaction between α-particles, generated from the radioactive decay of U and Th series isotopes, and stable nuclei of lighter elements such as oxygen (O), sodium (Na), aluminum (Al), and silicon (Si) (Faure, 1986). An estimate can be made of *in situ* produced ^{36}Cl for a given ground water system if the following contributing factors are known: 1) the U and Th content of the aquifer matrix; 2) the total Cl⁻ content of both the aquifer matrix and the water in the aquifer; 3) the irradiation time of the target nuclei; and 4) proximity of targets to neutrons. Andrews and others (1989) made such calculations for ^{36}Cl production in the Stripa granite. The Stripa results will be discussed in detail in Chapter 5, section 5.3.5. Using the Stripa study as a model, Beasley

and others (1993) calculated a theoretical *in situ* produced $^{36}Cl/Cl$ ratio of 1×10^{-18} for ground water moving through the basalt aquifer of the eastern Snake River Plain in southern Idaho. Because this ratio is not measurable even with AMS, *in situ* production within the ground water was determined to be inconsequential.

Thermonuclear explosions conducted during atmospheric tests over the Earth's oceans produced levels of ^{36}Cl that exceeded natural atmospheric production by up to three orders of magnitude at Long Island, New York (Bentley and others, 1982). This pulse is analogous to bomb-produced ^{3}H and can be used to trace and date ground water or determine net water-infiltration rates through the unsaturated zone in semi-arid areas. Peak bomb production of ^{36}Cl was in 1958 and Bentley and others (1986) modeled the fallout using data from a series of nuclear tests conducted during 1952-58.

As early as 1957, Begemann and Libby (1957) recognized the importance of ^{3}H input to the hydrologic environment as a result of weapons tests. However, this bomb pulse of ^{3}H is only a temporary tool to hydrogeologists due to the relatively short half-life of 12.26 years. The use of bomb-produced ^{3}H to identify water introduced into the hydrologic cycle during 1955-70 has become common practice and a review of studies of this type would be a major undertaking and is beyond the scope of this dissertation.

Chlorine-36, on the other hand, is a conservative tracing tool available with similar attributes as ^{3}H but with a much longer half-life. Advantages of using ^{36}Cl over ^{3}H in these kinds of studies include: 1) ^{36}Cl was produced by a limited number of tests between 1952-58 over oceans; 2) ^{36}Cl was washed out of the atmosphere relatively rapidly as opposed to bomb-produced ^{3}H; and 3) the weapons tests that produced ^{36}Cl were concentrated around the equator and global fallout was symmetrical in both hemispheres, whereas ^{3}H fallout was predominately in the northern hemisphere due to the location of the tests that produced it (Bentley and others, 1986).

An additional source of ^{36}Cl to the environment is the disposal of wastes from nuclear

facilities. At the INEEL, ground water concentrations up to 10^{12} atoms/L have been measured in samples near the INTEC (table 2.1). These concentrations are six orders of magnitude larger than calculated natural meteoric concentrations that will be presented in Chapter 5.

Table 2.1.   Total chloride concentrations, corrected chlorine-36/chloride ratios, and chlorine-36 concentrations with uncertainties in atoms/liter (atoms/L) for ground water collected at the Idaho National Engineering and Environmental Laboratory.

[See text for explanation of uncertainties. Symbols: T, indicates thief samples; P, indicates pumped samples. See figure 3.1 for well locations.]

Well Number & Date of collection	Total Chloride (mg/L)	Corrected ^{36}Cl/Cl Ratio ($\times 10^{-15}$)	^{36}Cl Concentration atoms/L ($\times 10^{8}$)
USGS 11 (7-21-66) T	9.2±0.5	1,040±50	1.6±0.1
USGS 11 (4-20-72) T	12±1	864±30	1.8±0.1
USGS 11 (9-20-77) T	12±1	1,320±270	2.7±0.1
USGS 11 (4-15-82) T	11±1	2,860±250	5.3±0.5
USGS 11 (4-14-83) T	12±1	8,040±380	16±1
USGS 11 (4-17-85) T	11±1	5,980±260	11±1
USGS 11 (3-13-87) T	12±1	2,920±330	6±1
USGS 11 (4-5-88) T	12±1	1,390±280	4.7±0.6
USGS 11 (10-26-95) P	11±1	2,890±800	5.4±0.2
USGS 14 (4-20-72) T	22±1	477±20	1.8±0.1
USGS 14 (9-20-77) T	29±1	739±18	3.6±0.1
USGS 14 (4-15-82) T	25±2	741±58	3.1±0.3
USGS 14 (4-14-83) T	30±1	716±60	3.6±0.3
USGS 14 (4-16-84) T	27±1	2,130±70	9.8±0.3
USGS 14 (4-17-85) T	27±1	1,910±150	8.8±0.7
USGS 14 (4-22-86) T	26±1	1,980±90	8.7±0.4
USGS 14 (4-8-87) T	21±2	5,250±50	19±0.2
USGS 14 (4-5-88) T	25±1	1,997±38	8.5±0.2
USGS 14 (10-01-93) P	18±1	1,740±90	5.3±0.3
USGS 14 (4-14-94) P	20±1	2,070±40	7±0.1
USGS 14 (10-26-95) P	20±1	1,690±50	6.3±0.2
USGS 19 (10-20-69) T	29±1	580±60	2.9±0.3
USGS 19 (4-24-70) T	21±1	971±36	3.5±0.1
USGS 19 (4-19-74) T	19±1	777±20	2.5±0.1
USGS 19 (4-1-76) T	15±1	2,000±70	5.1±0.2
USGS 19 (9-6-77) T	15±1	1,660±50	4.2±0.1
USGS 19 (4-17-80) T	15±1	854±33	2.2±0.1
USGS 19 (4-8-83) T	15±1	1,410±90	2.4±0.2
USGS 19 (4-30-85) T	14±1	1,040±100	2.5±0.2
USGS 19 (4-1-88) T	10±1	2,580±670	4.4±1.1
USGS 19 (10-1-93) P	11±1	570±30	1.1±0.1
USGS 20 (7-20-67) T	37±2	760,000±12,200	4,800±76
USGS 20 (5-25-68) T	27±1	623,000±25,300	2,900±120
USGS 20 (4-25-69) T	31±3	503,000±20,000	2,600±100
USGS 20 (10-17-70) T	27±1	745,000±28,000	3,400±130
USGS 20 (4-21-71) T	28±1	768,000±15,000	3,700±72
USGS 20 (4-18-72) T	27±1	847,000±20,600	3,900±94
USGS 20 (4-15-74) T	22±1	635,000±10,300	2,400±38
USGS 20 (9-6-77) T	20±1	562,000±16,200	1,900±55
USGS 20 (4-12-83) T	22±2	643,000±30,000	2,600±120
USGS 20 (4-4-88) T	28±3	815,000±20,000	3,300±82

Table 2.1.   Total chloride concentrations, corrected chlorine-36/chloride ratios, and chlorine-36 concentrations with uncertainties in atoms/liter (atoms/L) for ground water collected at the Idaho National Engineering and Environmental Laboratory—continued.

[See text for explanation of uncertainties. Symbols: T, indicates thief samples; P, indicates pumped samples. See figure 3.1 for well locations.]

Well Number & Date of collection	Total Chloride (mg/L)	Corrected ^{36}Cl/Cl Ratio ($\times 10^{-15}$)	^{36}Cl Concentration atoms/L ($\times 10^{8}$)
USGS 20 (10-19-93) P	23±1	903,000±26,300	3,500±100
USGS 20 (4-4-94) P	23±1	792,000±36,400	3,100±140
USGS 44 (4-30-67) T	8.3±0.5	76,300±3,720	110±5
USGS 44 (5-25-68) T	8.1±0.5	26,000±1,300	36±1
USGS 44 (5-8-69) T	12±1	21,500±4,000	44±8
USGS 44 (4-12-83) T	53±5	553,000±20,000	5,500±200 *
USGS 44 (4-9-88) T	17±2	54,100±2,000	140±5
USGS 44 (11-1-93) P	20±2	57,600±4,680	200±14
USGS 57 (5-8-69) T	47±5	2,100,000±58,000	18,000±490
USGS 57 (10-9-71) T	86±3	787,000±21,700	12,000±320
USGS 57 (9-5-77) T	92±3	1,360,000±60,000	20,000±940
USGS 57 (4-12-83) T	112±11	1,000,000±46,000	22,000±860
USGS 57 (3-31-88) P	69±7	1,930,000±64,000	28,000±910
USGS 57 (10-12-93) P	180±7	560,000±12,000	17,000±360
USGS 77 (5-10-68) T	65±3	1,450,000±20,000	16,000±220
USGS 77 (4-25-69) T	73±3	1,530,000±74,000	19,000±910
USGS 77 (4-21-71) T	71±3	1,410,000±46,000	17,000±560
USGS 77 (9-6-77) T	79±3	1,270,000±34,500	17,000±460
USGS 77 (11-1-93) P	120±5	614,000±8,900	12,500±180
USGS 85 (5-10-68) T	20±1	1,580,000±38,600	5,400±130
USGS 85 (4-25-69) T	21±2	1,480,000±40,000	6,000±160
USGS 85 (4-15-71) T	23±1	1,660,000±56,100	6,500±220
USGS 85 (4-29-72) T	28±1	1,250,000±24,300	5,900±120
USGS 85 (4-17-74) T	32±1	1,710,000±23,000	9,300±130
USGS 85 (9-28-77) T	34±2	1,490,000±39,000	8,600±220
USGS 85 (4-13-83) T	34±3	846,000±20,000	5,300±130
USGS 85 (11-4-93) P	74±3	240,000±27,000	3,000±34
SITE 14 (9-7-77) P	9.2±1	801±2	0.058±0.003
SITE 14 (10-15-93) P	8.2±1	1,600±9	0.44±0.01

*Note: The steel casing on the INTEC disposal well began to leak excessively in 1981 (Fromm, 1995). This elevated ^{36}Cl concentration in water from well USGS 44 may be a result of additional contaminant reaching this well due to the casing leaks. USGS 44 is approximately 500 meters downgradient from the INTEC disposal well (fig. 1.2)

CHAPTER 3

METHODS AND QUALITY ASSURANCE; WATER, SNOW, AND ICE SAMPLES

Discussions of the methods used to collect, process, analyze, and quality assure the water, snow, and ice samples follow. Some of the methods are standard but many are not and therefore, it is necessary to document the methods in some detail. The methods utilized to collect, process, and analyze the whole-rock samples are different from the methods described in this chapter and will be discussed later in sections 5.3.1, 5.3.2, and 5.3.3.

3.1   Sample Collection and Handling Methods

For the archived sample evaluation (Chapter 4), water samples were selected from the USGS sample archive library for sites within the eastern Snake River Plain aquifer system near and downgradient from the INTEC (fig. 3.1 and table 3.1), and were analyzed for $\delta^{37}Cl$ and ^{36}Cl. Additionally, water samples were collected from selected existing surface and ground water sampling locations for determination of ^{36}Cl concentrations. At the time of collection, two methods were used to obtain water from the wells. If a well was equipped with a dedicated submersible or turbine pump, it was pumped and the samples were collected at the end of the discharge pipe or at a spigot in the discharge pipe. A remotely operated thief sampler was used to obtain water samples from ground-water monitoring wells not equipped with dedicated pumps. Since sampling for ground water began in 1960, the proportion of wells with dedicated pumps has increased significantly. From the 1960s to the mid 1980s, thief samplers were used to collect most water samples. By the late 1980s, most wells were equipped with dedicated pumps.

Wells equipped with dedicated submersible or turbine pumps were pumped until the temperature, pH, and specific conductance of the water stabilized as described by Wood (1981) and Claassen (1982). When these properties of the water stabilized, suggesting that a steady-state water chemistry had been reached, a water sample was collected, provided an ample volume of
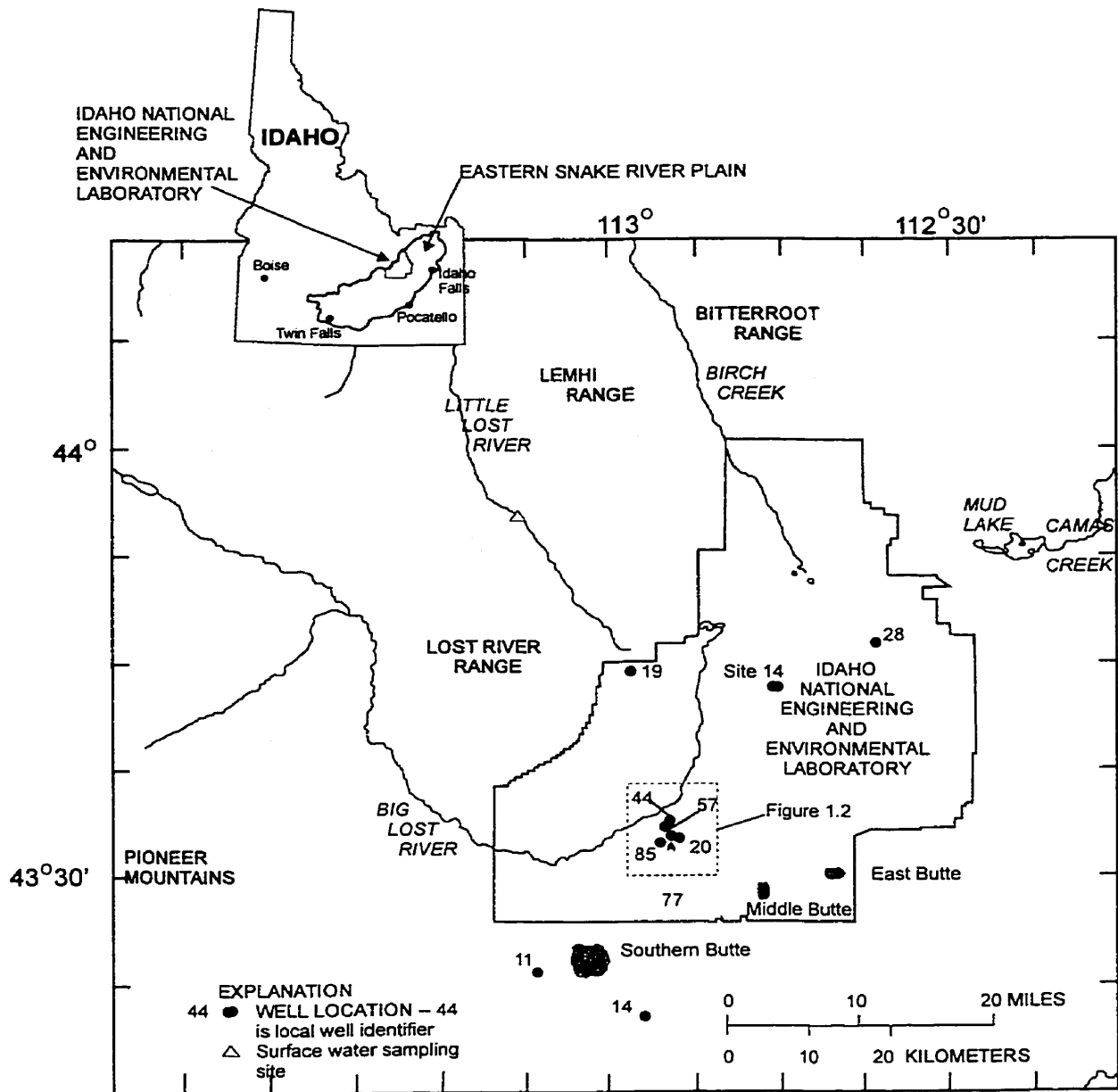
Figure 3.1. Location of the Idaho National Engineering and Environmental Laboratory and selected observation wells.

Notes: Water samples from USGS wells 14, 19, 20, 44, 57, and 85 were used for the archive-sample evaluation (table 3.1). Site 14 and USGS 14 are individual, separate observation wells.

Table 3.1. Archived ground water samples collected from selected wells for chloride isotopic analyses for evaluation of archive-sample suitability.

[See Figure 1.2 for well location. T, indicates thief sample; P, indicates pumped sample]

Well identifier	Total depth and interval of well perforated or open to aquifer (meters)	Type of Sample	Sample depth (meters)	Depth to water (meters)	Date depth to water measured	Date water sample was collected
USGS 14	229/216-225	T	222	215	04/15/1982	04/15/1982
		T	222	214	04/08/1987	04/08/1987
		P	222	215	04/16/1993	04/16/1993
USGS 19	120/86-92	T	87	80	10/28/1969	10/28/1969
		T	89	78	04/28/1983	04/08/1983
		P	97	83	04/07/1993	04/07/1993
USGS 20	203/140-143	T	159	137	04/28/1969	04/28/1969
	155-166	T	159	138	04/29/1983	04/12/1983
		P	150	137	04/04/1988	04/04/1988
		P	156	139	04/14/1993	04/14/1993
USGS44	195/138-195	T	150	136	08/05/1969	05/08/1969
		T	150	137	08/01/1983	04/12/1983
		T	150	137	04/09/1988	04/09/1988
		P	150	139	05/04/1993	05/04/1993
USGS 57	220/143-220	T	152	138	08/05/1969	05/08/1969
		T	165	140	08/01/1983	04/12/1983
		P	152	138	03/31/1988	03/31/1988
		P	152	140	04/15/1993	04/15/1993
USGS 85	191/157-191	T	171	144	04/25/1969	04/25/1969
		T	171	144	04/28/1983	04/13/1983
		P	157	146	04/19/1993.	04/19/1993

water had been pumped from the well. At most wells, a volume of water equivalent to a minimum of three wellbore volumes was pumped from each well; at many wells, 5 to 10 wellbore volumes were pumped prior to the collection of a sample.

For wells without dedicated pumps, a thief sampler was lowered inside the well casing to a predetermined level. The thief sampler is constructed in such a manner that water passes through the sampler while it is being lowered to the sampling level. Once at the sampling level, the ends of the sampler are closed, trapping about one liter of water.

On the basis of drillers' geophysical and fluid-conductivity logs, fracture zones have been identified in the basaltic rocks opposite perforations in the casing or in uncased intervals (table 3.1). For example, figure 3.2 from Morris and others (1964) illustrates the relation between ground water circulation, specific conductance, and well construction for well USGS 28. Water likely moves through the fracture zones, between about 77-83 meters below land surface for USGS 28 (figure 3.2), at a high velocity when compared with the velocity in unfractured zones. Each thief sample for all wells was taken at predetermined levels to obtain samples that represented water moving through the aquifer rather than water that may have stagnated in the wellbore and casing opposite unfractured zones. The thief sampler was cleaned and rinsed with a pressurized spray of deionized water prior to and after use at each well.

For surface water samples, pre-cleaned polypropylene bottles were submersed into the water-body and filled. All pre-cleaned bottles were rinsed with sample water an additional three times before filling. During the collection process, powderless plastic gloves were worn to minimize sample contamination.

The ice samples used in this research were processed for analyses at the National Ice Core Laboratory (NICL) in Denver, Colorado. Thanks are due Dr. Dave Naftz of the USGS for providing access to the glacial-ice samples used in this study. Thanks are due also to Dr. Joan Fitzpatrick and Geoffrey Hargreaves of the USGS for their help in processing portions of the ice core at the NICL.

The ice cores were cut from sections archived at the NICL using a band saw operated in a walk-in freezer where the air temperature is maintained at less than -10°C. Sections of the ice core selected for ^{36}Cl analysis were scraped with a stainless steel microtome and then rinsed with ultrapure (18 mega ohm (Mohm)) deionized water. The ice cores were then slowly melted in a microwave oven. A laboratory blank of the deionized water and a process blank (PRIME B-1, table 3.2) were prepared by the staff at PRIME Laboratory and analyzed with the melted ice cores. There was no ^{36}Cl in either of these blanks (table 3.1). The $^{36}Cl/Cl$ ratios measured in the

Specific conductance
(mhos/cm)

300   350

Construction
diagram
(USGS 28)

Point of
injection

Direction
of flow

Velocity
of flow
(meters/min)

Depth
(meters)

Water table -- 71 meters
from land surface

73 — 16 cm casing

76   Stagnant

Perforations

79

4.2
5.3
5.6
6.7

82

5.9
2.6

85   Stagnant

Welded joint

88

91   Stagnant

14 cm casing

94

97

Total depth 99 meters
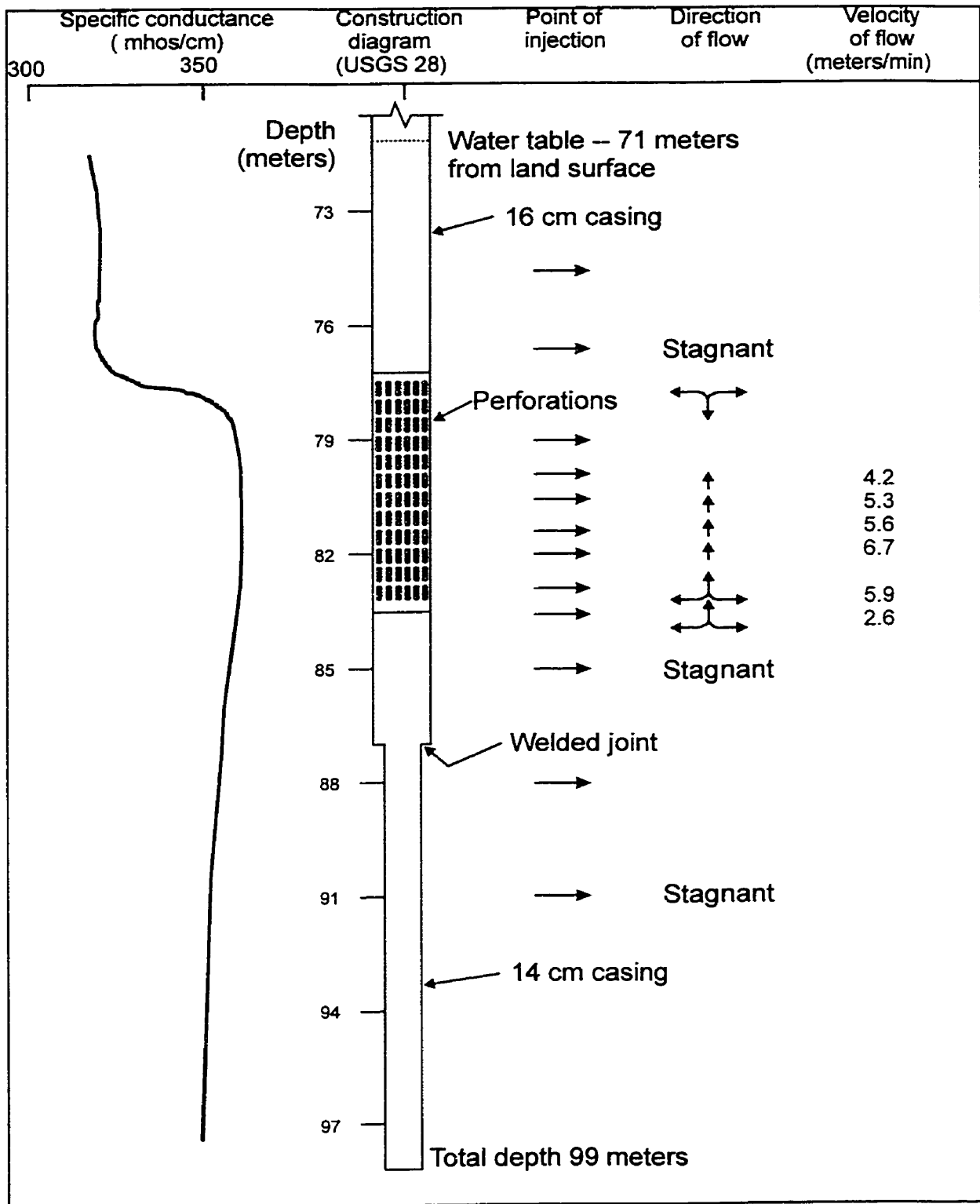
Figure 3.2.   Relation of ground water movement, specific conductance, and well constructions for well USGS 28.

Note: This figure was modified from Morris and others, 1964.

32

Table 3.2.   Dissolved-chloride concentration, amount of chlorine-36 free chloride carrier added, and measured chlorine-36/chlorine ratios in selected quality-assurance samples.

Site or sample identifier	Date of sample	Chloride concentration (mg/L)	^{36}Cl-free chloride carrier (mg)	Measured ^{36}Cl/Cl ($\times 10^{-15}$)
Deionized Water	1995	<0.01	1.71	16±16
PRIME B-1	1995	<0.01	1.01	1±1
PRIME B-2	1993	<0.01	3.83	12±2
PB-1	1991	<0.01	24	0±10
PB-2	1991	· <0.01	24	0±10
PB-3	1991	<0.01	24	15±10
PB-4	1991	<0.01	24	24±16

melted ice-core samples were corrected for the small ^{36}Cl concentration found in process blank B-2 (table 3.2). Chlorine was separated from the melted ice by precipitation as silver chloride (AgCl) and analyses for ^{36}Cl were performed as described by below. The rock-sample collection methods are described in section 5.3.1. During the field and laboratory work performed for this dissertation, conditions for each sample were documented and a chain-of-custody record was maintained from the time of collection and processing until the sample was delivered to the analytical laboratory. The field books, laboratory books, and chain-of-custody records are not included in the appendices in this dissertation but are available for inspection at the USGS's INEEL Global Research Ice-Core Project Office.

3.2   Analytical Methods

The following sections describe the analytical methods used for the determination of dissolved Cl, ^{36}Cl/Cl ratios, and ^{37}Cl/^{35}Cl ratios.

3.2.1   Dissolved Chloride

Dissolved Cl analyses presented in this dissertation were performed by three laboratories: DOE's Radiological and Environmental Sciences Laboratory (RESL); the University of Waterloo's Environmental Isotope Laboratory (EIL); and the USGS's National Water Quality Laboratory (NWQL). Methods of chloride determination included; 1) silver nitrate titration

(ASTM, 1982); 2) ion-selective electrode (ASTM, 1982); and 3) ion chromatography (Fishman and Friedman, 1989).

RESL performed all analyses listed in table 3.3 for dissolved Cl⁻ at date of sample collection. For those samples collected prior to May 1975, the method used was a silver-nitrate titration. In this method, a water sample was adjusted to a pH of 8.3 and then titrated in the presence of potassium chromate indicator solution. The end point in the titration was indicated by a red-brick silver chromate solution. For those analyses performed for Cl⁻ after May 1975, RESL staff used the ion-selective electrode method. In this method, the Cl⁻ ion concentration is determined potentiometrically with a Cl⁻ ion-selective electrode in tandem with a double-junction, sleeve-type reference electrode. Potentials were then read with either a selective-ion meter with a concentration scale for Cl⁻, or a pH meter with an expanded millivolt scale. The electrodes were calibrated to traceable standards.

The Cl⁻ analyses in table 3.3 by EIL and the NWQL were determined by the ion chromatography method.   Both laboratories employed a standard two-column ion chromatography technique. Water samples were placed in a liquid mobile phase (eluant) and pumped at a constant flow rate through two ion-exchange columns in tandem. Chloride ions were separated from solution in the first column on the basis of their affinity for exchange sites on an anion-specific resin. The second column decreased the background conductivity of the eluant to a minimal level to suppress interference. Separated Cl⁻ ions then were quantified with a specific-conductance cell and an anion chromatogram was produced. All other Cl⁻ results presented in this dissertation were performed by the NWQL using the ion chromatography method.

3.2.2   Accelerator Mass Spectrometry

Until 1979, ^{36}Cl in environmental samples was measured by counting beta-particle emissions during radioactive decay. These kinds of measurements were difficult due to the relatively long half-life of 301,000 years and the resultant small specific radioactivity of ^{36}Cl. Muller (1977) postulated that by using particle accelerators as mass spectrometers, radionuclides

34

Table 3.3.   Stable chlorine isotope results, dissolved chloride, and chlorine-36 concentrations for archived ground water samples collected from selected wells and the Little Lost River.

[These samples were selected to evaluate the archive-sample integrity. δ^{37}Cl, indicates delta chlorine-37, see text for explanation of uncertainties; Cl⁻, indicates dissolved chloride; ^{36}Cl, indicates chlorine-36; NA, indicates not applicable: R, analyses performed by Radiological and Environmental Sciences Laboratory; W, analyses performed by University of Waterloo Environmental Isotope Laboratory; N, analyses performed by USGS's National Water Quality Laboratory; P, analyses performed by Purdue University's PRIME Laboratory; NR, indicates blind replicate analyzed by the USGS's National Water Quality Laboratory; CRL, indicates blind replicate analyzed by Chalk River Laboratory.   Symbol: --, indicates no data available; *, indicates uncertainties estimated using equation 3.3-1 in text.]

Site identifier	Date Sample collected	δ^{37}Cl ±0.2 permil unless noted	Dissolved Cl⁻ at date sampled (mg/L)	Dissolved Cl⁻ in 1993 (mg/L) ±10 percent unless noted	Corrected (^{36}Cl/Cl) ×10⁻¹³	^{36}Cl (atoms/L) ×10⁸
USGS 14	04/15/1982	+0.47±0.01	25±2*R	21.4 W	7.41±0.58P	3.1±0.3
	04/08/1987	-0.44±0.5	21±2*R	28.4 W	52.5±0.5P	19±0.2
	10/01/1993	+0.20	NA	18±1 *N	17.4±0.9P	5.3±0.3
	10/01/1993	—	—	21±1 *NR	—	—
USGS 19	10/20/1969	+0.12	—	29.0 W	5.8±0.6P	2.9±0.3
	10/20/1969	--	--	—	7.0±0.7CRL	3.5±0.4
	04/08/1983	+0.10	21±1*R	14.9 W	14.1±0.9P	2.4±0.2
	10/01/1993	+0.02	NA	11±0.7 *N	5.7±0.3P	1.1±0.1
	10/01/1993	—	—	11±0.7 *NR	—	--
USGS 20	04/25/1969	+0.26	30±3*R	30.7 W	5,030±200P	2,600±100
	04/12/1983	+0.01	24±2*R	21.6 W	6,430±300P	2,600±130
	04/04/1988	+0.41	24±2*R	28.2 W	8,150±200P	3,300±82
	10/19/1993	+0.34	NA	23±1 *N	9,000±260P	3,500±100
USGS 44	05/08/1969	+0.21	12±1*R	10.6 W	215±40P	44±8
	04/12/1983	+0.19±0.15	59±6*R	52.8 W	5,530±200P	5,500±200
	04/09/1988	+0.11	15±2*R	17.0 W	541±20P	140±5
	11/01/1993	+0.42	NA	20.1 *N	580±42P	200±14
	11/01/1993	--	—	19±1 *NR	--	--
USGS 57	05/08/1969	-0.13±0.1	50±5*R	46.9 W	21,000±580P	18,000±490
	04/12/1983	+0.59±0.16	127±13*R	112 W	10,000±400P	22,000±860
	03/31/1988	-0.12±0.01	67±7*R	69.2 W	19,300±640P	28,000±910
	10/12/1993	+0.09	NA	180±7 *N	5,600±120P	17,000±360
	10/12/1993	--	—	190±8 *NR	--	—
USGS 85	04/25/1969	+0.12	24±2*R	21.3 W	14,800±400P	6,000±160
	04/13/1983	+0.21	37±4*R	33.8 W	8,460±200P	5,300±130
	11/04/1993	-0.05	NA	74±3*N	2,400±270P	3,000±34
	11/04/1993	—	—	73±3*NR	--	—
Little Lost River	04/03/1970	+0.27±0.23	—	13 W	--	—

35

with relatively long half-lives (such as carbon-14 (^{14}C) and beryllium-10 (^{10}Be)) could be measured at environmental concentrations. Researchers at McMaster University in Canada and the University of Rochester in the United States reported AMS measurements of ^{14}C later in 1977. In 1979, the first successful measurements of ^{36}Cl in ground water samples were carried out at the University of Rochester on a tandem Van De Graaff accelerator system, although the first such use of accelerators had been for helium-3 (^{3}He) measurements in 1939 by Alvarez and Cornog (Elmore and others, 1979). Since 1979, thousands of environmental samples have been measured for their ^{36}Cl content at more than twenty accelerator facilities worldwide. In addition to ^{36}Cl, AMS is now routinely used to measure ^{14}C, ^{26}Al, ^{10}Be, and ^{129}I.

With conventional beta decay counting methods, tens of grams of chloride were required and counting times as long as a week were common. With AMS, sample size has been reduced to as little as 1.0 mg/L total Cl⁻ and counting times of thirty minutes with 10 percent precision. Sensitivity has also improved with AMS; beta-counting methods have a sensitivity of about one ^{36}Cl atom in 10^{12} Cl atoms, and AMS methods have a sensitivity of about five atoms of ^{36}Cl in 10^{15} Cl atoms. For a typical ambient ^{36}Cl concentration in the eastern Snake River Plain, this AMS sensitivity corresponds to about one beta-particle emission every two years and this radioactivity is not detectable by scintillation counting (Appendix Table C-3).

AMS operates the same as conventional mass spectrometry by using the fact that all charged atomic and molecular species have unique masses. Just as in mass spectrometry, AMS is made up of four steps; (1) formation of a charged atomic or molecular species; (2) acceleration of this species through an electrostatic potential (ES); (3) separation of ions based on their mass-to-charge ratios; and (4) determination of the number of ions or atoms in a detector system. With AMS, acceleration is through ES of millions of volts of energy in contrast to ES of thousands of volts of energy found in conventional mass spectrometry.

Because particle accelerators are operating at these high energies, molecular ions are removed from the analytical line by gas-filled magnets; only target atoms (or atoms of the same

36

mass as the target, i.e. interfering atoms) remain at the detectors (Elmore and Phillips, 1987). In the case of ^{36}Cl, interferences from isobars are removed by selecting charge states that have no common factor with 36; for example, charge states 5, 7, 11, 13, or 17. Because the most common interference for ^{36}Cl measurements is from sulfur-36 (^{36}S), elimination of sulfate from water samples and selection of the correct charge state for ^{36}Cl analyses are crucial to obtaining meaningful results. Sulfate in ground water at the INEEL is a potential interference problem for ^{36}Cl analyses. In October 1995, sulfate concentrations in 66 ground water samples collected at the INEEL ranged from 11 to 230 mg/L (Bartholomay and others, 1995). These sulfate concentrations are representative of ground water at the INEEL since site operations started in 1953. Therefore, sulfate was removed from the water samples used in this research as outlined later in this section.

Water samples from the sample archive library and new samples collected for this research were analyzed for ^{36}Cl using Tandem Accelerator Mass Spectrometry (TAMS) at PRIME Laboratory, Purdue University. Ground and surface water samples, the glacial-runoff sample, the melted ice-core samples, and the deionized water and PRIME blanks B-1 and B-2 (table 3.2) also were analyzed for ^{36}Cl at PRIME Laboratory. The process blank water samples designated PB-1 through PB-4 in table 3.2 and the four snow samples (table 5.1) were analyzed for ^{36}Cl at the TAMS facility at the University of Rochester's Nuclear Structure Research Laboratory (NSRL) in New York. The PRIME TAMS facility is based on an upgraded 8-million volt tandem accelerator with a high intensity ion source, a 150-thousand volt ion-source injector, and a beam line and detector system. The 150 kV ion source is a cesium gun used to sputter chloride ions from a AgCl target. The accelerator at the NSRL is of the same configuration. The negative ions are focused and passed through a 90°-inflection magnet and accelerated toward a fixed positive potential located inside the tandem accelerator. At the midpoint of the tandem accelerator line, the negative ions pass through carbon foil that strips off valence electrons and breaks apart unwanted molecular species. The positive ions are accelerated away from the

positive terminal toward ground potential and continue through a series of mass/charge analyzers and a gas-ionization detector.

The Cl isotope laboratory within the EIL at the University of Waterloo was used to prepare some of the samples for TAMS analysis and the remaining samples were prepared at either PRIME Laboratory or the NSRL. Sample preparation for ^{36}Cl analysis includes preconcentration of Cl$^-$ in solution, precipitation of AgCl, and purification of the AgCl target. As previously mentioned, because ^{36}S is an interfering isobar, care must be taken to remove as much sulfate from the water sample as possible.

Before using the Cl isotope lab at EIL for TAMS target preparation, a laboratory swipe was taken from the countertops and overhead lamps on January 7, 1993. Approximately 1.2 g of material were dissolved in 20 mL of 18-Mohm deionized water. This solution was analyzed for Cl$^-$ at the EIL and for ^{36}Cl at the NSRL. The results are presented in table 3.4. Subsequent to receiving the results of the first lab swipe, all surfaces in the Cl$^-$ lab were cleaned with an Alconox soap solution, followed by a 2-percent ultrapure nitric acid solution with a final rinse with 18 Mohm deionized water. A second laboratory swipe was taken on April 15, 1993 and approximately 0.2 g of material were dissolved in 20 mL of 18-Mohm deionized water. The swipe taken after cleaning the Cl$^-$ laboratory was analyzed for Cl$^-$ at the EIL and for ^{36}Cl at NSRL and at PRIME Laboratory. The results of the dissolved Cl$^-$ and ^{36}Cl analyses showed a reduction in Cl$^-$ concentration from 282 ± 28 to 10 ± 1 mg/L and a reduction in ^{36}Cl/Cl from $263\pm21 \times 10^{-15}$ to $5\pm10 \times 10^{-15}$ (table 3.4). The Cl$^-$ lab at the EIL was then ready to be used to prepare AgCl targets for ^{36}Cl analyses.

The first step in sample preparation for ^{36}Cl analysis was preconcentration of Cl$^-$ as necessary. Because all the ground water samples in this research contained a minimum of 8.1 ± 0.5 mg/L of Cl$^-$ (table 2.1), it was determined that no preconcentration was necessary to ensure 8 to 10 mg of AgCl for a target in these samples. Alternatively, if the Cl$^-$ concentration in

Table 3.4.   Results of laboratory swipes taken at the University of Waterloo Environmental Isotope Laboratory before and after cleaning of the laboratory.

[EIL, analyses performed by the University of Waterloo Environmental Isotope Laboratory; NSRL, analyses performed by the University of Rochester Nuclear Structures Research Laboratory; PRIME, analyses performed by Purdue University's PRIME Laboratory.]

Sample	Laboratory	Dissolved chloride concentration (mg/L)	$(^{36}Cl/Cl) \times 10^{-15}$
Swipe before cleaning	EIL	282±28	—
	NSRL	—	263±21
Swipe after cleaning	EIL	10±1	—
	NSRL	—	5±10
	PRIME	—	5.8±4.0

a sample was small (less than one part per million, i.e. the melted ice-core samples) then ^{36}Cl-free carrier was added to ensure ample target mass. This method also was employed for samples suspected to have elevated ^{36}Cl concentrations to ensure no contamination of AMS ion sources during analyses. The next steps in preparing targets for TAMS measurements were precipitation and purification of AgCl targets.

Samples were acidified to pH 2 using ultrapure HNO_3. Chloride was then precipitated from the acidified samples as AgCl by the addition of 15 mL of 0.1 molar (M) ultrapure $AgNO_3$. The precipitate was filtered using a Millipore 250-mL filtering system with 0.45-mm cellulose nitrate filters. After filtration, the AgCl precipitate was washed several times with dilute ultrapure HNO_3. A few drops of ultrapure $AgNO_3$ were added to an aliquot of the filtrate to test for any remaining, unprecipitated Cl⁻. The AgCl was dissolved by the addition of 10 to 20 mL of 4-M ultrapure NH_4OH to the filter cup. Several rinses with 4-M NH_4OH ensured that all of the Cl⁻ was transferred to the test tube.

To remove sulfate from the AgCl precipitate, an ultrapure $Ba(NO_3)_2$ solution was

prepared by adding 100 mL of 1 M ultrapure HNO_3 to an excess of ultrapure $BaCO_3$ (approximately 25 g). A few drops of $Ba(NO_3)_2$ solution then were added to the sample to remove sulfate according to the following reaction:

$$Ba(NO_3)_2(aqueous) + SO_4^-(aqueous) \longrightarrow BaSO_4 \ (solid) + 2 \ NO_3^- \ (aqueous)$$
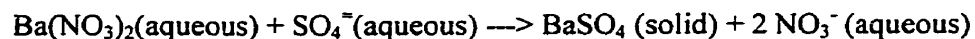
The sample was allowed to stand overnight to ensure complete precipitation of the $BaSO_4$. The sample was then gravity filtered, and the precipitate was washed and discarded. The sample was acidified to pH 1 by the addition of concentrated ultrapure HNO_3. This resulted in the reprecipitation of AgCl. The AgCl precipitate was isolated by centrifugation. After three washing and recentrifugation steps for purification, the final product was dried overnight in an oven at 90°C. Samples then were stored in amber glass vials to prevent photodecomposition of the AgCl.

3.2.3 Delta Chlorine-37

The $\delta^{37}Cl$ of a sample was determined by measurement of the $^{37}Cl/^{35}Cl$ ratio of methyl chloride (CH_3Cl) on a mass spectrometer. The addition of silver nitrate ($AgNO_3$) at pH less than two precipitated the Cl^- ions in solution by the following reaction;

$$Cl^- \ (aqueous) + AgNO_3 \ (aqueous) \longrightarrow AgCl \ (solid) + NO_3^- \ (aqueous)$$
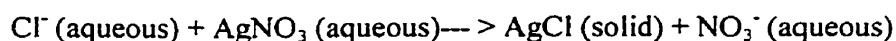
The 6 to 10 mg of AgCl was transferred to a reaction vessel that was then evacuated, and an excess (30 mL) of methyl iodide (CH_3I) was added. After 40 to 48 hours at 90°C, CH_3Cl was formed by the following reaction:.

$$AgCl \ (solid) + 2CH_3I \ (aqueous) \longrightarrow CH_3Cl \ (gas) + AgI \ (solid) + CH_3I \ (aqueous)$$
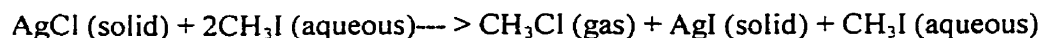
The reaction vessel was then attached to a preparation line where the CH_3Cl/CH_3I mixture was pushed with ultrapure helium through a gas chromatograph (Shimadzu-Porapak Q column). The methyl compounds were separated and the purified CH_3Cl was placed in a vessel for analysis on a VG SIRA 9 triple-collector mass spectrometer. The results were compared to commercial CH_3Cl gas. As no international standards for $\delta^{37}Cl$ are available, all results were reported relative to SMOC. (The EIL and other laboratories where stable Cl^- isotopes are determined in

40

environmental samples, have analyzed SMOC extensively). For the $\delta^{37}Cl$ values listed in table 3.3, the associated uncertainties were calculated from duplicate and triplicate analyses as noted. Otherwise, an associated uncertainty of $\pm$ 0.2 permil was determined from all measurements made during 1993 and was assigned to those values determined from a single analysis.

3.3   Quality Assurance

In addition to the measures described in section 3.2, quality assurance and reproducibility of measurements for $\delta^{37}Cl$, dissolved Cl^- and ^{36}Cl concentrations were tested in six ways: (1) National Institute of Standards and Technology (NIST) standard reference materials were used to calibrate the accelerators for mass spectrometric measurements at NSRL, PRIME, and Chalk River Laboratory; (2) two prepared blank water samples were measured for $^{36}Cl/Cl$ at Chalk River Laboratory; (3) five blind replicate samples were analyzed for dissolved Cl^- at the NWQL and one blind replicate sample was analyzed for ^{36}Cl at Chalk River Laboratory; (4) one laboratory blank was analyzed for $^{36}Cl/Cl$ at PRIME laboratory and a prepared spike sample was analyzed for Cl^- at EIL; (5) SMOC was measured once for $^{37}Cl/^{35}Cl$ for each six to eight water samples and NIST standard 975 was measured periodically; and (6) the SMOC used at the University of Waterloo was analyzed at the University of Arizona's laboratory for comparison.

The NSRL, PRIME, and Chalk River Laboratory facilities calibrate their respective AMS system with prepared solutions of ^{36}Cl traceable to NIST. Each AMS facility uses a solution prepared with ^{36}Cl of known radioactivity with the addition of an appropriate amount of ^{36}Cl-free Cl^- carrier. Control charts and documentation of the results of the calibrations are available at each facility for review.

Two AgCl targets were prepared using ^{36}Cl-free potassium chloride supplied by Chalk River Laboratory using the precipitation method outlined in section 3.2.2. One AgCl target was prepared using reagent-grade chemicals; a second target was prepared using ultrapure-grade chemicals. The $^{36}Cl/Cl$ ratio for the sample prepared with reagent-grade chemicals was 18.9 ± 6.7

$\times 10^{-15}$. The $^{36}Cl/Cl$ for the sample prepared with ultrapure-grade chemicals was $1.4\pm0.99 \times 10^{-15}$. Based on these results, the decision was made to use ultrapure-grade chemicals for all AgCl target preparation for AMS. Drs. Gwen Milton and Jack Cornett of Chalk River Laboratory in Ontario, Canada are thanked for their assistance on these ^{36}Cl quality-assurance samples.

Results of the blind replicate analyses performed by NWQL for Cl^- concentrations are given in table 3.5. All replicate and primary analyses agree at the 95 percent confidence level using equation 4.2-1 (page 56) with the exception of the sample from USGS 14 collected on October 1, 1993. However, the result of the blind replicate analysis for the sample collected on this date was within 6.6 percent of the result of the primary-sample analysis. Therefore, it was concluded that the primary analyses were acceptable as being representative of the Cl^- concentration in water from USGS 14 collected on this date. Additionally, one blind replicate sample was submitted to Chalk River Laboratory for comparison to the primary sample submitted to PRIME lab for ^{36}Cl analyses. The $^{36}Cl/Cl$ for the primary sample was $580\pm60 \times 10^{-15}$ and for the replicate the $^{36}Cl/Cl$ was $705\pm70 \times 10^{-15}$. These two analyses were in statistical agreement at

Table 3.5.   Statistical comparison of chloride concentrations in primary- and blind-replicate water samples collected from selected wells, Idaho National Engineering and Environmental Laboratory, Idaho.

[See figure 3.1 for location of wells. Analytical uncertainties expressed as one sample standard deviation estimated using equation 3 in this dissertation. All analyses performed by the U.S. Geological Survey National Water Quality Laboratory, Arvada. Co.]

Site Identifier	Date sampled	Concentration and analytical uncertainty, in milligrams per liter		Test statistic, if A>B, analytical results are statistically different; see text for explanation		Results are statistically different
		Primary	Replicate	A	B	
USGS 14	10/01/1993	18±1	21±1	3	2.8	YES
USGS 19	10/01/1993	11±0.7	11±0.7	0	1.7	NO
USGS 44	11/01/1993	20±1	19±1	1	2.8	NO
USGS 57	10/12/1993	180±7	190±8	10	20.8	NO
USGS 85	11/04/199.	74±3	73±7	1	8.3	NO

the 95 percent confidence level.

One prepared blank and one prepared spike sample were analyzed as part of the quality assurance for this research. A water sample was prepared at the PRIME lab with ^{36}Cl-free Cl⁻ carrier and analyzed with the submitted samples. The ^{36}Cl/Cl in that prepared blank was $12\pm2 \times 10^{-15}$ which was insignificant when compared to the results in table 3.3. However, this ratio was used to blank correct the ^{36}Cl/Cl ratios presented in table 3.3 for evaluation of the archive samples. Additionally, both AMS facilities used in this research routinely prepare internal blanks used to correct all reported results. A spike sample with 100 ± 4 mg/L Cl⁻ was prepared and submitted to EIL for analysis. The dissolved Cl⁻ result for this sample reported by EIL was 118 ± 12 mg/L, which was in acceptable agreement with the spike concentration.

The Cl⁻ concentrations in the snow and glacial ice and runoff samples were determined using a low-level ion chromatography (IC) system consisting of a Dionex AI-4500 IC, AS4A (4×250 mm) and AG4A (4×50 mm) columns, and a computer interface that downloaded the data directly to an IBM-compatible computer (Fishman and Friedman, 1989). A 1.8-mM sodium carbonate or 1.70-mM sodium bicarbonate eluant with a flow rate of 1.0 mL per minute was used. The concentration of the analytes was then determined using an anion micromembrane suppressor and a conductivity detector.

Eight hundred microliters of the sample were loaded onto the column. The anions were extracted on the stationary phase resin of the column. The anions were eluted off of the column at specific times and in a specific order using the carbonate/bicarbonate eluant. The sample stream passed through a suppressor that lowered the baseline conductivity, thereby lowering the method detection limit. The stream was then routed past a conductivity detector that showed increased conductivity when the number of ions in the stream increased. The timing of these peaks revealed which analyte was present and the magnitude of the peak revealed the amount of analyte in the sample.

Fifty percent of each group of ice-core samples were quality control (QC) samples. These consisted of Standard Reference Water Samples (SRWS), blanks, calibration standards and blind QC samples. Two separate blind sample programs submit samples to the Production Program of the NWQL. The NWQL's Quality Assurance Unit and the Branch of Technical Development and Quality Systems (BTD&QS, formerly BQA) administer these programs. Charts of the blind QC output are available from each of these groups. These charts indicate that this IC line was operating with no shifts in trends, no significant bias, and all data were within the acceptance limits. The QA/QC data and charts are available for inspection at the USGS, Global Ice-Core Research Project Office at the INEEL.

Based on reference samples, the Cl^- analysis performed by the NWQL on the ice-core samples had a standard deviation of 0.014 mg/L at concentrations of 0.07 mg/L. This standard deviation was calculated from on-line quality control data collected from 25 separate analyses of Standard Reference Water Sample (SRWS) P-13. The values used were collected from January 1996 to May 1996 and are similar to data collected from previous years. SRWS P-13 was made by the BTD&QS and is regularly used as a quality control sample on the analytical instrument used for this study. The on-line values for this SRWS are similar to values obtained by both the blind sample programs; one administered by BTD&QS, one administered by the Quality Assurance Unit of the NWQL.

With the exceptions noted earlier in this dissertation for some of the archived samples, the ground water, surface water, and snow samples also were analyzed for dissolved Cl^- by the ion-chromatography method (Fishman and Friedman, 1989). As in the low-level Cl^- measurements of glacial ice and runoff, internal standards were analyzed to ensure that all data were within acceptance limits. Both labs employed a standard two-column ion chromatography technique. Water samples were placed in an eluant and pumped at a constant flow rate through two ion-exchange columns in tandem. Chloride ions were separated from solution in the first column on the basis of their affinity for exchange sites on an anion-specific resin. The second

44

column decreased the background conductivity of the eluant to a minimal level to suppress interference. Separated Cl⁻ ions then were quantified with a specific-conductance cell and an anion chromatogram was produced.

The results of Cl⁻ analyses performed by NWQL and presented in this dissertation were not reported with a sample standard deviation; therefore, sample standard deviations were estimated. The USGS Branch of Quality Assurance conducts a Blind Sample Program (BSP) in which reference samples disguised as environmental samples are submitted to the NWQL for analyses (Maloney and others, 1993). These BSP data are stored in the USGS database (QADATA) and are accessible through the USGS computer system (Lucey, 1990). The statistical analyses generated through the QADATA program include equations generated by using linear-least-squares regression of a most probable value for a given analyte from the USGS's standard reference water sample program during the previous seven years against a corresponding sample standard deviation for that analyte. These linear-regression equations facilitate the calculation of a most probable deviation (MPD) at most concentrations for most analytes. The following equation from Maloney and others (1993) was used to estimate the sample standard deviations, or MPD, in tables 3.3 and 3.5 for Cl⁻ concentrations reported by the NWQL:

where:

x is the reported Cl⁻ concentration in mg/L, and

y is the calculated sample standard deviation in mg/L.

$$y = 0.039x + 0.16 \qquad\qquad \textbf{3.3-1}$$

As part of the QA/QC for this dissertation, several water samples were measured for ³⁶Cl/Cl ratios at both PRIME Laboratory and the NSRL. There was statistical agreement between the results from the two laboratories on blind duplicate samples and on duplicates of the same sample analyzed over several months (Beasley and others, 1993, table 1).

Table 3.6.　　Reproducibility of ^{36}Cl/Cl ratios for selected monitoring well waters at the Idaho National Engineering and Environmental Laboratory.

[Modified from Beasley, Cecil, and others, 1993.]

Sample Identifier	Date analyzed	AMS facility[a]	
		Rochester[b]	Purdue[c]
USGS 11	February 1990	1670 ● 110[d]	--
USGS 11	April 1990	1689 ± 104	--
USGS 14	February 1990	2030 ± 100	--
USGS 14	April 1990	2017 ± 105	--
CFA-1	May/September 1991[e]	2164 ± 105	2090 ± 170
Well 39	May/September 1991	1207 ± 89	1089 ± 74
Well 41	May/September 1991	536 ± 29	567 ± 35

[a] Each value represents the average of two separate AMS measurements.
[b] Nuclear Structure Research Laboratory (NSRL).
[c] PRIME.
[d] Samples were analyzed in May at NSRL and September at PRIME Lab.

46

CHAPTER 4

EVALUATION OF ARCHIVED GROUND WATER SAMPLES

To determine the quality and quantity of the archived samples, a complete inventory of the thousands of ground and surface water samples collected from 1966 through 1990 was conducted during February and March 1991. Samples were discarded that had questionable containers or did not have a complete historical record. The historical record for each sample included field notes taken during collection, laboratory notes compiled during analyses, chain-of-custody records maintained during processing (if available), and results of analyses requested and performed. The remaining samples were inventoried and catalogued. This inventory has been updated each year since the initial inventory in 1991 that was performed as part of this research.

Approximately 200 of the water samples were selected for possible processing for ^{36}Cl analyses based on location of sampling site, place in historical record, amount of water available, the dissolved Cl^- concentration, and sample/record integrity, as well as results of a ^{36}Cl survey of ground water from the Snake River Plain aquifer in 1990-91 (Cecil and others, 1992; and Beasley and others, 1993). Archived water samples collected from six sites over a number of years were selected for comparison to the results for samples from 1993 at the same sites. These samples were forwarded to the EIL for determination of $\delta^{37}Cl$.

4.1   Comparison of $\delta^{37}Cl$ in this Dissertation to Previous Investigations

A total of 430 measurements for $\delta^{37}Cl$ in water and rock samples were presented by Eggenkamp (1994). Delta ^{37}Cl values presented in that work ranged from -4.9 to +6.0 permil. However, for approximately 98 percent of the samples, $\delta^{37}Cl$ ranged from -1.4 to +1.5 permil and 62 percent of the samples were between -0.4 and +0.5 permil. The overall average for the 430 samples presented was -0.13 permil. The samples were collected from various geologic and
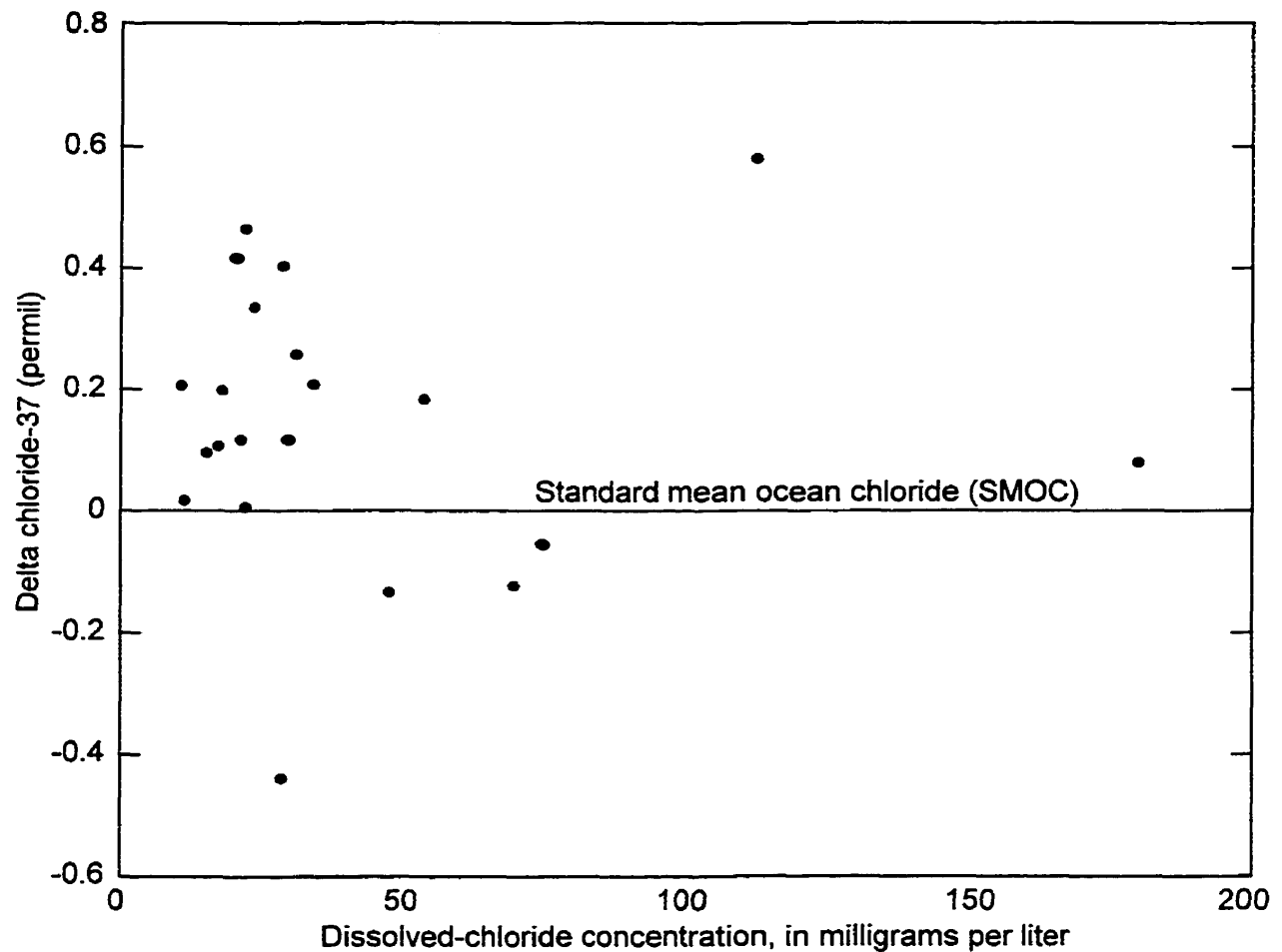
Figure 4.1. Dissolved-chloride concentration and delta chlorine-37.

Note: See table 3.3 for uncertainties. Analytical uncertainties omitted for clarity.

hydrologic environments, from volcanic to carbonate rock, and from low-salinity to high-salinity ground water.

The Eggencamp (1994) review also included data from Long and others (1993) that were among the first such analyses performed. The $\delta^{37}Cl$ from Long and others (1993) ranged from -1.5 to +2.0 permil for a total variation of 3.5 permil and included samples from ground water and brines.

The $\delta^{37}Cl$ data presented in this dissertation for water collected from the eastern Snake River Plain aquifer ranged from -0.44±0.5 to +0.59±0.16 permil with a mean of +0.15±0.27

48

permil (fig. 4.1 and table 3.3). The dissolved Cl⁻ data used in figure 4.1 were the 1993 concentrations from table 3.3. The variation in $\delta^{37}Cl$ is smaller than the variation for the 430 samples presented in the Eggenkamp review. This lack of extreme values makes it unlikely that measurable fractionation has occurred in these samples *in situ* or during storage in the USGS archive library. A linear regression analysis of the data presented in figure 4.1 produced a R^2 (fraction of variance explained by the regression) value of 0.07, suggesting that there may be little or no linear correlation between dissolved Cl⁻ concentrations and $\delta^{37}Cl$.

In addition to investigating possible fractionation of Cl⁻ isotopes in the archived water samples, dissolved Cl⁻ concentrations were measured again in 1993 and compared to the Cl⁻ concentration at the time of sample collection. Statistical comparisons of Cl⁻ concentrations in water from each site were made for the results from the 1993 analyses to the results at the time of sample collection to determine if significant Cl⁻ had been lost from the sample during storage.

Water samples collected from well USGS 19 were selected as representative of ambient or background $\delta^{37}Cl$ of the eastern Snake River Plain aquifer. Ambient values for this study are those values in water not affected by INEEL disposal practices. However, these ambient values may have been affected by fallout from nuclear weapons and/or irrigation practices. The ^{36}Cl concentrations listed in table 3.3 for water from USGS 19, $1.1\pm0.1 \times 10^8$ to $3.5\pm0.4 \times 10^8$ atoms/L, indicate that there may have been some influence from anthropogenic sources or evaporation. Additionally, the dissolved Cl⁻ concentration as measured in 1993 for water from USGS 19 that was sampled in 1969, 29.0 ± 2.9 mg/L (table 3.3), indicates an anthropogenic or evaporative influence on the water because background Cl⁻ concentrations are 10 mg/L or less for the eastern Snake River Plain aquifer (Robertson and others, 1974). This additional Cl⁻ may be due to surface flood irrigation in practice since the mid-1930s in the Little Lost River drainage upgradient from USGS 19 (Mundorff and others, 1963). The $\delta^{37}Cl$ for USGS 19 ranged from 0.02 ± 0.2 to 0.12 ± 0.2 permil, not statistically different from SMOC, and may represent a meteoric

δ^{37}Cl for water entering the Snake River Plain aquifer from the Little Lost River drainage. The δ^{37}Cl for water from the Little Lost River collected on April 3, 1970, also had a δ^{37}Cl value statistically the same as SMOC, +0.27±0.23 permil (table 3.3). The site where the Little Lost River sample was collected is about 18 km upgradient from USGS 19 (figure 3.1).

None of the δ^{37}Cl results for any of the wells listed in table 3.3 varied by more than 0.91 permil. Long and others (1993) reported δ^{37}Cl values of −1.5 permil to +0.8 permil for ground water, or a range of only 2.3 permil. These variations are in contrast to that presented by Eggenkamp (1994) for a greater variety of geologic media; the variation in that review was nearly 11 permil or almost an order of magnitude greater than the variations in water samples from the INEEL and vicinity and a factor of 5 compared to the ground water samples analyzed by Long and others (1993). The δ^{37}Cl results from the samples selected for this dissertation are consistent with two-thirds of the values presented by Eggenkamp. For the data presented in this dissertation, the largest variance was for well USGS 14, the most distant well downgradient from the waste Cl⁻ source at the INTEC. The average rate of Cl⁻ disposal to the Snake River Plain aquifer system has increased from 1971-95 (fig. 4.2). Figure 4.3 and table 3.3 show that ^{36}Cl significantly above ambient concentrations arrived in ground water at USGS 14 in 1984, the same year that the δ^{37}Cl in water from this well showed a shift from positive values to a negative value, suggesting waste-stream influences from INTEC. The most negative δ^{37}Cl value (-0.13±0.1 permil) and the largest ^{36}Cl/Cl ratio (21.000±580 × 10⁻¹³) in water samples collected from well USGS 57, the well located nearest to the discharge point at INTEC, was in 1969. The next most negative value (-0.12±0.01 permil) and the next largest ^{36}Cl/Cl (19,300±640 × 10⁻¹³) for well USGS 57 occurred in 1988 (fig. 4.4 and table 3.3). The most positive δ^{37}Cl values for USGS 14 and 57 were in thief samples that also had the smallest ^{36}Cl concentrations; 1982 for USGS 14, and 1983 for USGS 57. This suggests an inverse correlation between δ^{37}Cl and ^{36}Cl concentrations in the waste effluent from INTEC. Water from wells USGS 19, 20, 44, and 57
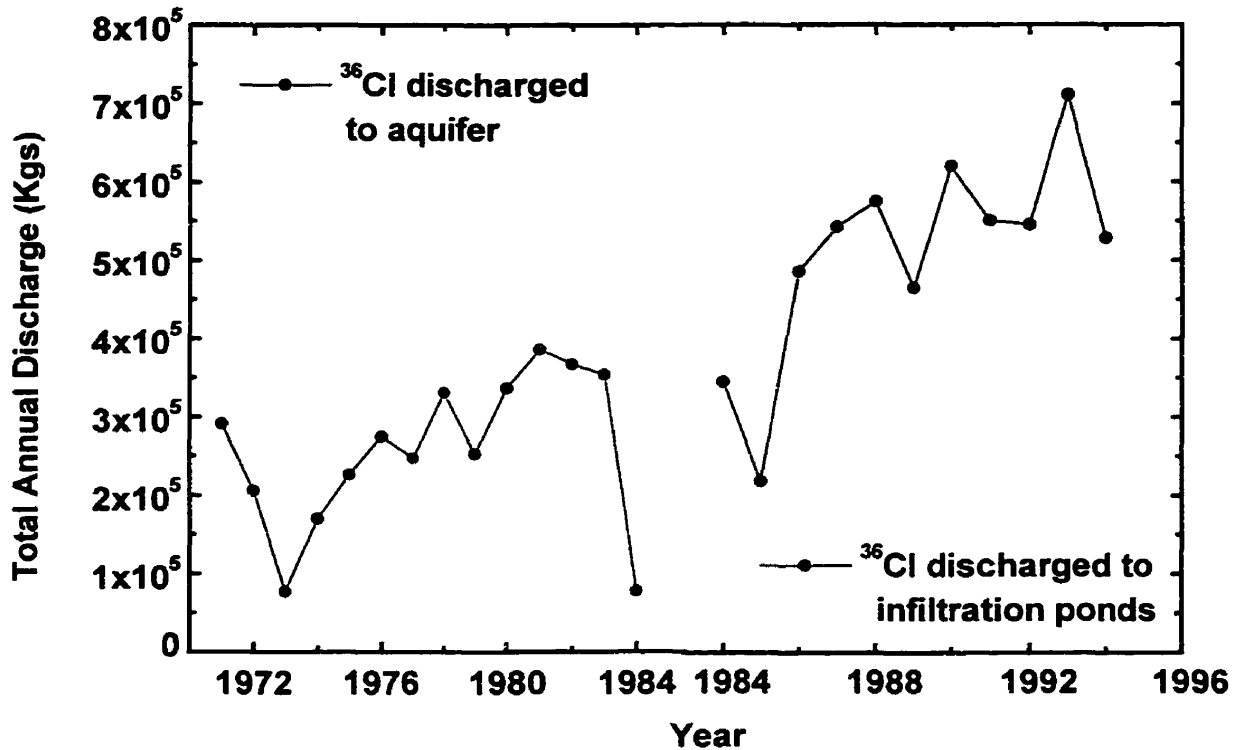
Figure 4.2. **Annual chloride discharge at the Idaho Nuclear Technology and Engineering Center, Idaho National Engineering and Environmental Laboratory, Idaho.**

showed this same inverse correlation in samples collected by the thief method; the largest ^{36}Cl concentrations are associated with the more negative $\delta^{37}Cl$. With the exception of USGS 85, all pumped samples had a positive $\delta^{37}Cl$ and range from +0.02 to +0.42 permil; the pumped sample from USGS 85 was -0.05 permil. The most negative $\delta^{37}Cl$ values occurred on the same dates as the largest ^{36}Cl concentrations in water from wells USGS 57 and 14, also suggesting an inverse correlation between $\delta^{37}Cl$ and ^{36}Cl concentrations. Wells 19, 20, and 44 had no negative $\delta^{37}Cl$ values in either thief or pumped samples (figure 4.5). It should also be noted that water from the well with the largest $^{36}Cl/Cl$ ratio, $21,000\pm580 \times 10^{-13}$, at USGS 57 collected on May 8, 1969, had the smallest dissolved Cl^- concentration for this well (by a factor of 3.7), 46.9 ± 4.7 mg/L (table 3.3). This suggests that measured ^{36}Cl concentrations in ground water from the eastern Snake River Plain aquifer are a good indicator of waste-disposal practices at the INTEC and that these

51
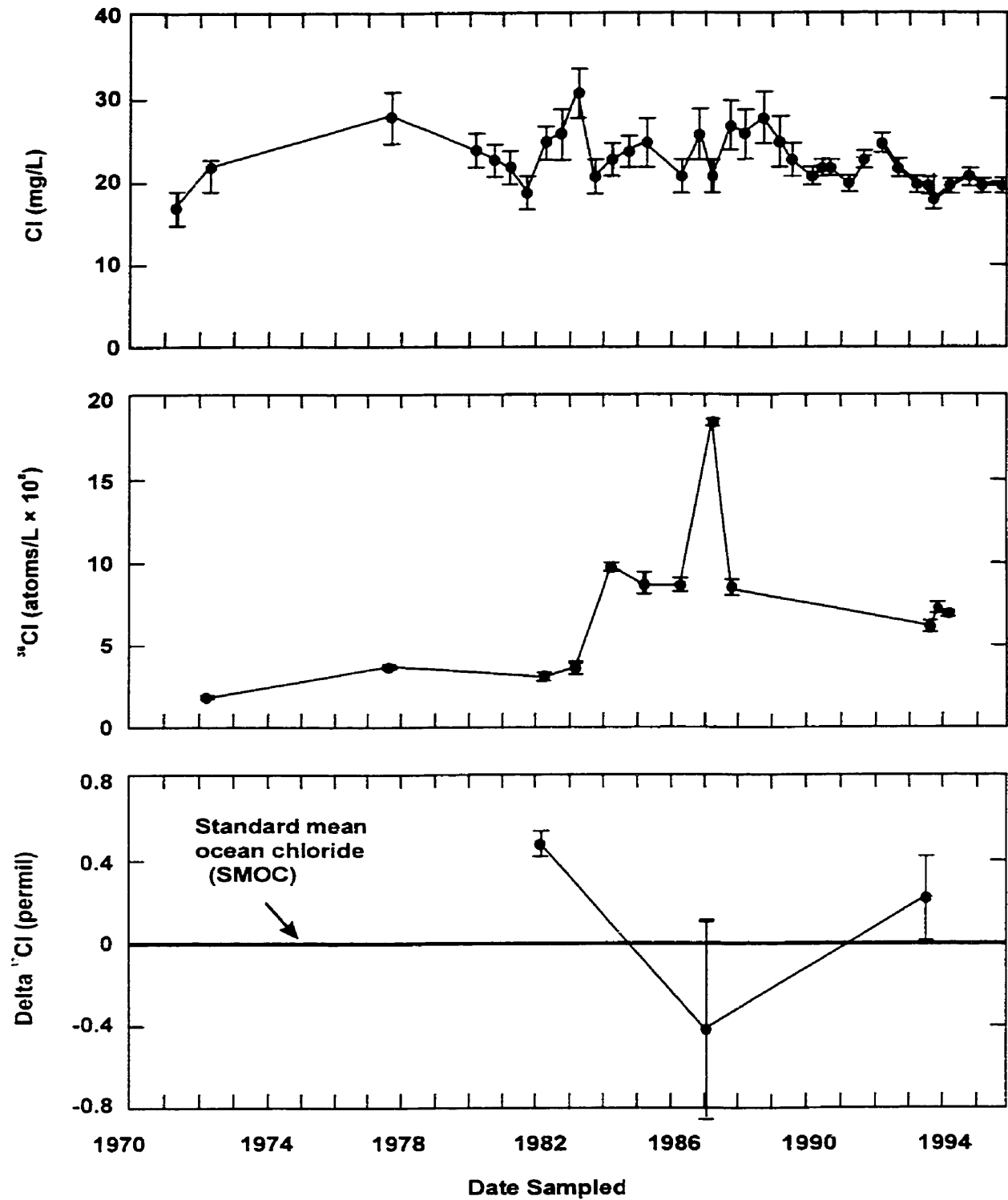
Figure 4.3. Concentration of dissolved chloride, chlorine-36, and delta chlorine-37 in relation to time, in ground water from well USGS 14, Idaho National Engineering and Environmental Laboratory, Idaho.

Note: See figure 3.1 for well location.
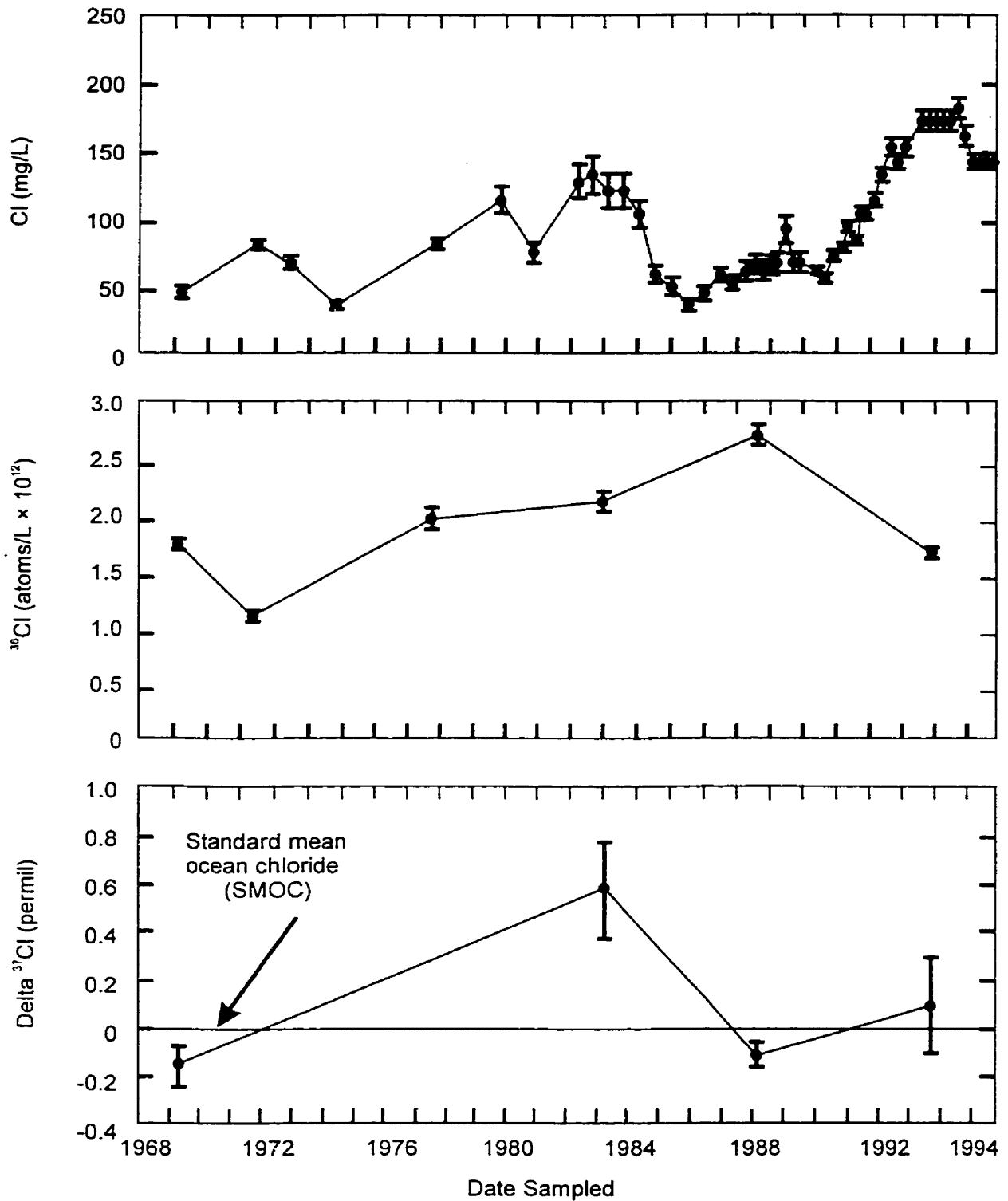
Figure 4.4.   Concentration of dissolved chloride, chlorine-36, and delta chlorine-37 in relation to time, in ground water from well USGS 57, Idaho National Engineering and Environmental Laboratory, Idaho.

Note: See figure 3.1 for well location.
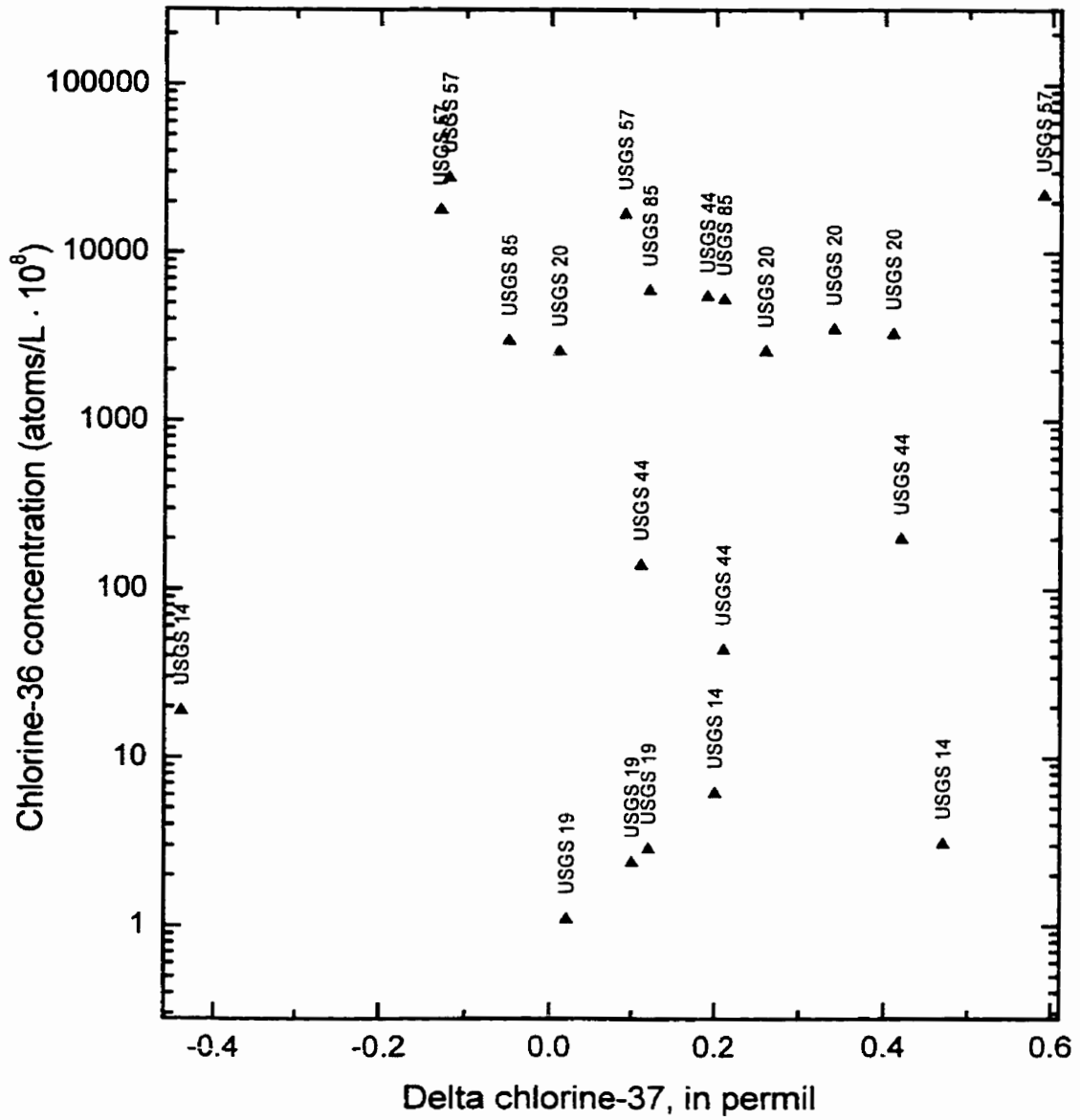
Figure 4.5. Chlorine-36 and delta chlorine-37 in selected wells, Idaho National Engineering and Environmental Laboratory, Idaho.

concentrations measured in archive samples were quantitative and useful in tracer studies utilizing Cl^- isotopic ratios. These data further suggest that processes fractionating stable Cl^- isotopic ratios or that are adding Cl^- with a ratio different than SMOC in the eastern Snake River Plain aquifer are from the facilities at the INEEL and that from the data presented here, no natural processes are quantifiable for Cl^- isotope fractionation. Additionally, these data also suggest that the radiochemical reprocessing of spent nuclear fuel at the INTEC may deplete the Cl^- released to the environment in terms of ^{37}Cl as compared to SMOC.

Evidence for this possibility comes from the inverse correlation of $\delta^{37}Cl$ and ^{36}Cl concentrations found in this evaluation and from the fact that in advective mixing of two sources of different concentrations, the larger concentration source (Cl^- from waste disposal at the INTEC) dominates the isotopic signature of the mixture. To confirm this, $\delta^{37}Cl$ measurements need to be performed on water from the effluent stream at the INTEC. The U.S. Environmental Protection Agency and the State of Idaho have not permitted this to date because the presence of other chemical and radiochemical constituents in the effluent stream dictates special sample handling.

Bartholomay (1993) showed that concentrations of ^3H and strontium-90 in water samples from wells with purge times greater than three hours at the INEEL are not affected measurably by purging one, two, or three borehole volumes. Descriptive statistics were presented that show reproducibility of analytical results in all but two sample pairs with defined numbers. Results from this study indicate that it is not necessary to purge three borehole volumes from wells with purge times greater than three hours; hence, data collected from the wells not purged with three borehole volumes in the past are probably reliable. Additionally, Olsen (1998) determined that there are no significant differences in water quality results collected by the thief method versus dedicated pumps in the Snake River Plain aquifer for wells that have substantial components of borehole flow. All of the wells selected for this research have purge times of one-half hour or

greater and components of borehole flow.

4.2   Statistical Comparison of Chloride Concentrations over Time

To determine if total CF concentrations in the archive samples had changed with time during storage, comparison of CF concentrations from the different sets of analyses was made using a modification of the t-test for unequal variances (Helsel and Hirsch, 1992, p. 126):

$$t = \frac{\overline{X} - \overline{Y}}{\sqrt{\dfrac{S_x^2}{n} + \dfrac{S_y^2}{m}}} \qquad\qquad 4.2-1$$

where: $\overline{X}$ is the mean of data in the first group,

$\overline{Y}$ is the mean of data in the second group,

S_x^2 is the sample variance of the first group,

S_y^2 is the sample variance of the second group,

n is the number of samples in the first group,

m is the number of samples in the second group, and

t is the test statistic.

This t-test can be used to determine if the means of two different sets of analyses are different. The assumption was made that the true variances for each set of CF analyses presented in this research, performed by different methods from different laboratories, were in fact unequal. In this research, a modification to equation 4.2-1 was used. The following equation was used for the comparison where n and m from equation 4.2-1 are equal to one:

$$|X - Y| > 1.96 ((S_x^2) + (S_y^2))^{1/2} \qquad\qquad 4.2\text{-}2$$

where:

X is the analytical result at the time of sample collection,

Y is the analytical result, for the same sample as X, analyzed in 1993,

$S_x{}^2$ is the sample variance of X,

$S_y{}^2$ is the sample variance of Y, and

1.96 is the test statistic (t in equation 4.2-1) for the 95 percent confidence limit

(Taylor, 1987, table C.2., p. 266).

In equation 4.2-2, if $| X - Y |$ exceeded the calculated value on the right-hand side of the equation, the two analytical results were considered to be statistically different. For this research, the statistical test for precision of results from the different methods was based on the sample standard deviations for reported concentrations from each laboratory. If the data were normally distributed and the sample standard deviations reported by the laboratories represented the true standard deviation, then the analytical results were considered to be statistically equal at the 95-percent confidence limit if $| X - Y |$ was less than or equal to the right-hand side of equation 4.2-2.

Concentrations of dissolved Cl⁻ in the archived water samples at time of collection ranged from 12 ± 1 to 127 ± 13 mg/L (table 3.3). The uncertainties were reported as one sample standard deviation and were estimated as 10 percent of the concentration by the RESL. The results of Cl⁻ analyses on these same archived water samples ranged from 10.6 ± 1.1 to 112 ± 11.2 mg/L in 1993. The concentrations reported by EIL for the analyses in 1993 also included uncertainties as one sample standard deviation, again estimated as 10 percent of the reported concentration. These sample standard deviations estimated as 10 percent for the Cl⁻ results reported by RESL and EIL were substituted into equation 4.2-2 for S_x and S_y. Therefore, this statistical evaluation must be considered as only a guide in testing for non-equivalence because the sample standard deviations were estimated and may not represent the true standard deviation.

Comparison of Cl⁻ concentrations at time of sample collection to the concentration determined in 1993 on the same samples indicated that the concentrations were statistically the same at the 95 percent level of confidence in all cases except for water samples from USGS 14 on

April 8, 1987 and from USGS 19 on April 8, 1983 (table 4.1). For the ^{36}Cl concentration in water from USGS 14, the smaller Cl$^-$ concentration was the value at the time of sample collection. Therefore, the ^{36}Cl concentration for the sample collected on April 8, 1987 at USGS 14 was a conservative estimate of that concentration. At USGS 19, the larger of the two concentrations listed in table 4.1 was the concentration at the time of sample collection on April 8, 1983; 21±1 mg/L. This suggests that the estimate of the ^{36}Cl concentration for water collected on this date may be as much as 29 percent too large.

4.3   Summary of the Chlorine Isotope Evaluation

Stable Cl isotopic ratios, ^{37}Cl/^{35}Cl, were determined on 21 ground water samples from six USGS observation wells for 1966-1993 and from one surface water site for 1970 (table 3.3). The ^{37}Cl/^{35}Cl ratio from the archived samples was measured at the EIL and was compared to the ^{37}Cl/^{35}Cl of SMOC. The resultant δ^{37}Cl values ranged from -0.44 to +0.59 permil and had a mean of +0.14 permil.   The largest variation in δ^{37}Cl for water from any individual well was 0.91 permil.   However, because of the associated uncertainties with these measurements, the data suggest an even smaller range of δ^{37}Cl values (table 3.3).   A review of available δ^{37}Cl data worldwide by Eggenkamp, 1994, showed a range of -4.6 to +6.0 permil, which is nearly 11 permil.   Long and others (1993) analyzed ground water samples and identified a range of −1.5 permil to +0.8 permil.   These ranges are up to an order of magnitude greater than the range of δ^{37}Cl for water from the INEEL and vicinity. The δ^{37}Cl range for water from the INEEL is indicative of a little or no fractionation. If there is any Cl isotope fractionation, it may be attributable to wastewater disposal and not to any processes operational during sample storage in the archive library or along the flowpath in the Snake River Plain aquifer. This is a topic to be pursued in future research.

Concentrations of ^{36}Cl were also measured in the archive samples selected for this evaluation. The historical ^{36}Cl concentrations ranged from 1.1±0.1 × 10^8 atoms/L to 28,000±910

Table 4.1.   Statistical comparison of chloride concentrations at time of sample collection and in 1993 for selected, archived ground water samples used in this evaluation.

[See figure 3.1 for location of wells. Analytical uncertainties expressed as one sample standard deviation estimated as 10 percent of the analytical result; RESL, Radiological and Environmental Sciences Laboratory; EIL, University of Waterloo Environmental Isotope Laboratory.]

Site Identifier	Date sampled	Concentration and analytical uncertainty, in milligrams per liter		Test statistic, if A>B, analytical results are statistically different; see text for explanation		Results are statistically different
		RESL (time of collection)	EIL (1993)	A	B	
USGS 14	04/14/1982	25±2	21.4±2.1	3.6	5.7	NO
	04/08/1987	21±2	28.4±2.8	7.4	6.7	YES
USGS 19	04/08/1983	21±1	14.9±1.5	6.1	4.9	YES
USGS 20	04/28/1969	30±3	30.7±3.1	0.7	6.1	NO
	04/12/1983	24±2	21.6±2.2	2.4	5.8	NO
	04/04/1988	24±2	28.2±2.8	4.2	6.7	NO
USGS 44	05/08/1969	12±1	10.6±1.1	1.4	2.9	NO
	04/12/1983	59±6	52.8±5.2	6.2	15.6	NO
	04/09/1988	15±2	17.0±1.7	2.0	5.1	NO
USGS 57	05/08/1969	50±5	46.9±4.7	3.1	13.4	NO
	04/12/1983	127±13	112±11.2	15	33.6	NO
	03/31/1988	67±2	69.2±6.9	2.2	19.3	NO
USGS 85	04/25/1969	24±2	21.3±2.1	2.7	5.7	NO
	04/13/1983	37±4	33.8±3.4	3.2	10.3	NO

× 10^8atoms/L. Based on the evaluation of the archived water samples in terms of $\delta^{37}Cl$, it was concluded that the ^{36}Cl concentrations measured in 1993 were representative of the concentrations at the time of sample collection. It follows, therefore, that ^{36}Cl concentrations measured on any of the archived samples used in this research are representative of the concentrations at the time of sample collection.

59

CHAPTER 5

SOURCES OF CHLORINE-36 IN THE ENVIRONMENT

To facilitate the use of ^{36}Cl as a hydrogeologic tracer at the INEEL, measurements were made on water, snow, and glacial-ice samples to determine the naturally- and weapons-produced fluxes of ^{36}Cl at mid-latitudes in North America. In addition to flux estimates, measurements were made for ^{36}Cl dissolved in ground and surface waters to determine initial (ambient) concentrations. This information was used to estimate meteoric and weapons-tests contributions of this nuclide to environmental inventories at and near the INEEL.

In addition to the determination of meteoric and weapons-tests inputs of ^{36}Cl to the environment, *in situ* neutron production rates and resultant maximum ^{36}Cl production were estimated. The ^{36}Cl concentrations from these sources are then compared to concentrations in ground water influenced by nuclear-waste disposal at the INEEL.

Eighteen surface water samples from six sites were selected for ^{36}Cl analyses from the USGS archive-sample library at the INEEL; these eighteen samples were collected during 1969-1995 (figure 5.1). The ^{36}Cl concentrations for the archived surface water samples ranged from $0.2 \pm 0.02 \times 10^8$ to $2.2 \pm 0.05 \times 10^8$ atoms/L (table 5.1). In 1994-95, an additional 14 surface water sites and two springs on the eastern Snake River Plain were sampled for ^{36}Cl analyses. The ^{36}Cl concentrations for these surface water and spring samples ranged from $0.014 \pm 0.001 \times 10^8$ to $6.2 \pm 0.7 \times 10^8$ atoms/L, similar to the range of concentrations in the 18 archived samples. For comparison, water from two monitoring wells at the INEEL had ^{36}Cl concentrations as low as $0.06 \pm 0.003 \times 10^8$ atoms/L for a well not influenced by site disposal practices (Site 14) and as large as $19,000 \pm 914 \times 10^8$ atoms/L for a well (USGS 77) just downgradient hydraulically from INTEC.

To aid in establishing meteoric concentrations, four snow samples also were collected in 1991 at and near the INEEL (table 5.1, fig. 1.1). The estimated ^{36}Cl flux for the sample collected

Figure 5.1. Location of the eastern Snake River Plain, the Department of Energy's Idaho National Engineering and Environmental Laboratory, selected facilities, and sampling sites for surface water, snow, and springs.

EXPLANATION

COPPER BASIN ● SNOW SAMPLING SITE—Entry, COPPER BASIN, is site identifier

TETON RIVER ▲ STREAMFLOW SITE—Entry, TETON RIVER, is name of gaging station

INTEC ◆ IDAHO NUCLEAR TECHNOLOGY AND ENGINEERING CENTER

TRA ◆ TEST REACTOR AREA

RWMC ◆ RADIOACTIVE WASTE MANAGEMENT COMPLEX

— BOUNDARY OF EASTERN SNAKE RIVER PLAIN

□ CITY OR TOWN

North

BEAVER CREEK

BIRCH CREEK

LITTLE LOST RIVER

MEDICINE LODGE CREEK

BIRCH CREEK

HARRIMAN STATE PARK

BIG SPRING

CAMAS CREEK

GIDDY HOT SPRING

HENRY'S FORK AT ST. ANTHONY

FALL RIVER

BIG LOST RIVER

LITTLE LOST RIVER

MUD LAKE

CAMAS CREEK

TETON RIVER

BIG LOST RIVER

IDAHO NATIONAL ENGINEERING AND ENVIRONMENTAL LABORATORY

SNAKE RIVER AT HEISE BRIDGE

COPPER BASIN

TRA

INTEC

INEEL #1

INEEL #2

RWMC

IDAHO FALLS

SNAKE RIVER

BIG WOOD RIVER

SILVER CREEK

Craters of the Moon National Monument

SNAKE RIVER AT SHELLEY

SNAKE RIVER AT KING HILL

EASTERN

BLACKFOOT RIVER

SNAKE RIVER AT IRWIN

KING HILL

SNAKE

LITTLE WOOD RIVER

RIVER

AMERICAN FALLS RESERVOIR

PORTNEUF RIVER

BIG WOOD RIVER

PLAIN

LAKE WALCOTT

SNAKE RIVER NEAR NEELY

TWIN FALLS

SNAKE RIVER AT MILNER

0   25   50 MILES

0   25   50 KILOMETERS

Table 5.1. Dissolved-chloride concentration, amount of ^{36}Cl-free chloride carrier added, ^{36}Cl concentration and calculated fluxes in surface water, ground water, spring, snow, and glacial-runoff samples.

[See figs. 1.1 and 3.1 for site locations. See text for explanation of uncertainties. SW, surface water sample; GW, ground water sample; SN, snow sample; SP, spring sample; GR, glacial runoff sample; USGS, U.S. Geological Survey; INEEL, Idaho National Engineering and Environmental Laboratory; ^{36}Cl, chlorine-36; and ND, not determined].

Site identifier	Date of sample	Chloride concentration (mg)	^{36}Cl-free chloride carrier (mg)	Corrected ^{36}Cl/Cl ratio ($\times 10^{-15}$)	^{36}Cl concentration (atoms/L$\times 10^8$)	^{36}Cl flux (atoms/cm^{2}sec $\times 10^{-1}$)
Little Lost River-SW	9/11/69	11±0.7	0	2,290±160	1.9±.0.1	ND
	10/4/77	7.4±0.6	0	2,070±190	0.3±0.01	ND
	4/8/83	13±0.8	0	3,220±250	2.1±0.2	ND
	4/1/88	11±0.7	0	950±198	0.7±0.1	ND
	10/11/94	13±0.8	0	998±24	2.2±0.05	ND
Big Lost River-SW	4/3/70	4.2±0.5	0	3,450±120	1.2±0.04	ND
	1990	4±0.5	0	2,461±99	1.7±0.07	ND
	1991	3±0.4	0	2,776±168	1.4±0.08	ND
	10/11/94	3.4±0.4	0	2,369±25	1.4±0.01	ND
Birch Creek-SW	4/3/70	5.1±0.5	0	960±40	0.2±0.01	ND
	1990	5±0.5	0	623±33	0.5±0.03	ND
	3/28/91	4.4±0.5	0	672±21	0.5±0.02	ND
	10/11/94	4.2±0.5	0	660±19	0.5±0.01	ND
Camas Creek-SW	4/3/70	5.9±0.5	0	390±50	0.2±0.02	ND
	10/3/77	7.3±0.6	0	2,170±60	0.5±0.02	ND
	10/11/94	7.4±0.6	0	843±25	1.1±0.03	ND
Fall River-SW	4/2/70	14±0.8	0	750±50	0.4±0.03	ND
Snake River below Jackson Dam-SW	4/2/70	4.8±0.5	0	2,310±70	0.4±0.01	ND
Blackfoot River-SW	3/1/94	13±0.8	0	689±51	1.5±0.1	ND
Snake River at Shelley-SW	3/1/94	12±0.8	0	567±33	1.2±0.1	ND
Snake River at Irwin-SW	3/2/94	6.8±0.6	0	894±42	1.0±0.05	ND
Snake River at Heise Bridge-SW	3/2/94	19±1	0	311±21	1.0±0.1	ND
Teton River-SW	3/2/94	3.3±0.4	0	2,630±210	1.5±0.1	ND
Henrys Fork at St. Anthony-SW	3/3/94	2.3±0.4	0	3,040±190	1.2±.0.1	ND
Beaver Creek-SW	3/3/94	4.4±0.5	0	8,300±970	6.2±0.7	ND
Portneuf River-SW	3/4/94	37±2	0	417±41	2.6±0.3	ND

Table 5.1. Dissolved-chloride concentration, amount of ^{36}Cl-free chloride carrier added, ^{36}Cl concentration and calculated fluxes in surface water, ground water, spring, snow, and glacial-runoff samples.

[See figs. 1.1 and 3.1 for site locations. See text for explanation of uncertainties. SW, surface water sample; GW, ground water sample; SN, snow sample; SP, spring sample; GR, glacial runoff sample; USGS, U.S. Geological Survey; INEEL, Idaho National Engineering and Environmental Laboratory; ^{36}Cl, chlorine-36; and ND, not determined].

Site identifier	Date of sample	Chloride concentration (mg)	^{36}Cl-free chloride carrier (mg)	Corrected ^{36}Cl/Cl ratio ($\times 10^{-15}$)	^{36}Cl concentration (atoms/L$\times 10^8$)	^{36}Cl flux (atoms/cm^{2}sec X 10^{-1})
Snake river Near Neely-SW	3/4/94	36±2	0	277±18	1.7±0.1	ND
Snake River at Milner-SW	3/4/94	29±1	0	387±15	1.9±0.1	ND
Snake River at King Hill-SW	3/5/94	25±1	0	442±33	1.9±0.1	ND
Big Wood River-SW	3/5/94	5.3±0.5	0	3,850±200	3.5±0.2	ND
Silver Creek-SW	3/5/94	4.4±0.5	0	4,180±200	3.1±0.2	ND
Liddy Hot Spring-SP	3/14/94	7.2±0.6	0	235±8	0.28±0.01	ND
Medicine Lodge Creek SW	3/3/94	6.3±0.5	0	2,230±120	2.4±0.1	ND
Big Spring-SP	6/27/95	2.6±0.4	0	33.6±2.5	0.014±0.001	ND
Site 14-GW	9/7/77	9.2±0.7	2.01	801±40	0.06±0.003	ND
	10/15/93	8.2±0.6	1.07	1,600±45	0.04±0.001	ND
USGS 77-GW	5/10/68	65±3	11.97	1,451,600±20,370	16,000±220	ND
	4/25/69	73±3	117.6	1,533,500±73,730	19,000±910	ND
	4/21/71	71±3	112.1	1,410,900±46,080	17,000±560	ND
	9/6/77	79±3	12.31	1,271,800±34,500	17,100±460	ND
	11/1/93	120±5	11.8	613,880±8,940	12,500±180	ND
Harriman State Park-SN	12/10/91	0.9±0.2	16	74±10	0.063±0.009	0.12±0.02
Copper Basin-SN	3/15/91	0.5±0.1	24	50±25	0.049±0.025	0.03±0.02
INEEL #1-SN	1/24/91	0.25±0.05	24	17,939±469	14±0.4	10±0.3
INEEL #2-SN	1/24/91	0.95±0.19	24	177,900±35,580	170±34	120±24
Galena Creek Rock Glacier-GR	8/30/95	0.079±0.004	0.722	170±25	0.032±0.005	0.16±0.02

in Harriman State Park, 150 km northeast of the INEEL, was $1.20\pm0.2 \times 10^{-2}$ atoms/square centimeter/second (atoms/cm^{2}sec). The estimated ^{36}Cl flux for the sample collected in Copper Basin, 100 km northwest of the INEEL, was $2.8\pm1.4 \times 10^{-3}$ atoms/cm^{2}sec. For comparison, two snow samples were collected at the INEEL during nuclear-fuel reprocessing operations downwind from INTEC. The estimated ^{36}Cl flux for the sample collected 11 km to the southwest of the effluent stack at the INTEC was 1.0 ± 0.03 atoms/cm^{2}sec and for the sample 1.5 km downwind, the flux was 12.0 ± 2.4 atoms/cm^{2}sec. The ^{36}Cl concentration in the four snow samples ranged nearly four orders of magnitude, from $4.9\pm2.5 \times 10^6$ to $1.7\pm0.3 \times 10^{10}$ atoms/L. The ^{36}Cl concentrations in the snow samples not influenced by INEEL disposal practices, $4.9\pm2.5 \times 10^6$ and $6.3\pm0.9 \times 10^6$ atoms/L, are two orders of magnitude smaller than the concentrations in the surface water samples. Evapotranspiration is the most probable mechanism for this apparent ^{36}Cl concentration in the surface water samples. This mechanism will be discussed in detail in section 5.3.6.

A 160-m ice core was collected from the Upper Fremont Glacier (43°07'N, 109°36'W) in the Wind River Mountain Range of Wyoming in the western United States in 1991 (fig. 1.4). In 1994-95, ice from this core was processed at the National Ice Core Laboratory in Denver, Colorado, and analyzed for ^{36}Cl. A ^{3}H bomb peak identified in the ice core was used as a marker to estimate the depth of bomb-produced ^{36}Cl. Tritium concentrations ranged from 0 TU for older ice to more than 360 TU at 29 m below the surface of the glacier, a depth that includes ice that was deposited as snow during nuclear-weapons tests through the early 1960s. Maximum ^{36}Cl production during nuclear-weapons tests was in the late 1950s; therefore, analyses were performed on ice from a depth of 29.8 to 35.3 m. Estimated flux for ^{36}Cl in ice deposited in the 1950s ranged from $9.0\pm0.2 \times 10^{-2}$ atoms/cm^{2}sec for ice from 34.2 to 34.8 m to $2.9\pm0.1 \times 10^{-1}$ atoms/cm^{2}sec for ice from 31.5 to 32.0 m. A mean global natural atmospheric production flux for ^{36}Cl of 1.1×10^{-3} atoms/cm^{2}sec has been reported (Lal and Peters, 1967). The peak atom/L

concentrations from these estimated fluxes were $7.7 \pm 0.2 \times 10^7$ atoms/L at a depth of about 32 m.

Ice samples from depths of less than 24.0 m and greater than 46.4 m were selected to represent pre- and post-weapons tests ^{36}Cl flux. These cores had estimated fluxes that ranged from $1.1 \pm 0.2 \times 10^{-2}$ atoms/cm^{2}sec to $2.0 \pm 0.2 \times 10^{-2}$ atoms/cm^{2}sec. For comparison, a glacial-runoff sample collected in 1995 at Galena Creek Rock Glacier, 180 km north of the Upper Fremont Glacier in Wyoming's Absaroka Mountains, had an estimated flux of $1.6 \pm 0.2 \times 10^{-2}$ atoms/cm^{2}sec. The atom/L concentrations in the pre- and post-bomb sections of glacial ice and runoff were all less than 1×10^7. It was concluded from the water, snow, and glacial-ice data presented below that atom concentrations of ^{36}Cl greater than 1×10^9 atoms/L are likely a result of waste-disposal practices at the INEEL.

In situ ^{36}Cl production due to nuclear interactions between non-radioactive (stable) nuclides and alpha particles given off during the radioactive transformation of uranium (U) and thorium (Th) decay-series isotopes was determined for 25 whole-rock samples collected from basalt, rhyolite, limestone, dolomite, shale, and quartzite of the eastern Snake River Plain aquifer system. The results will be discussed in section 5.3.

5.1   Meteoric Production

The most direct method to determine meteoric concentrations of ^{36}Cl is the long-term monitoring of wet precipitation and dry fallout. However, several problems must be addressed before the assumption can be made that these concentrations are representative of initial meteoric water. For arid regions such as the INEEL, precipitation events are infrequent and an accurate assessment of meteoric concentrations may take several years of measurements. Additionally, seasonal trends in ^{36}Cl deposition have been documented (Hainsworth and others, 1994) and maximum recharge to the local ground water may not correspond in time to periods of maximum precipitation and runoff due to possible lag time. Therefore, an attempt has been made in this dissertation, by analyzing several snow samples and a recent glacial-runoff sample combined

with measurements of ground and surface water from 1969-1994, to establish regional meteoric inputs of ^{36}Cl to the hydrogeologic environment.

Bentley and others (1986) have calculated the pre-weapons tests ^{36}Cl/Cl ratios in meteoric wet and dry deposition for the continental United States (figure 1.5). These calculations were for cosmogenically produced ^{36}Cl and stable Cl⁻, principally from transport of sea salts. The predicted pre-weapons tests ^{36}Cl/Cl ratios at the latitude of the INEEL average about 450 × 10^{-15} and represent the integrated ratios expected in uncontaminated ground water. As mentioned earlier, Cecil and others (1992) reported pre-weapons tests ^{36}Cl/Cl ratios of approximately 300 × 10^{-15} for soil in the unsaturated zone near the RWMC at the INEEL. Neither ET nor the addition of Cl⁻-free water (fig. 2.1) will change these ratios. However, as shown in figure 2.1, the absolute concentration of ^{36}Cl can change by these same processes. It is assumed that these processes affect the stable isotopes of Cl⁻ in the same way so that even though the absolute concentration of ^{36}Cl can change, the meteoric ratio of ^{36}Cl/Cl does not. The glacial-runoff sample, the two spring samples, the two snow samples, and the ground water samples not affected by INEEL waste-disposal practices, all had corrected ^{36}Cl/Cl ratios less than 300 × 10^{-15} (table 5.1). For comparison, the ground water samples from a well at the INEEL influenced by waste-disposal practices (USGS 77) had corrected ^{36}Cl/Cl ratios that ranged from about 600,000 × 10^{-15} to 1,500,000 × 10^{-15}, or up to four orders of magnitude larger than the meteoric ratios.

Using the reported ambient Cl⁻ concentration for ground water at the INEEL of 6 to 10 mg/L (Robertson and others, 1974) and the average pre-weapons tests ^{36}Cl/Cl ratio of 450 × 10^{-15} (Bentley and others, 1986), the concentration of ^{36}Cl in water should range from 4.6 to 7.6 × 10^7 atoms/L. (Using the larger ratio from Bentley and others (1986) for southeast Idaho of 600 × 10^{-15} results in a concentration of ^{36}Cl in water of 9.5 × 10^6 atoms/L). This compares to ranges of measured pre-weapons tests ^{36}Cl concentrations of 1.2 to 5.2 × 10^6 atoms/L for the Upper Fremont Glacier ice core and 4.0 to 6.0 × 10^6 atoms/L for ground water not affected by INEEL

disposal practices (Site 14). This suggests an anthropogenic or *in situ* component in the ambient Cl^- concentrations reported by Robertson and others (1974). Again, processes that could effect these concentrations are ET and the addition of Cl^- free ground water. Evapotranspiration is a significant process at and near the INEEL, a semi-arid high-plains desert environment. Extensive and long-term irrigation return flow will also influence the absolute concentrations.

A reevaluation of the Bentley and others model produced pre-bomb $^{36}Cl/Cl$ ratios for southeastern Idaho that ranged from 250×10^{-15} to 500×10^{-15} (Sterling, 2000, page 99), with an average of 375×10^{-15}. Using this average $^{36}Cl/Cl$ ratio, the concentration of ^{36}Cl in water would range from 3.8 to 6.4×10^7 atoms/L, or 17 percent smaller than the range calculated with data from the Bentley and others model used above.

The long-term (1980-99) precipitation-weighted average Cl^- concentrations at the National Atmospheric Deposition Program (NADP) station at Craters of the Moon National Monument (fig. 1.1), near the INEEL, is 0.19 mg/L. Using this average Cl^- concentration and the average pre-weapons tests $^{36}Cl/Cl$ ratio of 450×10^{-15}, the ^{36}Cl concentration in precipitation at the INEEL and vicinity should average about 1.5×10^6 atoms/L. If the larger ratio from Bentley and others is used (600×10^{-15}), then the average ^{36}Cl concentration should average about 1.9×10^6 atoms/L. These values are about an order of magnitude less than what can be measured in ground water uninfluenced by INEEL waste-disposal practices (table 5.1). Table 5.1 lists the concentrations of ^{36}Cl measured in glacial runoff (recent precipitation) and snow at nearly the same latitude as the INEEL. These concentrations range from $3.2\pm0.5 \times 10^6$ to $6.3\pm0.9 \times 10^6$ atoms/L water equivalent, in good agreement with the concentration calculated using the long-term average NADP data for Cl^- in precipitation, 1.5×10^6 atoms/L. For the two snow samples collected at the INEEL during active calcining operations (conversion of liquid high-level chemical and radioactive waste to a granular solid) in 1991, INEEL#1 and INEEL#2 (table 5.1), the ^{36}Cl concentrations are $14\pm0.4 \times 10^8$ and $1.7\pm0.3 \times 10^{10}$ atoms/L, respectively. These

concentrations are three to four orders of magnitude larger than the concentrations of ^{36}Cl in snow and glacial runoff unaffected by INEEL disposal operations.

For comparison, the ^{36}Cl concentration in the 32 surface water samples analyzed in this dissertation ranged from $0.20\pm0.02 \times 10^8$ to $6.2\pm0.7 \times 10^8$ atoms/L with an average ^{36}Cl concentration of 1.5 ± 0.3 atoms/L. This enrichment in ^{36}Cl concentrations for the surface water samples compared to the calculated and measured meteoric concentrations in precipitation is probably a result of extensive ET. The only other mechanism shown in figure 2.1 that could increase ^{36}Cl atom concentrations is subsurface (*in situ*) production. In 1993, Beasley and others estimated the contribution of 3×10^2 atoms/L to neutron activation of Cl$^-$ in ground water from this mechanism with corresponding ^{36}Cl/Cl ratios on the order of 10^{-18}. Additionally, *in situ* production in all major water-bearing rocks in the eastern Snake River Plain aquifer has been shown to be insignificant and to have no measurable impact on ^{36}Cl atom concentrations in ground water (Cecil and others, in press, and "*In situ* Production" section below).

The largest ^{36}Cl/Cl ratios from *in situ* production (discussed in greater detail in section 5.3), on the order of 4×10^{-14}, correspond to the largest ^{36}Cl atom concentrations in surface water listed in table 5.1 and shown on figure 5.2. For example, surface water from Beaver Creek near Spencer, Idaho, had the largest ^{36}Cl atom concentration of all the surface water sites, $6.2\pm0.7 \times 10^8$ atoms/L, and the calculated *in situ* ratios for the geology in this area ranged from 2.5×10^{-14} to 3.5×10^{-14}. If all the dissolved Cl$^-$ in water had been derived from the matrix in this area, then this *in situ* source at most would contribute 5.9×10^6 atoms/L. However, the water would have to be on the order of 1.5 million years in age to have this ^{36}Cl concentration. With ground water flow velocities on the order of 1 to 6 m/day and the travel distances in the Snake River Plain Aquifer, there is no water of this age in the effective flow system. Additionally, CFC dating of ground water at the INEEL indicates that water moving beneath the site in the 1990s was recharged to the system after 1940 (Busenburg and others, 1993). It is highly improbable that surface water would

be in contact with the rock matrix for a sufficient amount of time to produce measurable ^{36}Cl atom concentrations by *in situ* production. Additionally, this ^{36}Cl atom concentration is two orders of magnitude less than what has been measured in surface water in this area. This Beaver Creek ^{36}Cl atom/L concentration, $6.2\pm0.7 \times 10^8$, is probably a result of resuspension of bomb-produced ^{36}Cl and/or ET.

The maximum *in situ* contribution of ^{36}Cl has been estimated for all the major water-bearing rock types in the eastern Snake River Plain aquifer system and the results will be discussed in detail in later in this chapter. The largest calculated contribution to ^{36}Cl inventories from *in situ* production is 7.68×10^6 atoms/L for rhyolite (figure 5.2). This concentration compares well with meteoric concentrations (10^6 atoms/L) presented in this chapter.

Excluding anthropogenic input of ^{36}Cl to the hydrogeologic environment, the only enriching mechanism is ET. The ^{36}Cl/Cl ratios shown for these surface water sites in table 5.1 range from $390\pm50 \times 10^{-15}$ to $3450\pm120 \times 10^{-15}$ or about an order of magnitude. Excluding the two snow samples collected during nuclear-fuel reprocessing at the INTEC and the glacial-runoff and snow samples shown in figure 5.2, all the surface water concentrations are scattered about the line representing 1.5×10^8 atoms/L, the mean concentration for the 32 surface water samples. This distribution may be representative of evaporative processes in these surface water samples. Chlorine-36 concentrations between 1×10^8 and 1×10^9 atoms/L on figure 5.2 may be indicative of resuspension of weapons-test fallout, airborne disposal from the INTEC, or ET.

Additional independent data supporting the concept that evaporative processes are operable on recharge to the eastern Snake River Plain aquifer system were presented by Wood and Low (1988, figure 18, page D15). Oxygen-18 and deuterium isotopic ratios for surface and ground water samples collected from the Snake River Plain aquifer system are presented. The delta oxygen-18 values reported show a shift to heavier oxygen values suggesting evaporation prior to recharge in semiarid climates.
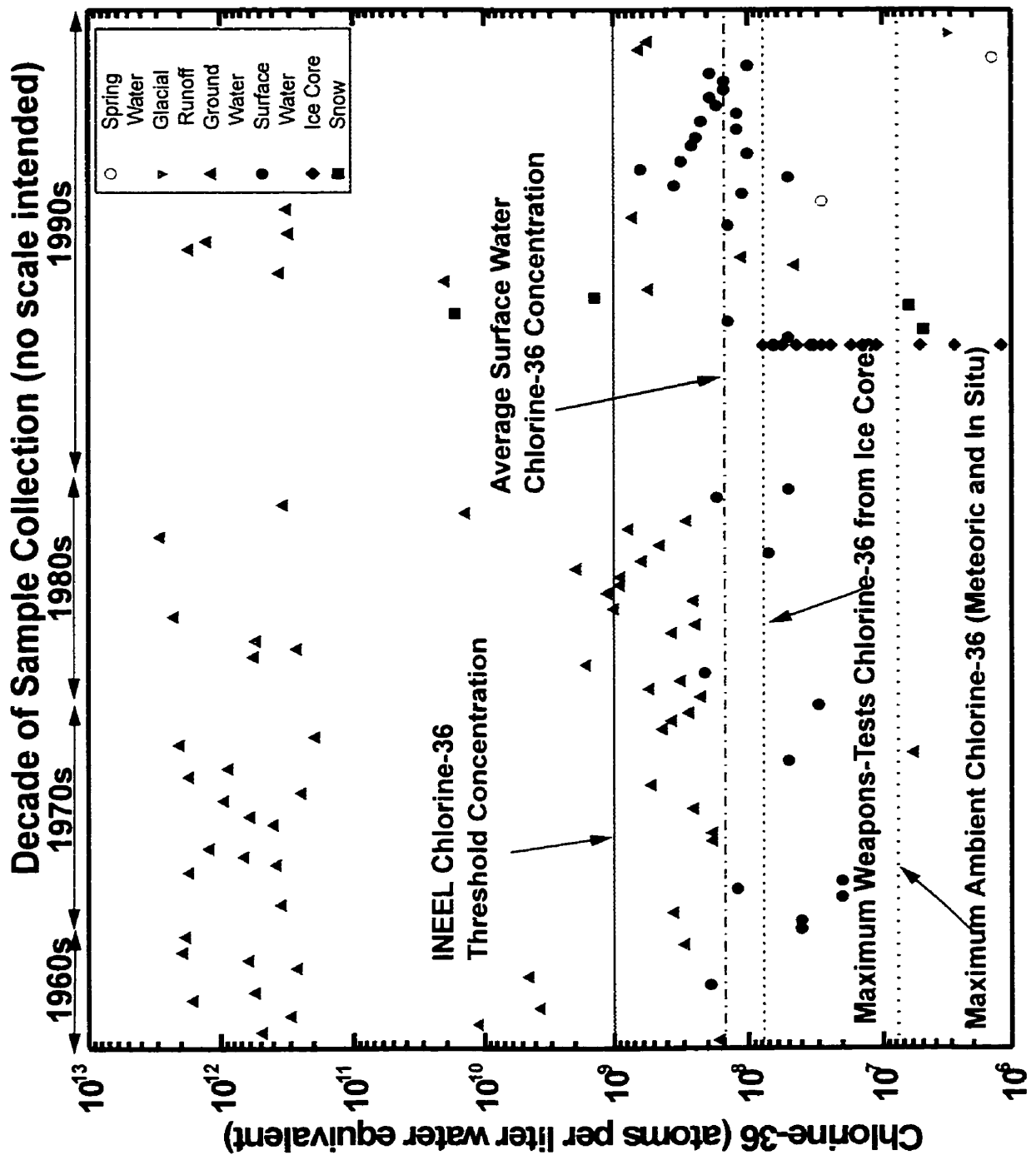
Figure 5.2. Chlorine-36 concentrations in spring-water, snow, ice-core, ground water, surface water, and glacial-runoff samples.

Note: Error bars were not included on this figure for clarity. For associated uncertainties see table 2.1 for ground water samples, table 5.1 for surface water, spring, snow, and glacial-runoff samples, and table 5.3 for ice-core samples.

Another useful geochemical selection criterion for determining meteoric ^{36}Cl inputs is the chloride/bromide (Cl⁻/Br⁻) mass ratio (Davis and others, 1998). For precipitation, this ratio is generally in the range of 80 to 160. Oil-field brines have ratios in the range 250 to 350 and brines produced from the dissolution of bedded salt and salt domes range from 1,500 to 15,000. Exceptions include precipitation within a few tens of kilometers from the coastline that may have ratios approaching 290 (the ratio found in seawater). For determining meteoric ^{36}Cl concentrations, ratios in excess of 200 indicate Cl⁻ sources other than precipitation; these waters should be avoided for determining meteoric inputs.

Water from several surface water sites, from Big Spring, the glacial-runoff samples, and two sections of ice from the Upper Fremont core were analyzed for Cl⁻ and Br⁻. The results indicate that, using the criterion outlined above, only water from Big Spring and from the glacial runoff is suitable for quantifying meteoric ^{36}Cl inputs at and near the INEEL (table 5.2). The ^{36}Cl concentrations in water from Big Spring and the glacial-runoff sample are less than 1 × 10^7 atoms/L and represent meteoric inputs on the eastern Snake River Plain. All the surface water samples indicate addition of Cl⁻ from sources other than meteoric. The ^{36}Cl/Cl ratios and atom/L concentrations given in table 5.1 (sample site locations are shown on fig. 5.1) also indicate enrichment of Cl⁻ in these samples. To date, only two ice-core samples have been analyzed for Cl⁻ /Br⁻ mass ratios from depths that include significant ^{36}Cl concentrations. The section of ice-core collected from a depth of 30.4 to 31.1 meters below the surface of the Upper Fremont Glacier (table 5.3) had a Cl⁻/Br⁻ mass ratio of 45 (table 5.2) and a ^{36}Cl concentration of 4.3±0.1 × 10^7 atoms/L water equivalent (table 5.3). The section of ice collected from 31.1 to 31.5 meters below the glacier surface had the maximum Cl⁻/Br⁻ mass ratio (633, table 5.2) and a ^{36}Cl concentration 0f 6.5±0.3 × 10^7 atoms/L water equivalent (table 5.3). The Cl⁻/Br⁻ mass ratio and ^{36}Cl concentration for this section of ice indicate anthropogenic sources of excess Cl⁻. Additional work is necessary to establish the Cl⁻/Br⁻ mass ratios for the glacial ice samples and to interpret the

results.

5.2   Weapons-Tests Production

The calculated ^{36}Cl concentrations in the sections of the Upper Fremont Glacier ice core are of similar magnitude to those found in Arctic and Antarctic ice cores (Synal and others, 1991; Elmore and others, 1982). Concentrations of 1×10^7 atoms/L water equivalent are typical values for pre- and post-bomb ^{36}Cl (figure 5.4). A direct comparison between the polar results and the mid-latitude results presented here should be done with caution because the ^{36}Cl flux depends on the precipitation rate that can vary considerably from one geographic location to another. Complex atmospheric dynamics may also contribute to larger atmospheric fallout of cosmogenic nuclides at mid-latitudes when compared to polar regions due to stratospheric-tropospheric air exchange mechanisms that are different at mid-latitudes (Moysey, 1999).

Table 5.2.   Mass ratios of chloride/bromide for selected water samples collected near the Idaho National Engineering and Environmental Laboratory, Idaho and for select ice-core samples from the Upper Fremont Glacier, Wyoming.

[Symbols: SP, spring sample; SW, surface water; GR, glacial runoff; and IC, ice core. Cl^-/Br^- analyses for the ice-core samples performed at Los Alamos National Laboratory.]

Site or sample identifier	Date of sample	Chloride content (mg/L)	Bromide content (mg/L)	Cl^-/Br^- mass ratio
Big Spring-SP	6-27-1995	2.6±0.4	0.02±0.005	130
Big Lost River-SW	6-28-1995	2.3±0.4	0.006±0.002	383
Birch Creek-SW	6-28-1995	4.8±0.5	0.007±0.002	686
Camas Creek-SW	6-28-1995	2.5±0.4	0.006±0.002	417
Little Lost River-SW	6-28-1995	23±9	0.044±0.011	523
Galena Creek Rock Glacier-GR	8-30-1995	0.079±0.004	0.0015±0.0004	53
Upper Fremont Glacier Ice, 30.4-31.1 meters, IC	1991	0.09±0.02	0.0011±0.0003	45
Upper Fremont Glacier Ice, 31.1-31.5 meters, IC	1991	0.2±0.04	0.0006±0.0002	633
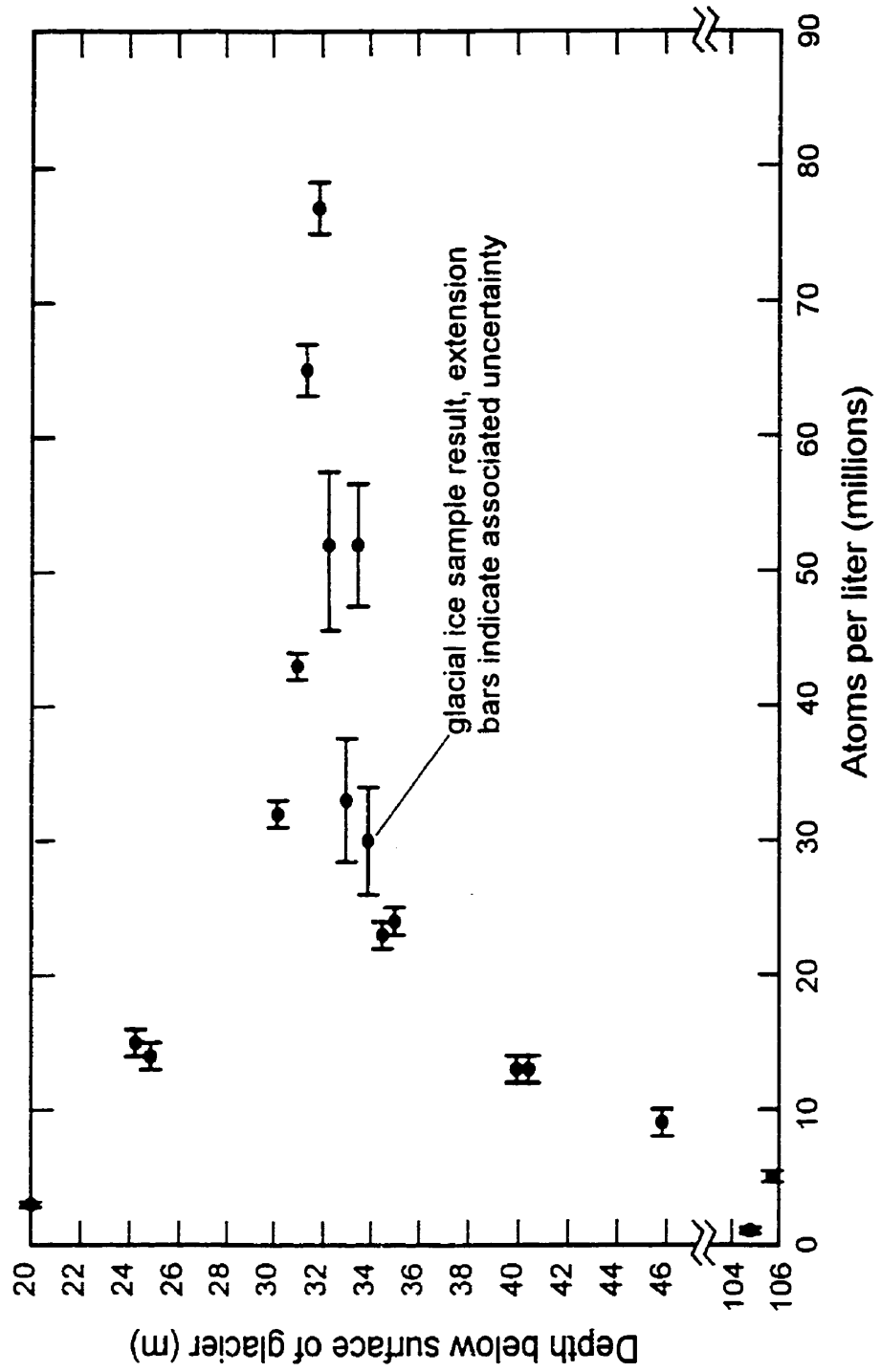
Figure 5.3. Chlorine-36 concentrations in glacial-ice samples, Upper Fremont Glacier, Wind River Range, Wyoming.

73

Table 5.3. Dissolved chloride content, amount of chlorine-36-free chloride carrier added to sample, chlorine-36 content and calculated fluxes for selected ice core sections collected in the summer of 1991 from the Upper Fremont Glacier, Wyoming.

[Symbols; PO, post-weapons test era; PR, pre-weapons test era.]

Depth below glacial surface (m)	Core length (m)	Dissolved chloride (mg/L) ± 20 percent	^{36}Cl-Free chloride carrier (mg)	Corrected *in situ* ^{36}Cl/Cl ($\times 10^{-15}$)	^{36}Cl concentration, water equivalent (atoms/L $\times 10^{8}$)	^{36}Cl Flux (atoms/cm^{2})/ secx10^{-1})
19.6-20.5, PO	0.9	0.19	1.03	860±80	0.028±0.003	0.11±0.02
24.0-24.5	0.5	0.25	0.85	3,900±100	0.17±0.006	0.63±0.03
24.5-25.0	0.5	0.11	0.99	7,600±200	0.14± 0.004	0.54±0.02
29.8-30.4	0.6	0.08	1.71	24,000±1,000	0.32± 0.01	1.2±0.1
30.4-31.1	0.7	0.09	1.69	28,000±1,000	0.43± 0.01	1.6±0.1
31.1-31.5	0.4	0.20	1.44	19,000±1,000	0.65± 0.02	2.5±0.1
31.5-32.0	0.5	0.16	1.69	28,000±1,000	0.77± 0.02	2.9±0.1
32.0-32.5	0.5	0.14	1.08	23,000±3,000	0.55± 0.07	2.1±0.3
32.5-33.1	0.6	0.13	1.00	16,000±2,000	0.34± 0.05	1.3±0.2
33.1-33.6	0.5	0.38	0.95	9,600±1,000	0.62± 0.06	2.4±0.2
33.6-34.2	0.6	0.12	1.02	16,000±2,000	0.32± 0.04	1.2±0.1
34.2-34.8	0.6	0.14	1.02	9,900±200	0.24± 0.01	0.90±0.02
34.8-35.3	0.5	0.38	1.02	4,300±100	0.28± 0.01	1.1±0.02
39.6-40.2	0.6	0.18	0.80	4,500±200	0.14± 0.005	0.53±0.01
40.2-40.6	0.4	0.09	0.81	8,900±300	0.14± 0.005	0.52±0.01
45.2-46.4	0.8	0.35	1.03	1,900±255	0.11± 0.002	0.49±0.07
104.7-105.5, PR	0.8	0.19	1.81	370±60	0.012± 0.002	0.045±0.007
105.5-106.3, PR	0.8	0.07	1.87	4,400±300	0.052± 0.004	0.20±0.02

74

However, a more quantitative comparison between the mid-latitude ice-core results and modern ^{36}Cl deposition over the continental United States can be made with some confidence. Knies and others (1994) reported an average ^{36}Cl concentration in wet fallout of 1.7×10^6 atoms/L, the volume-weighted average from measurements of all significant rainfall events during April 1992 and August 1993 at their field site in central Indiana. Similar ^{36}Cl concentrations in wet precipitation have been reported by Hainsworth and others (1994) for the east coast of the United States; the average for the period from February 1991 to January 1993 was $1.7\pm0.2 \times 10^6$ atoms/L. These averaged concentrations for wet precipitation agree well with the range of ^{36}Cl concentrations measured in pre- and post-bomb sections of the Upper Fremont Glacier ice core; $1.2\pm0.2 \times 10^6$ to $5.2\pm0.4 \times 10^6$ atoms/L water equivalent (table 5.3, figure 5.3). These concentrations also compare well with the two snow samples collected near the INEEL in 1991 and the glacial-runoff sample from the Galena Creek Rock Glacier collected in 1995 (table 5.1). The ^{36}Cl concentration in the Harriman State Park snow sample was $6.3\pm0.9 \times 10^6$ atoms/L, the concentration in the Copper Basin snow sample was $4.9\pm2.5 \times 10^6$ atoms/L, and the concentration in the Galena Creek Rock Glacier sample was $3.2\pm0.5 \times 10^6$ atoms/L (table 5.1). (The concentration of ^{36}Cl in the snow sample from Copper Basin was used in this dissertation for comparison purposes even though the concentration has a 50 percent associated uncertainty.)

Mean wet deposition fluxes of ^{36}Cl derived from these studies were $6.79\pm0.47 \times 10^{-3}$ atoms/cm^{2}sec (Knies and others, 1994), $3.86\pm0.54 \times 10^{-3}$ atoms/cm^{2}sec (Hainsworth and others, 1994), and $8.28\pm0.91\times 10^{-3}$ atoms/cm^{2}sec for pre- and post-bomb flux for the Upper Fremont Glacier. The wet-only flux determined in the central and the western United States appears to be about a factor of two larger than the flux for the eastern United States at similar latitudes. The mean non-weapons tests flux for the Upper Fremont Glacier site was determined by averaging the values in table 5.3 above 24.0 m and below 46.4 m in depth; this minimized the contribution of fallout from nuclear-weapons tests in the 1950-60s. The resulting mean flux was then reduced by

30 percent to account for dry deposition of ^{36}Cl (Hainsworth and others, 1994). The mean flux for the two snow samples collected near the INEEL in 1991 was 7.5±0.2 × 10^{-3} atoms/cm^{2}sec and for the Galena Creek Rock Glacier runoff the estimated flux was 16±2 × 10^{-3} atoms/cm^{2}sec. The average precipitation rates used to calculate the fluxes for the snow samples and the glacial-runoff sample were; 58 cm/year for Harriman State Park (L.L. Jones, Idaho Department of Parks and Recreation, oral commun., 1996); 2) 22 cm/year for INEEL #1 and #2 (Clawson and others, 1989, table D-1); 3) 18 cm/year for Copper Basin (S.M. Spencer, U.S. Forest Service, written commun., 1996); and 4) 160 cm/year for Galena Creek Rock Glacier (see discussion of precipitation rate for the Upper Fremont Glacier below). The precipitation rates used in calculation of ^{36}Cl flux for the four snow samples did not account for ET. Therefore, these calculated fluxes should be considered as minimum and may be increased by nearly two orders of magnitude due to evapotranspiration (Appendix tables C-4 and C-5). These calculations are much more sensitive to evapotranspiration rates than to average annual precipitation rates. The effects of ET on meteoric concentrations will be discussed in section 5.3.6, "Comparison of *In Situ* Produced Chlorine-36 with Other Sources".

In a detailed discussion of the radionuclide contents in the Upper Fremont Glacier ice core, more subtle effects such as dry deposition of ^{36}Cl, seasonal effects, and thawing-freezing cycles of the upper ice layer may play important roles. For instance, the total wet precipitation and dry fallout, ^{36}Cl flux determined by Hainsworth and others (1994) was 5.85±0.78 × 10^{-3} atoms/cm^{2}sec, about 30 percent higher than the wet-only precipitation flux. Non weapons-tests ^{36}Cl fluxes derived from the Upper Fremont Glacier ice core, again, assuming a constant net accumulation rate of 80 cm/yr, are also of similar magnitude; 4.5±0.7 × 10^{-3} to 20±2 × 10^{-3} atoms/cm^{2}sec, table 5.3. Hainsworth and others (1994) showed that the dry deposition of ^{36}Cl can account for about 30 percent of the total input as inferred from a direct comparison of analyses performed on samples collected in open (for dry deposition) and wet-only collectors. Significant

0.40

Dissolved chloride (milligrams per liter)

0.35

0.30

0.25

0.20

0.15

—O— NADP Station, Pinedale, Wyoming
—●— Knife Point Glacier, Wyoming
Correlation coefficient = 0.98

1981 1982 1983 1984 1985 1986 1987 1988
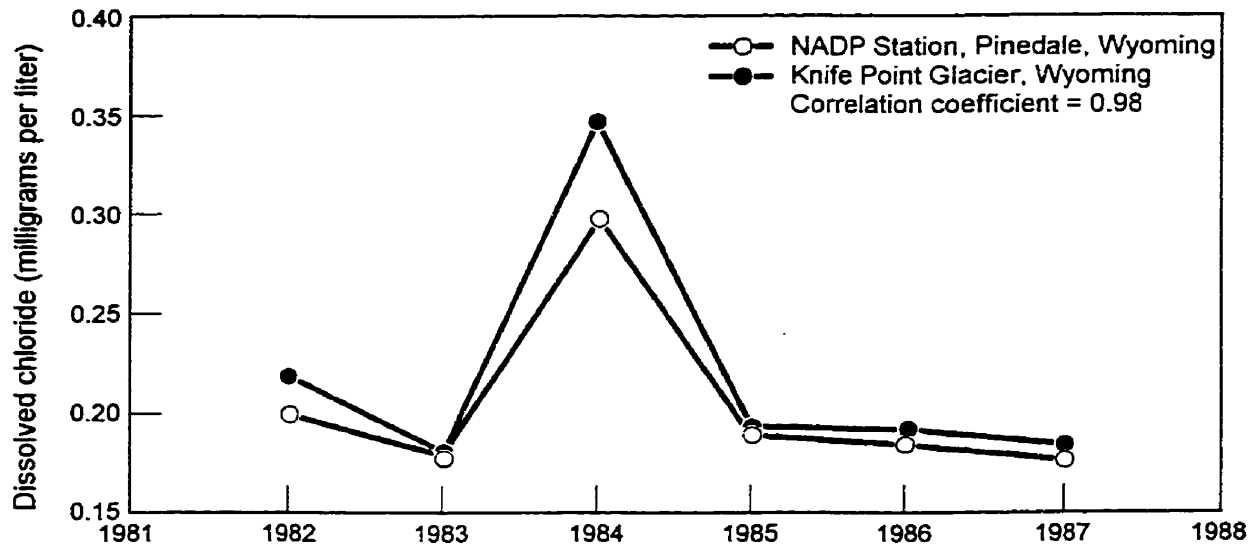
Figure 5.4.   Comparison of dissolved-chloride concentration in annual ice layers with the annual-weighted dissolved-chloride concentration at the National Atmospheric Deposition Program station near Pinedale, Wyoming.

Note: This figure was modified from Naftz and others, 1991.

seasonal effects have been reported by Knies and others (1994) for ^{36}Cl and other cosmogenic nuclide deposition, while recurring thawing-freezing events, resulting in downward percolation of meltwater in the ice core stratigraphy, will obscure any seasonal or other cyclic event preserved in the ice. All these variables might play a role in the fine structure of the results. However, these factors are of no immediate concern to the proper interpretation of the results presented in this dissertation as evidenced by data presented here and by related studies such as Naftz and others, 1991 (see below). It should be noted, however, that some ice- core sections analyzed here most likely do not cover a complete annual cycle so that any one or a combination of the effects outlined above might bear some significance in the interpretation.

In 1991, Naftz and others reported on a reconnaissance study to determine the relation between concentrations of selected chemical species dissolved in wet precipitation compared to the concentrations of the same species dissolved in annual ice layers collected from the Knife Point glacier in Wyoming's Wind River Range (fig. 5.3). Constituent concentrations calculated from annual-weighted means of wet deposition samples from the NADP station near Pinedale,

Wyoming (figure 1.4) for the years 1982-87 were compared to concentrations in the annual ice layers (fig. 5.5). The Cl⁻ concentrations in the deposition samples and in the corresponding ice layers showed a significant correlation coefficient of 0.98, indicating that, for determining Cl⁻, temperate glaciers from the Wind River Range may not be subject to severe meltwater contamination problems. Additionally, these data indicate that the annual ice layers may provide a reliable long-term record of the chemical composition of precipitation.

However, as shown in figure 5.5, the dissolved Cl⁻ concentrations in the annual ice layers at Knife Point glacier were consistently larger than the Cl⁻ concentrations in the annual-weighted wet deposition samples at the NADP station near Pinedale. This is further evidence that dry deposition of Cl⁻ may influence the dissolved concentrations in precipitation and ice as reported by Hainsworth and others (1994, up to 30 percent of total deposition) and by Sterling (2000, up to 60 percent of total deposition in Idaho).

Long-term records of accumulation and ablation of snow, firn, and ice were not available for the Upper Fremont Glacier location. Therefore, accumulation and ablation were calculated according to the following method to facilitate the estimation of an annual average precipitation flux for this site. An average annual accumulation flux of 80 g/cm^2yr was calculated using average core densities reported by Naftz (written communication, 1996) of 0.65 g/cm^3 for the 0- to 14-m section and 0.89 g/cm^3 for the remaining core down to the measured bomb ^3H peak at 29 m. An average annual accumulation flux of 76 g/cm^2yr was calculated using these same densities down to the depth of the measured ^{36}Cl peak at about 32 m. This average annual accumulation flux was in good agreement with the flux determined from the ^3H peak, 80 g/cm^2yr, Naftz (1992).

To account for all ^{36}Cl deposited at this high-altitude, mid-latitude site, ablation of snow, firn, and ice was also considered in the average annual precipitation flux for this study. Naftz and others (1996) reported an average ablation for 1990-91 at five sites on the Upper Fremont Glacier of 93 cm/yr. This cumulative ablation rate agreed well with the average annual ablation rate of 88 cm/year calculated by Marston and others (1991) on the Dinwoody Glacier for 1958-83.

78

Dinwoody Glacier is approximately 5 km north of the Upper Fremont Glacier and is at the same altitude (fig. 5.3).

Using the 88 cm/yr average annual rate and an assumed density of 0.5 g/cm^3, the average annual precipitation flux lost by ablation was estimated at 44 g/cm^2yr. The accumulated precipitation flux calculated from the ^{36}Cl bomb peak at 32 m depth was 76 g/cm^2yr. Considering accumulation and ablation, the combined average annual precipitation flux for this site was approximately 120 g/cm^2yr. This estimated average annual precipitation flux was used with the measured ^{36}Cl concentrations in atoms/L (table 5.3) to calculate ^{36}Cl fluxes. These ^{36}Cl fluxes are a first approximation only and are based on an estimated precipitation flux as described above. Estimated weapons-tests fluxes for the ten sections of ice between 29.8 and 35.3 m in depth range from $9.0\pm0.2 \times 10^{-2}$ to $2.9\pm0.1 \times 10^{-1}$ atoms/cm^2sec (table 5.3). These fluxes are up to two orders of magnitude larger than the mean global natural-production flux for ^{36}Cl (1.1×10^{-3} atoms/cm^2sec; Lal and Peters, 1967) and compared well with the weapons-tests flux reported by Elmore and others (1982) of 5×10^{-1} atoms/cm^2sec for the Dye-3 ice core from Greenland, deposited during the same period of time as the Upper Fremont Glacier ice. This continuous section of ice core represents the minimum ^{36}Cl produced by nuclear-weapons tests in the 1950-60s that was deposited at this site due to the assumption being made concerning ablation and the use of averages for precipitation flux. For the ice selected to represent pre-bomb tests ^{36}Cl flux centered at 105.1 m and 105.9 m, the estimated flux was $4.5\pm0.7 \times 10^{-3}$ and $2.0\pm0.2 \times 10^{-2}$ atoms/cm^2sec, respectively.

It is not understood at this time why the calculated flux of the section of ice centered at a depth of 105.9 m was nearly five times larger than the reported mean global average. The section of ice centered at 20.1 m had a calculated ^{36}Cl flux of $1.1\pm0.2 \times 10^{-2}$ atoms/cm^2sec and is representative of post-weapons fluxes. The sections of ice between 39.6 and 46.4 m had a range of calculated ^{36}Cl fluxes from $4.7\pm0.7 \times 10^{-2}$ to $5.3\pm0.1 \times 10^{-2}$ atoms/cm^2sec and most likely had a

component of weapons-tests produced ^{36}Cl. Additionally, the two sections of ice centered at 24.25 and 24.75 m had calculated ^{36}Cl fluxes of 6.3±0.3 × 10^{-2} and 5.4±0.2 × 10^{-2} atoms/cm^{2}sec respectively; these fluxes also probably had a component of weapons-tests-produced ^{36}Cl.

In terms of atom/L concentrations in water equivalent, the largest value for bomb ^{36}Cl identified in the Upper Fremont Glacier ice core was 7.7±0.2 × 10^7 atoms/L at a depth of about 32 m (table 5.3). This concentration is more than an order of magnitude larger than the meteoric concentration in water from Big Spring (1.4±0.1 × 10^6 atoms/L), Galena Creek Rock Glacier (3.2±0.5 × 10^6 atoms/L), the snow samples at Harriman State Park and Copper Basin (6.3±0.9 × 10^6 and 4.9±2.5 ×10^6 atoms/L, respectively), and the calculated long-term average concentration in precipitation at the Craters of the Moon NADP station (1.5 × 10^6 atoms/L). This concentration is about 1.5 to 2.5 orders of magnitude smaller than the concentrations in the two snow samples (INEEL #1, #2; table 5.1) collected during nuclear-fuel reprocessing operations at the INEEL and is nearly six orders of magnitude less than the atom concentrations in ground water from USGS 77 near the INTEC (table 5.1). All of the ice samples processed from the Upper Fremont Glacier had atom/L concentrations of ^{36}Cl that plotted below the 1.5 × 10^8 line in figure 5.2 suggesting that this value is the maximum for combined weapons-tests and meteoric ^{36}Cl concentrations in environmental samples collected in southeastern Idaho and western Wyoming.

5.3   *In Situ* Production: Analyses and Calculations

The purpose of this section is to estimate the contribution to ground water of natural, *in situ* produced ^{36}Cl in the eastern Snake River Plain aquifer system and to compare these concentrations in ground water to measured concentrations near the INEEL. Twenty-five samples from the six major water-bearing rock types (basalt, rhyolite, limestone, dolomite, shale, and quartzite) in the Snake River Plain aquifer system were evaluated for *in situ* ^{36}Cl production. Calculated ratios of ^{36}Cl/Cl in these rocks ranged from 1.4 × 10^{-15} for basalt to 45 × 10^{-15} for

rhyolite. The associated neutron production rates calculated for these rock types were 2.5 neutrons per gram of rock per year ((n/g)/yr) for the basalt and 29 (n/g)/yr for the rhyolite. The larger neutron production rate for the rhyolite is due to the larger U (11.5 ppm) and Th (22.2 ppm) concentration of the rhyolite; for comparison, the U and Th concentrations of the basalt were 0.8 ppm and 2.23 ppm, respectively. The calculated contribution included the estimation of neutron production rates based on the elemental composition of the rock samples and the proportion of the resultant neutrons that may be captured by Cl atoms within the rock to produce ^{36}Cl (Appendix tables C-6 and C-7).

Considering the Cl$^-$ concentration and minimum rock porosity with the calculated ^{36}Cl/Cl ratios, the estimated maximum corrected concentrations of ^{36}Cl in ground waters associated with the rock types analyzed in this study ranged from 2.45×10^5 atoms/L for ground water in the basalt to 7.68×10^6 atoms/L for ground water in the rhyolite (Appendix table C-8 and figure C-1). These values are six orders of magnitude smaller than concentrations measured in ground water at and near the INEEL. A ^{36}Cl concentration of $2.8 \pm 0.09 \times 10^{12}$ atoms/L has been measured in a ground water sample collected near the INTEC (USGS 57, table 2.1). Additionally, *in situ* ^{36}Cl/Cl ratios in ground water from rock with average compositions from this study ranged from 4.0×10^{-15} to 33.3×10^{-15}. For comparison, the range of ^{36}Cl/Cl for the 70 ground water samples collected from the Snake River Plain aquifer for this research at and near the INEEL was $47.7 \pm 0.2 \times 10^{-14}$ to $2.1 \pm 0.06 \times 10^{-9}$.

Determining the contribution of *in situ* production to ^{36}Cl inventories in ground water facilitated the identification of the source for this radionuclide in environmental samples. Based on the calculations in this dissertation, *in situ* production of ^{36}Cl was determined to be insignificant compared to concentrations measured in ground water near buried and injected nuclear waste at the INEEL. Maximum estimated ^{36}Cl concentrations in ground water from *in*

situ production are on the same order of magnitude as natural concentrations in meteoric water.

As described earlier in this dissertation, there are four sources of ^{36}Cl in the eastern Snake River plain aquifer; (1) natural production by cosmic ray interaction with ^{40}Ar and neutron activation of ^{36}Ar in the upper atmosphere that is then transported through the hydrologic environment as meteoric concentrations in precipitation (Cecil and others, 1999); (2) production by neutron activation of stable ^{35}Cl during nuclear-weapons tests of the 1950s-60s (Cecil and Vogt, 1997); (3) ^{36}Cl released during nuclear-waste processing at the INEEL (Cecil and others, 1992, 1998, 1999; Beasley and others, 1993); and (4) natural *in situ* production in the aquifer matrix at depth due primarily to neutron activation of stable ^{35}Cl. This section describes the contribution of *in situ* production, in the aquifer matrix at depth, to ^{36}Cl inventories measured in ground water. Meteoric, weapons tests, and nuclear-waste processing contributions to ^{36}Cl inventories have already been described earlier in this chapter (sections 5.1 and 5.2) and in the open literature by this author and colleagues (Cecil and others, 1992, 1998, 1999).

In this research, the solid-phase (rock) samples are designated SP, and their locations are shown on figure 1.1. The basalt flows that comprise the majority of the Snake River Plain are in layers of only a few meters thick and cover areas of tens to hundreds of square kilometers. Samples SP-15, SP-16, SP-18, SP-19, SP-20, SP-21, and SP-22 are representative of younger basalts on the eastern Snake River Plain (Appendix table A-1). Large-scale basalt flows, such as those in Oregon and Washington, have not been found in the Snake River Plain. The most recent volcanic eruptions on the Snake River Plain were at the Craters of the Moon National Monument (fig. 1.1) around 2,000 years ago (Kuntz and others, 1988).

Volcanism produced relatively thick flows of welded tuff, ash, and pumice that are exposed within and near the margins of the basin and are composed largely of rhyolite, latite, and andesite. The rhyolitic tuffs and rhyolite in this group are represented by samples SP-5, SP-6, SP-7, SP-8, SP-9, SP-10, SP-13, SP-17, and SP-23 (Appendix table A-1). Subsequent basalt

volcanism over the entire basin was predominately limited to outpourings of pahoehoe lava (Nace and others, 1975). Some eruptions however, such as the ones near Craters of the Moon, were violent enough to create pyroclastic rocks and significant deposits of cinders. None of these pyroclastic deposits are major aquifers in the basin. Pre-Cretaceous sedimentary and metamorphic rocks border the basin to the northwest and east and are represented in this study by samples SP-1, SP-2, SP-3, SP-4, SP-11, SP-12, SP-24, SP-25, and SP-26 (Appendix tables A-2 and A-3). Of the six rock types studied, basalt and rhyolite comprise the majority of the aquifer on the Plain and limestone and dolomite, with minor shale, quartzite, and medasediments, comprise the recharge areas to the north, west, and east.

The rock samples were submitted to the Idaho State University (ISU), Department of Geology, Geochemical Laboratory for elemental analysis. The geochemical laboratory prepared samples for analysis by three separate analytical methods, inductively coupled plasma-atomic emission spectrometry (ICP-AES), instrumental neutron activation analysis (INAA), and loss on ignition (LOI). In addition, selected solid-phase samples were submitted to the USGS, Branch of Geochemistry, to determine Cl⁻ concentration by ion-selective electrode potentiometry (ISEP). The data were received from the two laboratories and were processed into the form needed to make *in situ* production calculations for ^{36}Cl. The processed laboratory geochemical data are presented in Appendix tables A-1, A-2, and A-3.

5.3.1   Field Methods for *In Situ* Sample Collection

For the *in situ* ^{36}Cl production calculations it was assumed that the dominant mechanism of production was neutron activation of stable ^{35}Cl. At depths greater than about 10 m in most rocks, this assumption holds (Fabryka-Martin, 1988, tables h-3a through h-3h; Gifford and others, 1985, p. 418, Phillips, 2000, p. 304). Although some of the whole-rock samples collected for this study were collected from the upper 2 to 5 m of the rock formation at land surface and may have undergone some changes due to weathering, the chemical data presented in Appendix tables A-1,

83

A-2, and A-3 are assumed to be representative of the entire depth of the rock type both temporally and spatially. For basalt and rhyolite samples SP-15 through SP-21 (Appendix table A-1), the depth of collection was greater than 50 m in all cases; these samples were extracted from rock cores housed in the USGS Lithologic Core Library at the INEEL. All whole-rock samples were collected from fresh exposures or cores using standard methods and powderless gloves to minimize contamination.

5.3.2   Analytical Methods for *In Situ* Sample Processing

Sample processing for each of the following analytical methods began with the preparation of a homogeneous powdered sample. Each powdered sample subsequently underwent processing according to the specific analytical method to be applied. Additionally, rock samples sent to the ISU Geochemical Laboratory for analyses were further processed to insure that unweathered samples were used for all analyses. The analytical methods will be discussed in detail to aid in understanding how and why the resultant laboratory data were used in the *in situ* ^{36}Cl production calculations.

5.3.2.1 Inductively Coupled Plasma-Atomic Emission Spectroscopy (ICP-AES)

For analyses by ICP-AES, the sample must be prepared as a solution (Lichte and others, 1987). There are a variety of methods to prepare the solution and each method has advantages that are related to sample composition. Sequential acid dissolution using hydrofluoric acid (HF), aqua regia, perchloric acid ($HClO_4$), and HNO_3 is one procedure that has the disadvantage that Si and B are lost because of their volatility as fluorides. Several trace minerals, including chromite, are not completely dissolved by this procedure. Because of the silicic composition of volcanic rocks in the Snake River Basin, a fusion method of preparing sample solutions was used by the ISU laboratory as opposed to the sequential acid dissolution method.

The fusion method uses a flux to convert the sample to a glass bead, which is subsequently dissolved in dilute HNO_3 to prepare a solution for analysis. The specific procedure

used by the ISU Geochemical Laboratory involved mixing 0.1 g of powdered sample and 0.3 g of lithium metaborate in a graphite crucible and heating in a furnace for 20 minutes at 1,050 degrees °C. The contents of the crucible were immediately poured into 75 mL of 3.5 percent HNO_3 in a 250-mL beaker and stirred on a magnetic stirrer for five minutes or until the sample was clear. The contents of the beaker then were transferred to a 100-mL volumetric flask, and more dilute HNO_3 was added to bring the volume to 100 mL. The flask was capped and gently shaken to thoroughly mix the contents. Sample bottles were pretreated by rinsing with 5 mL of the sample solution that was then discarded. The pretreated sample bottle then was filled with 50 mL of the sample solution and was ready for analysis by ICP-AES. The ISU laboratory reported weight percent values for oxides of the following elements: Si, Na, titanium (Ti), Al, manganese (Mn), magnesium (Mg), calcium (Ca), potassium (K), and phosphorus (P). Using this method, the laboratory also determined strontium (Sr), zirconium (Zr), and yttrium (Y) concentrations in units of ppm by weight.

5.3.2.2 Instrumental Neutron Activation Analysis (INAA)

For analyses by INAA, a precisely known amount of powdered sample needs to be prepared to undergo irradiation without the loss of sample (Baedecker and McKown, 1987). The laboratory placed one g or less of powdered sample, weighed to the nearest milligram, into a 0.4-dram, reactor-safe, laboratory-grade polyvial, which then was heat-sealed. The 0.4-dram polyvial then was heat-sealed into a 2-dram, reactor-safe, laboratory-grade polyvial. Preparation for neutron activation then was complete. For calibration purposes, three reference standards were included with the samples: USGS rock standards BCR-1 and BHVO-1 and the National Institute of Science and Technology (NIST) traceable coal fly ash standard reference material (SRM) 1633-A.

The prepared standards and samples were sent to the Oregon State University Radiation Center for neutron activation in the TRIGA Reactor. Neutron activation lasted two hours under a

neutron flux of 3×10^{12} (n/cm^2)/sec. Once activated, the standards and samples were returned to ISU for analysis. Upon arrival at the laboratory, the inner 0.4-dram polyvials were transferred into new 2-dram polyvials for gamma counting.

Activation analysis is based on measurement of activity from radioactive nuclides produced by nuclear reactions on naturally occurring isotopes of the sample elements during the activation process. Gamma-ray spectroscopy at the ISU Geochemical Laboratory employed semiconductor detectors (high-purity germanium diodes) for gamma counting. These devices converted a gamma- ray signal from the irradiated samples to electronic pulses that could be sorted and processed by a multichannel analyzer and supporting electronics. The resulting spectra then were processed by computer software and the results were recorded. All standards and samples were counted three separate times in a sequence that optimized peak-to-background ratios for short-, intermediate-, and long-lived radionuclides, respectively. The first counts were for determining the short-lived radionuclides of Na, samarium (Sm), lanthanum, and U, and took place about five days after irradiation. The count periods were between 2,000 and 4,000 seconds. The next counts were for the intermediate-lived radionuclides of barium, rubidium, neodymium, ytterbium, and lutetium, and took place about 10 to 20 days after irradiation. The count periods were 8,000 to 10,000 seconds. The final counts were for the long-lived radionuclides of Fe, scandium, chromium, nickel, cobalt, cesium, cerium, europium, terbium (Tb), Th, hafnium, and tantalum, and took place about 30 to 40 days after irradiation. The count periods were 20,000 to 40,000 seconds. Results were reported in ppm by weight, except Na and Fe, which were reported as oxides of the elements in weight percent.

5.3.2.3 Loss on Ignition (LOI)

For analyses by LOI at the ISU Geochemical Laboratory, precisely 2 g of powdered sample weighed to within 0.0005 of a gram was placed in a clean ceramic crucible. The weight of the crucible and powder were determined and recorded. The open crucibles were heated

overnight (or for about 12 hours) at 90 °C. The crucibles were removed to a dessicator, cooled for two to three minutes, and reweighed. These raw weights were recorded and subtracted from the weights of the unheated crucibles and powdered sample. The difference represented the weight of volatile components that are not actually part of the sample. The samples were returned to a dessicator and a muffle furnace was heated to 950 °C. When the muffle furnace reached this temperature, lids were placed on the crucibles and they were heated for one hour. The crucibles were cooled two minutes, then the lids were removed and the crucibles were allowed to continue cooling in the dessicator until they reached room temperature (about five to seven minutes). After cooling, the weights of the crucibles were determined and subtracted from the raw weight of the crucible and sample determined previously. The weight difference in grams represents the LOI component of the sample. The difference was divided by the original sample weight (2 g ± 0.0005 g) and multiplied by 100. This value was reported along with the elemental oxides as LOI in weight percent.

5.3.2.4 Ion-Selective Electrode Potentiometry (ISEP)

For analyses of Cl^- by ISEP, 200 mg of powdered sample were weighed and placed into a confined area of the outer compartment of a Conway diffusion cell constructed of Teflon (Aruscavage, 1990). Oxidizing and reducing solutions were prepared. The reducing solution was made of 22.6 g of potassium hydroxide dissolved in 140 mL of deionized water and 1.12 g of anhydrous sodium sulfite. A 2.5-mL aliquot of reducing solution was pipetted into the inner compartment of the Conway diffusion cell. The oxidizing solution was made of 160 mL of HF added to a solution that contained 2.6 g of potassium permanganate ($KMnO_4$) dissolved in 50 mL of 15 percent sulfuric acid (H_2SO_4). A 3-mL aliquot of the oxidizing solution was added to the outer compartment of the Conway diffusion cell and digested the powdered sample by mixing overnight on an oscillating platform. The evolved Cl was converted to Cl^- by the reducing solution contained in the inner compartment of the Conway diffusion cell. Finally, the Cl^-

concentration was measured by an ISEP. The applicable concentration range for Cl⁻ by this method was 0.01 to 2.00 percent by weight, or 100 to 20,000 ppm by weight.

5.3.3 Data Reduction for In Situ Chlorine-36 Production Calculations

The methods used to determine the maximum *in situ* produced atom concentrations for ^{36}Cl in ground water have been documented in reports by Fabryka-Martin (1988) and Andrews and others (1989) and will be discussed in the section titled "Estimation of Neutron Production Rates and Chlorine-36 Production". Geochemical data for the rock samples generated by contract laboratories and used in this dissertation were converted for use in the necessary *in situ* production calculations using ion-specific methods described in the following sections.

5.3.3.1 Chloride

Results generated by the USGS Branch of Geochemistry were reported as percent by weight Cl⁻ with a reporting level of 0.01 percent. These numbers were converted directly to ppm by weight using the following equation:

$$(\text{weight percent Cl}^-/100) \times 1,000,000 \text{ g} = \text{ppm by weight Cl}^- \qquad (5.3\text{-}1)$$

For example, (0.04 weight percent Cl⁻/100) × 1,000,000 g = 400 ppm by weight Cl⁻.

Fourteen solid phase samples were selected for determination of Cl⁻ concentration. For the 11 of 14 Cl⁻ results that were larger than the reporting level, the converted results were used directly in Appendix tables A-1, A-2, and A-3. The Cl⁻ concentrations for the three samples that were determined to be less than the reporting level and for the samples that were not analyzed for Cl⁻ (marked with an asterisk in Appendix tables A-1, A-2, and A-3) were taken from a report by Parker (1967, table 19, p. D13-D14).

5.3.3.2 Gadolinium

Gadolinium (Gd) has the largest thermal neutron absorption cross section (49,000

barns/atom, table 5.4) of all major and trace elements used in the *in situ* calculations. Therefore, the determination of Gd in the rocks of the eastern Snake River Plain was essential for determining the total cross section of the rock available for thermal neutron absorption. As an example, table 5.4 lists the data used to calculate the thermal neutron cross section for neutron absorption, total neutron production rate, and *in situ* secular equilibrium $^{36}Cl/Cl$ ratio for sedimentary rock sample SP-1, a limestone. The data used for these calculations for the 25 whole-rock samples are given in Appendix tables B-1 (igneous rocks), B-2 (Sedimentary rocks), and B-3 (metamorphic rocks). The ISU Geochemical Laboratory reported concentrations of Sm and Tb directly in ppm; however, the laboratory did not determine Gd content.

Because Gd concentrations were needed to calculate *in situ* production of ^{36}Cl, and because the relationships between concentrations of Sm, Tb, and Gd in chondritic meteorites and terrestrial materials are systematic, the correlation among these three elements in chondritic meteorites and the measured concentrations of Sm and Tb in the samples were used to estimate Gd concentrations by interpolation. The Gd concentrations were calculated by normalizing the measured concentrations of Sm and Tb to their non-volatile mass concentrations in carbonaceous chondritic meteorites (designated the C1-chondrite) using values tabulated by Anders and Ebihara (1982, table 1). The values from Anders and Ebihara first were converted to non-volatile mass concentrations by subtracting volatile elements from the total, then normalizing to 100 percent. This process yielded appropriate values to which terrestrial samples were normalized using the following equations (Scott Hughes, ISU, written communication; 1999):

$$(Sm-N) = (Sm)/0.197, \text{ and} \tag{5.3-2}$$

$$(Tb-N) = (Tb)/0.047 \tag{5.3-3}$$

where

(Sm-N)	= C1-chondrite normalized concentration of samarium
(Sm)	= measured concentration of samarium in ppm

Table 5.4. Example of data used to calculate thermal neutron cross section for neutron absorption, total neutron production rate, and *in situ* secular equilibrium ^{36}Cl/Cl ratio for sedimentary rock sample SP-1, limestone.

[See figure 1.1 for location of sampling site. See text for explanation of Mass Stopping Power, Weighting Factor, X and Y factors, Weighted Neutron Yields, and Thermal Cross Sections. Mass Stopping Power, Neutron Yields, and Absorption Cross Sections supplied by Fabryka-Martin (1995). Mass Stopping Power is given for each element for an alpha particle of energy 8.0 million electron volts (MeV). Mass Stopping Power units: MeV per gram of rock per square centimeter. Sample parts per million (ppm) from Appendix table A-2; cm^2/g, square centimeters per gram; <, less than. See Appendix tables A-1, A-2, and A-3 for data for these calculations for all 25 whole rock samples.]

Element	Mass Stopping Power	Neutron Yield		Sample ppm	Weighting Factor	Weighted Neutron Yield	
		n/yr/g rock per ppm U	n/yr/g rock per ppm Th			n/yr/g rock per ppm U	n/yr/g rock per ppm Th
Si	454	0.69	0.339	7947	3.61	2.49	1.22
Al	444	5.116	2.585	1376	0.61	3.13	1.58
Fe	351	0.187	0.208	233	0.08	0.02	0.02
Ca	428	0.282	0.026	382508	163.71	46.17	4.26
Mg	461	5.834	2.564	4522	2.08	12.16	5.35
Na	456	12.535	5.959	74	0.03	0.42	0.20
K	414	0.89	0.08	415	0.17	0.15	0.01
P	433	4.473	0.573	87	0.04	0.17	0.02
Li	548	23.86	10.54	5	0.003	0.07	0.03
Be	529	265.948	91.561	0.5	0.0003	0.07	0.02
B	527	62.551	19.779	20	0.01	0.66	0.21
C	561	0.456	0.179	118201	66.31	30.24	11.87
F	472	41.33	16.362	330	0.16	6.44	2.55
O	527	0.236	0.084	483838.35	254.98	60.18	21.42
				Total 999556.85	491.80	162.35	48.76

Element	Atomic Weight (amu)	Sample ppm	Neutron Absorption Cross Section (barns/atom)	Thermal Neutron Cross Section (cm^2/g)
Si	28.1	7947	0.17	0.000029
Al	27.0	1376	0.233	0.000007
Fe	55.8	233	2.56	0.000006
Ca	40.1	382508	0.43	0.002469
Mg	24.3	4522	0.063	0.000007
Na	23.0	74	0.53	0.000001
K	39.1	415	2.1	0.000013
P	30.97	87	0.18	<0.000001
Li	6.9	5	71	0.000031
Be	9.01	0.5	0.0092	<0.000001
B	10.8	20	764	0.000852
C	12.0	118201	0.0035	0.000021
F	19.0	330	0.0096	<0.000001
H	1.0	340.37	0.33	0.000068
Ti	47.9	60	6.1	0.000005
Mn	54.9	77	13.3	0.000011
Sm	150.4	0.39	5600	0.000009
Gd	157.3	0.34	49000	0.000064
O	16.0	483838.35	0.00028	0.000005
		Total 1000034.95		0.0036

Neutron Production Rate (n/g/yr)

(X factor = 0.330) (Total U ppm = 1.9) = 0.67

(Y factor = 0.099) (Total Th ppm = 0.1) = 0.0099

^{238}U spontaneous fission = 0.815

Total neutron production rate (n/g/yr) = 1.5

Calculated
In Situ Secular
Equilibrium ^{36}Cl/Cl
Ratio ($\times 10^{-15}$) = 5.9

90

0.197   = Cl-chondrite total mass for samarium converted to non-volatile

(Tb-N)   = Cl-chondrite normalized concentration of terbium

(Tb)   = measured concentration of terbium in ppm, and

0.047   = Cl-chondrite total mass for terbium converted to non-volatile

            mass in ppm

The normalized concentrations of Sm and Tb then were used to calculate the normalized

concentration of Gd:

$$(Gd\text{-}N) = 10^{[\log\,(Sm\text{-}N)\,+\,2\log\,(Tb\text{-}N)]/3}\qquad\qquad(5.3\text{-}4)$$

where

    (Gd-N)   = Cl-chondrite normalized concentration of Gd

Finally, the normalized Gd concentrations were converted to the estimated Gd concentrations

shown in Appendix tables A-1, A-2. and A-3 using the following equation:

$$(Gd) = 0.26(Gd\text{-}N)\qquad\qquad(5.3\text{-}5)$$

where

    (Gd) = calculated concentration of Gd in ppm, and

    0.26 = Cl-chondrite total mass for Gd converted to non-volatile mass in ppm

The estimated Gd concentrations were evaluated by applying this method to an

independent data set that contained measured concentrations of Sm, Tb, and Gd in 56 basalt

samples from the eastern Snake River Plain (Knobel and others, 1995). The measured Sm and Tb

concentrations were used to estimate Gd concentrations using equations 5.3-2 through 5.3-5. The

estimated Gd concentrations were individually compared to the measured Gd concentrations to determine the percent differences of the estimated concentration relative to the measured concentration for all 56 samples. All 56 estimated Gd concentrations were within 25 percent of the measured concentrations: 51 were within 15 percent, and 47 were within 10 percent. A portion of these differences between estimated and measured Gd concentrations may be attributable to the analytical uncertainty associated with the measured concentrations.

Mean concentrations of the measured and estimated data sets were calculated along with the estimated uncertainties of the mean concentrations. The mean and the associated uncertainty for the mean of the measured Gd data set was 7.7 ± 1.8 ppm and 7.3 ± 1.7 ppm for the estimated Gd data set (table 5.5). The good agreement between the means of the two data sets suggest that Gd concentrations estimated using equations 5.3-2 through 5.3-5 are reasonable approximations of the true measured concentrations.

Another means of testing the acceptability of the estimated Gd concentrations is to plot the laboratory-measured results with the estimated Gd concentrations. If equations 5.3-2 through 5.3-5 produce exact estimates of the measured Gd concentrations, a straight line with a slope of one and a y-intercept of 0 should result. The data are plotted on figure 5.5 and a linear regression analysis gives a straight line with a slope of 0.87 and a y-intercept of 0.59. The correlation coefficient is 0.91, which suggests an acceptable match between the measured and estimated Gd concentrations. These comparisons suggest that equations 5.3-2 through 5.3-5 provide acceptable estimates of Gd concentrations in rocks from the eastern Snake River Plain aquifer system.

5.3.3.3 Lithium, beryllium, boron, carbon, and fluorine

The ISU Geochemical Laboratory did not measure the concentrations of these light elements in the samples listed in Appendix tables A-1, A-2, and A-3. Because these elements were needed for the calculation of *in situ* ^{36}Cl production, concentrations equivalent to average concentrations in the appropriate sample rock type were included in this analysis. These concen-
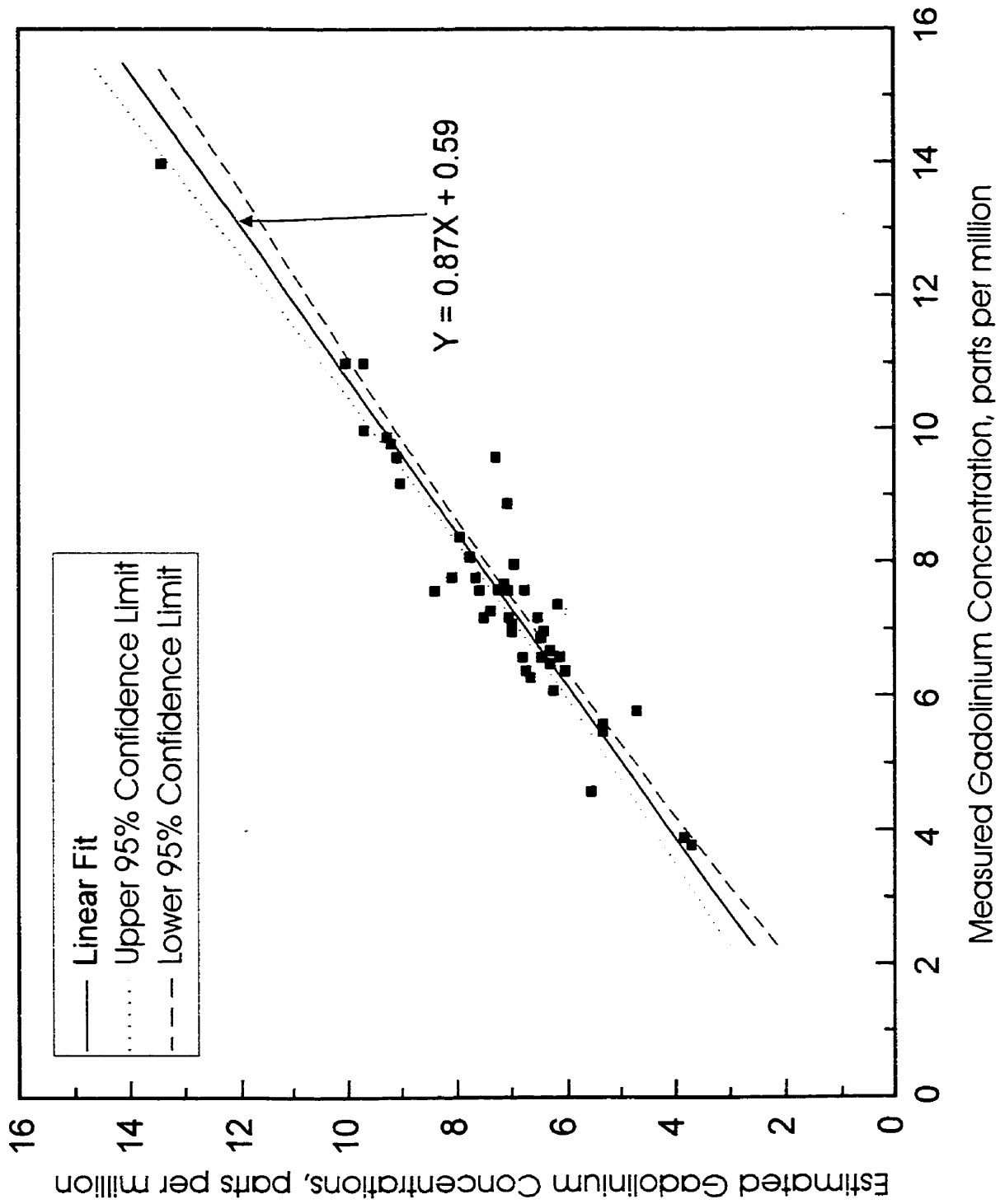
Figure 5.5. Comparison of the measured and estimated gadolinium concentrations for 56 basalt samples from the eastern Snake River Plain (95 percent confidence interval).

Table 5.5.   Measured and estimated Gd concentrations for 56 basalt samples from the eastern Snake River Plain aquifer.

[Measured Gd concentrations taken from Knobel and others, 1995. Estimated Gd concentrations calculated with equations 2-5 in text. ppm, parts per million.]

Measured Gd (ppm)	Estimated Gd (ppm)	Measured Gd (ppm)	Estimated Gd (ppm)
11	10	8.1	7.8
11	10	7.8	7.7
9.8	9.2	7.6	7.6
9.2	9	7.7	7.1
9.8	9.2	7.3	7.4
9.2	9.1	7.8	7.6
8.4	7.9	7.6	7.1
7.6	6.8	14	13
9.6	7.3	10	9.7
7.6	8.4	9.6	9.1
7.4	7.1	9.9	9.3
7.2	7.0	11	9.7
6.6	6.8	9.2	9.1
6.7	6.3	7.6	7.2
4.6	5.5	7.1	7.0
5.8	4.7	5.6	5.3
7.4	6.2	6.6	6.3
7	7.0	5.5	5.3
8	7.0	6.9	6.5
7.2	7.5	7.2	6.5
6.3	6.6	7.6	7.1
6.6	6.1	6.9	6.4
6.1	6.2	6.4	6
6.7	6.3	6.6	6.3
7	6.4	6.5	6.3
6.4	6.7	6.6	6.4
8.9	7.1	3.8	3.7
7.8	8.1	3.9	3.8

Measured mean and associated uncertainty, 7.67 ± 1.81 ppm
Estimated mean and associated uncertainty, 7.29 ± 1.66 ppm

trations were taken from Parker's study (1967, table 19, p. D13-D14) and were marked with asterisks in Appendix tables A-1, A-2, and A-3. Carbon (C) concentrations in these Appendix tables not marked with an asterisk were calculated using other methods. Those methods will be subsequently discussed in the sections titled "Carbonate sedimentary rocks" and "Noncarbonate sedimentary and metamorphic rocks".

Boron (B) has the largest absorption cross section of these five elements, 764 barns/atom, and so has the potential to significantly affect the overall thermal neutron cross section, depending on the B concentration in the sample. Therefore, a sensitivity analysis was performed on the samples to determine the effect of various B concentrations on the ^{36}Cl/Cl ratio. Average B concentrations taken from Parker's study ranged from 5 ppm for basalt to as much as 100 ppm for shale. A smaller B concentration in a sample generally corresponds to a larger ^{36}Cl/Cl ratio because more of the neutron flux is available for activation of ^{35}Cl. Therefore, the sensitivity analysis was performed under the assumption that the average B concentrations were lower by an order of magnitude.

The largest percent change in ^{36}Cl/Cl ratios occurred for sample SP-24, a quartzite. The calculated ^{36}Cl/Cl ratio using an average B concentration for quartzite taken from Parker's study (1967) was 1.5×10^{-15}, and the ^{36}Cl/Cl ratio adjusted for a smaller B concentration was 2.5×10^{-15}, or a 61-percent increase. The smallest percent change in ^{36}Cl/Cl ratios occurred for sample SP-20, a basalt. The calculated ^{36}Cl/Cl ratio was 1.4×10^{-15}, and the adjusted ^{36}Cl/Cl ratio was 1.5×10^{-15}, or an increase of only 0.7 percent. None of the ratios for the basalts changed by greater than 2.7 percent as a result of this change in B concentration. Ratios for the rhyolite samples, with the exception of SP-9, changed 8.6 percent or less. The average increases in ^{36}Cl/Cl ratios for the basalt and rhyolite samples were 2.3 and 7.5 percent, respectively. The average increases in ^{36}Cl/Cl ratios for the carbonate, opal, shale, and quartzite samples were 25, 24, 46, and 42 percent, respectively. The larger increase in the ^{36}Cl/Cl ratios of these samples was a result of the

decrease in B concentration in the samples. The order of magnitude decrease in the B concentration increased the available thermal neutron cross section for ^{35}Cl activation and, hence, the ^{36}Cl/Cl ratio.

As an example, there was a 46 percent change in the ^{36}Cl/Cl ratio for the shale sample (B concentration = 10 ppm) that was 20 times greater than the 2.3-percent ratio change for the average basalt sample (B concentration = 0.5 ppm). Thus, the change in the ^{36}Cl/Cl ratio in the shale sample as a result of the order of magnitude decrease in the B concentration was significant compared to the change in this ratio in basalt samples with a corresponding change in B concentrations. However, as mentioned earlier, the contribution of ^{36}Cl to ground water from shale is insignificant compared to the contribution from basalt because most of the aquifer on the Plain is composed of basalt.

The difference in initial B concentrations for the rock samples also affected the outcome of the sensitivity analysis. For example, the average B concentration for rhyolite was changed from 15 to 1.5 ppm. The average B concentration for basalt was changed from 5 to 0.5 ppm. Although all values were decreased by an order of magnitude, the rhyolite samples were affected more by the decrease in B concentration than the basalt samples were. The average change in B concentrations for the rhyolite samples was 13.5 ppm, and the average change in B for the basalt samples was 4.5 ppm. The resultant change in ^{36}Cl/Cl ratio was consequently 7.5 percent for rhyolite and only 2.3 percent for basalt.

Regardless of the initial B concentrations used in this sensitivity analysis, the Gd concentrations ultimately determined the degree of effect that the B concentrations had on the resultant ^{36}Cl/Cl ratio. With a Gd concentration of 10 ppm, the change in the B concentration had little or no effect on the ^{36}Cl/Cl ratio because Gd has such a large absorption cross section compared to B; 49,000 barns/atom for Gd and 764 barns/atom for B. Alternatively, if the Gd concentration is 0.01 ppm, the Gd will have very little effect on the ^{36}Cl/Cl ratio, enabling a

change in B concentration to have a significant effect.

5.3.3.4 Samarium, terbium, uranium, and thorium

Concentrations of Sm, Tb, U. and Th in Appendix tables A-1, A-2, and A-3 were the concentrations reported directly in ppm by the laboratory.

5.3.3.5 Elements reported as oxides

The laboratory reported the principal rock-forming elements as oxides in weight percent of the total sample weight. The ICP-AES and INAA analytical methods used by the ISU laboratory did not account for the volatile components in the sample; for example, water (H_2O) and carbon dioxide (CO_2). These constituents were measured using the LOI method, which provided a gross estimate of the total volatile fraction of the sample but did not distinguish between the component parts. The weight percent of the LOI fraction of the sample, added to weight percents of the major rock-forming elements, should equal 100 percent. However a total of 100 percent is rarely obtained because the LOI method of reporting results does not account for the trace-element content of the rock samples. Because selected trace elements were considered in this dissertation, the laboratory data were not normalized to 100 percent prior to conversion to ppm. Estimation of the volatile components of the sample required additional calculations as discussed in the section titled "Volatile components".

The principal rock-forming elements are Si, Al, Fe, Ca, Mg, Na, K, P, Ti, and Mn; the respective oxides are SiO_2, Al_2O_3, FeO, CaO, MgO, Na_2O, K_2O, P_2O_5, TiO_2, and MnO. (Some Fe_2O_3 does exist along with the FeO, but the quantity is small enough that the laboratory reported the total Fe concentration as FeO) Oxygen (O), which is reported as part of the oxides, also is considered to be a principal rock-forming element. The conversion of oxide weight percents to the needed units of ppm equivalent weight was done separately for each oxide.

The conversions were accomplished by reducing the weight percent to a fractional weight ratio and multiplying it by 1,000,000 g. This gave a result for the oxide in ppm equivalent

weight:

$$(\text{Weight percent oxide}/100) \times 1,000,000 \text{ g} = \text{ppm by weight oxide} \qquad (5.3\text{-}6)$$

The oxide in ppm by weight then was multiplied by the ratio of the elemental weight to the molecular weight of the oxide:

ppm by weight oxide $\times$ (elemental weight/molecular weight oxide) = ppm by weight

element. $\qquad (5.3\text{-}7)$

The ppm by weight of O in the oxide was determined by subtracting the ppm by weight of the element from the oxide:

ppm by weight oxide - ppm by weight element = ppm by weight O $\qquad (5.3\text{-}8)$

For example, the reported weight percent of SiO_2 for sample SP-15 of 45 weight percent used with the known elemental weight of Si (28.086 g) and molecular weight of SiO_2 (60.0848 g) gave the following:

1. From equation 5.3-6: $(45/100) \times 1,000,000$ g = 450,000 ppm by weight SiO_2.

2. From equation 5.3-7: $450,000 \times (28.086/60.0848)$ = 210,348 ppm by weight Si.

3. From equation 5.3-8: 450,000 - 210,348 = 239,652 ppm by weight O.

The ppm by weight of each element was calculated from the appropriate oxide and the results are listed in tables Appendix tables A-1, A-2, and A-3. The ppm by weight of the element O for each oxide was summed and is listed in tables Appendix tables A-1, A-2, and A-3 as oxygen, rock (O,r).

5.3.3.6 Volatile components

The principal volatile components of the rock samples submitted for analysis were CO_2

and H_2O. The importance of these two compounds in a sample depended on the amount of mineral material containing these compounds that was present in the samples. For example, the laboratory analyzes calcite ($CaCO_3$) in rock as CaO and CO_2, however, CO_2 is included as an undifferentiated component of the LOI result for the sample. Similarly, opal ($SiO_2 \cdot nH_2O$) in rock is analyzed as SiO_2 and H_2O in the laboratory with the H_2O included in the LOI result. Because LOI was undifferentiated, it was necessary to make some assumptions about its content and these assumptions were made on the basis of the typical mineralogy of the type of rock sample that was submitted for analysis. Also, because LOI was measured with a different analytical method than the oxides were measured, any adjustments necessary to make the ppm by weight values equal 1,000,000 ppm were made in the volatile component of the analysis. Because these assumptions and the resulting calculations depend on the rock type, they will be discussed in that way.

Basalt and Rhyolite—The extreme heat associated with the formation of basalt and rhyolite generally drives off most volatile components. Many surface samples of Snake River Plain basalt have coatings and void fillings of caliche, a mixture of calcite with clay that has been deposited by secondary moisture-related processes. In this case, LOI firing can remove CO_2 as a volatile, just like H_2O. However, the basalt samples in this research, with the exception of one sample, were taken from depths where the major sources of CO_2, caliche, and $CaCO_3$, are assumed minimal. Therefore, all of the LOI for the basalt and rhyolite in this study was assumed to be from H_2O and not CO_2. Some H_2O is trapped in vesicles as these rock types solidify from the molten magma and hydration of some minerals takes place. Because of these characteristics, the assumption was made that the difference in Appendix table A-1 between the raw total (the sum of previously discussed elements) and the adjusted (adj.) total was the result of H_2O lost during the analytical process. The ppm by weight oxide (H_2O) was calculated by subtracting the total raw values from the total adjusted values. Equations (5.3-7) and (5.3-8) were then used to calculate hydrogen (H) and O. These values were designated H,w and O,w and listed in Appendix

table A-1. Calculations for the sample from an opal deposit in rhyolite, SP-9, are discussed under the subsection entitled "Noncarbonate sedimentary and metamorphic rocks".

Carbonate sedimentary rocks—The idealized chemical formulas for carbonate rocks are $CaCO_3$ (limestone) and $CaMg(CO_3)_2$ (dolomite). The principal volatile component in both rocks is CO_2 and it was assumed in this dissertation that the LOI component of the carbonate samples was the result of CO_2 volatilization. For example, dolomite undergoes a two-stage volatilization:

(1) $CaMg(CO_3)_2 \rightarrow CaCO_3 + MgO + CO_2$ at about 800°C; and,

(2) $CaCO_3 \rightarrow CaO + CO_2$ at about 900°C.
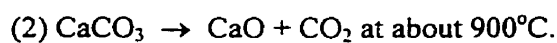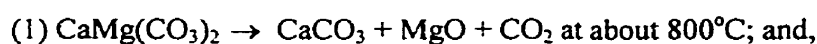
The LOI values thus were converted to ppm by weight of the oxide using equation (5.3-6). The remaining calculations were completed using equations (5.3-7) and (5.3-8). The calculated results for C are listed in Appendix table A-2 and the O values were included in the summation represented in table A-2 by O,r. The H,w and O,w values in Appendix table A-2 were calculated in the same manner as for the basalt and rhyolite samples in Appendix table A-1.

Noncarbonate sedimentary and metamorphic rocks—The amount of carbonate minerals in predominately noncarbonate sedimentary rock is variable and often is mirrored after the sum of Ca and Mg contained in the rock. For example, a predominantly silica sand may contain grains of calcite and dolomite that have not been removed by weathering processes. Conversely, opal, which is the weathering product of some igneous rocks, should not contain much carbonate material but should contain significant amounts of water.

Calcium and Mg in clays and shales generally are in the lattice of the complex aluminosilicate minerals contained in clay, and the presence of carbonate minerals should be limited in most cases. On the other hand, clay minerals commonly contain significant quantities of water. The average ppm by weight of carbon in clay and shales was taken from Parker's study

(1967, table 19) to represent the value listed in Appendix table A-2 for sample SP-25. The corresponding O value was calculated by first converting the element ppm by weight to the number of moles of the element. This was accomplished by dividing the sample elemental mass in grams (ppm by weight) by the elemental gram formula weight (gfw):

$$\text{element}_{ppm}/\text{element}_{gfw} = \text{element}_{moles} \tag{5.3-9}$$

For example, the ppm by weight for carbon in SP-25 is 10,000 g and the moles of C are calculated with equation (5.3-9) as follows:

$$10,000g/12.01115 \text{ g/mole} = 832.56 \text{ moles}$$

The chemical formula for carbon dioxide (CO_2) requires two moles of O for each mole of C (2 × 832.56 moles C) = 1,665.12 moles O for sample SP-25. Equation (5.3-9) was then modified to calculate the ppm by weight value for oxygen.

$$\text{element}_{ppm} = \text{element}_{moles} \times \text{element}_{gfw}$$

Therefore, O ppm by weight in grams = 1,665.12 moles × 15.9994 g/mole = 26,641 g of O. This O number was included as part of the sum of O listed as O,r in Appendix table A-2 for sample SP-25.

For the opal sample (SP-9) and the two quartzite samples (SP-11 and SP-24), the assumption was made that the number of moles of C was equal to the sum of the number of moles of Ca and Mg. Equation (5.3-9) was used to calculate the number of moles of calcium and magnesium. The ppm by weight of C was then calculated by using equation (5.3-8). These results were listed in Appendix tables A-1 and A-3. Once the moles of C were known, the moles of O were given by the relation $O_{moles} = (2) (C_{moles})$. The ppm by weight of O then was calculated with equation (5.3-8) and was summed into the appropriate O,r results listed in Appendix tables A-1 and A-3. The H,w and O,w values in Appendix tables A-1 and A-3 were calculated the same

way as for the basalt and rhyolite samples.

5.3.3.7 Anomalous data

Silica weight percents for samples SP-17 and SP-24 were outside the calibration range of the analytical instrument at the time the samples were analyzed, giving results that were larger than possible. Consequently, these two values were reduced so that the laboratory weight-percent totals equaled 100 percent.

The LOI weight percents for samples SP-16, SP-18, SP-19, SP-20, and SP-21 were reported as negative values because of analytical interferences by Fe in the samples. These values were adjusted so that the total (adj) value equaled 1,000,000 ppm by weight.

5.3.4   Estimation of Neutron Production Rates and Chlorine-36 Production

For the estimation of *in situ* neutron production rates and resultant ^{36}Cl production, calculations were restricted to the deep subsurface (greater than 10 m), under the assumption of rock-unit geochemical homogeneity. Additionally, as discussed in Chapter 2, the ^{35}Cl (n, γ) ^{36}Cl reaction is the only one that produces significant ^{36}Cl in the subsurface at a depth greater than about 10 m. Shallow subsurface sources for *in situ* produced ^{36}Cl were assumed to be minimal because seasonal ground water recharge moves rapidly through the shallow subsurface relative to the half-life of ^{36}Cl. Thus, concentrations of *in situ* produced ^{36}Cl do not have time to accumulate to levels that are significant when compared to the atmospheric fluxes.

To further support the assumption that ^{36}Cl production resulting from the neutron activation of ^{39}K is negligible compared to the production from ^{35}Cl, *in situ* secular equilibrium ^{36}Cl/Cl ratios from the reactions ^{39}K(n,α) ^{36}Cl and ^{35}Cl(n,γ) ^{36}Cl were calculated for each of the 25 rock samples (table 5.6 and Appendix table C-9). The ratios resulting from the activation of ^{39}K range from 1×10^{-21} to 5×10^{-17}, or three to six orders of magnitude smaller than the ratios due to the activation of ^{35}Cl. Thus the production of ^{36}Cl due to ^{39}K is negligible, and, since muon

activation of ^{40}Ca yields an even smaller ^{36}Cl production rate, these production mechanisms are insignificant compared to the neutron activation of ^{35}Cl.

In review for the neutron production rate calculations, the neutrons required for activation of ^{35}Cl and ^{39}K are produced by the interaction between alpha (α) particles, generated from the radioactive decay of U and Th series isotopes, and stable nuclei of lighter elements such as F, O, Na, Al, and silica (Faure, 1986). An estimate can be made of *in situ* produced ^{36}Cl for a given ground water system if the following contributing factors are known; (1) the U and Th content of the aquifer matrix; (2) the concentrations of target elements for (α,n) reactions; (3) proximity of the target elements to the neutrons: and (4) the concentration of target elements for neutron capture. Because of the heterogeneous nature of the eastern Snake River Plain aquifer, the proximity of target elements was not determined. Therefore, maximum equilibrium concentrations reported in this dissertation for ^{36}Cl in ground water were calculated with the assumption that all *in situ* produced atoms in the aquifer matrix were transferred to the fluids flowing through the aquifer. These maximum ^{36}Cl concentrations were used to determine the associated total Cl^{-} concentration transferred to the ground water.

Additionally, for the calculations of *in situ* produced ^{36}Cl, the following assumptions were made: (1) all neutrons were thermalized in all rocks below about 10 m in depth; (2) thermal neutron fluxes were directly proportional to neutron production rates at all depths (Fabryka-Martin, 1988, page 42); (3) all the U and Th decay series nuclides were in secular equilibrium and were homogeneously distributed throughout the rock; (4) all target nuclides were homogeneously distributed throughout the rock; and (5) all rocks were saturated with water. The thermal neutron flux and ^{36}Cl production are reduced in unsaturated rock due to neutron capture by other elements in addition to the ^{35}Cl and ^{39}K in the aquifer matrix. Therefore, *in situ* production in the deep unsaturated zone will be reduced by as much as 70 percent compared to the saturated zone (Fabryka-Martin, 1988). Applying these assumptions maximizes the *in situ* ^{36}Cl production calculations presented in this dissertation.

The total transferred rock-to-ground water Cl⁻ concentrations were compared to maximum ambient measured values and the maximum ^{36}Cl concentrations were adjusted accordingly. For example, for sample SP-1, the estimated maximum total transfer value for Cl⁻ was about 25 g/L. However, the maximum average ambient ground water concentration was 15 mg/L or 0.059 percent of the estimated total Cl⁻ transfer concentration. Therefore, the associated maximum ^{36}Cl concentration of 2.52×10^9 atoms/L was reduced by this method to 1.49×10^6 atoms/L to more accurately reflect the possible contribution to ground water concentrations from *in situ* production (Appendix Table C-7). Because of the assumptions made in these calculations, these corrected ^{36}Cl concentrations should be considered as maximum. Additionally, these maximum Cl⁻ concentrations in ground water would have to be supplied solely by rocks in the aquifer and from no other source.

As previously discussed, the dominant source of neutrons in the deep subsurface (below about 10 m) that are available for activation of stable ^{35}Cl and ^{39}K is the interaction of alpha-emitting progeny from the U and Th decay series and light nuclei. The neutron production rate from this interaction and from the spontaneous fission of naturally occurring ^{238}U can be calculated from the following equation modified from Fabryka-Martin (1988, pages 37 to 40):

$$Pn = X[U] + Y[Th] + 0.429[U] \tag{5.3-10}$$

where

Pn = neutron production rate, in (n/g)/yr;

X = production of secondary neutrons due to α decay of the U series [(n/g)/yr per ppm U];

[U] = U concentration of the rock, in ppm;

Y = production of secondary neutrons due to α decay of the Th series [(n/g)/yr per ppm Th];

[Th] = Th concentration of the rock, in ppm; and

0.429 [U] = neutrons produced by spontaneous fission of ^{238}U [(n/g)/yr per ppm U].

The X and Y factors are determined from the light-element composition of each different rock type in the study area. For example, X for limestone sample SP-1 was determined by dividing the total calculated (n/g)/yr per ppm U by the total weighting factor (table 5.4). The factor X is then multiplied with the U concentration in ppm to determine the neutron production rate from α-particle emissions from the U decay series. The Y factor is calculated in the same manner and multiplied with the Th concentration to determine the neutron production rate due to α-particle emissions from the Th decay series. The factor 0.429 [U] in equation (5.3-10) accounts for neutrons produced by the spontaneous fission of uranium-238 (^{238}U) and includes, (1) the atom concentration of a gram of ^{238}U; (2) the decay constant for spontaneous fission half-life for ^{238}U ($8.49\pm0.14 \times 10^{-17}$ yr^{-1}); (3) the average number of neutrons produced per spontaneous fission of ^{238}U; and (4) the fractional concentration of U in the sample in ppm (Fabryka-Martin, 1988, pages 39, 40).

Twenty-five samples of six different rock types were analyzed for this research. Table 5.6 lists the results for each of the samples. The calculated thermal neutron cross sections ranged from 0.0029 cm^2/g of rock in dolomite (SP-4, fig. 1.1) to 0.0165 cm^2/g of rock in basalt (SP-20, fig. 1.1). The total neutron production rate for each of the rock types ranged from 0.32 (n/g)/yr in dolomite (SP-4, fig. 1) to 29 (n/g)/yr in rhyolite (SP-17, fig. 1.1). The total neutron production rates were used in combination with the total reaction cross sections to calculate the *in situ* secular equilibrium ^{36}Cl/Cl ratios due to the two primary reactions that produce ^{36}Cl in the rock matrix at depth. For the reaction ^{35}Cl(n,γ) ^{36}Cl, the ratios ranged from 1.4×10^{-15} in basalt (SP-20, fig. 1.1) to 45×10^{-15} in rhyolite (SP-17, fig. 1.1). The larger neutron production rate for the rhyolite is due to the larger U (11.5 ppm) and Th (22.2 ppm) concentration of the rhyolite; for comparison, the U and Th concentrations of the basalt were 0.8 and 2.23 ppm, respectively.

For the reaction ^{39}K(n,α) ^{36}Cl, the ratios ranged from 0 in limestone (SP-26, fig. 1.1), to

2×10^{-15} in an opal deposit in rhyolite (SP-9, fig. 1.1) (table 5.6). The ^{36}Cl production by neutron activation of stable ^{35}Cl was at least one order of magnitude greater than production by neutron activation of ^{39}K for all samples analyzed. Table 5.6 also lists the calculated equilibrium ^{36}Cl content in the rock matrix. The ^{36}Cl content was smallest in quartzite (SP-24, fig. 1.1), 0.007×10^5 atoms/cm^3. The largest potential ^{36}Cl production was in rhyolite (SP-8, fig. 1.1) at 12×10^5 atoms/cm^3.

Table 5.4 shows an example of the thermal neutron cross section, the total neutron production rate and the *in situ* secular equilibrium ^{36}Cl/Cl ratios calculated for sedimentary rock sample SP-1, a limestone. The sample was analyzed for the elements shown in table 5.4 and a sample ppm was calculated using the methods outlined above. The weighting factors listed in table 5.4 were calculated by multiplying the mass stopping power for each element by the corresponding sample ppm expressed as a decimal fraction of the total ppm (J.T. Fabryka-Martin, written commun. 1995). The weighted neutron yields were calculated by multiplying the weighting factor by the original calculated neutron yields. The thermal neutron cross section for each of the analyzed elements was calculated by multiplying the sample ppm, as a decimal fraction of the total, by the absorption cross section in cm^2 and dividing by the atomic weight. The individual thermal neutron cross sections were then added to attain a total thermal neutron cross section.

The X and Y factors were calculated as discussed previously. The X and Y factors were then multiplied by the corresponding total U and Th sample ppm to arrive at a neutron production rate due to U and Th decay-series alpha emissions. In addition, the neutron production rate caused by ^{238}U spontaneous fission was calculated by multiplying the total U sample ppm by the factor of 0.429, as explained in equation 5.3-10. The individual neutron production rates were then added to give a total neutron production rate. To arrive at a ^{36}Cl/Cl ratio, the following equation was used (Fabryka-Martin, 1988, page 208):

Table 5.6.   Calculated thermal neutron cross sections for neutron absorption, total neutron production rate, *in situ* secular equilibrium ^{36}Cl/Cl ratios, and equilibrium ^{36}Cl concentrations in the rock matrix.

[See figure 1.1 for location of sampling sites. Note: Sample SP-26 had 0 ppm K as reported by the ISU Laboratory.]

Sample identifier and rock type	Thermal neutron cross section (× 10^{-6} cm^2/g)	Total neutron production rate (neutrons/ gram of rock/year)	*In Situ* secular equilibrium ^{36}Cl/Cl ratio due to ^{35}Cl(n,γ) ^{36}Cl (× 10^{-15})	*In Situ* secular equilibrium ^{36}Cl/Cl ratio due to ^{39}K(n,α) ^{36}Cl (× 10^{-15})	Equilibrium ^{36}Cl in rock matrix (× 10^5 atoms/cm^3)
Igneous, SP-5, rhyolite	0.0085	19	32	0.6	3.3
Igneous, SP-6, rhyolite	0.0084	19	32	0.7	3.4
Igneous, SP-7, rhyolite	0.0080	20	37	0.3	9.5
Igneous, SP-8, rhyolite	0.0078	22	41	0.3	12
Igneous, SP-9, opal deposit in rhyolite	0.0069	13	26	2	0.12
Igneous, SP-10, rhyolite	0.0082	20	38	0.8	4.0
Igneous, SP-13, rhyolite	0.0072	16	33	0.7	3.4
Igneous, SP-15, basalt	0.0094	2.9	4.5	0.1	0.10
Igneous, SP-16, basalt	0.0077	2.3	4.2	0.02	0.19
Igneous, SP-17, rhyolite	0.0093	29	45	0.8	4.9
Igneous, SP-18, basalt	0.0069	1.7	3.7	0.03	0.08
Igneous, SP-19, basalt	0.0077	1.7	3.3	0.02	0.15
Igneous, SP-20, basalt	0.0165	2.5	1.4	0.004	0.13
Igneous, SP-21, basalt	0.0113	8.2	10	0.08	0.93
Igneous, SP-22, basalt	0.0076	4.7	9.1	0.5	0.21
Igneous, SP-23, rhyolite	0.0083	19	34	0.6	3.6
Sedimentary, SP-1, limestone	0.0036	1.5	5.9	0.003	0.25
Sedimentary, SP-2, limestone	0.0037	1.9	7.5	0.003	0.65
Sedimentary, SP-3, limestone	0.0037	2.2	8.6	0.002	0.55
Sedimentary, SP-4, dolomite	0.0029	0.3	1.6	0.0003	0.28
Sedimentary, SP-12, limestone	0.0037	1.8	7.1	0.004	0.61
Sedimentary, SP-25, shale	0.0120	7.5	9.0	0.008	12
Sedimentary, SP-26, limestone	0.0042	3.2	11	0	0.72
Metamorphic, SP-11, quartzite	0.0048	2.1	6.4	0.06	0.30
Metamorphic, SP-24, quartzite	0.0035	0.4	1.5	0.04	0.007

$$\frac{^{36}Cl}{Cl} = \frac{(Pn) \times (N) \times (\sigma_{35Cl})}{(\sigma_T) \times (\lambda_{36Cl})}.$$ (5.3-11)

where Pn is the total neutron production rate, N is the ^{35}Cl isotopic abundance, σ_{35Cl} is the thermal neutron absorption cross section of ^{35}Cl, σ_T is the total thermal neutron cross section and λ_{36Cl} is

the decay constant for ^{36}Cl. The ^{35}Cl thermal neutron absorption cross section is 4.4×10^{-23} cm^2/atom, the percent isotopic abundance of ^{35}Cl is 0.7577 (Walker and others, 1989), and the ^{36}Cl decay constant is 2.3×10^{-6} yr^{-1} [(ln2)/301,000 years].

The $^{36}Cl/Cl$ ratios estimated for the 25 samples used in this study represent rock types of specific composition as opposed to average composition. Therefore, to arrive at values for rock types of average composition, the samples were grouped together into the categories of basalt, rhyolite, limestone and dolomite (carbonates), shale, and quartzite (table 5.7). The U and Th contents were averaged for each category, as were the thermal neutron cross sections, the total neutron production rates, and the *in situ* secular equilibrium $^{36}Cl/Cl$ ratios. The average values are compared in table 5.7 and figure 5.5 to average values taken from Parker (1967). The U and Th content, the thermal neutron cross section, and the total neutron production rates for all rock types compare well with the calculations performed with data from Parker. Additionally, the histogram shown in figure 5.5 shows good correlation between both data sets further supporting the methods outlined here for the calculated *in situ* secular equilibrium $^{36}Cl/Cl$ ratios for rocks of average composition from the eastern Snake River Plain.

5.3.5 Comparison of *In Situ* Chlorine-36 Production to Previous Studies

Andrews and others (1989) performed the calculations for ^{36}Cl production in the Stripa granite using the same methods outlined in this dissertation for *in situ* production of ^{36}Cl. The Stripa granite is composed of small amounts of neutron-absorbing elements and has a relatively large natural radio- element content. Thus the neutron flux generated within this granite is among the largest known for crustal rocks (Andrews and others, 1989). The theoretical flux for the Stripa granite was calculated to be 4.07 " 10-4 n/cm2/sec, while the theoretical neutron flux for the surrounding leptite was 0.80 ' 10-4 n/cm2/sec. These values agree to within 15 percent or better of the experimental neutron flux values measured by Andrews and others (1986).

Table 5.7.   Calculated thermal neutron cross sections for neutron absorption, total neutron production rates, and *in situ* secular equilibrium ^{36}Cl/Cl ratios for rock types of average composition.

[+, the values for the Snake River Plain shale represent only one sample and are not an average.
*, data not available from Parker (1967).]

Rock Type	Number of Samples	U Content (ppm)	Th Content (ppm)	Thermal Neutron Cross Section (cm²/g)	Total Neutron Production Rate (neutrons/ gram of rock/ year)	*In Situ* Secular Equilibrium ^{36}Cl/Cl Ratio (×10⁻¹⁵)
Basalt: Average Composition, Snake River Plain, this Study	7	1.14	3.03	0.0096	3.44	5.23
Basalt: Average Composition from Parker (1967)	*	1.00	4.00	0.0073	3.68	7.3
Rhyolite: Average Composition, Snake River Plain, this Study	9	5.96	24.01	0.0081	19.64	33.34
Rhyolite: Average Composition, from Parker for felsic granite (1967)	*	3.5	18	0.0069	14.62	30.71
Carbonate: Average Composition, Snake River Plain, this Study	6	2.35	0.19	0.0036	1.81	6.96
Carbonate: Average Composition, from Parker (1967)	*	2.2	1.7	0.0039	2.46	9.14
+ Shale: Snake River Plain, this Study	1	2.6	9.07	0.0120	7.49	9.05
Shale: Average Composition, from Parker (1967)	*	3.2	11.0	0.0098	9.27	13.71
Quartzite: Average Composition, Snake River Plain, this Study	2	0.85	2.16	0.0042	1.26	3.97
Quartzite: Average Composition, from Parker for sandstone (1967)	*	0.45	1.7	0.0061	0.73	1.73
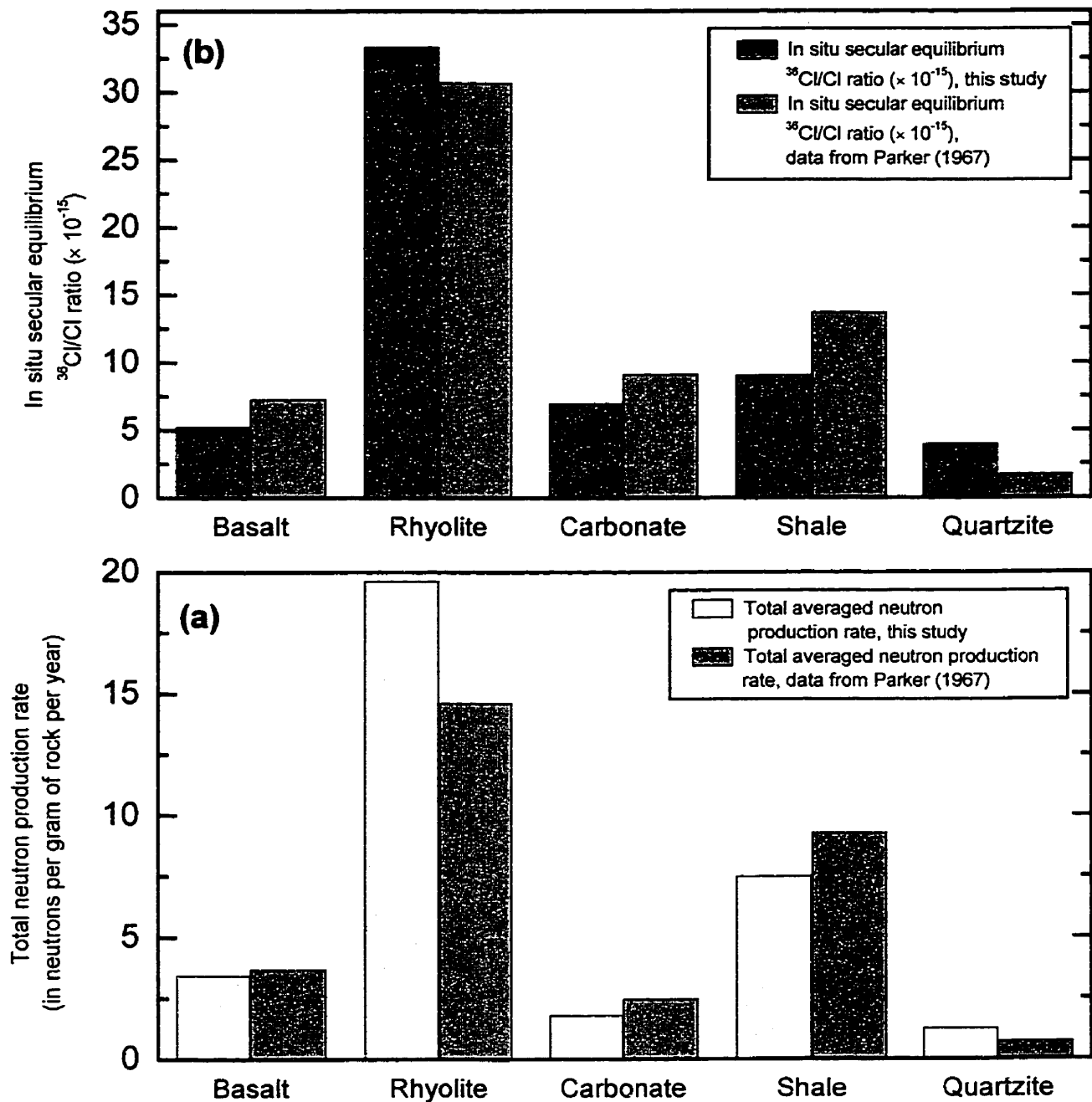
Figure 5.6. Neutron production rates (a) and *in situ* secular equilibrium chlorine-36/chloride ratios (b) for rocks of average composition presented in this study and for rocks of average composition from Parker (1967).

Note: The results from this study for shale represent only one sample and are not, therefore, a true average.

The theoretical flux value was used to calculate neutron-induced production rates of eight

isotopes within the Stripa granite, the fracture minerals, and the surrounding leptite. These

isotopes include helium-3 (^{3}He), ^{14}C, ^{36}Cl, ^{129}I, ^{37}Ar, ^{39}Ar, krypton-81 (^{81}Kr), and ^{85}Kr. In

calculating the production rates, two assumptions were made. The first assumption was that all of

the radioisotopes produced within the rock matrix were transferred to the fluids in the rock pore

spaces. The second assumption was that the minimum observed porosity for crystalline rocks is

one percent, an assumption independent of the micro-distribution of radionuclide production in

relation to the aqueous phase. The estimated equilibrium number of atoms of ^{36}Cl in one cm^3 of

the rock matrix was 1.5 × 10^6 for the reaction ^{35}Cl(n,γ) ^{36}Cl and 0.04 × 10^6 for the ^{39}K(n,α) ^{36}Cl

reaction. For the fracture fluid, the equilibrium number of atoms in one cm^3 was 2.5 × 10^6 for

neutron absorption by ^{35}Cl and was negligible for neutron activation of ^{39}K. For the surrounding

leptite rock matrix, the equilibrium number of atoms is 0.19 × 10^6 and 0.0067 × 10^6 for the two

reactions, respectively. As was the case for the rocks from the Snake River Plain aquifer

investigated in this dissertation, the production of ^{36}Cl via activation of ^{39}K in the Stripa Granite

was insignificant.

The equilibrium ^{36}Cl/Cl ratio that results from the experimental neutron flux in the rock

matrix for the Stripa granite is 215 × 10^{-15} after 1.5 million years. The equilibrium ^{36}Cl/Cl ratio

for the surrounding leptite is 41 × 10^{-15}. Although the ^{36}Cl/Cl ratios in the ground water may not

reach the same equilibrium ratio as in the aquifer matrix due to the smaller residence times, an

increase in salinity during transport through the fracture system could result in a Cl$^-$ concentration

and ^{36}Cl/Cl ratio signature characteristic of the Stripa granite (Andrews and others, 1989). Due to

the similarity in granitic and rhyolitic geochemistry, this ^{36}Cl/Cl ratio from the Stripa Granite is

comparable to the ^{36}Cl/Cl ratio for rhyolites from the eastern Snake River Plain. The estimated

equilibrium *in situ* ^{36}Cl/Cl ratio for the nine rhyolite samples used in this study ranged from 26 ×

10^{-15} to 45 × 10^{-15} with a mean of 35±5.5 × 10^{-15} (table 5.6). The slightly larger ^{36}Cl/Cl ratio from

the Stripa granite is due to the larger U and Th content of this granite compared to the average rhyolite from the eastern Snake River Plain; U is 44.1 ppm and Th is 33 ppm in the Stripa granite and U is 5.96 ppm and Th is 24.1 ppm for average rhyolitic composition from the eastern Snake River Plain (table 5.7).

If all of the Cl^- in the Stripa granite were transferred from the rock to the ground water, a ^{36}Cl concentration of 1.5×10^{11} atoms/L would be produced with an associated fluid chlorinity of 43 g/L. However, the maximum chlorinity present in ground water from the Stripa granite was only 700 mg/L, corresponding to 1.6 percent of the matrix Cl^- transferred to the pore fluids. The resultant corrected ^{36}Cl equilibrium concentration is 2.4×10^9 atoms/L and is on the same order of magnitude as measured ground water concentrations in the Stripa granite.

The ^{36}Cl content of Stripa ground water was determined to be a result of *in situ* production because it is much larger than what could be derived from cosmogenic or nuclear-fallout sources. Therefore, the input of ^{36}Cl into the ground water system from cosmogenic and nuclear-fallout sources was determined to be much less significant than the production of ^{36}Cl by neutron capture within the granite. Although this ultimately limits the use of ^{36}Cl concentrations for the estimation of ground water residence times in the Stripa granite, Andrews and others estimated residence time based on the rate of buildup of ^{36}Cl in the water.

Using the Stripa study as a model, Beasley and others (1993) calculated a theoretical *in situ* produced $^{36}Cl/Cl$ ratio of 1×10^{-18} for the basalt aquifer of the eastern Snake River Plain. This ratio is not measurable by any analytical techniques and *in situ* production was determined to be inconsequential. However, data presented here suggest that the maximum estimated *in situ* $^{36}Cl/Cl$ ratios in basalt rocks of the eastern Snake River Plain range from 1.4×10^{-15} to 1×10^{-14} (table 5.6) or three to four orders of magnitude larger than the theoretical ratio reported by Beasley and others.

This large difference in estimated $^{36}Cl/Cl$ ratios is due to the method of calculation.

Beasley and others (1993) estimated the *in situ* contribution for neutron activation of ^{35}Cl dissolved in ground water only. In the present study, possible neutron activation of ^{35}Cl in the aquifer matrix with complete transfer to the ground water also was considered. Therefore, the ratios calculated in this manner are expected to be orders of magnitude larger due to increased neutron production rates and Cl^- concentrations in the rock compared to the ground water.

In situ production of ^{36}Cl has been estimated in near-surface environments for a re-evaluation of cosmogenic production rates in terrestrial rocks (Phillips and others, 1996); this evaluation included 17 basalt samples collected from surface exposures on the eastern Snake River Plain. The *in situ* $^{36}Cl/Cl$ atom ratios for the 17 samples ranged from $22\pm2 \times 10^{-15}$ to $249\pm16 \times 10^{-15}$ with a mean of $125\pm17 \times 10^{-15}$. For comparison, the estimated *in situ* secular equilibrium $^{36}Cl/Cl$ ratios for the 7 basalt samples used in this study ranged from 1.4×10^{-15} to 10×10^{-15} with a mean of $5.2\pm3.3 \times 10^{-15}$ (table 5.6). The 17 basalt samples collected on the Snake River Plain by Phillips and others (1996) were all from surface outcrops. Only one of the seven basalt samples evaluated was an outcrop sample; the remaining six were from depths of 118 to 728 m below the surface. Therefore, the 17 measured $^{36}Cl/Cl$ atom ratios compare well with the seven estimated *in situ* ratios, since the surface ratios are expected to be larger by an order of magnitude or more due to enhanced surface production of ^{36}Cl by the interaction of cosmic rays with elements in the rocks. However, it is assumed in this dissertation that the contribution to ground water from this mechanism is insignificant for reasons outlined in the next section.

5.3.6   Comparison of *In Situ* Produced Chlorine-36 with Other Sources

In this section, meteoric, weapons-tests, and *in situ* ^{36}Cl results are compared to concentrations in ground water as a result of waste disposal practices at the INEEL. Earlier in this chapter, ^{36}Cl concentrations in water, snow, and glacial-ice samples collected at and near the INEEL were discussed. In southeastern Idaho and western Wyoming, meteoric concentrations

were determined to be less than 1×10^7 atoms/L for recharge and concentrations between 1×10^7 and 1×10^8 atoms/L were indicative of a nuclear weapons-tests component from peak ^{36}Cl production in the late 1950s. Chlorine-36 concentrations in ground water and surface water between 1×10^8 and 1×10^9 were determined to be representative of re-suspension of weapons-test fallout from the landscape, airborne disposal from nuclear-waste processing at the INTEC, or ET. Chlorine-36 concentrations larger than 1×10^9 were attributable to nuclear-waste disposal practices in the area.

Ground water samples collected just downgradient (within 1000 meters) from the INTEC have ^{36}Cl concentrations that range from $36\pm1\times 10^8$ to $2.8\pm0.1\times 10^{12}$ atoms/L (table 2.1). The associated total Cl⁻ concentrations ranged from 75 to 220 mg/L. Maximum estimated ^{36}Cl concentrations from *in situ* production for all rock types, corrected to ambient measured Cl⁻ concentrations, ranged from 2.45×10^5 to 7.68×10^6 atoms/L, or six to seven orders of magnitude smaller than concentrations in ground water near the INTEC (table 5.8). The ^{36}Cl concentrations in ground water near the INTEC were also three to four orders of magnitude larger than peak weapons-tests fallout for southeastern Idaho and Wyoming (Cecil and others, 1999). Additionally, *in situ* ^{36}Cl/Cl ratios for average rock compositions ranged from 4.0×10^{-15} to 33.3×10^{-15}. For comparison, the range of ^{36}Cl/Cl for the 70 ground water samples collected from the Snake River Plain aquifer at and near the INEEL was $47.7\pm0.2\times 10^{-14}$ to $2.1\pm0.06\times 10^{-9}$ (table 2.1).

In situ produced ^{36}Cl concentrations compare well with meteoric inputs that may be unaffected by evapotranspiration. For example, using calculated fallout rates for ^{36}Cl for precipitation presented in this dissertation, a range of possible meteoric concentrations in snow can be calculated. The ^{36}Cl fallout rates determined from separate snowfall events at two different stations during 1991 were 0.012 ± 0.002 atoms/cm²/sec at Harriman State Park near the

Table 5.8. Maximum calculated equilibrium ^{36}Cl and associated total chloride concentrations in ground water from *in situ* production due to neutron activation of stable ^{35}Cl for six rock types from the eastern Snake River Plain aquifer.

[See figure 1.1 for location of sampling sites. Source of data: percent porosity from Freeze and Cherry (1979); rock chloride content from U.S. Geological Survey Isotope Laboratory except values marked with an asterisk (*), which are from Parker (1967, table 19, p/ D13-14); maximum measured chloride content of ground water from L.L. Knobel (written commun., 1999). atoms/L, atoms per liter; g/cm^3, grams per cubic centimeter; g/L, grams per liter; mg/kg, milligrams per kilogram; mg/L, milligrams per liter. See text for explanation of the total transfer of ^{36}Cl and Cl$^-$ from rock to ground water and maximum corrected *in situ* ^{36}Cl contribution to ground water.]

Rock Type and Sample Identifier	Rock Density (g/cm^3)	Percent Porosity (min)	Chloride Content in rock (mg/kg)	Total Transfer of ^{36}Cl from Rock to Ground Water (atoms/L)	Total Transfer of Cl$^-$ from Rock to Ground Water (g/L)	Maximum Ambient Cl$^-$ Content of Ground Water (mg/L)	Maximum Corrected *In Situ* ^{36}Cl Contribution to Ground Water (atoms/L)
Igneous							
SP-5, rhyolite	2.51	1	*240	3.26E+10	60.24	10	5.42E+06
SP-6, rhyolite	2.51	1	*240	3.29E+10	60.24	10	5.45E+06
SP-7, rhyolite	2.51	1	600	9.42E+10	150.60	10	6.25E+06
SP-8, rhyolite	2.51	1	700	1.21E+11	175.70	10	6.91E+06
SP-9, opal deposit in rhyolite	2.51	1	*10	1.12E+09	2.51	10	4.47E+06
SP-10, rhyolite	2.51	1	*240	3.60E+10	60.24	10	5.98E+06
SP-13, rhyolite	2.51	1	*240	3.34E+10	60.24	10	5.54E+06
SP-15, basalt	2.61	5	*50	1.98E+08	2.61	10	7.59E+05
SP-16, basalt	2.61	5	100	3.73E+08	5.22	10	7.15E+05
SP-17, rhyolite	2.51	1	*240	4.81E+10	62.64	10	7.68E+06
SP-18, basalt	2.61	5	*50	1.65E+08	2.61	10	6.32E+05
SP-19, basalt	2.61	5	100	2.90E+08	5.22	10	5.56E+05
SP-20, basalt	2.61	5	200	2.55E+08	10.44	10	2.45E+05
SP-21, basalt	2.61	5	200	1.84E+09	10.44	10	1.77E+06
SP-22, basalt	2.61	5	*50	4.03E+08	2.61	10	1.55E+06
SP-23, rhyolite	2.51	1	*240	3.58E+10	62.64	10	5.71E+06
Sedimentary							
SP-1, limestone	2.54	1	100	2.52E+09	25.40	15	1.49E+06
SP-2, limestone	2.54	1	200	6.50E+09	50.80	15	1.92E+06
SP-3, limestone	2.54	1	*150	5.54E+09	38.10	15	2.18E+06
SP-4, dolomite	2.7	1	400	2.76E+09	101.60	15	4.08E+05
SP-12, limestone	2.54	1	200	6.12E+09	50.80	15	1.81E+06
SP-25, shale	2.42	1	*3000	1.17E+11	762.00	15	2.31E+06
SP-26, limestone	2.54	1	*150	7.18E+09	38.10	15	2.83E+06
Metamorphic							
SP-11, quartzite	2.74	1	100	2.98E+09	27.40	15	1.63E+06
SP-24, quartzite	2.74	1	*10	7.12E+07	2.74	15	3.90E+05

115

Wyoming border and 0.003±0.0015 atoms/cm^2/sec at Copper Basin in south central Idaho (fig. 1.1). Meteoric ^{36}Cl concentrations can be approximated using the ^{36}Cl fallout rate and a range of possible ET rates for the eastern Snake River Plain using the following equation:

$$\text{meteoric } ^{36}\text{Cl conc.} = \frac{\text{natural } ^{36}\text{Cl fallout rate ((atoms/cm}^2\text{)/sec))}}{\text{(average annual precip. (cm/yr))} - \text{(average annual ET (cm/yr))}} \qquad 5.4\text{-}1$$

where ET is the evapotranspiration rate; ranges of rates were used in these calculations in an attempt to account for differences in seasonal distributions of precipitation and ET.

Using the larger fallout rate for the Harriman site, 0.012±0.002 atoms/cm^2/sec, and ET rates of 0 and 95 percent, the range of meteoric concentrations is 6.5 × 10^6 atoms/L to 1.3 × 10^8 atoms/L. Cecil and others (1999) report a surface water mean ^{36}Cl concentration for 32 samples collected in southeastern Idaho of 1.5 × 10^8 atoms/L, indicating the effects of 95 percent or greater ET. In contrast, ^{36}Cl concentrations for average precipitation for the east coast of the United States where there is little or no ET have been determined to be 1.7±0.2 × 10^6 atoms/L for the period February 1997 through January 1993 (Hainsworth and others, 1994). This average is the same as for the calculated ^{36}Cl fallout rate presented here for precipitation not affected by ET in southeastern Idaho. Additionally, meteoric ^{36}Cl ground water concentrations from the eastern Snake River Plain aquifer range from 1.0 × 10^5 to 5.0 × 10^6 atoms/L, supporting the idea that no significant ^{36}Cl is being picked up in the shallow subsurface by rapidly infiltrating recharge that would not be significantly affected by ET. This is in contrast to the average ^{36}Cl concentration in the 32 surface water samples, 1.5 × 10^8 atoms/L, that would be expected to be influenced by ET processes.

For comparison to the measured ^{36}Cl concentrations in surface water presented in this dissertation, an average concentration of ^{36}Cl produced in surface water worldwide was

determined. Turekian (1969) compiled the average composition of surface water for nearly all the elements and these data were used to calculate an average *in situ* produced concentration for ^{36}Cl. An average *in situ* equilibrium ^{36}Cl concentration of 1.83×10^4 atoms/L was calculated. Although this relatively small ^{36}Cl concentration calculated in this manner is a first-order approximation, it suggests that the *in situ* contribution from surface water of average composition is insignificant compared to the contributions from weapons-tests fallout, natural atmospheric production, overland runoff containing near-surface produced ^{36}Cl, and concentrations as a result of nuclear-waste disposal at the INEEL.

Two snow samples were collected at the INEEL (INEEL #1 and INEEL#2, fig. 1.1) during nuclear-waste reprocessing operations and resultant ^{36}Cl fallout rates were determined for comparison to possible meteoric concentrations. The largest fallout rate, 12 ± 2.4 atoms/cm^2/sec for INEEL #2, was used to calculate a contribution of ^{36}Cl to the earth's surface from the INTEC (Appendix Table C-9). Again, using equation 5.4-1 and ET rates of 0 and 95 percent, the possible contribution to ground water concentrations in precipitation affected by waste-processing operations at the INEEL ranged from 1.7×10^{10} atoms/L for no ET to 3.8×10^{11} atoms/L for 95 percent ET. These concentrations are from four to five orders of magnitude larger than estimated natural meteoric contributions to ground water ^{36}Cl concentrations in the eastern Snake River Plain aquifer. Considering ground water residence time and rapid infiltration of recharge in the eastern Snake River Plain aquifer, it is highly unlikely that significant ^{36}Cl concentrations from *in situ* production occur.

5.4   Summary of *In Situ* Chlorine-36 Production

Twenty-five whole-rock samples were collected from basalt, rhyolite, limestone, dolomite, shale, and quartzite rock types in the eastern Snake River Plain aquifer. *In situ* production of ^{36}Cl in the rock samples resulting from nuclear interactions between stable nuclides and particles given off during the radioactive transformation of U and Th decay-series isotopes

was determined. Calculated ratios of ^{36}Cl/Cl in these rocks ranged from 1.4×10^{-15} for basalt to 45×10^{-15} for rhyolite. The associated neutron production rates calculated for these rock types were 2.5 (n/g)/yr for the basalt and 29 (n/g)/yr for the rhyolite. The larger neutron production rate for the rhyolite is due to the larger U (11.5 ppm) and Th (22.2 ppm) concentration of the rhyolite; for comparison, the U and Th concentrations of the basalt were 0.8 and 2.23 ppm, respectively.

Corrected concentrations of ^{36}Cl in ground water were estimated by taking into account Cl$^-$ concentration, minimum rock porosity (to maximize ^{36}Cl production), and the calculated ^{36}Cl/Cl ratios. In basalt and rhyolite, the maximum ^{36}Cl concentrations were 2.45×10^5 and 7.68×10^6 atoms/L, respectively. These maximum estimated ^{36}Cl concentrations in ground water from *in situ* production are on the same order of magnitude as natural concentrations in meteoric water. In contrast, the maximum ^{36}Cl concentration measured in ground water collected near the INTEC was $22 \pm 0.1 \times 10^{12}$ atoms/L, six orders of magnitude larger than *in situ* or meteoric concentrations. *In situ* ^{36}Cl/Cl ratios in ground water from rock with average compositions in this research ranged from 4.0×10^{-15} to 33.3×10^{-15}. For comparison, the range of ^{36}Cl/Cl for the 70 ground water samples collected from the Snake River Plain aquifer at and near the INEEL was $47.7 \pm 0.2 \times 10^{-14}$ to $2.1 \pm 0.06 \times 10^{-9}$ (table 2.1). Based on these results, *in situ* production of ^{36}Cl is insignificant compared to concentrations measured in ground water near buried and injected nuclear waste at the INEEL.

CHAPTER 6

ESTIMATION OF SELECT AQUIFER HYDRAULIC PROPERTIES FROM ENVIRONMENTAL CHLORINE-36 DATA

The purpose of this dissertation is to determine the sources of ^{36}Cl in the eastern Snake River Plain aquifer system and to describe the implications of using this isotopic tracer for estimating the environmental impact of waste disposal practices near a nuclear facility (INEEL). In chapter 5, the contributions to environmental concentrations of ^{36}Cl from all major sources in the study area were established. In this chapter the ^{36}Cl data are used in a 1-D system-response model to estimate select aquifer hydraulic properties. The selected aquifer hydraulic properties estimated are ground water flow velocities and effective longitudinal hydrodynamic dispersion. The flow velocities will be estimated from the apparent first-arrival times of ^{36}Cl in water from far-field monitoring wells (USGS 11 and USGS 14, fig. 6.1) downgradient from the INTEC. Additionally, the 1-D system response model will be utilized to estimate hydrodynamic dispersion. It is not the purpose of this research to construct a computer model that represents ground water flow, therefore, the purpose of this chapter is to utilize the knowledge gained in establishing the origin of ^{36}Cl in the eastern Snake River Plain to estimate select aquifer hydraulic properties. Special thanks are due to Dr. John A. Welhan, Idaho Geological Survey, for his insights of the ground-water flow in the eastern Snake River Plain aquifer system and his assistance and guidance on constructing and implementing the system-response model described here.

6.1   Conceptual Model of Ground water Movement

A brief review of the geologic framework presented in Chapter 1, section 1.2, is necessary to explain the conceptual model from which the aquifer-hydraulic properties will be estimated. The eastern Snake River Plain is a 28,000-km^2, downwarped, linear structure filled with basalt and sediment (fig. 1.1). Basalt-flow contacts in the subsurface typically are broken,
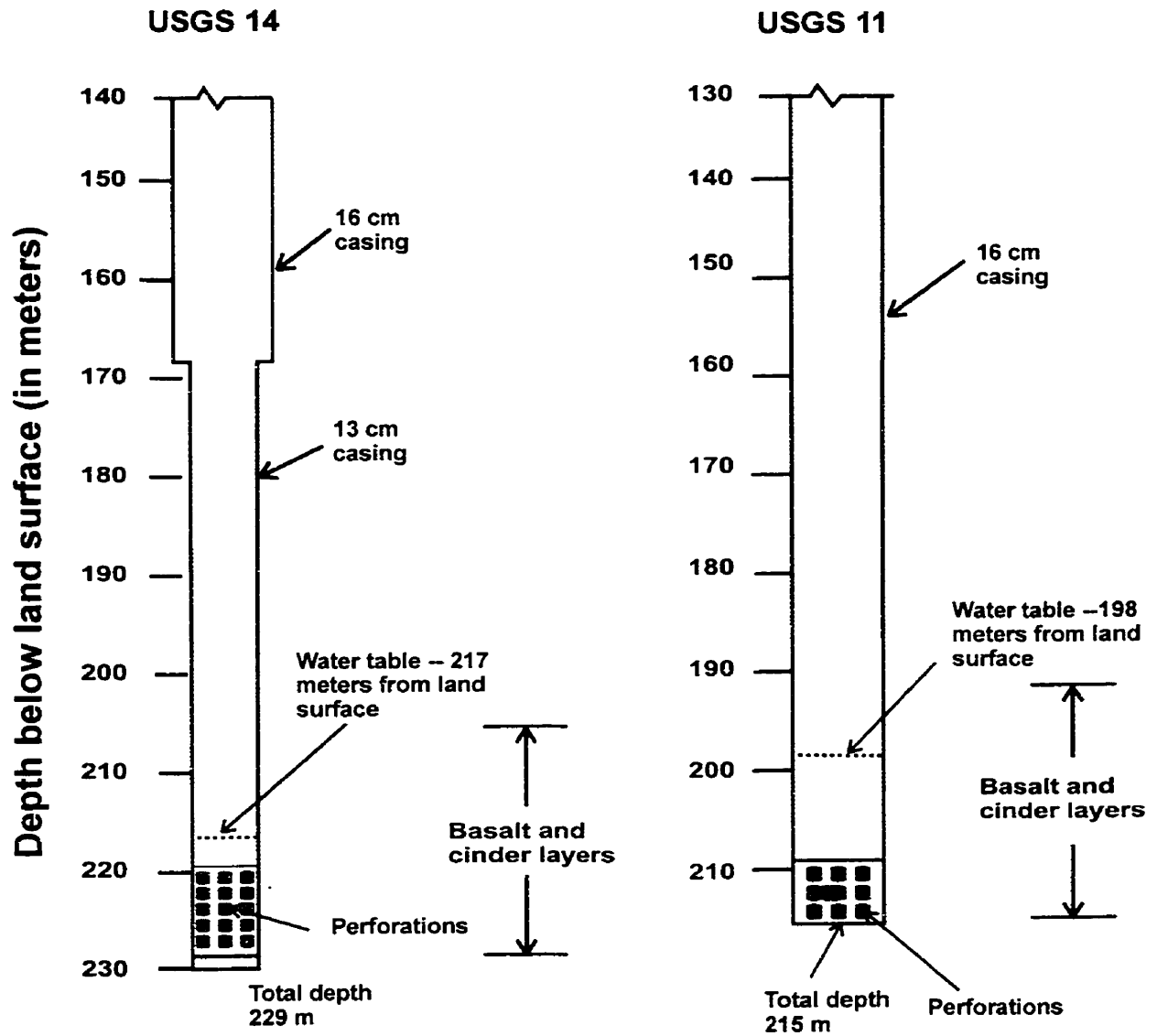
Figure 6.1. Construction diagram for wells USGS 11 and USGS 14.

Note: See Figure 3.1 for well locations.

and these zones may be highly transmissive of ground water. Reported transmissivities for the eastern Snake River Plain aquifer range from 0.1 to over 70,000 m^2/day, nearly six orders of magnitude (Ackerman, 1991). Depth to ground water at the INEEL in the basalt aquifer ranges from 60 m below land surface in the north to over 275 m in the south. The hydraulic gradient at the INEEL is about one m/km, and estimated horizontal ground water flow velocities are between 1 and 6 m/day. Regional ground water flow is from the northeast to the southwest (fig. 6.2).

Several attempts have been made to mathematically model waste plumes in the fractured basalt at the INEEL. The first report on computer-simulated transport of radionuclide and chemical waste in the Snake River Plain aquifer at the INEEL was published by Robertson (1974). That report documented the calibration of a 2-D computer model using data from the USGS for the period 1952 to 1972 and presented predictions of solute spreading in the aquifer at the INEEL to the year 2000. The calibrated longitudinal (α_L) and transverse (α_T) dispersivities were 90 and 140 m, respectively. This characteristic, $\alpha_T > \alpha_L$, is not expected theoretically and is still unique among field-scale investigations. A critical review of 59 published investigations of field-scale dispersion in aquifers showed that for 24 values of transverse dispersivity reported, all but those reported for the eastern Snake River Plain aquifer were one to two orders of magnitude less than the longitudinal values (Gelhar and others, 1992). Subsequent reevaluations of the simulation by Robertson (1974) and new attempts at modeling flow and transport have not resolved this apparent discrepancy (Duffy and Harison, 1987; Goode and Konikow, 1990). In light of the vertically stratified and inhomogeneous nature of this aquifer, an evaluation of its dispersive characteristics with a 2-D, vertically-averaged model, as was done by Robertson (1974), may not be fully representative of this complex aquifer system.

Previous work with isotopic tracers in the eastern Snake River Plain aquifer system suggest that first arrivals of [36]Cl and [129]I indicate that wastewater from the INTEC was detected in wells at the southern boundary of the INEEL as early as 1983 (Cecil and others, 1999, 2000b).

—— 4500 —— WATER—TABLE CONTOUR — Shows altitude of
water table. Intervals 10 and 100 feet.
Datum is sea level. Dashed where approximately
located

• WELL AT WHICH WATER LEVEL WAS MEASURED.
Open circle denotes water—level measurement
for February or June, 1995
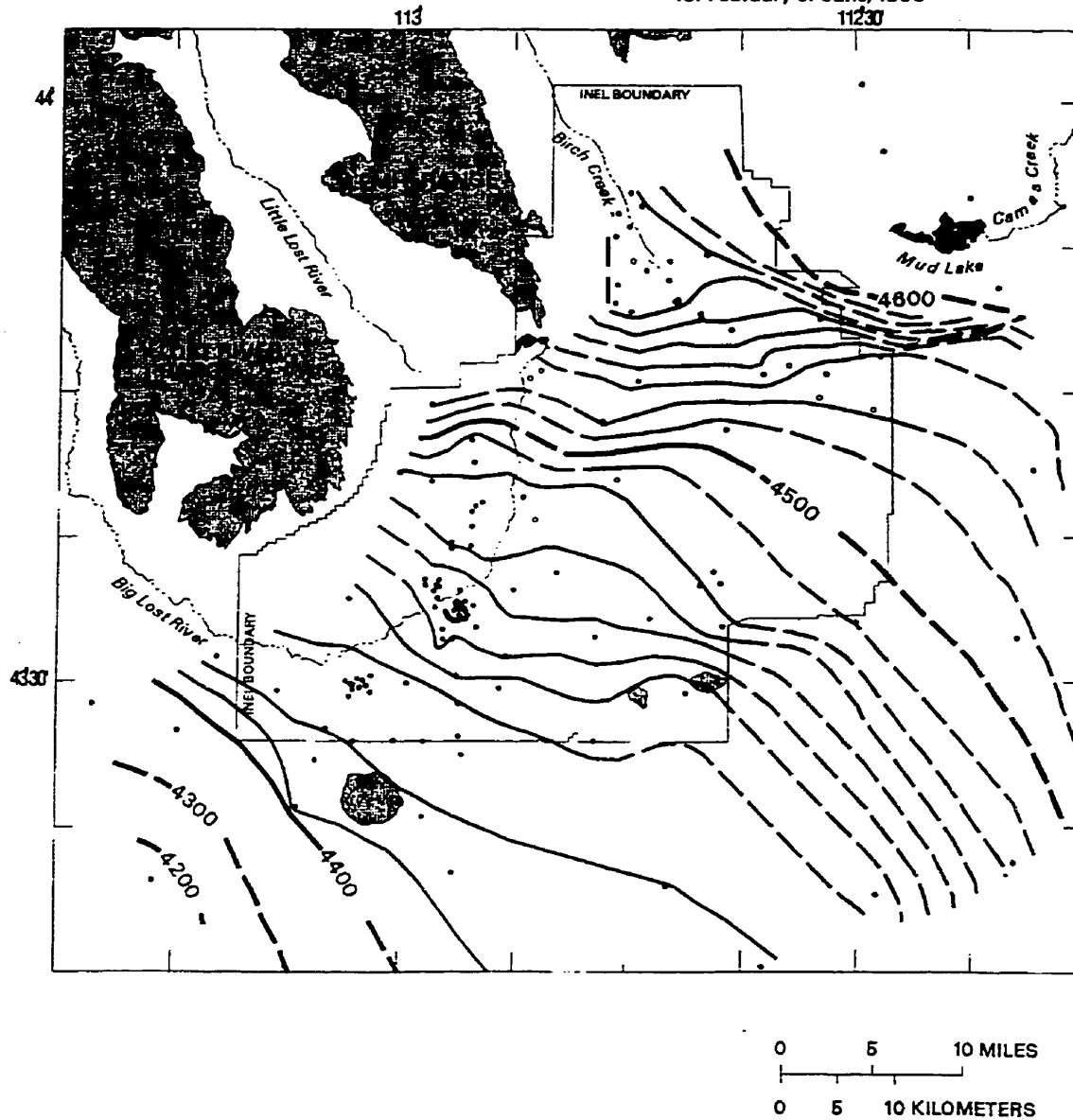
Figure 6.2.   Altitude of the water table in the Snake River Plain aquifer in the vicinity of
the Idaho National Engineering and Environmental Laboratory, March-May 1995.

This represents contaminant movement of about 13 km in 30 years, corresponding to an estimated minimum linear flow velocity of 1.2 m/day. Iodine-129 was detected in well USGS-11, about 24 km downgradient from the INTEC (fig. 3.1), at a concentration above background in 1991, corresponding to a linear flow velocity of 1.8 m/day (Mann and Beasley, 1994). Data presented in this dissertation indicates that the ^{36}Cl from INEEL operations was detectable at wells USGS 11 and USGS 14, about 26 km downgradient from the INEEL as early as 1977 (table 2.1). This represents contaminant movement of up to 26 km in 24 years and corresponds to an estimated minimum linear flow velocity of 3 m/day. The ^{36}Cl concentration in water from wells USGS 11 and USGS 14 in 1977 was $2.7\pm0.1 \times 10^8$ and $3.6\pm0.1 \times 10^8$ atoms/L, respectively. These concentrations represent the minimum first arrival of wastewater containing ^{36}Cl from INEEL disposal to the aquifer and are nearly three to four times the estimated maximum background (including weapons-test contributions) of 1×10^8 atoms/L (Chapter 5). The peak ^{36}Cl concentrations in water from wells USGS 11 and USGS 14 ($16\pm0.8 \times 10^8$ and $19\pm0.2 \times 10^8$, respectively, table 2.1) are an order of magnitude larger than concentrations reported for combined meteoric and weapons-test concentrations. This suggests that ^{36}Cl derived from nuclear-waste processing at the INTEC has been detected in water from far-field observation wells, and that the peak concentrations measured in water from these wells represent the maximum releases that occurred at the deep disposal well in 1958 (table 6.1).

Additionally, a calculation was performed to determine if the necessary amount of activated ^{35}Cl could have been processed at the INTEC to see the signature of ^{36}Cl measured in the ground water samples at the INEEL (Appendix table C-10). The amount of ^{35}Cl necessary for that signature is 35 grams/year. There is more than this amount of stable chlorine processed at the INTEC on a monthly basis (Steve Fernandez, INEEL, oral communication, 1997). This 35 grams of ^{36}Cl activated per year is equivalent to 1.2 curies per year. Over the period of nuclear fuel and nuclear-waste processing at the INTEC (1953 to 1991), the total ^{36}Cl inventory from

Table 6.1.   Input of tritium and calculated input of chlorine-36 to ground water through a deep-disposal well, Idaho Nuclear Technology and Engineering Center.

[See figure 1.2 for disposal well location.]

Year	Tritium (curies)	Estimated chlorine-36 (curies)	Volume of water discharged $(\times 10^9\ L)$	Chlorine-36 (atoms/L) $(\times 10^{10})$
1953	456	0.15	1.5	5070
1954	608	0.20	0.87	11600
1955	808	0.27	1.5	9120
1956	1,543	0.51	1.3	19900
1957	969	0.32	0.87	18600
1958	3,504	1.2	1.0	60800
1959	2,565	0.85	1.2	36900
1960	679	0.22	0.72	15500
1961	590	0.19	0.71	13600
1962	361	0.12	0.99	6140
1963	1,084	0.36	0.97	18800
1964	1,768	0.58	1.3	22600
1965	97	0.032	1.6	1010
1966	250	0.083	1.4	3000
1967	961	0.28	1.1	12900
1968	510	0.17	1.0	8610
1969	125	0.041	1.2	1730
1970	75	0.025	1.0	1270
1971	59	0.019	1.0	963
1972	298	0.098	1.3	3820
1973	32	0.011	1.3	429
1974	455	0.15	1.5	5070
1975	43	0.014	1.0	709
1976	43	0.014	1.4	507
1977	734	0.24	1.6	7600
1978	316	0.10	1.6	3170
1979	225	0.074	1.5	2500
1980	109	0.036	1.5	1220
1981	359	0.12	2.0	3040
1982	209	0.069	2.0	1750
1983	436	0.14	2.1	3380
1984	12	0.0040	2.1	96.5
1985	393	0.13	2.0	3290
1986	251	0.083	2.2	1910
1987	215	0.071	2.2	1640
1988	89	0.029	2.1	700
1989	0	0	1.7	0
1990	1	0.00033	2.3	7.27
1991	2	0.00066	2.1	15.9
1992	0.2	0.00007	2.4	1.48
1993	0	0	2.7	0
1994	0	0	2.1	0
1995	0.1	0.00003	1.7	0.894

Tritium total	$\cong$ 21,000

Chlorine-36 total	$\equiv$ 7

neutron-activated ^{35}Cl would be about 46 curies. This amount is more than six times the calculated amount of ^{36}Cl disposed to the environment at the INTEC (7 curies, table 6.1). Therefore, the concentrations of ^{36}Cl measured in the ground water samples at the INEEL could easily be from the INTEC (if assumptions used in Appendix table C-10 are correct).

The ^{36}Cl signal in wells USGS 11 and USGS 14 is similar and is characterized by relatively early arrivals of significant tracer activity, suggesting ground water velocities that are even larger than the minimum estimate of 1 to 6 m/day discussed previously. The 1958 peak in these monitoring wells is fairly sharp, with steep shoulders. However, the maximum ^{36}Cl activity observed in these wells is six orders of magnitude lower than the mean annual ^{36}Cl activity estimated in the INTEC disposal well during the 1958 releases. It would appear that the ^{36}Cl signal has been attenuated significantly through dilution, yet the sharpness of the peaks points to low effective dispersivity or an absence of significant mixing.

These two seemingly contradictory observations may be reconciled within a preferential-flow scenario. It has long been realized that a 3-D modeling approach may be required to adequately describe and predict flow and transport in the Snake River Plain aquifer system. However, the amount of detailed hydraulic and geologic information available to describe the vertical and lateral heterogeneity in the system is inadequate to construct and calibrate such a model. Work is in progress on a stochastic representation of 3-D flow arising from lithologically-controlled preferential flow-paths in the system (Gego and others, in press). Work started by Knutson and others (1990) and continued by Welhan and others (in press) supports the concept that the spatial distribution of high-conductivity zones may be localized along, and of the length scale of, rubble-encrusted and fissured basalt lava flows. Therefore, a conceptual model of preferential flow in which ground water is able to travel significant distances in highly conductive, subhorizontal conduits without significant lateral mixing, has been adopted for this application of ^{36}Cl tracer data to describe select hydraulic properties.

The evidence presented in this dissertation supports the concept that ^{36}Cl derived from

125
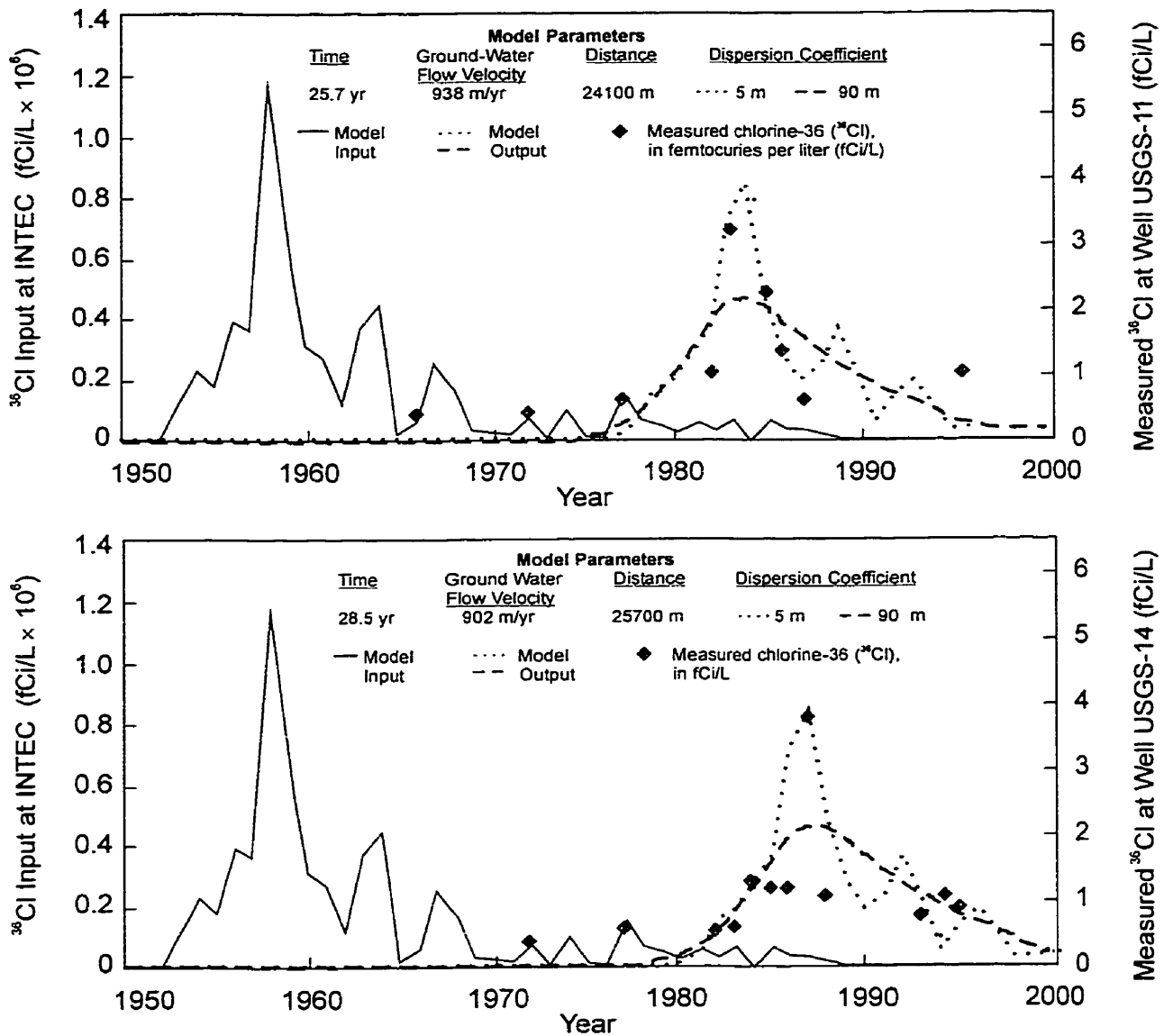
Figure 6.3. Modeled and measured chlorine-36 concentrations in ground water from monitoring wells USGS 11 and USGS 14. Note: See figure 3.1 for location of wells. Data from tables 2.1 and 6.1.

nuclear-waste processing at the INTEC was detected at wells USGS 11 and USGS 14, and that

the peak concentrations observed in these wells represent the maximum releases that occurred at

the INTEC deep-disposal well in 1958 (fig. 6.3). Recent measurements of CFCs support this

concept. Busenburg and others (in review) presented CFC analytical results for water collected

from USGS 11 and USGS 14 in 1995 (USGS 11) and 1994 (USGS 14). The CFC-11 results indicate that these samples were in equilibrium with 1968 and 1970 air, respectively. Therefore, it is probable that water collected from USGS 11 and USGS 14 in the mid-1980s could represent water that passed the INTEC in 1958.

In light of the vertically stratified and complex nature of the aquifer, an evaluation of its dispersive characteristics with a 2-D (vertically averaged) model, as was done by Robertson (1974), may be misleading. Robertson's fitted longitudinal dispersivity was of the order of 90 m, and appears to be reasonable for the scale and complex nature of the flow system. The transverse dispersivity was on the order of 140 m. However, this very high transverse/longitudinal dispersivity ratio has not been observed in any other aquifer system and has not been satisfactorily explained. For example, Goode and Konikow (1990) concluded that transient recharge normal to the regional flow direction could not account for these anomalous transverse dispersivities. Data presented by Goode and Konikow (1990) suggested that transients in the ground water flow field caused by episodic recharge in the Big Lost River channel near the INTEC (figure 1.2) made estimation of α_T and α_L ambiguous. They recalibrated Robertson's model using data from the USGS generated after 1972 and found that predictions of the shape of contaminant plume in the ground water downgradient from the INTEC were very insensitive to changes in dispersivities in both steady-state and transient simulations.

6.2   Transport Model Development

A 1-D, lumped-parameter, system-response model was chosen to interpret the tracer arrival record in terms of the tracer signal transformation characteristics of the system (i.e. the preferential flow path) between the point of injection and the point of monitoring. The dispersive impulse function of Maloszewski and Zuber (1982) was used for modeling the dispersive characteristics along a single assumed preferential flowpath, by fitting the predicted output response to the observed tracer record at given monitoring wells.

A system-response approach has not seen wide application in ground water studies

because of a lack of adequate records for temporal variations in tracer concentrations and primarily because of the need to assume steady flow. On a local scale, where tracer data are more likely to be available over the time scale of interest, the hydrologic steady state is a poor approximation of reality, but the steady-state assumption becomes less restrictive on a regional scale. However, it has not seen wide applicability in regional studies because the requisite input and output tracer data usually are not available over the time scales of interest. Despite its limitations, the method has been used successfully in the analysis of residence times and mixing in shallow soil and ground water flow and surface water runoff (Maloszewski et al., 1983; Stewart and McDonnel, 1991).

Because the total tracer (in this case, ^{36}Cl) injected at the INTEC disposal well is assumed to split into multiple, divergent preferential flow paths, each individual flow path carries a fraction of the total tracer input. This implicitly prevents fitting of absolute tracer concentrations since a 1-D model cannot account for flow splitting. Instead, the analysis presented in this dissertation focuses on the shape of tracer breakthrough curves to constrain the magnitude of the dispersion process. Although parameter fitting to peak shape and arrival times will limit overall accuracy, neither the amount of available tracer data nor the limited knowledge of the complexity of the flow processes operable in the eastern Snake River Plain aquifer system justify a more rigorous approach. However, as discussed in section 6.3 of this chapter, this fitting approach appears to be capable of constraining the magnitude of the apparent dispersion, based solely on the shape of the ^{36}Cl tracer arrival curves at wells USGS 11 and USGS 14 (fig. 6.3).

6.3   Model Construction

The intent is to examine the implications of preferential flow on the transport of contaminants over tens of kilometers in this complex aquifer. Since the necessary information for constraining a 2-D or 3-D transport model was lacking, a simple 1-D model was used to evaluate the dispersive characteristics associated with preferential flow in this system using ^{36}Cl tracer

records at wells USGS 11 and USGS 14 (fig. 3.1). Construction characteristic for wells USGS 11 and USGS 14 are shown n figure 6.1.

The amount of ^{3}H and the volume of wastewater discharged at the INTEC are shown in table 6.1. From 1953 to 1995 the amount of ^{3}H in wastewater discharged at the INTEC ranged from 0 to 3,504 curies per year (Ci/yr) and averaged about 500 Ci/yr. The amount of ^{36}Cl discharged annually is not known. However, an activity ratio of ^{36}Cl/^{3}H for a typical high-yield nuclear fuel reprocessed at the INTEC was used to calculate the annual amounts of ^{36}Cl listed in table 6.1; the activity ratio is 3.3 x 10^{-4} (Steve Fernandez, INEEL, oral communication, 1997). Because this ^{36}Cl/^{3}H ratio is representative of a high-yield nuclear fuel, the inventory of ^{36}Cl calculated using this value should be considered as maximum. Using this method, the total ^{36}Cl estimated to have been discharged to the environment at the INTEC is about 7 Ci (table 1). This amount is comparable to an estimate of 65 percent of the total INEEL discharge of 10 Ci of ^{36}Cl attributable to the INTEC (Cecil. unpublished data. 1999). These estimated ^{36}Cl source concentrations compose the tracer-input signal used in the 1-D system-response model for estimating a coefficient of dispersion. The ^{36}Cl concentrations over time for wells USGS 11 and USGS 14 are given in table 2.1.

The path length (x) along an individual flowline within this preferential-flow model is believed to be tortuous. However. until the results of stochastic flow modeling are available to impose constraints on the effective tortuosity. a straight-line distance between source and output is assumed. Therefore. the dispersivity derived from the x/v (mean flowpath length/mean velocity) fitting parameter represents a minimum estimate. The effect of flowpath tortuosity is countered by the fact that this model does not account for mixing at the intersections of flowpaths. Thus, the fitted dispersivity should provide a reasonable estimate of the magnitude of the dispersion process along a single preferential flowpath.

The results of model fits to the ^{36}Cl arrivals in USGS 11 and USGS 14 are shown in figure 6.3. As discussed previously. the tracer arrivals demonstrate very low concentrations

relative to the disposal well and are distinctly peaked, reflecting the 1958 disposal event. The ^{36}Cl concentrations in both wells are much less than that of the 1958 peak in the disposal well, suggesting dilution or loss of tracer mass by other than longitudinal dispersion. Because matrix diffusion is a second-order attenuation mechanism in flow systems dominated by advection and dispersion (such as suggested in this dissertation for the Snake River Plain aquifer) this process was assumed negligible and was not considered (Knox and others, 1993). In future research on the preferential flowpath scenario invoked here, a more rigorous analysis and discussion of matrix diffusion as a possible ^{36}Cl peak attenuation mechanism in the far field is warranted.

Maloszewski et al (1983) analyzed the annual variation of deuterium in precipitation and in an alpine stream using a systems-response approach, to characterize the distribution of runoff routing times. Welhan and others (in press) utilized stable oxygen-isotope variations in a shallow ground water flow system to constrain flow and transport parameters. In that work, a steady-state system response model was used to constrain tracer transport conditions in a shallow ground water flow system by modeling $\delta^{18}O$ variations with a transit-time distribution model incorporating dispersion. By considering a range of possible isotope recharge signals, the range of effective dispersivity and the effective distance from the recharge zone were constrained for use in subsequent distributed-parameter numerical modeling.

The availability of ^{36}Cl disposal rates at the INTEC well, the spatial scale of flow involved in the Snake River Plain aquifer south of the INTEC, and the availability of temporal records of ^{36}Cl variability in observation wells which span the time scale of interest make it likely that the method can be successfully applied in this hydrogeologic setting.

In a system-response model, transformation of an input signal, $C_{in}(t)$, traveling through a system at hydrologic steady-state is described by the convolution integral:

$$C_{out}(t) = \int_{0}^{t} C_{in}(t-t') f(t') dt'$$ (6.2-1)

where $C_{out}(t)$ is the concentration at a specific location and time, and $f(t)$ is a dispersive function used here to represent 1-D transport of a tracer along a path of infinite length under steady-state ground water flow. Because ^{36}Cl has a half-life of 301,000 years and this analysis was conducted over a relatively short time interval of 40 years, a radioactive decay term was not included in equation 6.2-1. The following equation from Maloszewski and Zuber (1982) best represents the dispersive, or system-response, function for this analysis:

$$f(t)=([(4\pi)(D/vx)]^{-1\,2}\,(t/r)^{-1\,2}(1/t))\,exp[-(1-t/r)^2(4(D/vx)(t/r))^{-1}]$$ (6.2-2)

where D/vx is the dimensionless dispersion parameter and r is the mean transit time, equal to system volume divided by average linear ground water velocity through the system or, in a homogeneous system, equal to flow path length (x) divided by mean velocity (v). Although this steady-state assumption is simplistic, it should be justifiable to first order, given the scale of flow (both spatial and temporal). The system-response modeling approach allows an estimate of the magnitude of dispersion and the flow velocity by model fitting of the observed ^{36}Cl-tracer output signal in downgradient observation wells to the ^{36}Cl-tracer input signal from disposal at the INTEC.

To generate the simulated tracer arrival, the convolution integral was evaluated using a numerical approach (Yurtsever, 1983) based on the tracer-input data from table 6.1. The calculations were implemented in a computer spreadsheet to maximize flexibility and interactive parameter fitting. In light of the uncertainties and step-like nature of the input function that was reconstructed at the disposal well, only annual or semi-annual average tracer concentrations could be used as input. The model's operation and output response were verified against a 1-D analytical model describing instantaneous injection of a slug into a uniform-flow field (Sauty, 1980). The results of comparisons between the numerical and analytical models showed that the system-response model fitting procedure was adequate for both long residence time or long travel

131

path (50 years and 26 km, respectively) and small and large dispersivity (5 to 90 m). The mean fitting errors were two percent and seven percent for residence time and dispersivity, respectively.

6.4. Discussion of Modeling Results

Another significant feature of the arrival record of isotopic tracers at wells USGS 11 and USGS 14 is that ^{36}Cl apparently arrives much earlier than predicted by this simple, 1-D, preferential-flow model (fig. 6.3). For example, the best-fit model predicts that no ^{36}Cl will have arrived at wells USGS 11 and USGS 14 by 1977, whereas observed radioactivity of ^{36}Cl in that year was 2.7±0.1 × 10^8 atoms/L at well USGS 11 and 3.6±0.1 × 10^8 atoms/L at well USGS 14. As already discussed, these concentrations are as much as four times larger than the combined meteoric and weapons-test contributions described in Cecil and others (1999), implying that some of the tracer moved at least twice as fast as is generally accepted for ground water flow velocities in this system. The earliest measured arrival at wells USGS 11 and USGS 14 corresponds to travel times of the order of 10 to 12 years, implying that effective maximum advective linear velocities may be as much as two times higher than velocities estimated from peak-to-peak arrival time, or up to 6 m/day.

Model fits for dispersivities of 5 and 90 m are shown in figure 6.3. Disregarding the single relatively enriched radioactivity due to ^{36}Cl measured in water from well USGS 14 collected in 1987, a 90-m dispersivity would provide a marginally acceptable fit. However, a 5-m dispersivity provides the best visual fit for data from both wells USGS 14 and USGS 11 when all the data points are considered, and the structure of the estimated input signal is retained using this value (fig. 6.3). A dispersivity of 90 m is similar to the longitudinal dispersivity estimated by Robertson (1974) in the 2-D, regional, equivalent porous-media model calibration (α_L = 90 m), and it plots in the middle of the spread of dispersivity values summarized by Gelhar and others (1992) for this scale of flow distance. The 5-m dispersivity is smaller than any previously reported dispersivity value for this scale of transport and is comparable to the only other reported

dispersivity in fractured rock, also estimated using an environmental tracer (Gelhar and others, 1992).

The implications of ^{36}Cl arrivals at wells USGS 11 and USGS 14 are important for three reasons: 1) these tracer results provide quantitative constraints on residence time or flow velocity and on dispersivity; 2) these constraints aid in refining the working conceptual model of preferential flow in this aquifer system. For example, the very early appearance of ^{36}Cl in water from wells USGS 11 and USGS 14 may be due to relatively fast flow in one or more flow conduits intersecting the open intervals in these wells. Such a conceptual model is consistent with the observation of spatially correlated transmissivities on the areal scale of individual basalt flows and consistent with known geologic or lithologic controls on preferential flow in this aquifer system (Welhan and others, in press); and 3) these results also suggest that high-conductivity interflow zones and lava tubes within individual basalt flows may be separated by lower conductivity sediment beds and massive basalt zones such that a range of preferential flowpaths and degrees of interconnection and effective velocities exist (fig. 6.1). This information also may provide a means for mapping preferential flowpaths within the eastern Snake River Plain aquifer.

Chapter 7

SUMMARY AND RECOMMENDATIONS FOR FUTURE RESEARCH

To facilitate the use of ^{36}Cl as a hydrogeologic tracer near a nuclear facilty in southeastern Idaho (the Idaho National Engineering and Environmental Laboratory (INEEL)), accelerator mass spectrometric (AMS) measurements were made for ^{36}Cl on 127 samples of ground water, surface water, snow, glacial ice and runoff, and spring water. From the AMS measurements of the $^{36}Cl/Cl$ ratios, atom concentrations of ^{36}Cl were calculated. The results of these analyses were used to determine meteoric, nuclear weapons-tests, and nuclear waste-processing contributions of this nuclide to inventories in the environment at and near the INEEL. An additional 25 rock samples were collected and processed for geochemical analyses for 23 elements to calculate *in situ* neutron production rates and resultant ^{36}Cl concentrations.

Beginning in 1966, the U.S. Geological Survey (USGS) has archived a suite of quarterly water samples collected at the INEEL each year. Samples were selected from the USGS library to evaluate the suitability of using these historical archives for determining changes in ^{36}Cl concentrations with time in water from the eastern Snake River Plain aquifer at and near the INEEL. Water samples from six monitoring wells and one surface water site covering the period 1966-1993 were selected for analysis of stable chlorine isotopic ratios ($^{37}Cl/^{35}Cl$). This information was used to determine if ^{36}Cl concentrations measured in the archived water samples in the 1990s are representative of the concentrations at the time of sample collection.

The $^{37}Cl/^{35}Cl$ ratio of the archived samples was measured at the Environmental Isotope Laboratory at the University of Waterloo, Ontario, Canada, and was compared to the $^{37}Cl/^{35}Cl$ of Standard Mean Ocean Water. The resultant delta ^{37}Cl ($\delta^{37}Cl$) data ranged from -0.44 ± 0.5 to $+0.59\pm0.16$ permil and had a mean of 0.15 ± 0.27 permil. The largest variation in $\delta^{37}Cl$ for water

from any individual well was 0.91 permil. However, considering the associated uncertainties with these data, this range is even smaller than this value. A review of avilable $\delta^{37}Cl$ data collected worldwide from a variety of geologic and hydrogeologic environments, showed a range of -4.9 to $+6.0$ permil, which is nearly 11 permil and is an order of magnitude greater than the range for water determined in this research. The range of $\delta^{37}Cl$ meaured in water from the INEEL is indicative of little or no fractionation. Based on the results of this evaluation of $\delta^{37}Cl$ in water collected from the eastern Snake River Plain aquifer at and near the INEEL, it was concluded that ^{36}Cl concentrations measured in the 1990s for samples collected from 1966-1993 were representative of the concentration at the time of sample collection.

Chlorine-36 concentrations in the archived water samples plus additional samples collected for this research were determined. The results of these analyses suggest a meteoric source of the ^{36}Cl for environmental samples collected in southeastern Idaho and western Wyoming if the concentration is less than 1×10^{7} atoms/L (table 7.1). Additonally, concentrations in water, snow, or glacial ice between 1×10^{7} atoms/L and 1×10^{8} atoms/L may be indicative of a weapons-tests component from peak ^{36}Cl production in the late 1950s. Chlorine-36 concentrations between 1×10^{8} atoms/L and 1×10^{9} atoms/L may be representative of resuspension of weapons-tests fallout, airborne disposal of ^{36}Cl from the INEEL, or of concentration by evapotranspiration. Additionally, the calculation of maximum ^{36}Cl contributions from *in situ* production in the aquifer matrix were less than 1×10^{7} atoms/L, or the same as meteoric concentrations (table 7.1). It was concluded that only concentrations of ^{36}Cl larger than 1×10^{9} atoms/L measured in the environment at and near the INEEL can be attributed with confidence to waste disposal at the site. (Table 7.1 lists the threshold values for the major ^{36}Cl sources at and near the INEEL determined from the analyses presented in this dissertation. These threshold values are specific to the sources listed in table 7.1 rather than ranges presented in this paragraph.)

This information was then used to construct a 1-D system response model to estimate aquifer dispersivity on the field scale out to 26 kilometers downgradient from the disposal source at the INEEL. Historical [36]Cl concentrations for monitoring wells USGS 11 and USGS 14 were measured in archived samples for the period 1966-1995. Chlorine-36 disposal to the aquifer was reconstructed from detailed tritium disposal records and a knowledge of the ratio of tritium and chlorine-36 for a high-yield fuel that was processed at the Idaho Nuclear Technology and Engineering Center, a nuclear fuel and waste processing facility at the INEEL. A 1958 disposal peak reconstructed from the [36]Cl input function for the 1-D model was identified in the historical data from wells USGS 11 and USGS 14 based on the threshold concentrations established from the [36]Cl souces identified through this research (table 7.1).

A preferential flowpath scenario was adopted for the flow in the aquifer and simple curve matching was applied to the model input and output to visually determine the best-fit dispersivity. It was determined that an effective longitudinal dispersivity of 5 m provided the best visual fit for data from both USGS 11 and USGS 14 when considering all data points. The structure of the estimated input signal also is best retained using this value.

Concentrations of the isotopic tracer [36]Cl have been established for all of the known sources in the environment at and near the INEEL. It is now understood that [36]Cl concentrations in ground water measured by AMS may provide an extremely sensitive far-field detection capability for certain types of contaminant plumes in certain geologic terrains. Additonally, based on the research presented here, it may now be possible to fully quantify the concentrations and fluxes of [36]Cl from nuclear-weapons tests archived in mid-latitude glacial ice in North America and to gain a better understanding of the distribution at mid-latitude of [36]Cl and other cosmogenic isotopes such as carbon-14, iodine-129, and beryllium-10. A list of additional research topics to be pursued as a result of this research follows:

(1) Additional spatial and temporal measurements of ^{36}Cl in both wet precipitation and dry deposition are needed to gain a better understanding of ^{36}Cl deposition patterns and processes in the study area.

(2) More measurements of the chloride/bromide mass ratio in ice cores would be useful in verifying the source of the chlorine.

(3) A transfer function needs to be developed for a more quantitative comparison of ^{36}Cl concentrations at higher altitudes (the Wind River Mountains) with concentrations deposited at lower altitudes (the Snake River Plain). One possibility for this suggestion is the measurement of the ^{36}Cl /^{137}Cs ratios in ice and snow in the Wind River Mountains for comparison to the ^{36}Cl /^{137}Cs ratios in soils on the Snake River Plain.

(4) Use the historical ^{36}Cl data in ground water developed for this research with available tritium data to model preferential flowpath "corridors" in the eastern Snake River Plain aquifer system (if they exist).

(5) The *in situ* ^{36}Cl production estimates could be improved by performing neutron flux measurements directly in wells at the INEEL. Fluxes determined in this way could be used to verify the neutron production estimates presented in this research.

(6) The monitoring well network at the INEEL needs to be improved to include nested piezometers with packer sampling to isolate water-bearing zones for improved tracer detection and interpretation.

(7) Measurements of ^{36}Cl and $\delta^{37}Cl$ in the effluent stream at the Idaho Nuclear Engineering and Technology Center would be useful in determining if there are

mechanisms operable at nuclear fuel and nuclear waste processing facilities that fractionate chlorine isotopes in a predictable manner. This information would be useful in understanding ground water movement at other sites throughout the DOE complex.

(8) Determine ^{36}Cl *in situ* production for sedimentary interbeds and fracture filling.

Table 7.1.   Summary of threshold chlorine-36 concentrations determined in this research.

Type of contribution to ^{36}Cl concentrations	Threshold ^{36}Cl concentration (atoms/L)	$(^{36}Cl/Cl) \times 10^{-15}$	Source of threshold concentration
Meteoric production	$\leq 7 \times 10^6$	300 to 600	Snow, surface water, and ground water samples
Deep *in situ* production	$\leq 8 \times 10^6$	≤ 45	Whole-rock analyses
Weapons-tests production	$\leq 8 \times 10^7$ *	1,900 to 30,000	Ice-core samples
INEEL contribution	$\geq 1 \times 10^9$	1,300 to $> 10^6$	All samples in table 1.1

* water equivalent concentration

REFERENCES

Ackerman, D.J., 1991, Transmissivity of the Snake River Plain aquifer at the Idaho National Engineering Laboratory, Idaho: U.S. Geological Survey Water-Resources Investigations Report 91-4058 (DOE/ID-22097), 35 p.

American Society for Testing and Materials, 1982, Standard test methods for chloride ion in water, in: Annual American Society for Testing and Materials, Standards, pt. 31, p. 353-361.

Anders, E., and Ebihara, M., 1982, Solar system abundance of the elements, *Geochemica et Cosmochemica Acta* 46, p. 2363-2380.

Andrews J.N., Edmunds W.M., Smedley P.L., Fontes J.-C., Fifield L.K. and Allan G.L., 1994, Chlorine-36 in ground water as a palaeoclimatic indicator: the East Midlands Triassic sandstone aquifer (UK). Earth Planet. Sci. Lett. 122, 159-171.

Andrews, J.N., Davis, S.N., Fabryka-Martin, J., Fontes, J-Ch., Lehmann, B.E., Loosli, H.H., Michelot, J-L., Moser, H., Smith, B., and Wolf, M., 1989, The *in situ* production of radioisotopes in rock matrices with particular reference to the Stripa granite: *Geochemica et Cosmochemica Acta*, v. 53, p. 1803-1815.

Andrews, J.N., Fontes, J-Ch, Michelot J-L., and Elmore, D., 1986, In situ 36Cl production and ground water evolution in crystalline rocks at Stripa, Sweden, Earth and Planetary Science Letters, 77, p. 49-58.

Andrews, J.N., and Fontes, J.-C., 1992, Importance of the *in situ* production of ^{36}Cl, ^{36}Ar and ^{14}C in hydrology and hydrogeochemistry: International Atomic Energy Agency, IAES-SM-319/12, p. 245-269.

Aruscavage, P., 1990, Determination of chloride in geologic materials by ion-selective electrode following $KMnO_4$-H_2SO_4-HF dissolution, in B.F. Arbogast, ed., Quality Assurance Manual for the Branch of Geochemistry: U.S. Geological Survey Open-File Report 90-668, p. 119-122.

Baedecker, P.A., and McKown, D.M., 1987, Instrumental neutron activation analysis of geochemical samples, in P.A. Baedecker, ed., Methods for geochemical analysis: U.S. Geological Survey Bulletin 1770, p. H1-H14.

Barraclough, J.T., Lewis, B.D., and Jensen R.G., 1982, Hydrologic conditions at the Idaho National Engineering Laboratory, Idaho--emphasis, 1974-1978: U.S. Geological Survey Water-Supply Paper 2191, 52 p.

Barraclough, J.T., and Jensen R.G., 1976, Hydrologic data for the Idaho National Engineering Laboratory site, Idaho 1971 to 1973: U.S. Geological Survey Open-File Report 75-318 (IDO-22055), 52 p.

Bartholomay, R.C., Orr, B.R., Liszewski, M.J., and Jensen, R.G., 1995, Hydrologic conditions and distributions of selected radiochemical and chemical constituents in water, Snake River Plain aquifer, Idaho National Engineering Laboratory, Idaho, 1989-91: U.S. Geological Survey Water-Resources Investigations Report 95-4175, 47 p.

Bartholomay, R.C., 1993, Concentrations of tritium and strontium-90 in water from selected wells at the Idaho National Engineering Laboratory after purging one, two, and three borehole volumes, U.S. Geological Survey Water Resources Investigations Report 93-4201, 21 p.

Beasley, T.M., Cecil, L.D., Sharma, P., Kubik, P.W., Fehn, U., Mann, L.J., and Gove, H.E., 1993, Chlorine-36 in the Snake River Plain Aquifer at the Idaho National Engineering Laboratory: Origin and Implications. Ground Water, vol. 31, no. 2.

Begemann, F., and Libby, W.F., 1957, Continental water balance, ground water inventory and storage time, surface ocean mixing rates and world-wide water circulation patterns from cosmic-ray and bomb tritium: Geochemica et Cosmochemica Acta, v. 12, p. 277-296.

Bentley, H.W., Phillips, F.W., and Davis, S.N., 1986a, Chlorine-36 in the terrestrial environment, in Handbook of Environmental Isotopes, vol. 2, p. 422-480, edited by P. Fritz and J-C. Fontes, Elsevier, New York.

Bentley, H.W., Phillips, F.M., Davis, S.N., Gifford, S, Elmore, D., Tubbs, L.E., and Gove, H.E., 1982, Thermonuclear ^{36}Cl pulse in Natural Water: Nature 300, p. 737-740.

Bentley H.W., Phillips F.M., Davis S.N., Airey P.L., Calf G.E., Elmore D., Habermehl M.A. and Torgersen T., 1986b, Chlorine-36 dating of very old ground water: I. The Great Artesian Basin, Australia. Water Resour. Res. 22, 1991-2002.

Busenberg E., Weeks, E.P., Plummer, L.N., and Bartholomay, R.C., 1993, Age dating ground water by use of chlorofluorocarbons (CCl$_3$F and CCl$_2$F$_2$), and distribution of chlorofluorocarbons in the unsaturated zone, Snake River Plain aquifer, Idaho National Engineering Laboratory, Idaho, U.S. Geological Survey Water Resources Investigations Report 93-4054, 47 p.

Busenburg, E., Plummer, L.N., and Bartholomsy, R.C., in review, Age of ground water at the Idaho National Engineering and Environmental Laboratory: results from chlorofluorocarbons, tritium-helium, sulfur hexafluoride, and other environmental tracers,

U.S. Geological Survey Water Resources Investigations Report.

Carlson C.A., Phillips F.M., Elmore D. and Bentley H.W., 1990, Chlorine-36 tracing of salinity sources in the Dry Valleys of Victoria Land, Antarctica. Geochimica et Cosmochimica. Acta. 54, 311-318.

Cecil, L.D., 1989, Definitions for the interpretation of analytical results for radionuclides of environmental concern, in: Pederson, G.L., and Smith, M.M., eds., U.S. Geological Survey 2nd National Symposium on Water Quality, Abstracts: U.S. Geological Survey Open-File Report 89-409, p. 9-10.

Cecil, L.D., Knobel, L.L., Wegner, S.J., and Moore, L.L., 1989, Evaluation of field sampling and preservation methods for strontium-90 in ground water at the Idaho National Engineering Laboratory: U.S. Geological Survey Water-Resources Investigations Report 89-4146, 24 p.

Cecil, L.D., Orr, B.R., Norton, T.J., and Anderson, S.R., 1991, Formation of perched ground water zones and concentrations of selected chemical constituents in water, Idaho National Engineering Laboratory, Idaho 1986-88: U.S. Geological Survey Water-Resources Investigations Report 91-4166, 53 p.

Cecil, L.D., Beasley, T.M., Pittman, J.R., Michel, R.L., Kubik, P.W. Sharma, P., Fehn, U., and Gove, H.E., 1992, Water infiltration rates in the unsaturated zone at the Idaho National Engineering Laboratory from chlorine-36 and tritium profiles, and neutron logging; in Water-Rock Interactions 7, Kharaka, Y.F., and Maest, A.S., editors, A.A. Balkema, Rotterdam, vol. 1, p. 709-714.

Cecil, L.D., and Vogt, S., 1997, Identification of bomb-produced chlorine-36 in mid-latitude glacial ice of North America. Nuclear Instruments and Methods, B123, p. 314-322.

Cecil, L.D., Frape, S.K., Drimmie, R., Flatt, H., and Tucker, B.J., 1998, Evaluation of archived water samples using chlorine isotopic data, Idaho National Engineering and Environmental Laboratory, Idaho, 1966-93. U.S. Geological Survey Water-Resources Investigations Report 98-4008, 27 p.

Cecil, L.D., Green, J.R., Vogt, S., Frape, S.K., Davis, S.N., Cottrell, G.L., and Sharma, P., 1999, Chlorine-36 in water, snow, and mid-latitude glacial ice of North America: Meteoric and weapons-tests production in the vicinity of the Idaho National Engineering and Environmental Laboratory, Idaho. U.S. Geological Survey Water-Resources Investigations Report 99-4037, 27 p.

Cecil, L.D., Knobel, L.L., Green, J.R., and Frape, S.K., 2000a, *In situ* production of chlorine-36 in eastern Snake River Plain aquifer, Idaho: Implications for describing ground water contamination near a nuclear facility. U.S. Geological Survey Water-Resources Investigations Report 00-4114, 35 p.

Cecil, L.D., Welhan, J.A., Green. J.R., Frape, S.K., and Sudicky, E.R., 2000b, Use of chlorine-36 to determine regional-scale aquifer dispersivity, eastern Snake River Plain aquifer, Idaho/USA. Nuclear Instruments and Methods in Physics Research B 172, p. 679-687.

Claasen, H.D., 1982, Guidelines and techniques for obtaining water samples that accurately represent the water chemistry of an aquifer: U.S. Geological Survey Open-File Report 82-1024, 49 p.

Clawsen, K.L., Start, G.E., and Ricks, N.R., eds, 1989, Climatography of the Idaho National Engineering Laboratory, U.S. Department of Commerce, National Oceanic and Atmospheric Administration, DOE/ID-12118, 155 p.

Conard, N.J., Elmore. D., Kubik, P.W., Gove, H.E., Tubbs, L.E., Chrunyk, B.A., and Wahlen M., 1986, The chemical preparation of AgCl for measuring chlorine-36 in polar ice with accelerator mass spectrometry: Radiocarbon, v. 28, p. 556-560.

Cook P.G., Jolly I.D., Leaney F.W., Walker G.R., Allan G.L., Fifield L.K. and Allison G.B., 1994, Unsaturated zone tritium and chlorine-36 profiles from southern Australia: Their use as tracers of soil water movement. Water Resour. Res. 30, 1709-1719.

Cornett R.J., Cramer J., Andrews H.R., Chant L.A., Davies W., Greiner B.F., Imahori Y., Koslowsky V., McKay J., Milton G.M. and Milton J.C.D. (1996) In situ production of ^{36}Cl in uranium ore: A hydrogeological assessment tool. Water Resour. Res. 32, 1511-1518.

CRC Handbook of Chemistry and Physics. 1991, Lide, D.R., ed., CRC Press, Boston, various pagination.

Currie, L.A., 1984, Lower limit of detection: Definition and elaboration of a proposed position for radiological effluent and environmental measurements: U.S. Nuclear Regulatory Commission, NUREG/CR-4007, 139 p.

Davie R.F., Kellett J.R., Fifield L.K., Evans W.R., Calf G.E., Bird J.R., Tropham S. and Ophel T.R. (1989) Chlorine-36 measurements in the Murray Basin: Preliminary results from the Victorian and South Australian Mailee region. BMR J. Aust. Geol. Geophys. 11, 261-272.

Davis, S.N., Cecil, L.D., Zareda, M., and Sharma, P., 1998, Chlorine-36 and the initial value problem, Hydrogeology Journal, Springer-Verlag, vol. 6, no. 1, p. 104-114.

Desaulniers, D.E., Kaufmann, R.S., Cherry, J.A., and Bentley, H.W., 1986, ^{37}Cl-^{35}Cl variations in a diffusion-controlled ground water system. Geochimica et Cosmochimica Acta, 50, p. 1757-1764.

Dowgiallo J., Nowicki Z., Beer J., Bonani G., Suter M., Synal H.A. and Wolfli W., 1990, ^{36}Cl in ground water of the Mazowsze Basin (Poland). J. Hydrol. 18, 373-385.

Duffy, C.J., and Harrison, J., 1987, The statistical structure and filter characteristics of tritium fluctuations in fractured basalt: Water Resources Research, v. 23, p. 556-560 and 894-902.

Eggenkamp, H.G.M., 1994, $\delta^{37}Cl$, The geochemistry of chlorine isotopes, Ph.D. dissertation, The University of Utrecht, The Netherlands.

Elmore, D., Fulton, B.R., Clover, M.R., Marsden, J.R., Gove, H.E., Naylor, H., Purser, K.H., Kilius, L.R., Beukens, R.P., and Litherland, A.E., 1979, Analysis of ^{36}Cl in environmental water samples using an electrostatic accelerator: Nature, v. 127, p. 22-25.

Elmore, D., Tubbs, L.E., Newman, D., Ma, X.Z., Finkel, R., Nishiizumi, K., Beer, J., Oeschger, H., and Andree, M., 1982, ^{36}Cl bomb pulse measured in a shallow ice core from Dye 3, Greenland: Nature, v. 300, no. 5894, p. 735-737.

Elmore, D., and Phillips, F.M., 1987, Accelerator mass spectrometry for measurement of long-lived radioisotopes: Science, v. 236, p. 543-550.

Eriksson, E., 1960, The yearly circulation of chloride and sulfur in nature, II. Meteorological, geochemical, and pedological implications, Tellus, 12: 63-109.

Erickson, G.E., 1981, Geology and origin of the Chilean nitrate deposits: U.S. Geological Survey Professional Paper 1188, 37 p.

Fabryka-Martin, J.T., Wolfsberg, A.V., Dixon, P.R., Levy, S.S., Musgrave, J.A., and Turin, H.J., 1997, Summary report of chlorine-36 studies: sampling, analysis, and simulation of chlorine-36 in the exploratory studies facility, Los Alamos National Laboratory Publication, LA-13352-MS, 110 p.

Fabryka-Martin, J.T., 1988, Production of radionuclides in the earth and their hydrogeologic significance with emphasis on chlorine-36 and iodine-129: Ph.D. dissertation at the University of Arizona, 400 p.

Fabryka-Martin J., Davis S.N. and Elmore D., 1987, Applications of 129I and 36Cl to hydrology. Nucl. Instrum. Meth. Phys. Res. B29, 361-371.

Fabryka-Martin J., Davis S.N., Roman D., Airey P.L., Elmore D. and Kubik P.W., 1988, Iodine-129 and chlorine-36 in uranium ores: 2. Discussion of AMS measurements. Chem. Geol. 72, 7-16.

Fabryka-Martin J.T., Wightman S.J., Murphy W.J., Wickham M.P., Caffee M.W., Nimz G.J., Southon J.R. and Sharma P., 1993, Distribution of chlorine-36 in the unsaturated zone at Yucca Mountain: An indicator of fast transport paths. In FOCUS '93: Site Characteristics and Model Validation. pp. 58-68. American Nuclear Society, La Grange Park, Illinois.

Fabryka-Martin, J.T., 1995, written communication on file at the USGS Global Ice-Core Research Project Office, Idaho Falls, Idaho, USA.

Faure, Gunter, 1986, Principles of isotope geology: John Wiley and Sons, New York., 589 p.

Finkel, R.C., Nishiizumi, K., Elmore, D., Ferraro, R.D., and Gove, H.E., 1980, ^{36}Cl in polar ice, rainwater and seawater: Geophysical Research Letters, v. 7, no. 11, p. 983-986.

Fishman, M.J., and Friedman, L.C., eds, 1989, Methods for determination of inorganic substances in water and fluvial sediments: U.S. Geological Survey Techniques Water-Resources Investigations, 3rd ed., book 5, Chap. A1, 545 p.

Fromm, J.M., 1995, Characterizing aquifer hydrogeology and anthropogenic chemical influences on ground water near the Idaho Chemical Processing Plant, Idaho National Engineering Laboratory, Idaho, Master's thesis, Idaho State University, 312 p.

Fryar, A.E., and Domenico, P.A., 1989, Analytical inverse modeling of regional-scale tritium waste migration: Journal of Contaminant Hydrology, 4, p. 113-125.

Garabedian, S.P., 1992, Hydrology and digital simulation of the regional aquifer system, eastern Snake River Plain, Idaho, U.S. Geological Survey Professional Paper 1408-F, 102 p.

Gego, E.L., Johnson, G.S., Wylie, A.H., and Welhan, J.A., in press. Geological Society of America Special Paper.

Gelhar, L.W., Welty, C., and Rehfeldt, K.R., 1992, A critical review of data on field-scale dispersion in aquifers: Water Resources Research, v. 28, no. 7, p. 1955-1974.

Gifford, S.K., Bentley, H., and Graham, D.L., 1985, Chlorine isotopes as environmental tracers in Columbia River basalt ground water, Memoirs, Hydrogeology of Rocks of Low Permeability, International Association of Hydrgeologist, Tucson, AZ, v. VII, part 1, p. 417-429.

Gifford S.K.I., 1987, Use of chloride and chlorine isotopes in the unsaturated zone to characterize recharge at the Nevada Test Site. Unpublished MS thesis, University of Arizona, Tucson.

Goode, D.J., and Konikow, L.F., 1990, Reevaluation of large-scale dispersivities for a waste chloride plume: Effects of transient flow, in: Modelcare 90: Calibration and reliability of ground water modeling, IAHS Publ. no. 195, p. 417-426.

Hainsworth, L.J., Mignerey, A.C., Helz, G.R., Sharma, P., and Kubik, P.W., 1994, Modern chlorine-36 deposition in southern Maryland, U.S.A., Nuclear Instruments and Methods in Physics Research, B 92, Elsevier Science, Holland, p. 345-349.

Hedenquist J.W., Goff F., Phillips F.M., Elmore D. and Stewart M.K., 1990, Ground water dilution and residence times, and constraints on chloride source, in the Mokai geothermal system, from chemical, stable isotope, tritium, and 36Cl data. J. Geophys. Res. 95, 19 365-19 375.

Herczeg A.L., Leaney F.W.J., Stadter M.F., Allan G.L. and Fifield L.K., 1997, Chemical and isotopic indicators of point-source recharge to a karst aquifer, South Australia. J. Hydrol. 192, 271-299.

Helsel, D.R., and Hirsch, R.M., 1992, Statistical methods in water resources, New York, Elsevier Science Publishing Company, Inc., 522 p.

Hossain, T.Z., 1988, Measurement of the $^{36}Ar(n,p)$ ^{36}Cl cross section: Annual report of the Nuclear Structure Research Laboratory, University of Rochester, Rochester, New York, p. 157-159.

Jannik N.O., Phillips F.M., Smith G.I. and Elmore D., 1991, A ^{36}Cl chronology of lacustrine sedimentation in the Pleistocene Owens River Systems, Eastern California. Geol. Soc. Am. Bull, 103, 1146-1159.

Jones, L.L., 1996, Idaho State Park Service, Harriman State Park, personal communication.

Kaufmann, R.S., Long, A., Bentley, H., and Davis S.N., 1984, Natural chlorine variations: Nature, v. 309, p. 338-340.

Kaufman A., Magaritz M., Paul M., Hillaire-Marcel C., Hollus G., Boaretto E. and Taieb M. (1990) The ^{36}Cl ages of the brines in the Magadi-Natron basin, East Africa. Geochim. Cosmochim. Acta 54, 2827-2834.

Kellett J.R., Evans W.R., Allan G.L. and Fifield L.K., 1993, Reinterpretation of ^{36}Cl age data: physical processes, hydraulic interconnections, and age estimates in ground water systems-Discussion. Appl. Geochem. 8, 653-658.

Knies, D.L., Elmore, D., Sharma, P., Vogt, S., Li, R., Lipschutz, M.E., Petty, G., Farrel, J., Monaghan, M.C., Fritz, S., and Agee, E., 1994, ^{7}Be, ^{10}Be, ^{36}Cl in precipitation, Nuclear Instruments and Methods, B92, p. 340-344.

Knobel, L.L., Cecil, L.D., and Woods, T., 1995, Chemical composition of selected core samples, Idaho National Engineering Laboratory, Idaho, U.S. Geological Survey Open-File Report 95-748, 59 p.

Knutson, C.F., McCormick, K.A., Smith, R.P. Hackett, W.R., O'Brian, J.P. and Crocker, J.C., 1990, EG&G Idaho, Report EGG-WM-8949, 126 p. plus appendices.

Kuntz, M.A., Champion, D.E., Lefevzre, R.F., and Covington, H.R., 1988, Geologic map of the Craters of the Moon, Kings Bowl, and Wapi Lava Fields in the Great Rift Volcanic Rift Zone, south-central Idaho, U.S., Geological Survey; Miscellaneous Investigations Series Map, I-1632, scale 1:1,000,000.

Lal, D., and Peters, B., 1967, Cosmic ray produced radioactivity on the earth, Handbuch der Physik, Sitte, K., ed., 46/2, Springer-Verlag, Berlin, p. 551-612.

Lewis, B.D, and Jensen, R. G., 1985, Hydrologic conditions at the Idaho National Engineering Laboratory 1979-81: U.S. Geological Survey Open-File Report 84.

Lichte, R.E., Golightly, D.W., and LaMothe, P.J., 1987, Inductively coupled plasma-atomic emission spectrometry, in Climate change in continental isotopic records, Steward, P.K., Lohman, K.C., McKenzie, J., and Savin, S., eds., American Geophysical Union, Washington, D.C., p. 55-66.

Lodemann M., Fritz P., Wolf M., Ivanovich M., Hansen B.T. and Nolte E., 1997, On the origin of saline fluids in the KTB (continental deep drilling project of Germany). Appl. Geochem. 12, 831-849.

Long, A., Eastoe, C.J., Kaufmann, R.S., Martin, J.G., Wirt L., and Finley, J.B., 1993, High-precision measurement of chlorine stable isotope ratios, Geochimica et Cosmochimica Acta, v. 57, p. 2907-2912.

Lucey, K.J., 1990, QADATA User's Manual: An interactive computer program for the retrieval and analysis of the results from the external blind sample quality-assurance project of the U.S. Geological Survey: U.S. Geological Survey Open-File Report 90-162.

Lyons W.B., Welch K.A. and Sharma P., 1998, Chlorine-36 in the waters of the McMurdo Dry Valley lakes, southern Victoria Land, Antarctica: Revisited. Geochim. Cosmochim. Acta 62, 185-192.

Magaritz M., Kaufman A., Paul M., Boaretto E. and Hollos G., 1990, A new method to determine regional evapotranspiration. Water Resour. Res. 26, 1759-1762.

Maloney, T.J., Lutke, A.S., Krizman, T.L., 1993, Quality assurance for routine water analysis in the laboratories of the U.S. Geological Survey for water year 1990:U.S.Geological Survey Water-Resources Investigations Report 93-4081, 145 p.

Maloszewski, P., and Zuber, A., 1982, Determing the turnover time of ground water systems with the aid of environmental tracers, 1. Models and their applicability, Journal of Hydrology, v. 57, p. 207-231.

Maloszewski, P. Rauert, W., Stickler, W., and Herrmann, A., 1983, Journal of Hydrology, v. 66, p. 319-330.

Mann, L.J., and Beasley, T.M., 1994, Iodine-129 in the Snake River Plain aquifer at and near the Idaho National Engineering Laboratory, Idaho, 1990-91: U.S. Geological Survey Water-Resources Investigations Report 94-4053, 27 p.

Marston, R.A., Pochop, L.O., Kerr, G.L., Varujka, M.L., and Veryzer, D.J., 1991, Recent glacier changes in the Wind River Range, Wyoming: Physical Geography, v. 12, p 115-123.

Milton G.C.D., Milton G.M., Andrews H.R., Chant L.A., Cornett R.J.J., Davies W.G., Greiner B.F., Imanori Y., Koslowsky V.T., Kotzer T., Kramer S.J. and McKay J.W., 1997a, A new interpretation of the distribution of bomb-produced chlorine-36 in the environment, with special reference to the Laurentian Great Lakes. Nucl. Instrum. Meth. Phys. Res. B123, 382-386.

Milton G.M., Kramer S.J., Kotzer T.G., Milton J.C.D., Andrews H.R., Chant L.A., Cornett R.J., Davies W.G., Greiner B.F., Imahori Y., Koslowsky V.T. and McKay J.W., 1997b, ^{36}Cl - a potential paleodating tool. Nucl. Instrum. Meth. Phys. Res. B123, 371-377.

Muller, R.A., 1977, Radioisotope dating with a cyclotron: Science, v. 196, n. 4289, p. 489-494.

Morris, D.A., Barraclough, J.T., Chase, G.H., Teasdale, W.E., and Jensen, R.G., 1964, Hydrology of subsurface waste disposal, National Reactor Testing Station, Idaho, Annual Progress Report, IDO-22047-USGS, 147 p.

Moysey, S., 1999, Meteoric ^{36}Cl in the contiguous United States, Master's Thesis, Univ. of Arizona, 163 p.

Mundorff, M.J., Broom, H.C., and Kilburn, Chabot, 1963, Reconnaissance of the hydrology of the Little Lost River Basin, Idaho: U.S. Geological Survey Water-Supply Paper 1539-Q, 51 p. and 3 plates.

147

Nace, R.L., Voegeli, P.T., Jones, J.R., and Deutsch, Morris, 1975, Generalized geologic framework of the National Reactor Testing Station, Idaho, U.S. Geological Survey Professional Paper 725-B, 49 p.

Naftz, D.L., Rice, J.A., and Ranville, J.R., 1991, Glacial ice composition: A potential long-term record of the chemistry of atmospheric deposition, Wind River Range, Wyoming. Water Resources Research, vol. 27, no. 6, p. 1231-1238.

Naftz, D.L., 1993, Ice-core records of the chemical quality of atmospheric deposition and climate from mid-latitude glaciers, Wind River Range, Wyoming. Unpublished Doctoral dissertation, Colorado School of Mines, 204 p.

Naftz, D.L., Michel, R.L., and Miller, K.A., 1993, Isotopic indicators of climate in ice cores from the Wind River Range, Wyoming; in Lohmann, K.C., and others, eds., Climate change in continental isotopic records, Geophysical Monograph 78, American Geophysical Union, p. 55-66.

Naftz, D.L., Klusman, R.W., Michel, R.L., Schuster, P.F., Reddy, M.M., Taylor, H.E., Yanosky, T.M., and McConnaughey, E.A., 1996, Little Ice Age evidence from a south-central North American ice core, U.S.A.: Arctic and Alpine Research, v. 28, no. 1, p. 35-41.

Nolte E., Krauthan P., Korschinek G., Maloszewski P., Fritz P. and Wolf M., 1991, Measurements and interpretations of ^{36}Cl in ground water, Milk River aquifer, Alberta, Canada. Appl. Geochem. 6, 435-445.

Norris A.E., Wolfsberg K., Gifford S.K., Bentley H.W. and Elmore D., 1987, Infiltration at Yucca Mountain traced by 36Cl. Nucl. Instrum. Meth. Phys. Res. B29, 361-371.

Olsen, J.H., 1998, Thief sampling and geophysical logging for determination of vertical variations in Snake River Plain aquifer chemistry at the Idaho National Engineering and Environmental Laboratory, Master's Thesis, University of Idaho, 117 p.

Orr, B.R., and Cecil, L.D., 1991, Hydrologic Conditions and Distribution of Selected Chemical Constituents in Water, Snake River Plain Aquifer, Idaho National Engineering Laboratory, Idaho 1986 to 1988: U.S. Geological Survey Water-Resources Investigations Report 91-4047, 56 p.

Parker, R.L., 1967, Composition of the Earth's crust: U.S. Geological Survey Professional Paper 440-D, 19 p.

Paul M., Kaufman A., Magaritz M., Fink D., Henning W., Kalm R., Kutschera W. and Meirav O., 1986, A new ^{36}Cl hydrological model and ^{36}Cl systematics in the Jordan River/Dead Sea

system. Nature 321, 511-515.

Pearson Jr. F.J., Balderer W., Loosli H.H., Lehmann B.E., Matter A., Peters T., Schmassmann H. and Gautschi A., 1991, Applied Isotope Hydrogeology: A Case Study in Northern Switzerland. Elsevier, New York.

Phillips F.M., Goff F., Vuataz F., Bentley H.W., Elmore D. and Gove H.E., 1984a, ^{36}Cl as a tracer in geothermal systems: Example from Valles caldera. Geophys. Res. Lett. 11, 1227-1230.

Phillips F.M., Trotman K.N., Bentley H.W. and Davis S.N., 1984b, The bomb-36Cl pulse as a tracer for soil water movement near Socorro, New Mexico. In Selected Papers on Water Quality and Pollution in New Mexico. ed. W.J. Stone, pp. 271-280. New Mexico Bureau of Mines and Mineral Resources Hydrologic Report 7.

Phillips F.M., Bentley H.W., Davis S.N., Elmore D. and Swannick G.B., 1986, Chlorine-36 dating of very old ground water II: Milk River aquifer, Alberta. Water Resour. Res. 22, 2003-2016.

Phillips F.M., Davis S.N. and Kubik P., 1990, A proposal to use chlorine-36 for monitoring the movement of radionuclides from nuclear explosions. Ground Water Monit. Rev. 10(3), 106-113.

Phillips F.M., 1993, Comment on Reinterpretation of ^{36}Cl data: physical processes, hydraulic interconnections and age estimates in ground water systems by E. Mazor. Appl. Geochem. 8, 643-647.

Phillips F.M., 1994, Environmental tracers for water movement in desert soils of the American Southwest. Soil Sci. Soc. Amer. J. 58, 15-24.

Phillips F.M., Rogers D.B., Dreiss S.J., Jannik N.O. and Elmore D., 1995, Chlorine-36 in Great Basin waters: Revisited. Water Resour. Res. 31, 3195-3204.

Phillips, F.M., Zreda, M.G., Flinsch, M.R., Elmore, D., and Sharma, P., 1996, A reevaluation of cosmogenic ^{36}Cl production rates in terrestrial rocks, Geophysical Research Letters, v. 23 (9), p. 949-952.

Phillips, F.M., 2000, Chlorine-36, In Environmental Tracers in Subsurface Hydrology. Cook, P.G., and Herczeg, A.L., editors, Kluwer Academic Publishers, Boston, p. 299-348.

Pittman, J.R., Jensen, R.G., and Fischer, P.R., 1988, Hydrologic conditions at the Idaho National Engineering Laboratory, 1982 to 1985: U.S. Geological Survey Water-Resources Investigations Report 89-4008, 73 p.

Plummer M.A., Phillips F.M., Fabryka-Martin J., Turin H.J., Wigand P.E. and Sharma P., 1997, Chlorine-36 in fossil rat urine: an archive of cosmogenic nuclide deposition over the past 40,000 years. Science 277, 538-541.

Prych E.A., 1995, Using chloride and chlorine-36 as soil-water tracers to estimate deep percolation at selected locations on the U.S. Department of Energy Hanford Site, Washington. U.S. Geological Survey, Open-File Rept. 94-514.

Prych E.A., 1996, Estimating deep percolation of precipitation at the U.S. Department of Energy Hanford site using two chloride-tracer methods. In Joint U.S. Geological Survey, U.S. Nuclear Regulatory Commission Workshop on Research Related to Low-Level Radioactive Waste Disposal, eds. P. R. Stevens and T. J. Nicholson, pp. 103-107. U.S. Geological Survey, Water-Resources Investigations Report 95-4015.

Purdy C.B., 1991, Isotopic and chemical tracer studies of ground water in the Aquia Formation, southern Maryland, including ^{36}Cl, ^{14}C, ^{18}O, and ^{3}H. Unpubl. PhD thesis, University of Maryland, College Park.

Purdy C.B., Helz G.R., Mignerey A.C., Kubik P.W., Elmore D., Sharma P. and Hemmick T., 1996, Aquia aquifer dissolved Cl- and ^{36}Cl/Cl: implications for flow velocities. Water Resour. Res. 32, 1163-1172.

Rao U., Fehn U., Teng R.T.D. and Goff F., 1996, Sources of chloride in hydrothermal fluids from the Valles caldera, New Mexico: a ^{36}Cl study. J. Volcanol. Geotherm. Res. 72, 59-70.

Robertson, J.B., 1974, Digital modeling of radioactive and chemical waste transport in the Snake River Plain aquifer at the National Reactor Testing Station, Idaho 1952-1970: U.S. Geological Survey Open-File Report, IDO-22054, 41 p.

Robertson, J.B., Schoen, R., and Barraclough, J.T., 1974, The influence of liquid waste disposal on the geochemistry of water at the National Reactor Testing Station, Idaho: U.S. Geological Survey Open-File Report IDO-22053, 231 p.

Rose T.P., Denneally J.M., Smith D.K., Davisson M.L., Hudson G.B. and Rego J.A.H., 1997, Chemical and isotopic data for ground water in southern Nevada. Report UCRLID-12800, Lawrence Livermore National Laboratory, Livermore, California, 36 pp.

Sauty, J-P., 1980, Water Resources Research, vol. 16, no. 1, p. 145-158.

Scanlon B.R., 1992, Evaluation of liquid and vapor water flow in desert soils based on chlorine-36 and tritium tracers and nonisothermal flow simulations. Water Resour. Res. 28, 285-298.

Schaeffer, O.A., Thompson, S.O., and Lark, N.L, 1960, Chlorine-36 radioactivity in rain: Journal of Geophysical Research, v. 65, p. 4013-4016.

Sienko, M.J., and Plane, R.A., 1966, Chemistry: principles and properties: McGraw-Hill, New York, 623 p.

Sterling, J.M., 2000, Spatial Distribution of chloride and ^{36}Cl Deposition in the conterminous United States, Master's Thesis, New Mexico Institute of Mining and Technology, 155p.

Stewart, M.K., and McDonald, J.J., 1991, Water Resources Research, vol. 27, no. 10, p. 2681-2693.

Synal, H.A., Beer, J., Bonani, G, Suter, M., and Woelfli, W., 1991, Atmospheric transport of bomb-produced ^{36}Cl, Nuclear Instruments and Methods, B52, p. 483-488.

Taylor, J.K., 1987, Quality Assurance of Chemical Measurements: Chelsea, Michigan, Lewis Publishers, Inc., 328 p.

Torgersen T., Habermehl M.A., Phillips F.M., Elmore D., Kubik P., Jones B.G., Hemmick T. and Gove H.E., 1991, Chlorine-36 dating of very old ground water: III. Further studies in the Great Artesian Basin, Australia. Water Resour. Res. 27, 3201-3214.

Trotman K.N., 1983, Thermonuclear 36Cl in arid soil. Unpublished MS thesis, University of Arizona, Tucson.

Turekian, K.K., 1969, The oceans, streams, and atmosphere, in Wedepohl, K.H., ed., Handbook of Geochemistry, v. 1, New York, Springer-Verlag p. 297-323.

Tyler S.W., Chapman J.B., Conrad S.H., Hammermeister D.P., Blout D.O., Miller J.J., Sully M.J. and Ginanni J.M., 1996, Soil-water flux in the southern Great Basin, United States: temporal and spatial variations over the last 120 000 years. Water Resour. Res. 32, 1481-1499.

Walker, W.W., Parrington, J.R., and Feiner, F., 1989, Nuclides and Isotopes, chart of the nuclides 14th Edition, General Electric Co., San Jose, 57 p.

Walker G.R., Jolly I.D., Stadter M.H., Leaney F.W., Davie R.F., Fifield L.K., Ophel T.R. and Bird J.R., 1991, Evaluation of the use of chlorine-36 in recharge studies. In Isotope Techniques in Water Resources Development 1991, pp. 19-29. IAEA, Vienna.

Welhan, J.A., Johannsen, C.M., Glover, J.A., Davis, L.L., and Reeves, K.S., in press. Idaho Geological Survey Bulletin, Tectonic and Magmatic Evolution of the Snake River Plain, editors, W. Bonnichesen, W. White, and M. McCurry.

Whitehead, R.L., 1992, Geohydrologic framework of the Snake River Plain regional aquifer

system, Idaho, and eastern Oregon: U.S. Geological Survey Professional Paper 1408-B, 32 p.

Wood, W.W., 1981, Guidelines for collection and field analysis of ground water samples for selected unstable constituents: U.S. Geological Survey Techniques of Water-Resources Investigation, Book 1, Chap. D2, 24 p. (Reprinted 1981).

Wood, W.W., and Low, W.H., 1988, Solute Geochemistry of the Snake River Plain regional aquifer system, Idaho and eastern Oregon: U.S. Geological Survey Professional Paper 1408-D, 79 p.

Yechieli Y., Ronen D., and Kaufman A., 1996, The source and age of ground water brines in the Dead Sea area, as deduced from ^{36}Cl, Geochimica et Cosmochimica Acta 60, 1909-1916.

Yurtsever, Y., 1983, IAEA Technical Report Series no. 228, p. 381-402.

ABBREVIATIONS USED IN THE APPENDIX TABLES

Al	Aluminum
amu	Atomic mass unit: mass of all isotopes relative to the mass of pure carbon-12
At. Wt.	Weighted average mass of all isotopes relative to the mass of pure carbon-12
B	Boron
Be	Beryllium
C	Carbon
Ca	Calcium
Cl	Chlorine
F	Fluorine
Fe	Iron
Gd	Gadolinium
H,w	Hydrogen from water
ICP-AES	Inductively coupled plasma-atomic emission spectrometry
ISEP	Ion-selective electrode potentiometry
INAA	Instrumental neutron activation analysis
K	Potassium
Li	Lithium
LOI	Loss on ignition
Mg	Magnesium
Mn	Manganese
n/g/yr	Neutrons per gram per year
Na	Sodium
O,r	Oxygen as structural component of rock matrix
O,w	Oxygen as part of water molecule in rock pore spaces
P	Phosphorus
ppm	Parts per million by weight
Si	Silicon
Sm	Samarium
Tb	Terbium
Th	Thorium
Ti	Titanium
Total (adj.)	Sum of all elements including H,w and O,w from water adjusted to equal 1,000,000 ppm
Total (raw)	Sum of all elements except H,w and O,w from water adjusted to equal 1,000,000 ppm
U	Uranium
Z	Atomic number

APPENDIX A

ELEMENTAL DATA FOR CALCULATING THERMAL CROSS-SECTIONS FOR NEUTRON ABSORPTION

Table A-1. Data for calculating thermal cross-sections for neutron absorption, igneous rock samples.

[Sample locations are shown on figure 1.1. Source of data: major rock-forming elements as oxides in weight percent, trace elements in ppm equivalent weight, and volatile components in weight percent are from the Idaho State University, Department of Geology,- Geochemistry Laboratory and were determined by ICP-AES, INAA, or LOI; unmarked chlorine values in weight percent are from the U.S. Geological Survey, Branch of Geochemistry Laboratory and were determined by ISEP; values marked with an asterisk (*) are from Parker [directly for basalts and from geochemical equivalent for rhyolites (felsic granite)] (1967, table 19, p. D13-D14). Calculations: Gd values were calculated using chondritic trace-element ratios; carbon values marked with an "at" symbol (@) were calculated using the assumption that the moles of carbon were equivalent to the sum of the moles of calcium and magnesium; values for H,w and O,w were calculated using the assumption that the difference between the raw and adj. totals plus excess LOI values were attributable to water content (both water of hydration and pore water); the value for O,r was calculated from oxide weight-percent data. For a detailed explanation of calculations and conversions, see section 5.3.3 of text on data reduction. Symbols: <, less than.]

			Sample identifier and type					
Z	Element	At. Wt. amu	SP-5 ppm, rhyolite, outcrop	SP-6 ppm, rhyolite, outcrop	SP-7 ppm, rhyolite, outcrop	SP-8 ppm, rhyolite, depth, 10 meters	SP-9 ppm, opal in rhyolite, depth, 10 meters	SP-10 ppm, rhyolite, outcrop
14	Si	28.1	343302	345718	314633	353104	345625	338660
13	Al	27.0	56153	64410	58588	60864	64780	64304
26	Fe	55.8	10649	13137	12670	10338	2254	14458
20	Ca	40.1	15223	5503	36664	3859	1572	4431
12	Mg	24.3	5549	724	603	422	121	603
11	Na	23.0	25223	26633	26262	25965	964	27820
19	K	39.1	38935	44746	43500	44580	7222	44497
15	P	30.97	175	218	131	131	175	175
3	Li	6.9	*40	*40	*40	*40	*15	*40
4	Be	9.01	*5.5	*5.5	*5.5	*5.5	*0.5	*5.5
5	B	10.8	*15	*15	*15	*15	*35	*15
6	C	12.0	*300	*300	*300	*300	@531	*300
9	F	19	*800	*800	*800	*800	*270	*800
1	H.w	1.0	3506.37	2018.39	6242.28	1944.54	13180.9	3630.32
22	Ti	47.9	719	1079	959	899	1439	1499
25	Mn	54.9	77	1007	232	310	<77	232
62	Sm	150.4	17.3	15.7	11.1	13.6	4.28	12.9
65	Tb	158.9	2.28	2.2	1.33	1.94	0.43	1.89
64	Gd	157.3	15.37	14.53	9.26	12.74	3.17	12.30
8	O.r	16.0	471195	477325	448158	480228	457162	469421
8	O.w	16.0	27828.18	16018.88	49541.63	15432.78	104610.09	28811.89
92	U	238.0	4.9	4.4	5.1	6.2	5.3	5.3
90	Th	232.0	25.1	25.4	28.8	27.7	20.3	24.9
17	Cl	35.5	*240	*240	600	700	*10	*240
	Total (raw)		968665.45	981962.73	944216.09	982622.68	882208.98	967557.79
	Total (adj.)		1000000	1000000	1000000	1000000	1000000	1000000

Table A-1.   Data for calculating thermal cross-sections for neutron absorption, igneous rock samples—Continued.

			Sample identifier and type					
Z	Element	At. Wt. amu	SP-13 ppm, rhyolite, outcrop	SP-15 ppm, basalt, depth, 728 meters	SP-16 ppm, basalt, depth, 158 meters	SP-17 ppm, rhyolite, depth, 136 Meters	SP-18 ppm, basalt, depth, 180 meters	SP-19 ppm, basalt, depth, 118 meters
14	Si	28.1	346419	210348	212685	(353337)	222969	215490
13	Al	27.0	62081	69861	77800	66156	85739	83622
26	Fe	55.8	8550	90945	85504	12903	81618	97164
20	Ca	40.1	11078	77545	73614	5003	79332	76259
12	Mg	24.3	784	33291	49575	1025	50359	46982
11	Na	23.0	25594	15727	17582	31974	18250	18695
19	K	39.1	44165	12369	3653	38187	3736	4400
15	P	30.97	175	3710	1091	87	1397	1920
3	Li	6.9	*40	*15	*15	*40	*15	*15
4	Be	9.01	*5.5	*0.4	*0.4	*5.5	*0.4	*0.4
5	B	10.8	*15	*5	*5	*15	*5	*5
6	C	12.0	*300	*100	*100	*300	*100	*100
9	F	19	*800	*370	*370	*800	*370	*370
1	H.w	1.0	2579.75	7065.57	5863.45	103.33	1034.88	1375.94
22	Ti	47.9	480	16247	10491	959	10611	13069
25	Mn	54.9	310	1471	1317	387	1317	1394
62	Sm	150.4	9.91	7.51	4.75	15.44	4.8	5.68
65	Tb	158.9	1.57	0.94	0.05	4.31	0.6	0.75
64	Gd	157.3	9.96	6.45	3.87	22.63	4.12	5.05
8	O.r	16.0	475864	404786	413688	487582	434872	428105
8	O.w	16.0	20474.11	56075.49	46534.97	820.09	8213.29	10920.08
92	U	238.0	5.1	1.1	0.8	11.5	0.6	0.5
90	Th	232.0	19.1	2.54	1.71	22.2	1.31	1.6
17	Cl	35.5	*240	*50	100	*240	*50	100
	Total (raw)		976946.14	936858.94	947601.58	999076.58	990751.83	987703.98
	Total (adj.)		1000000	1000000	1000000	1000000	1000000	1000000

Table A-1.   Data for calculating thermal cross-sections for neutron absorption, igneous rock samples—Continued.

Z	Element	At. Wt. amu	Sample identifier and type			
			SP-20 ppm, basalt, depth, 193 meters	SP-21 ppm, basalt, depth, 259 meters	SP-22 ppm, basalt, outcrop	SP-23 ppm, rhyolite, outcrop
14	Si	28.1	209880	214555	227176	347775
13	Al	27.0	79388	70390	75683	60864
26	Fe	55.8	98719	94055	66071	15002
20	Ca	40.1	70970	57176	66610	3431
12	Mg	24.3	43665	30035	45293	543
11	Na	23.0	18917	23294	17211	26707
19	K	39.1	5230	14611	26980	41840
15	P	30.97	2662	1353	2269	131
3	Li	6.9	*15	*15	*15	*40
4	Be	9.01	*0.4	*0.4	*0.4	*5.5
5	B	10.8	*5	*5	*5	*15
6	C	12.0	*100	*100	*100	*300
9	F	19	*370	*370	*370	*800
1	H,w	1.0	3882.04	8489.93	5241.73	2813.21
22	Ti	47.9	16247	15887	4736	1259
25	Mn	54.9	1471	1549	1162	465
62	Sm	150.4	7.39	13.77	5.07	14.25
65	Tb	158.9	0.96	2.22	0.73	2.2
64	Gd	157.3	6.50	13.99	4.78	14.07
8	O,r	16.0	417451	400495	419409	475383
8	O,w	16.0	30809.68	67380.12	41600.81	22326.97
92	U	238.0	0.8	3.0	1.2	5.8
90	Th	232.0	2.23	6.57	5.28	23.0
17	Cl	35.5	200	200	*50	*240
	Total (raw)		965308.28	924129.95	953157.46	974859.82
	Total (adj.)		1000000	1000000	1000000	1000000

Table A-2. Data for calculating thermal cross-sections for neutron absorption, sedimentary rock samples.

[Sample locations are shown on figure 1.1. Source of data: major rock-forming elements as oxides in weight percent, trace elements in ppm equivalent weight, and volatile components in weight percent are from the Idaho State University, Department of Geology, Geochemistry Laboratory and were determined by ICP-AES, INAA, or LOI; unmarked chlorine values in weight percent are from the U.S. Geological Survey, Branch of Geochemistry Laboratory and were determined by IES; values marked with an asterisk (*) are from Parker directly (1967, table 19, p. D13-14). Calculations: Gd values were calculated using chondritic trace-element ratios; carbon was calculated using the assumption that LOI values resulted from volatilization of carbonate; values for H,w and O,w were calculated using the assumption that the difference between the raw and adj. totals plus excess LOI values was attributable to water content; the value for O,r was calculated from oxide weight-percent and LOI data. For a detailed explanation of calculations and conversions, see section 5.3.3 of text on data reduction. Symbol: -bd-, below detection limit; <, less than.]

			Sample identifier and type						
Z	Element	At. Wt. amu	SP-1 ppm, limestone, outcrop	SP-2 ppm, limestone, depth, 10 meters	SP-3 ppm, limestone, outcrop	SP-4 ppm, dolomite, outcrop	SP-12 Ppm, limestone, outcrop	SP-25 ppm, shale, outcrop	SP-26 ppm, limestone, outcrop
14	Si	28.1	7947	10564	8554	3085	19960	226241	-bd-
13	Al	27.0	1376	2064	1217	1429	1747	62452	-bd-
26	Fe	55.8	233	544	233	1166	777	30704	311
20	Ca	40.1	382508	381865	383586	217555	369572	63394	385939
12	Mg	24.3	4522	2714	3317	120681	3076	38659	2835
11	Na	23.0	74	148	74	223	74	6825	148
19	K	39.1	415	830	249	747	913	26731	0
15	P	30.97	87	131	44	44	218	1222	262
3	Li	6.9	*5	*5	*5	*5	*5	*60	*5
4	Be	9.01	*0.5	*0.5	*0.5	*0.5	*0.5	*3	*0.5
5	B	10.8	*20	*20	*20	*20	*20	*100	*20
6	C	12.0	118201	117164	117519	128108	116318	*10000	115718
9	F	19	*330	*330	*330	*330	*330	*500	*330
1	H.w	1.0	340.37	284.27	569.56	1459.63	250.74	12664.38	3243.86
22	Ti	47.9	<60	60	<60	<60	60	3477	240
25	Mn	54.9	<77	<77	<77	155	<77	1704	155
62	Sm	150.4	0.39	0.69	0.72	0.12	0.64	4.53	0.72
65	Tb	158.9	0.05	0.09	0.11	0.01	0.07	0.66	0.06
64	Gd	157.3	0.34	0.61	0.71	0.08	0.50	4.30	0.47
8	O.r	16.0	481137	480816	479607	513007	484485	411732	464892
8	O.w	16.0	2701.35	2256.13	4520.32	11584.32	1990.03	100510.46	25744.81
92	U	238.0	1.9	2.5	2.9	0.2	2.3	2.6	4.3
90	Th	232.0	0.1	0.21	0.18	0.14	0.22	9.07	0.28
17	Cl	35.5	100	200	*150	400	200	*3000	*150
	Total (raw)		996958.28	997459.60	994910.12	986956.05	997759.23	886825.16	971011.33
	Total (adj.)		1000000	1000000	1000000	1000000	1000000	1000000	1000000

Table A-3.   Data for calculating thermal cross-sections for neutron absorption, metamorphic rock samples.

[Sample locations are shown on figure 1.1. Source of data: major rock-forming elements as oxides in weight percent, trace elements in ppm equivalent weight, and volatile components in weight percent are from the Idaho State University, Department of Geology, Geochemistry Laboratory and were determined by ICP-AES, INAA, or LOI (value in parenthesis indicates that the element's concentration was outside the calibration range of the instrument during analysis and that the value was reduced to make the adjusted weight percent data equal 100 percent); unmarked chlorine values in weight percent are from the U.S. Geological Survey, Branch of Geochemistry Laboratory and were determined by IES; values marked with an asterisk (*) are from Parker [directly for basalts and from geochemical equivalent for quartzite (sandstone)] (1967, table 19, p. D13-14). Assumption: LOI values provided by the ISU Laboratory were assumed to result from volatilization of carbonate or water. Calculations: GD values were calculated using chondritic trace-element ratios; carbon values marked with an at (@) were calculated using the assumption that the moles of carbon were equivalent to the sum of the moles of calcium and magnesium; values for H,w and O,w were calculated using the assumption that the difference between the raw and adj. totals plus the excess LOI values were attributable to water content (both the water of hydration and pore water); the value for O,r was calculated from oxide weight percent and LOI data. For a detailed explanation of calculations and conversions, see section of text on data reduction. Symbols: - bd-, below detection limit; <, less than.]

Z	Element	At. Wt. amu	SP-11 ppm, quartzite, outcrop	SP-24 ppm, quartzite, outcrop
14	Si	28.1	342353	(463513)
13	Al	27.0	16883	-bd-
26	Fe	55.8	5441	155
20	Ca	40.1	69969	0
12	Mg	24.3	5126	181
11	Na	23.0	371	148
19	K	39.1	8966	2657
15	P	30.97	524	131
3	Li	6.9	*15	*15
4	Be	9.01	*0.5	*0.5
5	B	10.8	*35	*35
6	C	12.0	@23501	@89
9	F	19	*270	*270
1	H,w	1.0	2379.16	295.54
22	Ti	47.9	719	420
25	Mn	54.9	620	155
62	Sm	150.4	2.01	0.28
65	Tb	158.9	0.27	0.04
64	Gd	157.3	1.81	0.26
8	O,r	16.0	503836	529578
8	O,w	16.0	18882.17	2345.53
92	U	238.0	1.4	0.3
90	Th	232.0	3.68	0.55
17	Cl	35.5	100	*10
	Total (raw)		978738.67	997358.93
	Total (adj.)		1000000	1000000

APPENDIX B

THERMAL NEUTRON CROSS-SECTIONS, TOTAL NEUTRON PRODUCTION RATES, AND *IN SITU* SECULAR EQUILIBRIUM ^{36}Cl/Cl RATIOS FOR ROCK TYPES INVESTIGATED

160

Table B-la. Calculated thermal neutron cross section for neutron absorption, total neutron production rate, and *in situ* secular equilibrium ^{36}Cl/Cl ratio for igneous rock sample SP-5, rhyolite.

[See figure 1.1 for location of sampling site. See text for explanation of Mass Stopping Power, Weighting Factor, X and Y factors, Weighted Neutron Yields, and Thermal Cross-Sections. Mass Stopping Power, Neutron Yields, and Absorption Cross Sections supplied by Fabryka-Martin (1995). Mass Stopping Power is given for each element for an alpha particle of energy 8.0 million electron volts (MeV). Mass Stopping Power units: MeV per gram of rock per square centimeter. Sample ppm from Appendix table A-1; cm^2/g, square centimeters per gram; <, less than.]

| Element | Mass Stopping Power | Neutron Yield | | Sample ppm | Weighting Factor | Weighted Neutron Yield | |
		n/yr/g rock per ppm U	n/yr/g rock per ppm Th			n/yr/g rock per ppm U	n/yr/g rock per ppm Th
Si	454	0.69	0.339	343302	155.86	107.54	52.84
Al	444	5.116	2.585	56153	24.93	127.55	64.45
Fe	351	0.187	0.208	10649	3.74	0.70	0.78
Ca	428	0.282	0.026	15223	6.52	1.84	0.17
Mg	461	5.834	2.564	5549	2.56	14.92	6.56
Na	456	12.535	5.959	25223	11.50	144.17	68.54
K	414	0.89	0.08	38935	16.12	14.35	1.29
P	433	4.473	0.573	175	0.08	0.34	0.04
Li	548	23.86	10.54	40	0.02	0.52	0.23
Be	529	265.948	91.561	5.5	0.00	0.77	0.27
B	527	62.551	19.779	15	0.01	0.49	0.16
C	561	0.456	0.179	300	0.17	0.08	0.03
F	472	41.33	16.362	800	0.38	15.61	6.18
O	527	0.236	0.084	499023.18	262.99	62.06	22.09
			Total	995392.68	484.86	490.95	223.62

Element	Atomic Weight (amu)	Sample ppm	Neutron Absorption Cross Section (barns/atom)	Thermal Neutron Cross Section (cm^2/g)
Si	28.1	343302	0.17	0.001250
Al	27.0	56153	0.233	0.000292
Fe	55.8	10649	2.56	0.000294
Ca	40.1	15223	0.43	0.000098
Mg	24.3	5549	0.063	0.000009
Na	23.0	25223	0.53	0.000350
K	39.1	38935	2.1	0.001259
P	30.97	175	0.18	0.000001
Li	6.9	40	71	0.000248
Be	9.01	5.5	0.0092	<0.000001
B	10.8	15	764	0.000639
C	12.0	300	0.0035	<0.000001
F	19.0	800	0.0096	<0.000001
H	1.0	3506.37	0.33	0.000697
Ti	47.9	719	6.1	0.000055
Mn	54.9	77	13.3	0.000011
Sm	150.4	17.3	5600	0.000388
Gd	157.3	15.37	49000	0.002882
O	16.0	499023.18	0.00028	0.000005
	Total	999727.72		**0.008478**

Neutron Production Rate (n/g/yr)

(X factor = 1.013) (Total U ppm = 4.9) = 4.9637

(Y factor = 0.461) (Total Th ppm = 25.1) = 11.5711

^{238}U spontaneous fission = 2.102

Total neutron production rate (n/g/yr) = 19

In Situ Secular Equilibrium ^{36}Cl/Cl Ratio (x 10^{-15}) = 32

Table B-1b. Calculated thermal neutron cross section for neutron absorption, total neutron production rate, and *in situ* secular equilibrium ^{36}Cl/Cl ratio for igneous rock sample SP-6, rhyolite.

[See figure 1.1 for location of sampling site. See text for explanation of Mass Stopping Power, Weighting Factor, X and Y factors, Weighted Neutron Yields, and Thermal Cross Sections. Mass Stopping Power, Neutron Yields, and Absorption Cross Sections supplied by Fabryka-Martin (1995). Mass Stopping Power is given for each element for an alpha particle of energy 8.0 million electron volts (MeV). Mass Stopping Power units: MeV per gram of rock per square centimeter. Sample ppm from Appendix table A-1; cm^2/g, square centimeters per gram; <, less than.]

Element	Mass Stopping Power	Neutron Yield		Sample ppm	Weighting Factor	Weighted Neutron Yield	
		n/yr/g rock per ppm U	n/yr/g rock per ppm Th			n/yr/g rock per ppm U	n/yr/g rock per ppm Th
Si	454	0.69	0.339	345718	156.96	108.30	53.21
Al	444	5.116	2.585	64410	28.60	146.31	73.93
Fe	351	0.187	0.208	13137	4.61	0.86	0.96
Ca	428	0.282	0.026	5503	2.36	0.66	0.06
Mg	461	5.834	2.564	724	0.33	1.95	0.86
Na	456	12.535	5.959	26633	12.14	152.23	72.37
K	414	0.89	0.08	44746	18.52	16.49	1.48
P	433	4.473	0.573	218	0.09	0.42	0.05
Li	548	23.86	10.54	40	0.02	0.52	0.23
Be	529	265.948	91.561	5.5	0.00	0.77	0.27
B	527	62.551	19.779	15	0.01	0.49	0.16
C	561	0.456	0.179	300	0.17	0.08	0.03
F	472	41.33	16.362	800	0.38	15.61	6.18
O	527	0.236	0.084	493343.88	259.99	61.36	21.84
			Total	995593.38	484.19	506.06	231.62

Element	Atomic Weight (amu)	Sample ppm	Neutron Absorption Cross Section (barns/atom)	Thermal Neutron Cross Section (cm^2/g)
Si	28.1	345718	0.17	0.001259
Al	27.0	64410	0.233	0.000335
Fe	55.8	13137	2.56	0.000363
Ca	40.1	5503	0.43	0.000036
Mg	24.3	724	0.063	0.000001
Na	23.0	26633	0.53	0.000369
K	39.1	44746	2.1	0.001447
P	30.97	218	0.18	0.000001
Li	6.9	40	71	0.000248
Be	9.01	5.5	0.0092	<0.000001
B	10.8	15	764	0.000639
C	12.0	300	0.0035	<0.000001
F	19.0	800	0.0096	<0.000001
H	1.0	2018.39	0.33	0.000401
Ti	47.9	1079	6.1	0.000083
Mn	54.9	1007	13.3	0.000147
Sm	150.4	15.7	5600	0.000352
Gd	157.3	14.53	49000	0.002725
O	16.0	493343.88	0.00028	0.000005
	Total	999728		0.008410

Neutron Production Rate (n/g/yr)

(X factor = 1.045) (Total U ppm = 4.4) = 4.598

(Y factor = 0.478) (Total Th ppm = 25.4) = 12.1412

^{238}U spontaneous fission = 1.888

Total neutron production rate (n/g/yr) = 19

In Situ Secular Equilibrium ^{36}Cl/Cl Ratio (x 10^{-15}) = 32

162

Table B-1c. Calculated thermal neutron cross section for neutron absorption, total neutron production rate, and *in situ* secular equilibrium ^{36}Cl/Cl ratio for igneous rock sample SP-7, rhyolite.

[See figure 1.1 for location of sampling site. See text for explanation of Mass Stopping Power, Weighting Factor, X and Y factors, Weighted Neutron Yields, and Thermal Cross Sections. Mass Stopping Power, Neutron Yields, and Absorption Cross Sections supplied by Fabryka-Martin (1995). Mass Stopping Power is given for each element for an alpha particle of energy 8.0 million electron volts (MeV). Mass Stopping Power units: MeV per gram of rock per square centimeter. Sample ppm from Appendix table A-1; cm^2/g, square centimeters per gram; <, less than.]

| Element | Mass Stopping Power | Neutron Yield | | Sample ppm | Weighting Factor | Weighted Neutron Yield | |
		n/yr/g rock per ppm U	n/yr/g rock per ppm Th			n/yr/g rock per ppm U	n/yr/g rock per ppm Th
Si	454	0.69	0.339	314633	142.84	98.56	48.42
Al	444	5.116	2.585	58588	26.01	133.08	67.24
Fe	351	0.187	0.208	12670	4.45	0.83	0.93
Ca	428	0.282	0.026	36664	15.69	4.43	0.41
Mg	461	5.834	2.564	603	0.28	1.62	0.71
Na	456	12.535	5.959	26262	11.98	150.11	71.36
K	414	0.89	0.08	43500	18.01	16.03	1.44
P	433	4.473	0.573	131	0.06	0.25	0.03
Li	548	23.86	10.54	40	0.02	0.52	0.23
Be	529	265.948	91.561	5.5	0.00	0.77	0.27
B	527	62.551	19.779	5	0.00	0.16	0.05
C	561	0.456	0.179	300	0.17	0.08	0.03
F	472	41.33	16.362	800	0.38	15.61	6.18
O	527	0.236	0.084	497699.63	262.29	61.90	22.03
			Total	991901.13	482.18	483.96	219.34

Element	Atomic Weight (amu)	Sample ppm	Neutron Absorption Cross Section (barns/atom)	Thermal Neutron Cross Section (cm^2/g)
Si	28.1	314633	0.17	0.001146
Al	27.0	58588	0.233	0.000304
Fe	55.8	12670	2.56	0.000350
Ca	40.1	36664	0.43	0.000237
Mg	24.3	603	0.063	0.000001
Na	23.0	26262	0.53	0.000364
K	39.1	43500	2.1	0.001406
P	30.97	131	0.18	<0.000001
Li	6.9	40	71	0.000248
Be	9.01	5.5	0.0092	<0.000001
B	10.8	15	764	0.000639
C	12.0	300	0.0035	<0.000001
F	19.0	800	0.0096	<0.000001
H	1.0	6242.28	0.33	0.001240
Ti	47.9	959	6.1	0.000074
Mn	54.9	232	13.3	0.000034
Sm	150.4	11.1	5600	0.000249
Gd	157.3	9.26	49000	0.001737
O	16.0	497699.63	0.00028	0.000005
	Total	999364.77		**0.008034**

Neutron Production Rate (n/g/yr)

(X factor = 1.004)	(Total U ppm =	5.1)	= 5.1204	
(Y factor = 0.455)	(Total Th ppm =	28.8)	= 13.104	
	^{238}U spontaneous fission		= 2.188	*In Situ* Secular Equilibrium ^{36}Cl/Cl
	Total neutron production rate (n/g/yr)		= 20	Ratio (x 10^{-15}) = 37

Table B-1d. Calculated thermal neutron cross section for neutron absorption, total neutron production rate, and *in situ* secular equilibrium ^{36}Cl/Cl ratio for igneous rock sample SP-8, rhyolite.

[See figure 1.1 for location of sampling site. See text for explanation of Mass Stopping Power, Weighting Factor, X and Y factors, Weighted Neutron Yields, and Thermal Cross-Sections. Mass Stopping Power, Neutron Yields, and Absorption Cross Sections supplied by Fabryka-Martin (1995). Mass Stopping Power is given for each element for an alpha particle of energy 8.0 million electron volts (MeV). Mass Stopping Power units: MeV per gram of rock per square centimeter. Sample ppm from Appendix table A-1; cm^2/g, square centimeters per gram; <, less than.]

Element	Mass Stopping Power	Neutron Yield n/yr/g rock per ppm U	Neutron Yield n/yr/g rock per ppm Th	Sample ppm	Weighting Factor	Weighted Neutron Yield n/yr/g rock per ppm U	Weighted Neutron Yield n/yr/g rock per ppm Th
Si	454	0.69	0.339	353104	160.31	110.61	54.34
Al	444	5.116	2.585	60864	27.02	138.25	69.86
Fe	351	0.187	0.208	10338	3.63	0.68	0.75
Ca	428	0.282	0.026	3859	1.65	0.47	0.04
Mg	461	5.834	2.564	422	0.19	1.13	0.50
Na	456	12.535	5.959	25965	11.84	148.41	70.55
K	414	0.89	0.08	44580	18.46	16.43	1.48
P	433	4.473	0.573	131	0.06	0.25	0.03
Li	548	23.86	10.54	40	0.02	0.52	0.23
Be	529	265.948	91.561	5.5	0.00	0.77	0.27
B	527	62.551	19.779	15	0.01	0.49	0.16
C	561	0.456	0.179	300	0.17	0.08	0.03
F	472	41.33	16.362	800	0.38	15.61	6.18
O	527	0.236	0.084	495660.78	261.21	61.65	21.94
			Total	996084.28	484.95	495.36	226.37

Element	Atomic Weight (amu)	Sample ppm	Neutron Absorption Cross Section (barns/atom)	Thermal Neutron Cross Section (cm^2/g)
Si	28.1	353104	0.17	0.001286
Al	27.0	60864	0.233	0.000316
Fe	55.8	10338	2.56	0.000286
Ca	40.1	3859	0.43	0.000025
Mg	24.3	422	0.063	0.000001
Na	23.0	25965	0.53	0.000360
K	39.1	44580	2.1	0.001441
P	30.97	131	0.18	<0.000001
Li	6.9	40	71	0.000248
Be	9.01	5.5	0.0092	<0.000001
B	10.8	15	764	0.000639
C	12.0	300	0.0035	<0.000001
F	19.0	800	0.0096	<0.000001
H	1.0	1944.54	0.33	0.000386
Ti	47.9	899	6.1	0.000069
Mn	54.9	310	13.3	0.000045
Sm	150.4	13.6	5600	0.000305
Gd	157.3	12.74	49000	0.002389
O	16.0	495660.78	0.00028	0.000005
	Total	999264.16		0.007802

Neutron Production Rate (n/g/yr)

(X factor = 1.021) (Total U ppm = 6.2) = 6.3302

(Y factor = 0.467) (Total Th ppm = 27.7) = 12.9359

^{238}U spontaneous fission = 2.660

Total neutron production rate (n/g/yr) = 22

In Situ Secular Equilibrium ^{36}Cl/Cl Ratio (x 10^{-15}) = 41

164

Table B-1e.   Calculated thermal neutron cross section for neutron absorption, total neutron production rate, and *in situ* secular equilibrium ^{36}Cl/Cl ratio for igneous rock sample SP-9, opal deposit in rhyolite.

[See figure 1.1 for location of sampling site. See text for explanation of Mass Stopping Power, Weighting Factor, X and Y factors, Weighted Neutron Yields, and Thermal Cross Sections. Mass Stopping Power, Neutron Yields, and Absorption Cross Sections supplied by Fabryka-Martin (1995). Mass Stopping Power is given for each element for an alpha particle of energy 8.0 million electron volts (MeV). Mass Stopping Power units: MeV per gram of rock per square centimeter. Sample ppm from Appendix table A-1; cm^2/g, square centimeters per gram; <, less than.]

Element	Mass Stopping Power	Neutron Yield		Sample ppm	Weighting Factor	Weighted Neutron Yield	
		n/yr/g rock per ppm U	n/yr/g rock per ppm Th			n/yr/g rock per ppm U	n/yr/g rock per ppm Th
Si	454	0.69	0.339	345625	156.91	108.27	53.19
Al	444	5.116	2.585	64780	28.76	147.15	74.35
Fe	351	0.187	0.208	2254	0.79	0.15	0.16
Ca	428	0.282	0.026	1572	0.67	0.19	0.02
Mg	461	5.834	2.564	121	0.06	0.33	0.14
Na	456	12.535	5.959	964	0.44	5.51	2.62
K	414	0.89	0.08	7222	2.99	2.66	0.24
P	433	4.473	0.573	175	0.08	0.34	0.04
Li	548	23.86	10.54	15	0.01	0.20	0.09
Be	529	265.948	91.561	0.5	0.00	0.07	0.02
B	527	62.551	19.779	35	0.02	1.15	0.36
C	561	0.456	0.179	531	0.30	0.14	0.05
F	472	41.33	16.362	270	0.13	5.27	2.09
O	527	0.236	0.084	561772.09	296.05	69.87	24.87
			Total	985336.59	487.21	341.28	158.25

Element	Atomic Weight (amu)	Sample ppm	Neutron Absorption Cross Section (barns/atom)	Thermal Neutron Cross Section (cm^2/g)
Si	28.1	345625	0.17	0.001259
Al	27.0	64780	0.233	0.000337
Fe	55.8	2254	2.56	0.000062
Ca	40.1	1572	0.43	0.000010
Mg	24.3	121	0.063	<0.000001
Na	23.0	964	0.53	0.000013
K	39.1	7222	2.1	0.000234
P	30.97	175	0.18	0.000001
Li	6.9	15	71	0.000093
Be	9.01	0.5	1.119	<0.000001
B	10.8	35	764	0.001491
C	12.0	531	0.0035	<0.000001
F	19.0	270	0.0096	<0.000001
H	1.0	13180.93	0.33	0.002619
Ti	47.9	1439	6.1	0.000110
Mn	54.9	77	13.3	0.000011
Sm	150.4	4.28	5600	0.000096
Gd	157.3	3.17	49000	0.000594
O	16.0	561772.09	0.00028	0.000006
Total		1000040.97		0.006935

Neutron Production Rate (n/g/yr)

(X factor = 0.700)	(Total U ppm =	5.3)	= 3.71
(Y factor = 0.325)	(Total Th ppm =	20.3)	= 6.5975
	^{238}U spontaneous fission		= 2.274
Total neutron production rate (n/g/yr)			= 13

In Situ Secular Equilibrium ^{36}Cl/Cl Ratio (x 10^{-15}) =   26

Table B-1f.   Calculated thermal neutron cross section for neutron absorption, total neutron production rate, and *in situ* secular equilibrium ^{36}Cl/Cl ratio for igneous rock sample SP-10, rhyolite.

[See figure 1.1 for location of sampling site. See text for explanation of Mass Stopping Power, Weighting Factor, X and Y factors, Weighted Neutron Yields, and Thermal Cross Sections. Mass Stopping Power, Neutron Yields, and Absorption Cross Sections supplied by Fabryka-Martin (1995). Mass Stopping Power is given for each element for an alpha particle of energy 8.0 million electron volts (MeV). Mass Stopping Power units: MeV per gram of rock per square centimeter. Sample ppm from Appendix table A-1; cm^2/g, square centimeters per gram; <, less than.]

		Neutron Yield				Weighted Neutron Yield	
Element	Mass Stopping Power	n/yr/g rock per ppm U	n/yr/g rock per ppm Th	Sample ppm	Weighting Factor	n/yr/g rock per ppm U	n/yr/g rock per ppm Th
Si	454	0.69	0.339	338660	153.75	106.09	52.12
Al	444	5.116	2.585	64304	28.55	146.07	73.80
Fe	351	0.187	0.208	14458	5.07	0.95	1.06
Ca	428	0.282	0.026	4431	1.90	0.53	0.05
Mg	461	5.834	2.564	603	0.28	1.62	0.71
Na	456	12.535	5.959	27820	12.69	159.02	75.60
K	414	0.89	0.08	44497	18.42	16.40	1.47
P	433	4.473	0.573	175	0.08	0.34	0.04
Li	548	23.86	10.54	40	0.02	0.52	0.23
Be	529	265.948	91.561	5.5	0.00	0.77	0.27
B	527	62.551	19.779	15	0.01	0.49	0.16
C	561	0.456	0.179	300	0.17	0.08	0.03
F	472	41.33	16.362	800	0.38	15.61	6.18
O	527	0.236	0.084	498232.89	262.57	61.97	22.06
			Total	994341.39	483.88	510.45	233.77

Element	Atomic Weight (amu)	Sample ppm	Neutron Absorption Cross Section (barns/atom)	Thermal Neutron Cross Section (cm^2/g)
Si	28.1	338660	0.17	0.001233
Al	27.0	64304	0.233	0.000334
Fe	55.8	14458	2.56	0.000399
Ca	40.1	4431	0.43	0.000029
Mg	24.3	603	0.063	0.000001
Na	23.0	27820	0.53	0.000386
K	39.1	44497	2.1	0.001439
P	30.97	175	0.18	0.000001
Li	6.9	40	71	0.000248
Be	9.01	5.5	1.119	<0.000001
B	10.8	15	764	0.000639
C	12.0	300	0.0035	<0.000001
F	19.0	800	0.0096	<0.000001
H	1.0	3630.32	0.33	0.000721
Ti	47.9	1499	6.1	0.000115
Mn	54.9	232	13.3	0.000034
Sm	150.4	12.9	5600	0.000289
Gd	157.3	12.3	49000	0.002307
O	16.0	498232.89	0.00028	0.000005
	Total	999727.91		**0.008180**

Neutron Production Rate (n/g/yr)

(X factor = 1.055)   (Total U ppm =   5.3)   = 5.5915

(Y factor = 0.483)   (Total Th ppm =   24.9)   = 12.0267

^{238}U spontaneous fission   = 2.274   *In situ* Secular Equilibrium ^{36}Cl/Cl

Total neutron production rate (n/g/yr)   = 20   Ratio (x 10^{-15}) =   35

Table B-1g.   Calculated thermal neutron cross section for neutron absorption, total neutron production rate, and *in situ* secular equilibrium ^{36}Cl/Cl ratio for igneous rock sample SP-13, rhyolite.

[See figure 1.1 for location of sampling site. See text for explanation of Mass Stopping Power, Weighting Factor, X and Y factors, Weighted Neutron Yields, and Thermal Cross Sections. Mass Stopping Power, Neutron Yields, and Absorption Cross Sections supplied by Fabryka-Martin (1995). Mass Stopping Power is given for each element for an alpha particle of energy 8.0 million electron volts (MeV). Mass Stopping Power units: MeV per gram of rock per square centimeter. Sample ppm from Appendix table A-1; cm^2/g, square centimeters per gram; <, less than.]

Element	Mass Stopping Power	Neutron Yield n/yr/g rock per ppm U	Neutron Yield n/yr/g rock per ppm Th	Sample ppm	Weighting Factor	Weighted Neutron Yield n/yr/g rock per ppm U	Weighted Neutron Yield n/yr/g rock per ppm Th
Si	454	0.69	0.339	346419	157.27	108.52	53.32
Al	444	5.116	2.585	62081	27.56	141.02	71.25
Fe	351	0.187	0.208	8550	3.00	0.56	0.62
Ca	428	0.282	0.026	11078	4.74	1.34	0.12
Mg	461	5.834	2.564	784	0.36	2.11	0.93
Na	456	12.535	5.959	25594	11.67	146.29	69.55
K	414	0.89	0.08	44165	18.28	16.27	1.46
P	433	4.473	0.573	175	0.08	0.34	0.04
Li	548	23.86	10.54	40	0.02	0.52	0.23
Be	529	265.948	91.561	5.5	0.00	0.77	0.27
B	527	62.551	19.779	15	0.01	0.49	0.16
C	561	0.456	0.179	300	0.17	0.08	0.03
F	472	41.33	16.362	800	0.38	15.61	6.18
O	527	0.236	0.084	496338.11	261.57	61.73	21.97
			Total	996344.61	485.12	495.65	226.13

Element	Atomic Weight (amu)	Sample ppm	Neutron Absorption Cross Section (barns/atom)	Thermal Neutron Cross Section (cm^2/g)
Si	28.1	346419	0.17	0.001262
Al	27.0	62081	0.233	0.000323
Fe	55.8	8550	2.56	0.000236
Ca	40.1	11078	0.43	0.000072
Mg	24.3	784	0.063	0.000001
Na	23.0	25594	0.53	0.000355
K	39.1	44165	2.1	0.001428
P	30.97	175	0.18	0.000001
Li	6.9	40	71	0.000248
Be	9.01	5.5	1.119	<0.000001
B	10.8	15	764	0.000639
C	12.0	300	0.0035	<0.000001
F	19.0	800	0.0096	<0.000001
H	1.0	2579.75	0.33	0.000512
Ti	47.9	480	6.1	0.000037
Mn	54.9	310	13.3	0.000045
Sm	150.4	9.91	5600	0.000222
Gd	157.3	9.96	49000	0.001868
O	16.0	496338.11	0.00028	0.000005
	Total	999734.23		**0.007254**

Neutron Production Rate (n/g/yr)

(X factor = 1.022)   (Total U ppm =   5.1)   = 5.2122

(Y factor = 0.466)   (Total Th ppm =   19.1)   = 8.9006

^{238}U spontaneous fission   = 2.188

Total neutron production rate (n/g/yr)   = 16

In Situ Secular Equilibrium ^{36}Cl/Cl Ratio (x 10^{-15}) =   33

Table B-1h. Calculated thermal neutron cross section for neutron absorption, total neutron production rate, and *in situ* secular equilibrium ^{36}Cl/Cl ratio for igneous rock sample SP-15, basalt.

[See figure 1.1 for location of sampling site. See text for explanation of Mass Stopping Power, Weighting Factor, X and Y factors, Weighted Neutron Yields, and Thermal Cross Sections. Mass Stopping Power, Neutron Yields, and Absorption Cross Sections supplied by Fabryka-Martin (1995). Mass Stopping Power is given for each element for an alpha particle of energy 8.0 million electron volts (MeV). Mass Stopping Power units: MeV per gram of rock per square centimeter. Sample ppm from Appendix table A-1; cm^2/g, square centimeters per gram; <, less than.]

Element	Mass Stopping Power	Neutron Yield		Sample ppm	Weighting Factor	Weighted Neutron Yield	
		n/yr/g rock per ppm U	n/yr/g rock per ppm Th			n/yr/g rock per ppm U	n/yr/g rock per ppm Th
Si	454	0.69	0.339	210348	95.50	65.89	32.37
Al	444	5.116	2.585	69861	31.02	158.69	80.18
Fe	351	0.187	0.208	90945	31.92	5.97	6.64
Ca	428	0.282	0.026	77545	33.19	9.36	0.86
Mg	461	5.834	2.564	33291	15.35	89.54	39.35
Na	456	12.535	5.959	15727	7.17	89.89	42.74
K	414	0.89	0.08	12369	5.12	4.56	0.41
P	433	4.473	0.573	3710	1.61	7.19	0.92
Li	548	23.86	10.54	15	0.01	0.20	0.09
Be	529	265.948	91.561	0.4	0.00	0.06	0.02
B	527	62.551	19.779	5	0.00	0.16	0.05
C	561	0.456	0.179	100	0.06	0.03	0.01
F	472	41.33	16.362	370	0.17	7.22	2.86
O	527	0.236	0.084	460861.49	242.87	57.32	20.40
			Total	975147.89	463.99	496.06	226.90

Element	Atomic Weight (amu)	Sample ppm	Neutron Absorption Cross Section (barns/atom)	Thermal Neutron Cross Section (cm^2/g)
Si	28.1	210348	0.17	0.000766
Al	27.0	69861	0.233	0.000363
Fe	55.8	90945	2.56	0.002512
Ca	40.1	77545	0.43	0.000501
Mg	24.3	33291	0.063	0.000052
Na	23.0	15727	0.53	0.000218
K	39.1	12369	2.1	0.000400
P	30.97	3710	0.18	0.000013
Li	6.9	15	71	0.000093
Be	9.01	0.4	0.009	<0.000001
B	10.8	5	764	0.000213
C	12.0	100	0.0035	<0.000001
F	19.0	370	0.0096	<0.000001
H	1.0	7065.57	0.33	0.001404
Ti	47.9	16247	6.1	0.001246
Mn	54.9	1471	13.3	0.000215
Sm	150.4	7.51	5600	0.000168
Gd	157.3	6.45	49000	0.001210
O	16.0	460861.49	0.00028	0.000005
	Total	999945.42		0.009377

Neutron Production Rate (n/g/yr)

(X factor = 1.069)   (Total U ppm =   1.1)   = 1.1759

(Y factor = 0.489)   (Total Th ppm =   2.54)   = 1.2421

^{238}U spontaneous fission   = 0.472

Total neutron production rate (n/g/yr)   = 2.9

In situ Secular Equilibrium ^{36}Cl/Cl Ratio (x 10^{-15}) =   4.5

Table B-1i. Calculated thermal neutron cross section for neutron absorption, total neutron production rate, and *in situ* secular equilibrium ^{36}Cl/Cl ratio for igneous rock sample SP-16, basalt.

[See figure 1.1 for location of sampling site. See text for explanation of Mass Stopping Power, Weighting Factor, X and Y factors, Weighted Neutron Yields, and Thermal Cross Sections. Mass Stopping Power, Neutron Yields, and Absorption Cross Sections supplied by Fabryka-Martin (1995). Mass Stopping Power is given for each element for an alpha particle of energy 8.0 million electron volts (MeV). Mass Stopping Power units: MeV per gram of rock per square centimeter. Sample ppm from Appendix table A-1; cm^2/g, square centimeters per gram; <, less than.]

| Element | Mass Stopping Power | Neutron Yield | | Sample ppm | Weighting Factor | Weighted Neutron Yield | |
		n/yr/g rock per ppm U	n/yr/g rock per ppm Th			n/yr/g rock per ppm U	n/yr/g rock per ppm Th
Si	454	0.69	0.339	212685	96.56	66.63	32.73
Al	444	5.116	2.585	77800	34.54	176.72	89.29
Fe	351	0.187	0.208	85504	30.01	5.61	6.24
Ca	428	0.282	0.026	73614	31.51	8.88	0.82
Mg	461	5.834	2.564	49575	22.85	133.33	58.60
Na	456	12.535	5.959	17582	8.02	100.50	47.78
K	414	0.89	0.08	3653	1.51	1.35	0.12
P	433	4.473	0.573	1091	0.47	2.11	0.27
Li	548	23.86	10.54	12	0.01	0.16	0.07
Be	529	265.948	91.561	0.4	0.00	0.06	0.02
B	527	62.551	19.779	5	0.00	0.16	0.05
C	561	0.456	0.179	100	0.06	0.03	0.01
F	472	41.33	16.362	370	0.17	7.22	2.86
O	527	0.236	0.084	460222.97	242.54	57.24	20.37
			Total	982214.37	468.25	559.99	259.24

Element	Atomic Weight (amu)	Sample ppm	Neutron Absorption Cross Section (barns/atom)	Thermal Neutron Cross Section (cm^2/g)
Si	28.1	212685	0.17	0.000775
Al	27.0	77800	0.233	0.000404
Fe	55.8	85504	2.56	0.002362
Ca	40.1	73614	0.43	0.000475
Mg	24.3	49575	0.063	0.000077
Na	23.0	17582	0.53	0.000244
K	39.1	3653	2.1	0.000118
P	30.97	1091	0.18	0.000004
Li	6.9	12	71	0.000074
Be	9.01	0.4	1.119	<0.000001
B	10.8	5	764	0.000213
C	12.0	100	0.0035	<0.000001
F	19.0	370	0.0096	<0.000001
H	1.0	5863.45	0.33	0.001165
Ti	47.9	10491	6.1	0.000804
Mn	54.9	1317	13.3	0.000192
Sm	150.4	4.75	5600	0.000106
Gd	157.3	3.87	49000	0.000726
O	16.0	460222.97	0.00028	0.000005
	Total	999894.44		0.007744

Neutron Production Rate (n/g/yr)

(X factor = 1.196)	(Total U ppm =	0.8)	= 0.9568
(Y factor = 0.554)	(Total Th ppm =	1.71)	= 0.9473
	^{238}U spontaneous fission		= 0.343
	Total neutron production rate (n/g/yr)		= 2.3

In Situ Secular Equilibrium ^{36}Cl/Cl Ratio (x 10^{-15}) = 4.2

Table B-1j.   Calculated thermal neutron cross section for neutron absorption, total neutron production rate, and *in situ* secular equilibrium ^{36}Cl/Cl ratio for igneous rock sample SP-17, rhyolite.

[See figure 1.1 for location of sampling site. See text for explanation of Mass Stopping Power, Weighting Factor, X and Y factors, Weighted Neutron Yields, and Thermal Cross Sections. Mass Stopping Power, Neutron Yields, and Absorption Cross Sections supplied by Fabryka-Martin (1995). Mass Stopping Power is given for each element for an alpha particle of energy 8.0 million electron volts (MeV). Mass Stopping Power units: MeV per gram of rock per square centimeter. Sample ppm from Appendix table A-1; cm²/g, square centimeters per gram; <, less than.]

| Element | Mass Stopping Power | Neutron Yield | | Sample ppm | Weighting Factor | Weighted Neutron Yield | |
		n/yr/g rock per ppm U	n/yr/g rock per ppm Th			n/yr/g rock per ppm U	n/yr/g rock per ppm Th
Si	454	0.69	0.339	353337	160.41	110.69	54.38
Al	444	5.116	2.585	66156	29.37	150.27	75.93
Fe	351	0.187	0.208	12903	4.53	0.85	0.94
Ca	428	0.282	0.026	5003	2.14	0.60	0.06
Mg	461	5.834	2.564	1025	0.47	2.76	1.21
Na	456	12.535	5.959	31974	14.58	182.76	86.88
K	414	0.89	0.08	38187	15.81	14.07	1.26
P	433	4.473	0.573	87	0.04	0.17	0.02
Li	548	23.86	10.54	40	0.02	0.52	0.23
Be	529	265.948	91.561	5.5	0.00	0.77	0.27
B	527	62.551	19.779	15	0.01	0.49	0.16
C	561	0.456	0.179	300	0.17	0.08	0.03
F	472	41.33	16.362	800	0.38	15.61	6.18
O	527	0.236	0.084	488402.09	257.39	60.74	21.62
			Total	998234.59	485.32	540.39	249.17

Element	Atomic Weight (amu)	Sample ppm	Neutron Absorption Cross Section (barns/atom)	Thermal Neutron Cross Section (cm²/g)
Si	28.1	353337	0.17	0.001287
Al	27.0	66156	0.233	0.000344
Fe	55.8	12903	2.56	0.000356
Ca	40.1	5003	0.43	0.000032
Mg	24.3	1025	0.063	0.000002
Na	23.0	31974	0.53	0.000444
K	39.1	38187	2.1	0.001235
P	30.97	87	0.18	<0.000001
Li	6.9	40	71	0.000248
Be	9.01	5.5	1.119	<0.000001
B	10.8	15	764	0.000639
C	12.0	300	0.0035	<0.000001
F	19.0	800	0.0096	<0.000001
H	1.0	103.33	0.33	0.000021
Ti	47.9	989	6.1	0.000076
Mn	54.9	387	13.3	0.000056
Sm	150.4	15.44	5600	0.000346
Gd	157.3	22.63	49000	0.004244
O	16.0	488402.09	0.00028	0.000005
	Total	999751.99		0.009334

Neutron Production Rate (n/g/yr)

(X factor = 1.113)   (Total U ppm =   11.5)   = 12.7995

(Y factor = 0.513)   (Total Th ppm =   22.5)   = 11.5425

^{238}U spontaneous fission   = 4.934

Total neutron production rate (n/g/yr)   = 29

In Situ Secular Equilibrium ^{36}Cl/Cl Ratio (x 10^{-15}) =   45

Table B-1k.   Calculated thermal neutron cross section for neutron absorption, total neutron production rate, and *in situ* secular equilibrium $^{36}Cl/Cl$ ratio for igneous rock sample SP-18, basalt.

[See figure 1.1 for location of sampling site. See text for explanation of Mass Stopping Power, Weighting Factor, X and Y factors, Weighted Neutron Yields, and Thermal Cross Sections. Mass Stopping Power, Neutron Yields, and Absorption Cross Sections supplied by Fabryka-Martin (1995). Mass Stopping Power is given for each element for an alpha particle of energy 8.0 million electron volts (MeV). Mass Stopping Power units: MeV per gram of rock per square centimeter. Sample ppm from Appendix table A-1; cm^2/g, square centimeters per gram; <, less than.]

| Element | Mass Stopping Power | Neutron Yield | | Sample ppm | Weighting Factor | Weighted Neutron Yield | |
		n/yr/g rock per ppm U	n/yr/g rock per ppm Th			n/yr/g rock per ppm U	n/yr/g rock per ppm Th
Si	454	0.69	0.339	222969	101.23	69.85	34.32
Al	444	5.116	2.585	85739	38.07	194.76	98.41
Fe	351	0.187	0.208	81618	28.65	5.36	5.96
Ca	428	0.282	0.026	79332	33.95	9.58	0.88
Mg	461	5.834	2.564	50359	23.22	135.44	59.52
Na	456	12.535	5.959	18250	8.32	104.32	49.59
K	414	0.89	0.08	3736	1.55	1.38	0.12
P	433	4.473	0.573	1397	0.60	2.71	0.35
Li	548	23.86	10.54	15	0.01	0.20	0.09
Be	529	265.948	91.561	0.4	0.00	0.06	0.02
B	527	62.551	19.779	5	0.00	0.16	0.05
C	561	0.456	0.179	100	0.06	0.03	0.01
F	472	41.33	16.362	370	0.17	7.22	2.86
O	527	0.236	0.084	443085.29	233.51	55.11	19.61
			Total	986975.69	469.33	586.14	271.79

Element	Atomic Weight (amu)	Sample ppm	Neutron Absorption Cross Section (barns/atom)	Thermal Neutron Cross Section (cm^2/g)
Si	28.1	222969	0.17	0.000812
Al	27.0	85739	0.233	0.000445
Fe	55.8	81618	2.56	0.002254
Ca	40.1	79332	0.43	0.000512
Mg	24.3	50359	0.063	0.000079
Na	23.0	18250	0.53	0.000253
K	39.1	3736	2.1	0.000121
P	30.97	1397	0.18	0.000005
Li	6.9	15	71	0.000093
Be	9.01	0.4	1.119	<0.000001
B	10.8	5	764	0.000213
C	12.0	100	0.0035	<0.000001
F	19.0	370	0.0096	<0.000001
H	1.0	1034.88	0.33	0.000206
Ti	47.9	10611	6.1	0.000813
Mn	54.9	1317	13.3	0.000192
Sm	150.4	4.8	5600	0.000108
Gd	157.3	4.12	49000	0.000773
O	16.0	443085.29	0.00028	0.000005
	Total	999947.49		0.006883

Neutron Production Rate (n/g/yr)

(X factor = 1.249)   (Total U ppm =   0.6)   = 0.7494

(Y factor = 0.579)   (Total Th ppm =   1.31)   = 0.7585

^{238}U spontaneous fission   = 0.257

Total neutron production rate (n/g/yr)   = 1.8

In Situ Secular Equilibrium $^{36}Cl/Cl$ Ratio (x 10^{-15}) =   3.7

171

Table B-11.   Calculated thermal neutron cross section for neutron absorption, total neutron production rate, and *in situ* secular equilibrium ^{36}Cl/Cl ratio for igneous rock sample SP-19, basalt.

[See figure 1.1 for location of sampling site. See text for explanation of Mass Stopping Power, Weighting Factor, X and Y factors, Weighted Neutron Yields, and Thermal Cross Sections. Mass Stopping Power, Neutron Yields, and Absorption Cross Sections supplied by Fabryka-Martin (1995). Mass Stopping Power is given for each element for an alpha particle of energy 8.0 million electron volts (MeV). Mass Stopping Power units: MeV per gram of rock per square centimeter. Sample ppm from Appendix table A-1; cm²/g, square centimeters per gram; <, less than.]

Element	Mass Stopping Power	Neutron Yield n/yr/g rock per ppm U	Neutron Yield n/yr/g rock per ppm Th	Sample ppm	Weighting Factor	Weighted Neutron Yield n/yr/g rock per ppm U	Weighted Neutron Yield n/yr/g rock per ppm Th
Si	454	0.69	0.339	215490	97.83	67.50	33.17
Al	444	5.116	2.585	83622	37.13	189.95	95.98
Fe	351	0.187	0.208	97164	34.10	6.38	7.09
Ca	428	0.282	0.026	76259	32.64	9.20	0.85
Mg	461	5.834	2.564	46982	21.66	126.36	55.53
Na	456	12.535	5.959	18695	8.52	106.86	50.80
K	414	0.89	0.08	4400	1.82	1.62	0.15
P	433	4.473	0.573	1920	0.83	3.72	0.48
Li	548	23.86	10.54	15	0.01	0.20	0.09
Be	529	265.948	91.561	0.4	0.00	0.06	0.02
B	527	62.551	19.779	5	0.00	0.16	0.05
C	561	0.456	0.179	100	0.06	0.03	0.01
F	472	41.33	16.362	370	0.17	7.22	2.86
O	527	0.236	0.084	439025.08	231.37	54.60	19.43
			Total	984047.48	466.15	573.85	266.50

Element	Atomic Weight (amu)	Sample ppm	Neutron Absorption Cross Section (barns/atom)	Thermal Neutron Cross Section (cm²/g)
Si	28.1	215490	0.17	0.000785
Al	27.0	83622	0.233	0.000434
Fe	55.8	97164	2.56	0.002684
Ca	40.1	76259	0.43	0.000492
Mg	24.3	46982	0.063	0.000073
Na	23.0	18695	0.53	0.000259
K	39.1	4400	2.1	0.000142
P	30.97	1920	0.18	0.000007
Li	6.9	15	71	0.000093
Be	9.01	0.4	1.119	<0.000001
B	10.8	5	764	0.000213
C	12.0	100	0.0035	<0.000001
F	19.0	370	0.0096	<0.000001
H	1.0	1375.94	0.33	0.000273
Ti	47.9	13069	6.1	0.001002
Mn	54.9	1394	13.3	0.000203
Sm	150.4	5.68	5600	0.000127
Gd	157.3	5.05	49000	0.000947
O	16.0	439025.08	0.00028	0.000005
	Total	999897.15		0.007740

Neutron Production Rate (n/g/yr)

(X factor = 1.231)   (Total U ppm =   0.5)   = 0.6155

(Y factor = 0.572)   (Total Th ppm =   1.6)   = 0.9152

^{238}U spontaneous fission   = 0.215

Total neutron production rate (n/g/yr)   = 1.7

In Situ Secular
Equilibrium ^{36}Cl/Cl
Ratio (x 10^{-15}) =   3.3

172

Table B-1m. Calculated thermal neutron cross section for neutron absorption, total neutron production rate, and *in situ* secular equilibrium ^{36}Cl/Cl ratio for igneous rock sample SP-20, basalt.

[See figure 1.1 for location of sampling site. See text for explanation of Mass Stopping Power, Weighting Factor, X and Y factors, Weighted Neutron Yields, and Thermal Cross Sections. Mass Stopping Power, Neutron Yields, and Absorption Cross Sections supplied by Fabryka-Martin (1995). Mass Stopping Power is given for each element for an alpha particle of energy 8.0 million electron volts (MeV). Mass Stopping Power units: MeV per gram of rock per square centimeter. Sample ppm from Appendix table A-1; cm^2/g, square centimeters per gram; <, less than.]

Element	Mass Stopping Power	Neutron Yield n/yr/g rock per ppm U	Neutron Yield n/yr/g rock per ppm Th	Sample ppm	Weighting Factor	Weighted Neutron Yield n/yr/g rock per ppm U	Weighted Neutron Yield n/yr/g rock per ppm Th
Si	454	0.69	0.339	209880	95.29	65.75	32.30
Al	444	5.116	2.585	79338	35.23	180.22	91.06
Fe	351	0.187	0.208	98719	34.65	6.48	7.21
Ca	428	0.282	0.026	70970	30.38	8.57	0.79
Mg	461	5.834	2.564	43665	20.13	117.44	51.61
Na	456	12.535	5.959	18917	8.63	108.13	51.40
K	414	0.89	0.08	5230	2.17	1.93	0.17
P	433	4.473	0.573	2662	1.15	5.16	0.66
Li	548	23.86	10.54	15	0.01	0.20	0.09
Be	529	265.948	91.561	0.4	0.00	0.06	0.02
B	527	62.551	19.779	5	0.00	0.16	0.05
C	561	0.456	0.179	100	0.06	0.03	0.01
F	472	41.33	16.362	370	0.17	7.22	2.86
O	527	0.236	0.084	448260.68	236.23	55.75	19.84
			Total	978132.08	464.09	557.07	258.08

Element	Atomic Weight (amu)	Sample ppm	Neutron Absorption Cross Section (barns/atom)	Thermal Neutron Cross Section (cm^2/g)
Si	28.1	209880	0.17	0.000764
Al	27.0	79388	0.233	0.000412
Fe	55.8	79388	2.56	0.002193
Ca	40.1	98719	0.43	0.000637
Mg	24.3	70970	0.063	0.000111
Na	23.0	43665	0.53	0.000606
K	39.1	18917	2.1	0.000612
P	30.97	5230	0.18	0.000018
Li	6.9	2662	71	0.016490
Be	9.01	0.4	1.119	<0.000001
B	10.8	5	764	0.000213
C	12.0	100	0.0035	<0.000001
F	19.0	370	0.0096	<0.000001
H	1.0	3882.04	0.33	0.000771
Ti	47.9	16247	6.1	0.001246
Mn	54.9	1471	13.3	0.000215
Sm	150.4	7.39	5600	0.000166
Gd	157.3	6.5	49000	0.001219
O	16.0	448260.68	0.00028	0.000005
	Total	1079169.01		0.025677

Neutron Production Rate (n/g/yr)

(X factor = 1.200)   (Total U ppm = 0.8)   = 0.96

(Y factor = 0.556)   (Total Th ppm = 2.23)   = 1.2399

^{238}U spontaneous fission   = 0.343

Total neutron production rate (n/g/yr)   = 2.5

In Situ Secular Equilibrium ^{36}Cl/Cl Ratio (x 10^{-15}) =   1.4

Table B-1n.   Calculated thermal neutron cross section for neutron absorption, total neutron production rate, and *in situ* secular equilibrium ^{36}Cl/Cl ratio for igneous rock sample SP-21, basalt.

[See figure 1.1 for location of sampling site. See text for explanation of Mass Stopping Power, Weighting Factor, X and Y factors. Weighted Neutron Yields, and Thermal Cross Sections. Mass Stopping Power, Neutron Yields. and Absorption Cross Sections supplied by Fabryka-Martin (1995). Mass Stopping Power is given for each element for an alpha particle of energy 8.0 million electron volts (MeV). Mass Stopping Power units: MeV per gram of rock per square centimeter. Sample ppm from Appendix table A-1; cm^2/g, square centimeters per gram; <, less than.]

Element	Mass Stopping Power	Neutron Yield		Sample ppm	Weighting Factor	Weighted Neutron Yield	
		n/yr/g rock per ppm U	n/yr/g rock per ppm Th			n/yr/g rock per ppm U	n/yr/g rock per ppm Th
Si	454	0.69	0.339	214555	97.41	67.21	33.02
Al	444	5.116	2.585	70390	31.25	159.89	80.79
Fe	351	0.187	0.208	94055	33.01	6.17	6.87
Ca	428	0.282	0.026	57176	24.47	6.90	0.64
Mg	461	5.834	2.564	30035	13.85	80.78	35.50
Na	456	12.535	5.959	23294	10.62	133.15	63.30
K	414	0.89	0.08	14611	6.05	5.38	0.48
P	433	4.473	0.573	1353	0.59	2.62	0.34
Li	548	23.86	10.54	15	0.01	0.20	0.09
Be	529	265.948	91.561	0.4	0.00	0.06	0.02
B	527	62.551	19.779	5	0.00	0.16	0.05
C	561	0.456	0.179	100	0.06	0.03	0.01
F	472	41.33	16.362	370	0.17	7.22	2.86
O	527	0.236	0.084	467875.12	246.57	58.19	20.71
			Total	973834.52	464.06	527.96	244.67

Element	Atomic Weight (amu)	Sample ppm	Neutron Absorption Cross Section (barns/atom)	Thermal Neutron Cross Section (cm^2/g)
Si	28.1	214555	0.17	0.000781
Al	27.0	70390	0.233	0.000366
Fe	55.8	94055	2.56	0.002598
Ca	40.1	57176	0.43	0.000369
Mg	24.3	30035	0.063	0.000047
Na	23.0	23294	0.53	0.000323
K	39.1	14611	2.1	0.000472
P	30.97	1353	0.18	0.000005
Li	6.9	15	71	0.000093
Be	9.01	0.4	1.119	<0.000001
B	10.8	5	764	0.000213
C	12.0	100	0.0035	<0.000001
F	19.0	370	0.0096	<0.000001
H	1.0	8489.93	0.33	0.001687
Ti	47.9	15887	6.1	0.001218
Mn	54.9	1549	13.3	0.000226
Sm	150.4	13.77	5600	0.000309
Gd	157.3	13.99	49000	0.002624
O	16.0	443085.29	0.00028	0.000005
	Total	974998.38		0.011334

Neutron Production Rate (n/g/yr)

(X factor = 1.138)   (Total U ppm =   3.00)   = 3.4140

(Y factor = 0.527)   (Total Th ppm =   6.57)   = 3.4624

^{238}U spontaneous fission   = 1.287

Total neutron production rate (n/g/yr)   = 8.2

In Situ Secular Equilibrium ^{36}Cl/Cl Ratio (x 10^{-15}) =   10

Table B-1o. Calculated thermal neutron cross section for neutron absorption, total neutron production rate, and *in situ* secular equilibrium [36]Cl/Cl ratio for igneous rock sample SP-22, basalt.

[See figure 1.1 for location of sampling site. See text for explanation of Mass Stopping Power, Weighting Factor, X and Y factors, Weighted Neutron Yields, and Thermal Cross Sections. Mass Stopping Power, Neutron Yields, and Absorption Cross Sections supplied by Fabryka-Martin (1995). Mass Stopping Power is given for each element for an alpha particle of energy 8.0 million electron volts (MeV). Mass Stopping Power units: MeV per gram of rock per square centimeter. Sample ppm from Appendix table A-1; cm^2/g, square centimeters per gram; <, less than.]

Element	Mass Stopping Power	Neutron Yield		Sample ppm	Weighting Factor	Weighted Neutron Yield	
		n/yr/g rock per ppm U	n/yr/g rock per ppm Th			n/yr/g rock per ppm U	n/yr/g rock per ppm Th
Si	454	0.69	0.339	227176	103.14	71.17	34.96
Al	444	5.116	2.585	75683	33.60	171.91	86.86
Fe	351	0.187	0.208	66071	23.19	4.34	4.82
Ca	428	0.282	0.026	66610	28.51	8.04	0.74
Mg	461	5.834	2.564	45293	20.88	121.81	53.54
Na	456	12.535	5.959	17211	7.85	98.38	46.77
K	414	0.89	0.08	26980	11.17	9.94	0.89
P	433	4.473	0.573	2269	0.98	4.39	0.56
Li	548	23.86	10.54	15	0.01	0.20	0.09
Be	529	265.948	91.561	0.4	0.00	0.06	0.02
B	527	62.551	19.779	5	0.00	0.16	0.05
C	561	0.456	0.179	100	0.06	0.03	0.01
F	472	41.33	16.362	370	0.17	7.22	2.86
O	527	0.236	0.084	461009.81	242.95	57.34	20.41
			Total	988793.21	472.52	554.98	252.59

Element	Atomic Weight (amu)	Sample ppm	Neutron Absorption Cross Section (barns/atom)	Thermal Neutron Cross Section (cm^2/g)
Si	28.1	227176	0.17	0.000827
Al	27.0	75683	0.233	0.000393
Fe	55.8	66071	2.56	0.001825
Ca	40.1	66610	0.43	0.000430
Mg	24.3	45293	0.063	0.000071
Na	23.0	17211	0.53	0.000239
K	39.1	26980	2.1	0.000872
P	30.97	2269	0.18	0.000008
Li	6.9	15	71	0.000093
Be	9.01	0.4	1.119	<0.000001
B	10.8	5	764	0.000213
C	12.0	100	0.0035	<0.000001
F	19.0	370	0.0096	<0.000001
H	1.0	5241.73	0.33	0.001041
Ti	47.9	4736	6.1	0.000363
Mn	54.9	1162	13.3	0.000169
Sm	150.4	5.07	5600	0.000114
Gd	157.3	4.78	49000	0.000896
O	16.0	461009.81	0.00028	0.000005
	Total	999942.79		0.007560

Neutron Production Rate (n/g/yr)

(X factor = 1.175)   (Total U ppm = 1.2)   = 1.41

(Y factor = 0.535)   (Total Th ppm = 5.28)   = 2.8248

[238]U spontaneous fission   = 0.515

Total neutron production rate (n/g/yr)   = 4.8

In Situ Secular Equilibrium [36]Cl/Cl Ratio (x 10^{-15}) =   9.1

175

Table B-1p.　Calculated thermal neutron cross section for neutron absorption, total neutron production rate, and *in situ* secular equilibrium ^{36}Cl/Cl ratio for igneous rock sample SP-23, rhyolite.

[See figure 1.1 for location of sampling site. See text for explanation of Mass Stopping Power, Weighting Factor, X and Y factors, Weighted Neutron Yields, and Thermal Cross Sections. Mass Stopping Power, Neutron Yields, and Absorption Cross Sections supplied by Fabryka-Martin (1995). Mass Stopping Power is given for each element for an alpha particle of energy 8.0 million electron volts (MeV). Mass Stopping Power units: MeV per gram of rock per square centimeter. Sample ppm from Appendix table A-1; cm^2/g, square centimeters per gram; <, less than.]

Element	Mass Stopping Power	Neutron Yield		Sample ppm	Weighting Factor	Weighted Neutron Yield	
		n/yr/g rock per ppm U	n/yr/g rock per ppm Th			n/yr/g rock per ppm U	n/yr/g rock per ppm Th
Si	454	0.69	0.339	347775	157.89	108.94	53.52
Al	444	5.116	2.585	60864	27.02	138.25	69.86
Fe	351	0.187	0.208	15002	5.27	0.98	1.10
Ca	428	0.282	0.026	3431	1.47	0.41	0.04
Mg	461	5.834	2.564	543	0.25	1.46	0.64
Na	456	12.535	5.959	26707	12.18	152.66	72.57
K	414	0.89	0.08	41840	17.32	15.42	1.39
P	433	4.473	0.573	131	0.06	0.25	0.03
Li	548	23.86	10.54	40	0.02	0.52	0.23
Be	529	265.948	91.561	2.2	0.00	0.31	0.11
B	527	62.551	19.779	15	0.01	0.49	0.16
C	561	0.456	0.179	300	0.17	0.08	0.03
F	472	41.33	16.362	800	0.38	15.61	6.18
O	527	0.236	0.084	497709.97	262.29	61.90	22.03
			Total	995160.17	484.32	497.29	227.88

Element	Atomic Weight (amu)	Sample ppm	Neutron Absorption Cross Section (barns/atom)	Thermal Neutron Cross Section (cm^2/g)
Si	28.1	347775	0.17	0.001267
Al	27.0	60864	0.233	0.000316
Fe	55.8	15002	2.56	0.000414
Ca	40.1	3431	0.43	0.000022
Mg	24.3	543	0.063	0.000001
Na	23.0	26707	0.53	0.000370
K	39.1	41840	2.1	0.001353
P	30.97	131	0.18	<0.000001
Li	6.9	40	71	0.000248
Be	9.01	5.5	1.119	<0.000001
B	10.8	15	764	0.000639
C	12.0	300	0.0035	<0.000001
F	19.0	800	0.0096	<0.000001
H	1.0	2813.21	0.33	0.000559
Ti	47.9	1259	6.1	0.000097
Mn	54.9	465	13.3	0.000068
Sm	150.4	14.25	5600	0.000319
Gd	157.3	14.07	49000	0.002639
O	16.0	497709.97	0.00028	0.000005
	Total	999729		0.008317

Neutron Production Rate (n/g/yr)

(X factor = 1.027)　(Total U ppm = 5.8)　= 5.9566

(Y factor = 0.471)　(Total Th ppm = 23.0)　= 10.8330

　　^{238}U spontaneous fission　= 2.488

Total neutron production rate (n/g/yr)　= 19

In Situ Secular Equilibrium ^{36}Cl/Cl Ratio (x 10^{-15}) =　34

176

Table B-2a.   Calculated thermal neutron cross section for neutron absorption, total neutron production rate, and *in situ* secular equilibrium ^{36}Cl/Cl ratio for sedimentary rock sample SP-1, limestone.

[See figure 1.1 for location of sampling site. See text for explanation of Mass Stopping Power, Weighting Factor, X and Y factors, Weighted Neutron Yields, and Thermal Cross Sections. Mass Stopping Power, Neutron Yields, and Absorption Cross Sections supplied by Fabryka-Martin (1995). Mass Stopping Power is given for each element for an alpha particle of energy 8.0 million electron volts (MeV). Mass Stopping Power units: MeV per gram of rock per square centimeter. Sample ppm from Appendix table A-2; cm^2/g, square centimeters per gram; <, less than.]

Element	Mass Stopping Power	Neutron Yield n/yr/g rock per ppm U	Neutron Yield n/yr/g rock per ppm Th	Sample ppm	Weighting Factor	Weighted Neutron Yield n/yr/g rock per ppm U	Weighted Neutron Yield n/yr/g rock per ppm Th
Si	454	0.69	0.339	7947	3.61	2.49	1.22
Al	444	5.116	2.585	1376	0.61	3.13	1.58
Fe	351	0.187	0.208	233	0.08	0.02	0.02
Ca	428	0.282	0.026	382508	163.71	46.17	4.26
Mg	461	5.834	2.564	4522	2.08	12.16	5.35
Na	456	12.535	5.959	74	0.03	0.42	0.20
K	414	0.89	0.08	415	0.17	0.15	0.01
P	433	4.473	0.573	87	0.04	0.17	0.02
Li	548	23.86	10.54	5	0.00	0.07	0.03
Be	529	265.948	91.561	0.5	0.00	0.07	0.02
B	527	62.551	19.779	20	0.01	0.66	0.21
C	561	0.456	0.179	118201	66.31	30.24	11.87
F	472	41.33	16.362	330	0.16	6.44	2.55
O	527	0.236	0.084	483838.35	254.98	60.18	21.42
			Total	999556.85	491.80	162.35	48.76

Element	Atomic Weight (amu)	Sample ppm	Neutron Absorption Cross Section (barns/atom)	Thermal Neutron Cross Section (cm^2/g)
Si	28.1	7947	0.17	0.000029
Al	27.0	1376	0.233	0.000007
Fe	55.8	233	2.56	0.000006
Ca	40.1	382508	0.43	0.002469
Mg	24.3	4522	0.063	0.000007
Na	23.0	74	0.53	0.000001
K	39.1	415	2.1	0.000013
P	30.97	87	0.18	<0.000001
Li	6.9	5	71	0.000031
Be	9.01	0.5	0.0092	<0.000001
B	10.8	20	764	0.000852
C	12.0	118201	0.0035	0.000021
F	19.0	330	0.0096	<0.000001
H	1.0	340.37	0.33	0.000068
Ti	47.9	60	6.1	0.000005
Mn	54.9	77	13.3	0.000011
Sm	150.4	0.39	5600	0.000009
Gd	157.3	0.34	49000	0.000064
O	16.0	483838.35	0.00028	0.000005
	Total	1000034.95		**0.003598**

Neutron Production Rate (n/g/yr)

(X factor 0.330)   (Total U ppm = 1.9)   = 0.627

(Y factor 0.099)   (Total Th ppm = 0.1)   = 0.0099

^{238}U spontaneous fission   = 0.815

Total neutron production rate (n/g/yr)   = **1.5**

In Situ Secular Equilibrium ^{36}Cl/Cl Ratio (× 10^{-15}) =   **5.9**

177

Table B-2b. Calculated thermal neutron cross section for neutron absorption, total neutron production rate, and *in situ* secular equilibrium ^{36}Cl/Cl ratio for sedimentary rock sample SP-2, limestone.

[See figure 1.1 for location of sampling site. See text for explanation of Mass Stopping Power, Weighting Factor, X and Y factors, Weighted Neutron Yields, and Thermal Cross Sections. Mass Stopping Power, Neutron Yields, and Absorption Cross Sections supplied by Fabryka-Martin (1995). Mass Stopping Power is given for each element for an alpha particle of energy 8.0 million electron volts (MeV). Mass Stopping Power units: MeV per gram of rock per square centimeter. Sample ppm from Appendix table A-2; cm^2/g, square centimeters per gram; <, less than.]

Element	Mass Stopping Power	Neutron Yield		Sample ppm	Weighting Factor	Weighted Neutron Yield	
		n/yr/g rock per ppm U	n/yr/g rock per ppm Th			n/yr/g rock per ppm U	n/yr/g rock per ppm Th
Si	454	0.69	0.339	10564	4.80	3.31	1.63
Al	444	5.116	2.585	2064	0.92	4.69	2.37
Fe	351	0.187	0.208	544	0.19	0.04	0.04
Ca	428	0.282	0.026	381865	163.44	46.09	4.25
Mg	461	5.834	2.564	2714	1.25	7.30	3.21
Na	456	12.535	5.959	148	0.07	0.85	0.40
K	414	0.89	0.08	830	0.34	0.31	0.03
P	433	4.473	0.573	131	0.06	0.25	0.03
Li	548	23.86	10.54	5	0.00	0.07	0.03
Be	529	265.948	91.561	0.5	0.00	0.07	0.02
B	527	62.551	19.779	20	0.01	0.66	0.21
C	561	0.456	0.179	117164	65.73	29.97	11.77
F	472	41.33	16.362	330	0.16	6.44	2.55
O	527	0.236	0.084	483072.13	254.58	60.08	21.38
			Total	999451.63	491.54	160.11	47.91

Element	Atomic Weight (amu)	Sample ppm	Neutron Absorption Cross Section (barns/atom)	Thermal Neutron Cross Section (cm^2/g)
Si	28.1	10564	0.17	0.000038
Al	27.0	2064	0.233	0.000011
Fe	55.8	544	2.56	0.000015
Ca	40.1	381865	0.43	0.002465
Mg	24.3	2714	0.063	0.000004
Na	23.0	148	0.53	0.000002
K	39.1	830	2.1	0.000027
P	30.97	131	0.18	<0.000001
Li	6.9	5	71	0.000031
Be	9.01	0.5	0.0092	<0.000001
B	10.8	20	764	0.000852
C	12.0	117164	0.0035	0.000021
F	19.0	330	0.0096	<0.000001
H	1.0	284.27	0.33	0.000056
Ti	47.9	60	6.1	0.000005
Mn	54.9	77	13.3	0.000011
Sm	150.4	0.69	5600	0.000015
Gd	157.3	0.61	49000	0.000114
O	16.0	483072.13	0.00028	0.000005
	Total	999874.2		0.003674

Neutron Production Rate (n/g/yr)

(X factor = 0.326)	(Total U ppm =	2.5)	= 0.815
(Y factor = 0.097)	(Total Th ppm =	0.21)	= 0.0204
	^{238}U spontaneous fission		= 1.073

Total neutron production rate (n/g/yr) = 1.9

In Situ Secular Equilibrium ^{36}Cl/Cl Ratio (x 10^{-15}) = 7.53

Table B-2c.   Calculated thermal neutron cross section for neutron absorption, total neutron production rate, and *in situ* secular equilibrium ^{36}Cl/Cl ratio for sedimentary rock sample SP-3, limestone.

[See figure 1.1 for location of sampling site. See text for explanation of Mass Stopping Power, Weighting Factor, X and Y factors, Weighted Neutron Yields, and Thermal Cross Sections. Mass Stopping Power, Neutron Yields, and Absorption Cross Sections supplied by Fabryka-Martin (1995). Mass Stopping Power is given for each element for an alpha particle of energy 8.0 million electron volts (MeV). Mass Stopping Power units: MeV per gram of rock per square centimeter. Sample ppm from Appendix table A-2; cm^2/g, square centimeters per gram; <, less than.]

| Element | Mass Stopping Power | Neutron Yield | | Sample ppm | Weighting Factor | Weighted Neutron Yield | |
		n/yr/g rock per ppm U	n/yr/g rock per ppm Th			n/yr/g rock per ppm U	n/yr/g rock per ppm Th
Si	454	0.69	0.339	8554	3.88	2.68	1.32
Al	444	5.116	2.585	1217	0.54	2.76	1.40
Fe	351	0.187	0.208	233	0.08	0.02	0.02
Ca	428	0.282	0.026	383586	164.17	46.30	4.27
Mg	461	5.834	2.564	3317	1.53	8.92	3.92
Na	456	12.535	5.959	74	0.03	0.42	0.20
K	414	0.89	0.08	249	0.10	0.09	0.01
P	433	4.473	0.573	44	0.02	0.09	0.01
Li	548	23.86	10.54	5	0.00	0.07	0.03
Be	529	265.948	91.561	0.5	0.00	0.07	0.02
B	527	62.551	19.779	20	0.01	0.66	0.21
C	561	0.456	0.179	117519	65.93	30.06	11.80
F	472	41.33	16.362	330	0.16	6.44	2.55
O	527	0.236	0.084	484127.32	255.14	60.21	21.43
			Total	999275.82	491.60	158.79	47.18

Element	Atomic Weight (amu)	Sample ppm	Neutron Absorption Cross Section (barns/atom)	Thermal Neutron Cross Section (cm^2/g)
Si	28.1	8554	0.17	0.000031
Al	27.0	1217	0.233	0.000006
Fe	55.8	233	2.56	0.000006
Ca	40.1	383586	0.43	0.002476
Mg	24.3	3317	0.063	0.000005
Na	23.0	74	0.53	0.000001
K	39.1	249	2.1	0.000008
P	30.97	44	0.18	<0.000001
Li	6.9	5	71	0.000031
Be	9.01	0.5	0.0092	<0.000001
B	10.8	20	764	0.000852
C	12.0	117519	0.0035	0.000021
F	19.0	330	0.0096	<0.000001
H	1.0	569.56	0.33	0.000113
Ti	47.9	60	6.1	0.000005
Mn	54.9	77	13.3	0.000011
Sm	150.4	0.72	5600	0.000016
Gd	157.3	0.71	49000	0.000133
O	16.0	484127.32	0.00028	0.000005
	Total	999983.81		**0.003721**

Neutron Production Rate (n/g/yr)

(X factor = 0.323)   (Total U ppm =   2.9)   = 0.9367

(Y factor = 0.096)   (Total Th ppm =   0.18)   = 0.0173

^{238}U spontaneous fission   = 1.244

Total neutron production rate (n/g/yr)   = 2.2

In Situ Secular Equilibrium ^{36}Cl/Cl Ratio ($\times 10^{-15}$) =   8.6

Table B-2d. Calculated thermal neutron cross section for neutron absorption, total neutron production rate, and *in situ* secular equilibrium ^{36}Cl/Cl ratio for sedimentary rock sample SP-4, dolomite.

[See figure 1.1 for location of sampling site. See text for explanation of Mass Stopping Power, Weighting Factor, X and Y factors, Weighted Neutron Yields, and Thermal Cross Sections. Mass Stopping Power, Neutron Yields, and Absorption Cross Sections supplied by Fabryka-Martin (1995). Mass Stopping Power is given for each element for an alpha particle of energy 8.0 million electron volts (MeV). Mass Stopping Power units: MeV per gram of rock per square centimeter. Sample ppm from Appendix table A-2; cm^2/g, square centimeters per gram; <, less than.]

| Element | Mass Stopping Power | Neutron Yield | | Sample ppm | Weighting Factor | Weighted Neutron Yield | |
		n/yr/g rock per ppm U	n/yr/g rock per ppm Th			n/yr/g rock per ppm U	n/yr/g rock per ppm Th
Si	454	0.69	0.339	3085	1.40	0.97	0.47
Al	444	5.116	2.585	1429	0.63	3.25	1.64
Fe	351	0.187	0.208	1166	0.41	0.08	0.09
Ca	428	0.282	0.026	217555	93.11	26.26	2.42
Mg	461	5.834	2.564	120681	55.63	324.57	142.65
Na	456	12.535	5.959	223	0.10	1.27	0.61
K	414	0.89	0.08	747	0.31	0.28	0.02
P	433	4.473	0.573	44	0.02	0.09	0.01
Li	548	23.86	10.54	5	0.00	0.07	0.03
Be	529	265.948	91.561	0.5	0.00	0.07	0.02
B	527	62.551	19.779	20	0.01	0.66	0.21
C	561	0.456	0.179	128108	71.87	32.77	12.86
F	472	41.33	16.362	330	0.16	6.44	2.55
O	527	0.236	0.084	524591.32	276.46	65.24	23.22
			Total	997984.82	500.12	462.00	186.81

Element	Atomic Weight (amu)	Sample ppm	Neutron Absorption Cross Section (barns/atom)	Thermal Neutron Cross Section (cm^2/g)
Si	28.1	3085	0.17	0.000011
Al	27.0	1429	0.233	0.000007
Fe	55.8	1166	2.56	0.000032
Ca	40.1	217555	0.43	0.001404
Mg	24.3	120681	0.063	0.000188
Na	23.0	223	0.53	0.000003
K	39.1	747	2.1	0.000024
P	30.97	44	0.18	<0.000001
Li	6.9	5	71	0.000031
Be	9.01	0 5	0.0092	<0.000001
B	10.8	20	764	0.000852
C	12.0	128108	0.0035	0.000022
F	19.0	330	0.0096	<0.000001
H	1.0	1459.63	0.33	0.000290
Ti	47.9	60	6.1	0.000005
Mn	54.9	155	13.3	0.000023
Sm	150.4	0.12	5600	0.000003
Gd	157.3	0.08	49000	0.000015
O	16.0	524591.32	0.00028	0.000006
	Total	999659.65		0.002917

Neutron Production Rate (n/g/yr)

(X factor = 0.924)   (Total U ppm =   0.2)   = 0.9367

(Y factor = 0.374)   (Total Th ppm =   0.14)   = 0.0173

^{238}U spontaneous fission   = 0.086

Total neutron production rate (n/g/yr)   = 0.3

In Situ Secular Equilibrium ^{36}Cl/Cl Ratio (x 10^{-15}) =   1.6

180

Table B-2e. Calculated thermal neutron cross section for neutron absorption, total neutron production rate, and *in situ* secular equilibrium ^{36}Cl/Cl ratio for sedimentary rock sample SP-12, limestone.

[See figure 1.1 for location of sampling site. See text for explanation of Mass Stopping Power, Weighting Factor, X and Y factors, Weighted Neutron Yields, and Thermal Cross Sections. Mass Stopping Power, Neutron Yields, and Absorption Cross Sections supplied by Fabryka-Martin (1995). Mass Stopping Power is given for each element for an alpha particle of energy 8.0 million electron volts (MeV). Mass Stopping Power units: MeV per gram of rock per square centimeter. Sample ppm from Appendix table A-2; cm^2/g, square centimeters per gram; <, less than.]

Element	Mass Stopping Power	Neutron Yield		Sample ppm	Weighting Factor	Weighted Neutron Yield	
		n/yr/g rock per ppm U	n/yr/g rock per ppm Th			n/yr/g rock per ppm U	n/yr/g rock per ppm Th
Si	454	0.69	0.339	19960	9.06	6.25	3.07
Al	444	5.116	2.585	1747	0.78	3.97	2.01
Fe	351	0.187	0.208	777	0.27	0.05	0.06
Ca	428	0.282	0.026	369572	158.18	44.61	4.11
Mg	461	5.834	2.564	3076	1.42	8.27	3.64
Na	456	12.535	5.959	74	0.03	0.42	0.20
K	414	0.89	0.08	913	0.38	0.34	0.03
P	433	4.473	0.573	218	0.09	0.42	0.05
Li	548	23.86	10.54	5	0.00	0.07	0.03
Be	529	265.948	91.561	0.5	0.00	0.07	0.02
B	527	62.551	19.779	20	0.01	0.66	0.21
C	561	0.456	0.179	116318	65.25	29.76	11.68
F	472	41.33	16.362	330	0.16	6.44	2.55
O	527	0.236	0.084	486475.03	256.37	60.50	21.54
			Total	999485.53	492.01	161.82	49.19

Element	Atomic Weight (amu)	Sample ppm	Neutron Absorption Cross Section (barns/atom)	Thermal Neutron Cross Section (cm²/g)
Si	28.1	19960	0.17	0.000073
Al	27.0	1747	0.233	0.000009
Fe	55.8	777	2.56	0.000021
Ca	40.1	369572	0.43	0.002386
Mg	24.3	3076	0.063	0.000005
Na	23.0	74	0.53	0.000001
K	39.1	913	2.1	0.000030
P	30.97	218	0.18	0.000001
Li	6.9	5	71	0.000031
Be	9.01	0.5	1.119	<0.000001
B	10.8	20	764	0.000852
C	12.0	116318	0.0035	0.000020
F	19.0	330	0.0096	<0.000001
H	1.0	250.74	0.33	0.000050
Ti	47.9	60	6.1	0.000005
Mn	54.9	77	13.3	0.000011
Sm	150.4	0.64	5600	0.000014
Gd	157.3	0.5	49000	0.000094
O	16.0	486475.03	0.00028	0.000005
	Total	999874.41		**0.003607**

Neutron Production Rate (n/g/yr)

(X factor = 0.329) (Total U ppm = 2.3) = 0.7567

(Y factor = 0.100) (Total Th ppm = 0.22) = 0.0220

^{238}U spontaneous fission = 0.987

Total neutron production rate (n/g/yr) = **1.8**

In Situ Secular Equilibrium ^{36}Cl/Cl Ratio ($\times 10^{-15}$) = 7

181

Table B-2f. Calculated thermal neutron cross section for neutron absorption, total neutron production rate, and *in situ* secular equilibrium ^{36}Cl/Cl ratio for sedimentary rock sample SP-25, shale.

[See figure 1.1 for location of sampling site. See text for explanation of Mass Stopping Power, Weighting Factor, X and Y factors, Weighted Neutron Yields, and Thermal Cross.Sections. Mass Stopping Power, Neutron Yields, and Absorption Cross Sections supplied by Fabryka-Martin (1995). Mass Stopping Power is given for each element for an alpha particle of energy 8.0 million electron volts (MeV). Mass Stopping Power units: MeV per gram of rock per square centimeter. Sample ppm from Appendix table A-2; cm^2/g, square centimeters per gram; <, less than.]

| Element | Mass Stopping Power | Neutron Yield | | Sample ppm | Weighting Factor | Weighted Neutron Yield | |
		n/yr/g rock per ppm U	n/yr/g rock per ppm Th			n/yr/g rock per ppm U	n/yr/g rock per ppm Th
Si	454	0.69	0.339	226241	102.71	70.87	34.82
Al	444	5.116	2.585	62452	27.73	141.86	71.68
Fe	351	0.187	0.208	30704	10.78	2.02	2.24
Ca	428	0.282	0.026	63394	27.13	7.65	0.71
Mg	461	5.834	2.564	38659	17.82	103.97	45.70
Na	456	12.535	5.959	6825	3.11	39.01	18.55
K	414	0.89	0.08	26731	11.07	9.85	0.89
P	433	4.473	0.573	1222	0.53	2.37	0.30
Li	548	23.86	10.54	60	0.03	0.78	0.35
Be	529	265.948	91.561	3	0.00	0.42	0.15
B	527	62.551	19.779	100	0.05	3.30	1.04
C	561	0.456	0.179	10000	5.61	2.56	1.00
F	472	41.33	16.362	500	0.24	9.75	3.86
O	527	0.236	0.084	512242.46	269.95	63.71	22.68
			Total	979133.46	476.77	458.12	203.95

Element	Atomic Weight (amu)	Sample ppm	Neutron Absorption Cross Section (barns/atom)	Thermal Neutron Cross Section (cm^2/g)
Si	28.1	226241	0.17	0.000824
Al	27.0	62452	0.233	0.000324
Fe	55.8	30704	2.56	0.000848
Ca	40.1	63394	0.43	0.000409
Mg	24.3	38659	0.063	0.000060
Na	23.0	6825	0.53	0.000095
K	39.1	26731	2.1	0.000864
P	30.97	1222	0.18	0.000004
Li	6.9	60	71	0.000372
Be	9.01	3	1.119	<0.000001
B	10.8	100	764	0.004259
C	12.0	10000	0.0035	0.000002
F	19.0	500	0.0096	<0.000001
H	1.0	12664.38	0.33	0.002516
Ti	47.9	3477	6.1	0.000267
Mn	54.9	1704	13.3	0.000249
Sm	150.4	4.53	5600	0.000102
Gd	157.3	4.3	49000	0.000806
O	16.0	512242.46	0.00028	0.000005
	Total	996987.67		0.012006

Neutron Production Rate (n/g/yr)

(X factor = 0.961) (Total U ppm = 2.6) = 2.4986

(Y factor = 0.428) (Total Th ppm = 9.07) = 3.8820

^{238}U spontaneous fission = 1.115

Total neutron production rate (n/g/yr) = 7.5

In Situ Secular Equilibrium ^{36}Cl/Cl Ratio (x 10^{-15}) = 9

182

Table B-2g.   Calculated thermal neutron cross section for neutron absorption, total neutron production rate, and *in situ* secular equilibrium ^{36}Cl/Cl ratio for sedimentary rock sample SP-26, limestone.

[See figure 1.1 for location of sampling site. See text for explanation of Mass Stopping Power, Weighting Factor, X and Y factors, Weighted Neutron Yields, and Thermal Cross Sections. Mass Stopping Power, Neutron Yields, and Absorption Cross Sections supplied by Fabryka-Martin (1995).   Mass Stopping Power is given for each element for an alpha particle of energy 8.0 million electron volts (MeV).   Mass Stopping Power units: MeV per gram of rock per square centimeter. Sample ppm from Appendix table A-2; cm^2/g, square centimeters per gram; <, less than.]

Element	Mass Stopping Power	Neutron Yield		Sample ppm	Weighting Factor	Weighted Neutron Yield	
		n/yr/g rock per ppm U	n/yr/g rock per ppm Th			n/yr/g rock per ppm U	n/yr/g rock per ppm Th
Si	454	0.69	0.339	-bd-	--	--	--
Al	444	5.116	2.585	-bd-	--	--	--
Fe	351	0.187	0.208	311	0.11	0.02	0.02
Ca	428	0.282	0.026	385939	165.18	46.58	4.29
Mg	461	5.834	2.564	2835	1.31	7.62	3.35
Na	456	12.535	5.959	148	0.07	0.85	0.40
K	414	0.89	0.08	0	0.00	0.00	0.00
P	433	4.473	0.573	262	0.11	0.51	0.07
Li	548	23.86	10.54	5	0.00	0.07	0.03
Be	529	265.948	91.561	0.5	0.00	0.07	0.02
B	527	62.551	19.779	20	0.01	0.66	0.21
C	561	0.456	0.179	115718	64.92	29.60	11.62
F	472	41.33	16.362	330	0.16	6.44	2.55
O	527	0.236	0.084	490636.81	258.57	61.02	21.72
			Total	996205.31	490.43	153.44	44.29

Element	Atomic Weight (amu)	Sample ppm	Neutron Absorption Cross Section (barns/atom)	Thermal Neutron Cross Section (cm^2/g)
Si	28.1	-bd-	0.17	--
Al	27.0	-bd-	0.233	--
Fe	55.8	311	2.56	0.000009
Ca	40.1	385939	0.43	0.002491
Mg	24.3	2835	0.063	0.000004
Na	23.0	148	0.53	0.000002
K	39.1	0	2.1	<0.000001
P	30.97	262	0.18	0.000001
Li	6.9	5	71	0.000031
Be	9.01	0.5	1.119	<0.000001
B	10.8	20	764	0.000852
C	12.0	115718	0.0035	0.000020
F	19.0	330	0.0096	<0.000001
H	1.0	3243.86	0.33	0.000644
Ti	47.9	240	6.1	0.000018
Mn	54.9	155	13.3	0.000023
Sm	150.4	0.72	5600	0.000016
Gd	157.3	0.47	49000	0.000088
O	16.0	490636.81	0.00028	0.000005
	Total	999845.36		0.004205

Neutron Production Rate (n/g/yr)

(X factor = 0.313)   (Total U ppm =   4.3)   = 1.3459

(Y factor = 0.090)   (Total Th ppm =   0.28)   = 0.0252

^{238}U spontaneous fission   = 1.845

Total neutron production rate (n/g/yr)   = 3.2

In Situ Secular Equilibrium ^{36}Cl/Cl Ratio ($\times 10^{-15}$) =   11

Table B-3a.   Calculated thermal neutron cross section for neutron absorption, total neutron production rate, and *in situ* secular equilibrium ^{36}Cl/Cl ratio for metamorphic rock sample SP-11, quartzite.

[See figure 1.1 for location of sampling site. See text for explanation of Mass Stopping Power, Weighting Factor, X and Y factors, Weighted Neutron Yields, and Thermal Cross Sections. Mass Stopping Power, Neutron Yields, and Absorption Cross Sections supplied by Fabryka-Martin (1995). Mass Stopping Power is given for each element for an alpha particle of energy 8.0 million electron volts (MeV). Mass Stopping Power units: MeV per gram of rock per square centimeter. Sample ppm from Appendix table A-3; cm^2/g, square centimeters per gram; <, less than.]

| Element | Mass Stopping Power | Neutron Yield | | Sample ppm | Weighting Factor | Weighted Neutron Yield | |
		n/yr/g rock per ppm U	n/yr/g rock per ppm Th			n/yr/g rock per ppm U	n/yr/g rock per ppm Th
Si	454	0.69	0.339	342353	155.43	107.25	52.69
Al	444	5.116	2.585	16883	7.50	38.35	19.38
Fe	351	0.187	0.208	5441	1.91	0.36	0.40
Ca	428	0.282	0.026	69969	29.95	8.44	0.78
Mg	461	5.834	2.564	5126	2.36	13.79	6.06
Na	456	12.535	5.959	371	0.17	2.12	1.01
K	414	0.89	0.08	8966	3.71	3.30	0.30
P	433	4.473	0.573	524	0.23	1.01	0.13
Li	548	23.86	10.54	15	0.01	0.20	0.09
Be	529	265.948	91.561	0.5	0.00	0.07	0.02
B	527	62.551	19.779	35	0.02	1.15	0.36
C	561	0.456	0.179	23501	13.18	6.01	2.36
F	472	41.33	16.362	270	0.13	5.27	2.09
O	527	0.236	0.084	522718.17	275.47	65.01	23.14
			Total	996172.67	490.06	252.33	108.80

Element	Atomic Weight (amu)	Sample ppm	Neutron Absorption Cross Section (barns/atom)	Thermal Neutron Cross Section (cm^2/g)
Si	28.1	342353	0.17	0.001247
Al	27.0	16883	0.233	0.000088
Fe	55.8	5441	2.56	0.000150
Ca	40.1	69969	0.43	0.000452
Mg	24.3	5126	0.063	0.000008
Na	23.0	371	0.53	0.000005
K	39.1	8966	2.1	0.000290
P	30.97	524	0.18	0.000002
Li	6.9	15	71	0.000093
Be	9.01	0.5	1.119	<0.000001
B	10.8	35	764	0.001491
C	12.0	23501	0.0035	0.000004
F	19.0	270	0.0096	<0.000001
H	1.0	2379.16	0.33	0.000473
Ti	47.9	719	6.1	0.000055
Mn	54.9	620	13.3	0.000090
Sm	150.4	2.01	5600	0.000045
Gd	157.3	1.81	49000	0.000339
O	16.0	522718.17	0.00028	0.000006
	Total	999894.65		0.004837

Neutron Production Rate (n/g/yr)

(X factor = 0.515)   (Total U ppm =   1.4)   = 0.7210

(Y factor = 0.222)   (Total Th ppm =   3.68)   = 0.8170

^{238}U spontaneous fission   = 0.601

Total neutron production rate (n/g/yr)   = 2.1

In Situ Secular Equilibrium ^{36}Cl/Cl Ratio ($\times 10^{-15}$) =   6.4

Table B-3b. Calculated thermal neutron cross section for neutron absorption, total neutron production rate, and *in situ* secular equilibrium ^{36}Cl/Cl ratio for metamorphic rock sample SP-24, quartzite.

[See figure 1.1 for location of sampling site. See text for explanation of Mass Stopping Power, Weighting Factor, X and Y factors, Weighted Neutron Yields, and Thermal Cross Sections. Mass Stopping Power, Neutron Yields, and Absorption Cross Sections supplied by Fabryka-Martin (1995). Mass Stopping Power is given for each element for an alpha particle of energy 8.0 million electron volts (MeV). Mass Stopping Power units: MeV per gram of rock per square centimeter. Sample ppm from Appendix table A-3; cm^2/g, square centimeters per gram; <, less than.]

Element	Mass Stopping Power	Neutron Yield		Sample ppm	Weighting Factor	Weighted Neutron Yield	
		n/yr/g rock per ppm U	n/yr/g rock per ppm Th			n/yr/g rock per ppm U	n/yr/g rock per ppm Th
Si	454	0.69	0.339	463513	210.43	145.20	71.34
Al	444	5.116	2.585	-bd-	—	—	—
Fe	351	0.187	0.208	155	0.05	0.01	0.01
Ca	428	0.282	0.026	0	0.00	0.00	0.00
Mg	461	5.834	2.564	151	0.07	0.41	0.18
Na	456	12.535	5.959	148	0.07	0.85	0.40
K	414	0.89	0.08	2657	1.10	0.98	0.09
P	433	4.473	0.573	131	0.06	0.25	0.03
Li	548	23.86	10.54	15	0.01	0.20	0.09
Be	529	265.948	91.561	0.5	0.00	0.07	0.02
B	527	62.551	19.779	35	0.02	1.15	0.36
C	561	0.456	0.179	89	0.05	0.02	0.01
F	472	41.33	16.362	270	0.13	5.27	2.09
O	527	0.236	0.084	531923.53	280.32	66.16	23.55
			Total	999088.03	492.31	220.56	98.17

Element	Atomic Weight (amu)	Sample ppm	Neutron Absorption Cross Section (barns/atom)	Thermal Neutron Cross Section (cm^2/g)
Si	28.1	463513	0.17	0.001688
Al	27.0	-bd-	0.233	—
Fe	55.8	155	2.56	0.000004
Ca	40.1	0	0.43	<0.000001
Mg	24.3	181	0.063	<0.000001
Na	23.0	148	0.53	0.000002
K	39.1	2657	2.1	0.000086
P	30.97	131	0.18	<0.000001
Li	6.9	15	71	0.000093
Be	9.01	0.5	1.119	<0.000001
B	10.8	35	764	0.001491
C	12.0	89	0.0035	<0.000001
F	19.0	270	0.0096	<0.000001
H	1.0	295.54	0.33	0.000059
Ti	47.9	420	6.1	0.000032
Mn	54.9	155	13.3	0.000023
Sm	150.4	0.28	5600	0.000006
Gd	157.3	0.26	49000	0.000049
O	16.0	531923.53	0.00028	0.000006
	Total	999989.11		0.003539

Neutron Production Rate (n/g/yr)

(X factor = 0.448)   (Total U ppm = 0.30)   = 0.1344

(Y factor = 0.199)   (Total Th ppm = 0.55)   = 0.1095

^{238}U spontaneous fission   = 0.129

Total neutron production rate (n/g/yr)   = 0.4

In Situ Secular Equilibrium ^{36}Cl/Cl Ratio (x 10^{-15}) =   1.5

185

APPENDIX C

EXAMPLES OF CALCULATIONS PERFORMED IN THIS RESEARCH

Table C-1.   Sample calculation for determining atoms of ^{36}Cl per liter for archived ground water sample USGS 14 (collection date = 04-08-1987).

USGS 14 (collection date = 04-08-1987)

Total dissolved Cl⁻ as measured by RESL, 1993   =   21±1.0 mg/L

Volume of water sample   =   400 mL

Cl⁻   =   (400mL/1000mL)×(21 mg/L)

                                                  =   0.0084 g/L

Measured $^{36}Cl/Cl$ ratio   =   5250±50 × 10^{-15}

Atoms of chloride added:

$$atoms\ Cl^- = \frac{(0.00\ g/L)}{(35.453\ g/\ g\ atom)}\left(6.023 \times 10^{23}\ atoms/\ g\ atom\right) = 0$$

Calculated atoms of native chloride/L:

$$atoms\ Cl^- = \frac{(0.0084\ g/0.4L)}{(35.453\ g/\ g\ atom)}\left(6.023 \times 10^{23}\ atoms/\ g\ atom\right) = 3.57 \times 10^{20}$$

Calculated atoms of $^{36}Cl/L$:

$$atoms\ ^{36}Cl = \left(3.57 \times 10^{20}\ atoms\ native\ Cl^-\right)\left(5250 \times 10^{-15}\right) = 18.7 \times 10^{8}\ atoms\ /\ L$$

187

Table C-2.   Calculation of average precipitation flux at the Upper Fremont Glacier, Wyoming, USA.

Depth of weapons-tests produced ^{36}Cl peak $\cong$ 32 meters

Densities (from Naftz, 1992):

0-14 meter depth	0.65 g/cm^3	(snow, firn, and ice mixed)
14-32 meter depth	0.89 g/cm^3	(ice)

(14,000 cm) × (0.65 g/cm^3) + (1,800) × (0.89 g/cm^3)   =   2,152 g/cm^2

=   Total accumulation rate of "wet" precipitation. (Can't measure the dry deposition here, only can estimate it.)

^{36}Cl peak at 32 m depth produced in about 1958. Ice core was collected in 1991.

$$\begin{array}{r} 1991 \\ -1958 \\ \hline 33 \text{ years} \end{array}$$

Average accumulation rate is:

$$\frac{2,512 \text{ g/cm}^2}{33 \text{ years}} = (76 \text{ g/cm})/\text{year}$$

For ablation, long-term average from Marston and others (1991) is 88 cm/year. Assumed density for the ablated portion of "wet" precipitation is 0.5 g/cm^3 (Naftz, 1992). Average ablation rate is therefore, 44 (g/cm^2)/yr. It follows that,

$$\text{Total "Wet" precipitation flux} = \frac{\begin{array}{l} 76 \,(\text{g/cm}^2)/\text{year (accumulation flux)} \\ + 44 \,(\text{g/cm}^2)/\text{year (ablation flux)} \end{array}}{120 \,(\text{g/cm}^2)/\text{year}}$$

Note: These calculations may have as much as a 50 percent associated uncertainty.

Table C-3.   Comparison of accelerator mass spectrometry and conventional decay counting method sensitivities.

The following information applies to an ambient ^{36}Cl/Cl ratio calculated for a representative (1 liter) ground-water sample from the eastern Snake River Plain aquifer. The accelerator mass spectrometry (AMS) measurement is accomplished with a 5 mg silver chloride (AgCl) target for a half-hour count. The conventional beta-decay counting method, for the same ambient ground water sample, requires grams of AgCl and no detection of the ^{36}Cl is accomplished because of the extremely long counting time required for a single beta-particle emission (about 2 years).

AMS MEASUREMENT

- Chlorine-36:   Half life = 301,000 years

- Sample Size: 5 mg of AgCl (1.25 mg Cl⁻)

- Ratio Measured: 1×10^{-14}

- Calculated atoms of ^{36}Cl: 2×10^{5}

- Calculated Radioactivity: 9.8×10^{-7} disintegrations per minute (dpm)

CONVENTIONAL DECAY COUNTING

- Calculated disintegrations from the ambient sample with a measured ratio of 1×10^{-14} for a ground water sample from the eastern Snake River Plain, Idaho

  $(9.8 \times 10^{-7}$ dpm)(525,600 min/yr) $= 0.52$ disintegrations per year

- On average, this is one beta-particle decay every 2 years, this is not detectable by conventional counting methods

Table C-4.   Meteoric ^{36}Cl concentration in the Harriman State Park snow sample.

$$meteoric\ ^{36}Cl\ concentration = \frac{natural\ ^{36}Cl\ fallout\ rate\left(atoms/cm^2yr\right)}{\left(average\ annual\ precip\ in\ cm/yr\right) - \left(average\ annual\ ET\ in\ cm/yr\right)}$$

Example #1: Harriman State Park (data from Cecil and others, 1999)

Fallout Rate   = 0.012±0.002 atoms/cm^{2}sec
                      = 3.8 × 10^5 atoms/cm^{2}yr

Average annual precip = 58 cm/yr
Estimated annual ET   = 29 cm/yr   (1st guess, 50 percent ET rate)

(50 percent ET) $y = \dfrac{3.8 \times 10^5\ atoms/cm^2 yr}{\left(58\ cm/yr\right) - \left(29\ cm/yr\right)}$

$= 1.3 \times 10^4\ atoms/cm^3$

$= 1.3 \times 10^4\ atoms/mL$

$= 1.3 \times 10^7\ atoms/L$

(No ET) $y = \dfrac{3.8 \times 10^5\ atoms/cm^2 yr}{\left(58\ cm/yr\right)}$

$= 6.5 \times 10^3\ atoms/cm^3$

$= 6.5 \times 10^6\ atoms/L$

(95 percent ET) $y = \dfrac{3.8 \times 10^5\ atoms/cm^2 yr}{\left(\left(58\ cm/yr\right) - \left(55\ cm/yr\right)\right)}$

$= 1.3 \times 10^5\ atoms/cm^3$

$= 1.3 \times 10^8\ atoms/L$

Table C-5.   Anthropogenic chlorine-36 concentration in INEEL snow sample #2.

Fallout Rate $= 12 \pm 2.4$ atoms/cm^{2}sec (water equivalent)
                              $= 3.8 \times 10^8$ atoms/cm^{2}yr

Average annual precip $= 22$ cm/yr
Estimated annual ET $= 21$ cm/yr   (95% estimated ET from Cecil & others, 1992)

(95 percent ET)

$$y = \frac{3.8 \times 10^8 \ atoms/cm^2 yr}{(22 \ cm/yr) - (21 \ cm/yr)}$$

$$= 3.8 \times 10^8 \ atoms/cm^3$$

$$= 3.8 \times 10^{11} \ atoms/L$$

(No ET)

$$y = \frac{3.8 \times 10^8 \ atoms/cm^2 yr}{(22 \ cm/yr)}$$

$$= 1.7 \times 10^7 \ atoms/cm^3$$

$$= 1.7 \times 10^{10} \ atoms/L$$

(50 percent ET)

$$y = \frac{3.8 \times 10^8 \ atoms/cm^2 yr}{((22 \ cm/yr) - (11 \ cm/yr))}$$

$$= 3.5 \times 10^7 \ atoms/cm^3$$

$$= 3.5 \times 10^{10} \ atoms/L$$

Table C-6.   Calculation of chlorine-36/chlorine as a result of *in situ* production for sample SP-1, limestone.

The following is modified from equation 5.3-11, page 107:

$$Ratio = \frac{(\text{isotopic abundance})(^{35}Cl \text{ cross section})(thermal\ neutron\ flux)}{decay\ \text{constant}}$$

$\Rightarrow$ Thermal neutron flux for SP-1 = P_n (neutron production rate)/ σ_T (neutron absorption cross section)

- $\bullet$ = (1.45 [n/g]/yr)/ (0.003598 cm^2/g)

- $\bullet$ = 404 n/cm^2/yr

- $\bullet$ isotopic abundance   =   0.7577 for ^{35}Cl

- $\bullet$ ^{35}Cl cross section   =   44 barns/atom = (4.4 × 10^{-23} cm^2/atom)

- $\bullet$ thermal neutron flux   =   404 n/cm^2 yr

- $\bullet$ decay constant   =   2.3 × 10^{-6} /yr

$$\frac{^{36}Cl}{Cl} Ratio = \frac{(0.7577)(4.4 \times 10^{-23})(404)}{2.3 \times 10^{-6}}$$

$$= 5.9 \times 10^{-15}$$

Table C-7.   Sample calculation to determine atoms of chlorine-36 in solution in ground water from *in situ* production.

Example: SP-1, Limestone

Cl⁻ (USGS lab)	=	100 mg/kg	=	0.1 mg/g
^{36}Cl/Cl (calculated)	=	5.9×10^{-15}		
limestone density	=	2.54 g/cm³		
Cl⁻ (g/cm³) .	=	$(0.1 \times 10^{-3})(2.54 \text{ g/cm}^3)$		
	=	0.254×10^{-3} g/cm³		

$$\frac{atoms\ Cl^-}{cm^3} = \left(\frac{0.254 \times 10^{-3}\ g/cm^3}{35.453\ g/g\ atom}\right)\left(6.023 \times 10^{23}\ atoms/g\ atom\right) = 4.32 \times 10^{18}\ atoms/cm^3$$

$$\frac{atoms\ ^{36}Cl}{cm^3} = \left(5.9 \times 10^{-15}\right)\left(4.32 \times 10^{18}\ atoms/cm^3\right) = 2.55 \times 10^4\ atoms/cm^3$$

Total transfer from rock to fluid using 1% porosity:

$$Total\ Transfer = \left(2.55 \times 10^4\ atoms/cm^3\right)\left(100\right) = 2.55 \times 10^9\ atoms/L$$

$$Associated\ Fluid\ Chlorinity = \left(\frac{2.55 \times 10^4\ atoms/cm^3}{5.9 \times 10^{-15}\left(^{36}Cl^- / Cl^-\right)}\right) = 4.32 \times 10^{23}\ atoms\ Cl^-/L$$

$$\frac{x\ (g/L)}{35.453\ g/g\ atom}\left(6.023 \times 10^{23}\ atoms/g\ atom\right) = 4.32 \times 10^{23}\ atoms\ Cl^-/L$$

$$\therefore\quad x \quad = \quad 25.4\ g/L$$

Ambient dissolved Cl⁻ (maximum for ground water from limestone in the eastern Snake River Plain aquifer) is 15 mg/L, or 0.059 percent of the associated chlorinity for complete transfer of *in situ* produced ^{36}Cl. Therefore, the corrected ^{36}Cl atoms/L is;

$$2.55 \times 10^9\ atoms/L\ (total\ transfer)(0.00059) = 1.49 \times 10^6\ atoms\ ^{36}Cl/L$$

$$(maximum\ ^{36}Cl\ atoms/L\ in\ ground\ water)$$

193

Table C-8. Calculations to determine atoms of chlorine-36 per cubic centimeter (atoms/cm^3) of rock that is transferred from the rock matrix to the available pore space within the aquifer matrix.
[See figure C.1 for conceptual model of these calculations.]

[The following calculations were performed to determine the number of atoms of chlorine-36 that could be transferred to the aquifer pore spaces for a given rock unit. The calculations are performed for various percentages of porosity and an assumed initial ^{36}Cl concentration of one million atoms per cubic centimeter of rock (1 × 10^6 atoms of ^{36}Cl /cm^3) produced *in situ*.]

1.   Consider a one cubic meter section of rock:

$$1 \text{ m}^3 \quad = \quad 1 \times 10^6 \text{ cm}^3$$

2.   Maximum ^{36}Cl atoms available for transfer to the pore spaces in the rock:

$$(1 \times 10^6 \text{ atoms/cm}^3) \times (1 \times 10^6 \text{ cm}^3) \quad = \quad 1 \times 10^{12} \text{ atoms}$$

Therefore: Only a portion of the maximum 1 × 10^{12} atoms will be transferred into pore spaces of the aquifer matrix.

3.   For an aquifer matrix with one percent porosity;

$$1 \text{ percent of 1 m}^3 \text{ of rock is, } 0.01 \text{ m}^3 \quad = \quad 10,000 \text{ cm}^3$$

It follows that the number of atoms of ^{36}Cl that can be transferred to the pore spaces is:

$$(10,000 \text{ cm}^3) \times (X \text{ atoms/cm}^3) \quad = \quad 1 \times 10^{12} \text{ atoms}$$
$$X \quad = \quad 100 \times 10^6 \text{ atoms}$$

For an aquifer matrix with 5 percent porosity;

$$5 \text{ percent of 1 m}^3 \text{ of rock is, } 0.05 \text{ m}^3 \quad = \quad 50,000 \text{ cm}^3$$
$$(50,000 \text{ cm}^3) \times (X \text{ atoms/cm}^3) \quad = \quad 1 \times 10^{12} \text{ atoms}$$
$$X \quad = \quad 20 \times 10^6 \text{ atoms}$$

For an aquifer matrix with 10 percent porosity;

$$10 \text{ percent of 1 m}^3 \text{ of rock is, } 0.1 \text{ m}^3 \quad = \quad 100,000 \text{ cm}^3$$
$$(100,000 \text{ cm}^3) \times (X \text{ atoms/cm}^3) \quad = \quad 1 \times 10^{12} \text{ atoms}$$
$$X \quad = \quad 10 \times 10^6 \text{ atoms}$$

For an aquifer matrix with 50 percent porosity;

$$50 \text{ percent of 1 m}^3 \text{ of rock is, } 0.5 \text{ m}^3 \quad = \quad 500,000 \text{ cm}^3$$
$$(500,000 \text{ cm}^3) \times (X \text{ atoms/cm}^3) \quad = \quad 1 \times 10^{12} \text{ atoms}$$
$$X \quad = \quad 2 \times 10^6 \text{ atoms}$$

For an aquifer matrix with 75 percent porosity;

$$75 \text{ percent of 1 m}^3 \text{ of rock is, } 0.75 \text{ m}^3 = 750,000 \text{ cm}^3$$
$$(750,000 \text{ cm}^3) \times (X \text{ atoms/cm}^3) \quad = \quad 1 \times 10^{12} \text{ atoms}$$
$$X \quad = \quad 1.33 \times 10^6 \text{ atoms}$$

1 m^3 of rock matrix with 1 percent porosity

1 percent porosity

Rock Matrix

Transfer of ^{36}Cl atoms from rock matrix to pore spaces
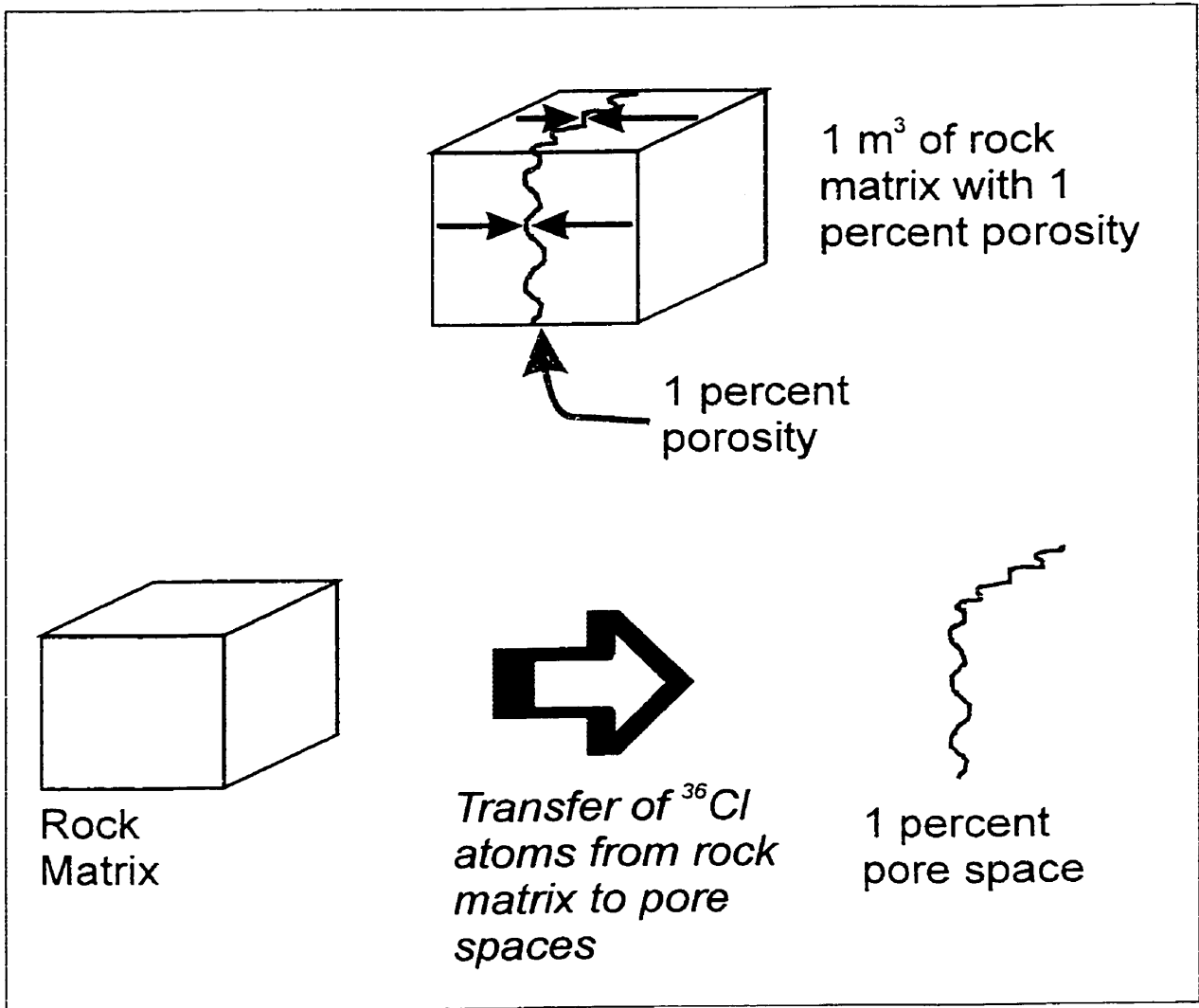
1 percent pore space

Figure C.1. Conceptual model of the transfer of ^{36}Cl atoms in the rock matrix to the pore spaces within the rock matrix.

Table C-9.   Contribution to ^{36}Cl/Cl ratio from the *in situ* reaction ^{39}K(n,α)^{36}Cl.

Sample SP-5, rhyolite

Atom concentration of potassium ion (K$^+$) in sample SP-5, rhyolite:

$$K^+ = 38,935 \ \mu g/g \ = 38,935 \ mg/kg \ = 38.9 \ mg/g$$

Rhyolite density $= 2.61$ g/cm^3

$$(38.9 \ mg/g)(2.61 \ g/cm^3) = \ (0.0389 \ g/g)(2.61 g/cm^3) \ = \ 0.102 \ g/cm^3$$

$$\frac{atoms \ K}{cm^3} = \left(\frac{0.102 \ g/cm^3}{39.0983 \ g/g \ atom}\right)\left(6.023 \times 10^{23} \ atoms/g \ atom\right) = 1.56 \times 10^{21} \ atoms/cm^3$$

atom concentration of Cl$^-$ in SP-5:

$$Cl- = 240 \ \mu g/g \ = 0.24 \ mg/g \ = 0.24 \times 10^{-3} \ g/g$$

$$(0.24 \times 10^{-3} \ g/g)(2.61 \ g/cm^3) \ = 0.62 \times 10^{-3} \ g/cm^3$$

$$\frac{atoms \ Cl}{cm^3} = \left(\frac{0.62 \times 10^{-3} \ g/cm^3}{35.453 g/g \ atom}\right)\left(6.023 \times 10^{23} \ atoms/g \ atom\right) = 1.06 \times 10^{19} \ atoms/cm^3$$

- neutron production rate   = 18.63 n/yr/g
- absorption cross section   = 8478 $\times$ 10^{-6} cm^2/g
- isotopic abundance   = 0.9326 four ^{39}K

Using equation 5.3-11, page 107:

$$\frac{^{36}Cl}{Cl} = \left[\frac{(0.9326)(1.56 \times 10^{21})(0.0043 \times 10^{-24})(18.63)}{(0.0000023)(1.06 \times 10^{19})(8478 \times 10^{-6})}\right] \cong 6 \times 10^{-16}$$

Table C-10. Calculation of amount of ^{35}Cl that is activated per year at the INTEC to produce the chlorine-36 inventory estimated to be in the environment at the INEEL.

The following equation is from West and others, 1958, Nuclear Engineering Handbook, 1st edition, McGraw-Hill, New York, NY

$$N(^{36}Cl) = \frac{N(^{35}Cl)(\sigma)(\phi)(1 - e^{-\lambda t})}{\lambda}$$

Where
N = number of atoms

λ = decay constant of chlorine-36

ϕ = neutron flux (estimated)

σ = thermal neutron absorption cross sectional area of ^{35}Cl, and

t = time, note: if t is short compared to the half-life of the product nuclide, then $1-e^{-\lambda t}$ is approximately equal to λt

$$N(^{35}Cl) = \frac{\left(1.5 \times 10^{23}\ atoms/yr\right)\left(7.5 \times 10^{-14}\ /sec\right)}{\left(43 \times 10^{-24}\right)\left(1 \times 10^{14}\ n/cm^2\ sec\right)\left(7.5 \times 10^{-14}\ /sec\right)(2\ yr)}$$

= 6 × 10^{23} atoms/yr (one gram atom of ^{35}Cl)

= 35 grams ^{35}Cl or 57 grams NaCl/year

Assumptions:

- All chloride in the target sample is ^{35}Cl and all ^{35}Cl is neutron activated
- 100 percent of the neutron flux is thermal
- irradiation time is 2 years
- ^{36}Cl atoms per year concentration is based on measurements of ground water near INEEL

APPENDIX D

COMPREHENSIVE LIST OF GLOBAL RESEARCH CONCERNING CHLORINE-36 STUDIES IN VARIOUS GEOLOGIC AND HYDROLOGIC ENVIRONMENTS

Table D-1.   Comprehensive list of global research concerning ^{36}Cl studies in various geologic and hydrologic environments.

Type of Application	Study Area	Author(s)	Date of Publication
Vadose Zone Tracing	Socorro, New Mexico	Trotman	1983
	Socorro, New Mexico	Phillips and others	1984b
	Southeastern New Mexico	Phillips and others	1990a
	Nevada Test Site	Fabryka-Martin and others	1993, 1997
	Nevada Test Site	Gifford	1987
	Nevada Test Site	Norris and others	1987
	West Texas	Scanlon	1992
	INEEL, Idaho	Cecil and others	1992
	Central Washington	Prych	1995, 1996
	South Australia	Cook and others	1994
	South Australia	Walker and others	1991
	Southwest U.S.A.	Phillips	1994
	Southern Nevada	Plummer	1997
	Southern Nevada	Tyler and others	1996
^{36}Cl bomb pulse in ground water and ice	Borden, Ontario	Bentley and others	1982; 1986a
	Milk River Aquifer, Canada	Phillips and others	1986
	East Midlands Triassic sandstone aquifer, UK	Andrews and others	1994
	Aquia aquifer, Maryland	Purdy and others	1996
	South Australia	Herczeg and others	1997
	Sturgeon Falls, Ontario	Milton and others	1997b
	INEEL, Idaho	Cecil and others	1992
	Wyoming, U.S.A.	Cecil and Vogt	1997
	INEEL, Idaho	Cecil and others	1998a
	Wyoming, U.S.A.	Cecil and others	1998b
	INEEL, Idaho	Cecil and others	1999
	INEEL, Idaho	Cecil and others	2000a
	INEEL, Idaho	Cecil and others	2000b
	Wyoming, U.S.A.; Nepal	Green and others	2000
	INEEL Idaho	Beasley and other	1993
^{36}Cl as a tracer for salinity balances	Jordan River	Paul and others	1986
	Jordan River	Magaritz and others	1990
	Jordan River	Yechieli and others	1986
	North America	Milton and others	1997a
	Victoria Land, Antarctica	Carlson and others	1990
	Victoria Land, Antarctica	Lyons and others	1998

Type of Application	Study Area	Author(s)	Date of Publication
	East African Rift	Kaufman and others	1990
	Southern Great Basin, U.S.A.	Phillips and others	1993
	Southern Great Basin, U.S.A.	Jannik and others	1991
	Western Great Basin, U.S.A.	Phillips and others	1995
Decay Dating of Ground Water using ^{36}Cl	Great Artesian Basin, Australia	Bentley and others	1986b
	Great Artesian Basin, Australia	Torgersen and others	1991
	Milk River Aquifer, Alberta, Canada	Phillips and others	1986
	Milk River Aquifer, Alberta, Canada	Nolte and others	1991
	Murray Basin, Australia	Davie and others	1989
	Murray Basin, Australia	Kellet and others	1993
	Nevada Test Site	Rose and others	1997
	Columbia Plateau flood basalts	Gifford and others	1985
	Aquia aquifer, Maryland	Purdy	1991
	Aquia aquifer, Maryland	Purdy and others	1996
	Carrizo Aquifer, southern Texas	Bentley and others	1986a
	Switzerland	Pearson and others	1991
	Midlands Triassic sandstone aquifer, England	Andrews and others	1994
	Dead Sea	Yechieli and others	1996
	Mazowsze Basin, Poland	Dowgiallo and others	1990
	East Africa Rift Zone	Kaufman and others	1990
	Stripa site, Sweden	Andrews and others	1986
	Germany	Lodemann and others	1997
	Australia and Canada	Fabryka-Martin and others	1987; 1988
	Canada	Cornett and others	1996
	Switzerland	Pearson and others	1990
^{36}Cl in Geothermal Systems	Valles caldera, New Mexico	Phillips and others	1984a
	Valles caldera, New Mexico	Rao and others	1996
	New Zealand	Hedenquist and others	1990
	Long Valley, California	Phillips and others	1995